INFORMATION TO USERS

This material was produced from a microfilm copy of the original document. While the most advanced technological means to photograph and reproduce this document have been used, the quality is heavily dependent upon the quality of the original submitted.

The following explanation of techniques is provided to help you understand markings or patterns which may appear on this reproduction.

1. The sign or "target" for pages apparently lacking from the document photographed is "Missing Page(s)". If it was possible to obtain the missing page(s) or section, they are spliced into the film along with adjacent pages. This may have necessitated cutting thru an image and duplicating adjacent pages to insure you complete continuity.

2. When an image on the film is obliterated with a large round black mark, it is an indication that the photographer suspected that the copy may have moved during exposure and thus cause a blurred image. You will find a good image of the page in the adjacent frame.

3. When a map, drawing or chart, etc., was part of the material being photographed the photographer followed a definite method in "sectioning" the material. It is customary to begin photoing at the upper left hand corner of a large sheet and to continue photoing from left to right in equal sections with a small overlap. If necessary, sectioning is continued again — beginning below the first row and continuing on until complete.

4. The majority of users indicate that the textual content is of greatest value, however, a somewhat higher quality reproduction could be made from "photographs" if essential to the understanding of the dissertation. Silver prints of "photographs" may be ordered at additional charge by writing the Order Department, giving the catalog number, title, author and specific pages you wish reproduced.

5. PLEASE NOTE: Some pages may have indistinct print. Filmed as received.

Xerox University Microfilms
300 North Zeeb Road
Ann Arbor, Michigan 48106

Downloaded from SHAREOK. Persistent Handle URL: https://hdl.handle.net/11244/3685

74-9873

MCALLISTER, David Lee, 1946-
ELECTROCHEMICAL STUDIES OF SELECTED PTERIDINES AND RELATED COMPOUNDS.

The University of Oklahoma, Ph.D., 1973
Chemistry, analytical

University Microfilms, A XEROX Company, Ann Arbor, Michigan

THIS DISSERTATION HAS BEEN MICROFILMED EXACTLY AS RECEIVED.

THE UNIVERSITY OF OKLAHOMA

GRADUATE COLLEGE

ELECTROCHEMICAL STUDIES OF SELECTED PTERIDINES AND RELATED COMPOUNDS

A DISSERTATION

SUBMITTED TO THE GRADUATE FACULTY

in partial fulfillment of the requirements for the

degree of

DOCTOR OF PHILOSOPHY

BY

DAVID LEE MCALLISTER

1973

ELECTROCHEMICAL STUDIES OF SELECTED PTERIDINES

AND RELATED COMPOUNDS

APPROVED BY

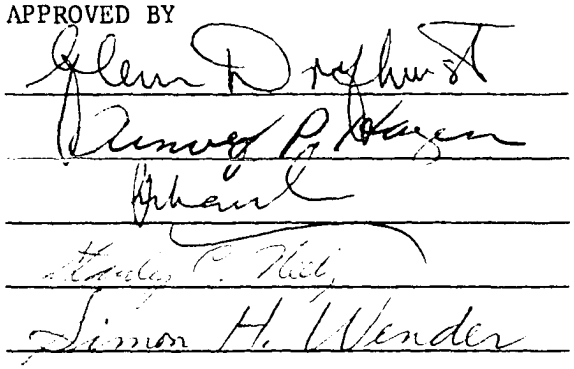

DISSERTATION COMMITTEE

ACKNOWLEDGEMENTS

The author wishes to express his gratitude to Dr. Glenn Dryhurst, who suggested these problems, for guidance and support during the course of this research.

Financial assistance in the form of a National Defense Graduate Fellowship from the Department of Health, Education and Welfare, and summer fellowships from the Electrochemical Society and the Division of Analytical Chemistry of the American Chemical Society is gratefully acknowledged.

Discussions with the chemistry faculty and my fellow graduate students have been very helpful. Their generosity in the use of research equipment has been especially beneficial.

Finally, I am most indebted to my parents who encouraged my early interest in science, and to my wife, without whose patience and understanding graduate work would have been impossible.

TABLE OF CONTENTS

Page

LIST OF TABLES vi

LIST OF ILLUSTRATIONS ix

Chapter

1. INTRODUCTION 1

2. ELECTROCHEMICAL REDUCTION OF PTERIDINE 11

Introduction 11

Results and Discussion 12

Experimental 71

Summary 77

Appendix 2 79

References 86

3. ELECTROCHEMICAL REDUCTION OF 6- AND 7-HYDROXYPTERIDINE 88

Introduction 88

Results and Discussion 91

6-hydroxypteridine 91

7-hydroxypteridine 118

Analytical Application 121

Experimental 124

Summary 125

Page

References 127

4. ELECTROCHEMICAL OXIDATION OF 6- AND 7-HYDROXYPTERIDINE 128

Introduction 128

Results and Discussion 129

Experimental 163

Summary 176

References 177

5. THE ELECTROCHEMICAL REDUCTION OF OXAMIDE 179

Introduction 179

Results and Discussion 180

Mechanism 196

Experimental 200

Summary 203

Appendix 5 204

References 210

LIST OF TABLES

Table		Page
2-1.	Effect of Mercury Column Height and Temperature on the Limiting Current of Pteridine	22
2-2.	Separation of Anodic and Cathodic Peak Potentials for Pteridine	29
2-3.	Heterogeneous Rate Constants (k_s) for Pteridine Wave I at the PGE and HMDE	31
2-4.	Comparison of Experimental and Theoretical Peak Currents for Pteridine Peak I_c	32
2-5.	Variation of $i_p/v^{1/2}$ as a Function of $v^{1/2}$ for Voltammetric Peak I_a of Pteridine	36
2-6.	Variation of $(i_p)_a/(i_p)_c$ with $k_2C\tau$, for $a\tau = 4$	40
2-7.	Values of $(i_p)_a/(i_p)_c$ and k_2 for Pteridine at the HMDE	41
2-8.	Coulometric Determination of the Number of Electrons Involved in the Reduction of Pteridine on the Plateau of Polarographic Wave I	43
2-9.	Comparison of Properties of Pteridine and Dihydropteridine	64
A-2-1.	Variation of ψ with Peak Separation	81
3-1.	Effect of Corrected Mercury Column Height and Temperature on the Limiting Current for 6-hydroxy-pteridine	94

Table Page

3-2. Effect of Mercury Column Height on the Limiting Current of the Prewave for 6-hydroxypteridine at pH 9.8 93

3-3. Coulometric n-values for the Electrochemical Reduction of 6-hydroxypteridine 115

3-4. Comparison of UV Spectra and Voltammetric Oxidation Peak Potentials for 7,8-dihydro-6-hydroxypteridine and Product of Electrochemical Reduction of 6-hydroxypteridine 115

3-5. Coulometric n-values for the Electrochemical Reduction of 7-hydroxypteridine 120

4-1. Peak Current Values for the Oxidation of 6- and 7-hydroxypteridine at the PGE 129

4-2. Coulometric Determination of the Number of Electrons Involved in the Oxidation of Peak I_a of 6-hydroxypteridine 138

4-3. Coulometric Determination of the Number of Electrons Involved in the Oxidation of 6,7-dihydroxypteridine 144

4-4. Material Balance for the Oxidation of 6,7-dihydroxypteridine 148

4-5. Percentage of Oxamide and Carbon Dioxide Originating from Positions 6 and 7 of 6,7-dihydroxypteridine 152

4-6. Comparison of Quantities of Oxidation Products of 6,7-dihydroxypteridine Predicted by the Proposed Reaction Schemes with the Quantities Found by Analysis 162

5-1. Effect of Corrected Mercury Column Height and Temperature on the Limiting Current for Oxamide 182

Table | Page

5-2. Coulometric n-values for the Electrochemical Reduction of Oxamide at Mercury 184

5-3. Values of Homogeneous Rate Constant, k_f, for the Chemical Step in the Electrochemical Reduction of Oxamide at a Mercury Electrode 192

A-5-1. Values of $i/ACv^{1/2}$ at Various Sweep Rates for $k_f = 10$ 208

LIST OF ILLUSTRATIONS

Figure		Page
2-1.	Equilibrium of Pteridine in Aqueous Solution	13
2-2.	Variation of $E_{1/2}$ with pH for Pteridine waves I, II and III	14
2-3.	Variation of the Diffusion Current Constant, I, with pH for Pteridine waves I, II and III	16
2-4.	D.C. Polarograms of Pteridine at pH 7.0	17
2-5.	D.C. Polarograms of Pteridine in 1 M acetic acid	18
2-6.	Log Plots of Pteridine Wave I at pH 7.1, 8.1 and 10.8	20
2-7.	(A) Triangular Waveform for Cyclic Voltammetry. (B) Cyclic Voltammogram for a Reversible Electrochemical Reaction	23
2-8.	Cyclic Voltammogram of Pteridine at pH 7.0 at the PGE	25
2-9.	Variation of E_p with pH for Pteridine at the PGE	26
2-10.	Cyclic Voltammogram of Pteridine at the PGE at pH 2.8	27
2-11.	Cyclic Voltammograms of Pteridine at pH 9.0 at the PGE	33
2-12.	Cyclic Voltammograms of Pteridine at pH 10.0 and 7.0 at the PGE	34

Figure Page

2-13. Variation of $(i_p)_a/(i_p)_c$ with Log $(k_2C\tau)$ at $a\tau = 4$ 40

2-14. Polarograms of Pteridine During Electrochemical Reduction at pH 4.7 44

2-15. Dependence of $E_{1/2}$ and E_p upon pH for (A) Pteridine waves II, IV, and V and (B) the Oxidation Peak Observed at the PGE after Reduction of Pteridine 46

2-16. Ultraviolet Spectra Recorded During the Electro-Chemical Reduction of Pteridine at pH 4.7 47

2-17. Log Plot for Pteridine Wave IV at pH 7.0 49

2-18. Voltammograms at the PGE of Pteridine at pH 7.0 During Reduction 51

2-19. Mass, NMR and IR Spectra of Pteridine Wave I Reduction Product 54

2-20. Mass, NMR and IR Spectra of Pteridine 55

2-21. Proposed Fragmentation Pattern for Pteridine Wave I Product 58

2-22. Mass, NMR and IR Spectra of the Pteridine Wave IV Reduction Product 61

2-23. Proposed Mass Spectral Fragmentation Pattern for Pteridine Wave IV Reduction Product 65

2-24. Proposed Electrochemical Reduction Mechanism for Pteridine 66

2-25. Electrochemical Reduction Mechanism for (A) 2-amino-4-hydroxypteridines and (B) Quinoxalines 68

2-26. Proposed Mechanism for the Reaction of 5,8-dihydropteridine with Pteridine to Form a Dimer 70

A-2-1. Variation of ψ with Peak Separation 81

Figure Page

A-2-2. Hypothetical Cyclic Voltammogram for the Couple Ox ± ne ⇌ Red 82

3-1. Equilibrium of 6-hydroxypteridine in Aqueous Solution 90

3-2. Variation of $E_{1/2}$ and E_p with pH for 6- and 7-hydroxypteridine 92

3-3. Variation of the Diffusion Current Constant, I, with pH for 6- and 7-hydroxypteridine 93

3-4. (A) D.C. Polarogram of 6-hydroxypteridine at pH 9.8. (B) A.C. Polarogram of 6-hydroxypteridine at pH 9.8. (C) A.C. Polarogram of 7,8-dihydro-6-hydroxypteridine at pH 9.8 95

3-5. Variation of Wave Height and $E_{1/2}$ with Concentration for 6-hydroxypteridine at pH 9.8 97

3-6. (A) D.C. Polarogram of 6-hydroxypteridine at pH 9.8. (B) A.C. Polarogram of 6-hydroxypteridine at pH 9.8 98

3-7. (A) D.C. Polarogram of 6-hydroxypteridine at pH 8.1. (B) A.C. Polarogram of 6-hydroxypteridine at pH 8.1 99

3-8. Fundamental A.C. Polarograms of 6-hydroxypteridine at Various Concentrations at pH 5.6 102

3-9. Potential Range of the Sharp Depression Observed in A.C. Polarography of 6-hydroxypteridine at pH 7.1 as a Function of Concentration 104

3-10. Change in Differential Capacity at -0.55 V as a Function of Concentration for (A) 6-hydroxypteridine, pH 6.0 and 7,8-dihydro-6-hydroxypteridine, pH 9.8. (B) 7-hydroxypteridine,

Figure Page

pH 6.0 and 5,6-dihydro-7-hydroxypteridine, pH 6.0 . . . 106

3-11. Differential Capacity vs $t^{1/2}$ Curves for 6-hydroxypteridine at pH 6.0 at the HMDE 107

3-12. Cyclic Voltammograms of (A) 6-hydroxypteridine and (B) 7,8-dihydro-6-hydroxypteridine at the PGE at pH 11.1 111

3-13. Variation of (A) Peak Current Function with Square Root of Scan Rate, and (B) i_p/C with Concentration for 6-hydroxypteridine 113

3-14. (A) Possible Two-dimensional Hydrogen-bonded Polymer of 7,8-dihydro-6,7-dihydroxypteridine. (B) Possible Two-dimensional Hydrogen-bonded Dimeric Form of 7,8-dihydro-6,7-dihydroxypteridine 117

3-15. Proposed Reaction Scheme for the Electrochemical Reduction of 6-hydroxypteridine 119

3-16. Cyclic Voltammograms of (A) 7-hydroxypteridine and (B) 5,6-dihydro-7-hydroxypteridine at the PGE at pH 7.0 122

3-17. Proposed Reaction Scheme for the Electrochemical Reduction of 7-hydroxypteridine 123

4-1. Voltammograms at the PGE of 1 mM Solutions of 6-hydroxypteridine at pH 7.0 and 7-hydroxypteridine in 2 M H_2SO_4 130

4-2. Variation of E_p with pH for 6-hydroxypteridine at the PGE 131

4-3. Variation of $i_p/ACv^{1/2}$ with pH for Peak I_a of 6-hydroxypteridine at the PGE 133

Figure Page

4-4. Variation of Peak Current Function with Voltage Sweep Rate for 6- and 7-hydroxypteridine at the PGE . . 134

4-5. Variation of i_p/C with Concentration of 6- and 7-hydroxypteridine at the PGE 136

4-6. Plot of Peak Current vs Concentration for 6- and 7-hydroxypteridine 137

4-7. Proposed Reaction Scheme for the Electrochemical Oxidation of 6- and 7-hydroxypteridine at the PGE . . . 140

4-8. Variation of E_p with pH for 6,7-dihydroxypteridine at the PGE 141

4-9. Variation of Peak Current Function with Scan Rate for 6,7-dihydroxypteridine at the PGE 143

4-10. D.C. Polarograms of Solution after Oxidation of 6,7-dihydroxypteridine 146

4-11. Proposed Initial and Secondary Electrochemical Oxidation of 6,7-dihydroxypteridine 157

4-12A. Proposed Reaction Scheme for the Rearrangement of the Diol to Oxamide, Followed by Fragmentation of 4,5-diketopyrimidine 159

4-12B. Proposed Reaction Scheme for the Rearrangement and Oxidation of the Diol to Tetraketopiperazine and Urea 161

4-13. Mass and IR Spectra of Oxamide 167

4-14. Mass and IR Spectra of Tetraketopiperazine 169

4-15. Mass and IR Spectra of Oxamic Acid 171

5-1. Variation of the Diffusion Current Constant with pH for Oxamide 181

Figure		Page
5-2.	Cyclic Voltammograms of Oxamide at the HMDE at pH 10.0	185
5-3.	Cyclic Voltammograms of Oxamide at the HMDE in 50% Acetonitrile - 50% pH 10.0 Carbonate Buffer	187
5-4.	Variation of the Peak Current Function of Oxamide Peak I_c at the HMDE with the Square Root of Scan Rate in Various Buffer Systems	189
5-5.	Comparison of Experimental and Theoretical Current-time Curves for the Electrochemical Reduction of Oxamide at the HMDE	194
5-6.	Proposed Mechanism for the Electrochemical Reduction of Oxamide to Glycolamide and Ammonia	197
5-7.	Linear Variation of the Limiting Current *vs* Concentration of Oxamide	199
5-8.	Mass, NMR and Infrared Spectra of Glycolamide	202
A-5-1.	i_t *vs* $t^{-1/2}$ for Oxamide at pH 7 at the HMDE	205
A-5-2.	Variation of the Peak Current Function with k_f/a for the Second Charge-transfer Step of an ECE Reaction	207

CHAPTER 1

INTRODUCTION

The pteridine ring system (1), consisting of a pyrazine ring fused with a pyrimidine ring, is found quite widely distributed in nature,

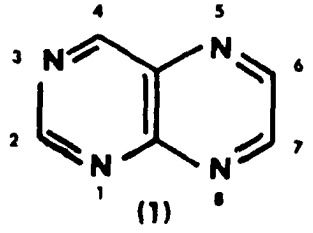

(1)

although the amounts of pteridine derivatives found in biological systems are generally very small.

The first investigations of natural pteridines were those of Hopkins,[1] who found that the wing pigments of the English brimstone butterfly and the white cabbage butterfly were pteridine derivatives. At about the same time, Kübling[2] prepared the first synthetic pteridines. However, the structure of the pteridines and the relationship between the natural and synthetic substances was not recognized until about 1940 by Wieland and co-workers.[3-5] In subsequent years, much research has been devoted to the chemistry and biology of pteridines.

The very low concentration of pteridines in biological systems has in general prohibited detailed study of their biochemical reactions. However, it is known that the reduced forms of some pteridines are of

metabolic importance as coenzymes in hydroxylation reactions[6] and as intermediates in the photosynthetic electron transport process.[7] Also, the in vitro oxidation of hydroxypteridines by xanthine oxidase has been studied.[8,9]

Because of the similar nature of certain electrochemical and enzymatic electron-transfer reactions, electrochemical methods have been used in investigations of electron-transfer reactions (both oxidations and reductions) of biologically important compounds. For example, it has been shown that for certain purines, the electrochemical oxidation mechanism closely parallels the enzymatic oxidation.[10-12] The present study was initiated to determine whether a comparable similarity exists for the electrochemical and enzymatic oxidations and reductions of certain pteridines. Another goal of the investigation was a more thorough understanding of the electrochemical reactions of pteridines as a class of compounds.

Biological Significance of Pteridines

Although pteridines were first observed in biological systems in 1891[1] and have since been found to be quite widely distributed in nature, in only a few instances has the role of these compounds in metabolic processes been clearly defined. Since naturally occurring pteridines are found in highest concentrations as pigments in butterflies and fish, most early work was directed toward the isolation and characterization of these compounds.[13] It was some fifty years after the initial isolation of these pigments that the structures were firmly established.[14-16] The three pigments occurring in highest

concentrations are now known by the trivial names xanthopterin (2), leucopterin (3), and isoxanthopterin (4). Many other pigments have

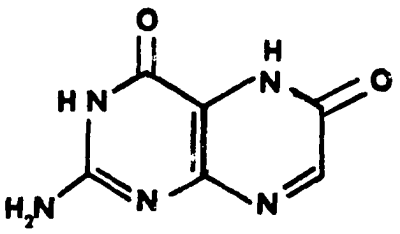

(2)

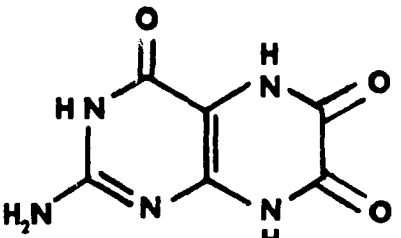

(3)

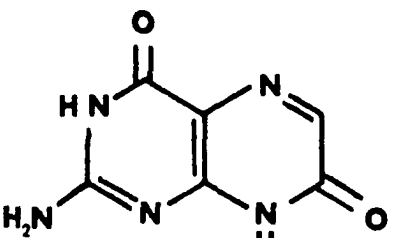

(4)

subsequently been isolated and identified as pteridines.[13]

One of the first pteridines isolated from mammalian sources was urothione (5) which was found in human urine by Koschara[17] in 1940. This compound is present in the liver of man and cattle. The structure

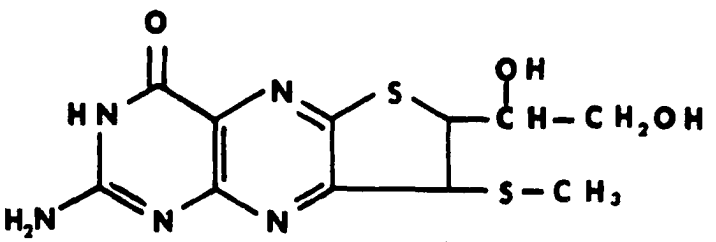

(5)

of urothione has been elucidated by Tschesche[18] following the initial work by Koschara.[19] Because of the very low concentrations of naturally-occurring urothione, the biological significance of this compound is unknown.

One of the most widely occurring pteridines is biopterin,[13] which was first isolated from human urine.[20] The structure of biopterin, shown below (6), was established by Patterson.[21] Dihydrobiopterin has been identified as a cofactor in the conversion of phenylalanine to tyrosine and probably also in the conversion of tyrosine to dihydroxyphenylalanine.[22]

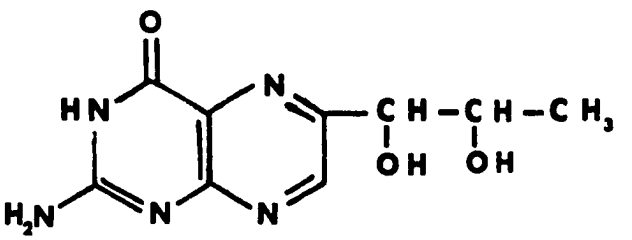

(6)

Fuller and Nugent[7] showed that the dihydro forms of certain 2-amino-4-hydroxy-6-substituted pteridines can be reduced to the tetrahydro compounds by the action of light in the presence of chromatophores from photosynthetic bacteria. Pteridines of this type were found in association with the pigment-protein complex characteristic of the reaction center of chromatophore fractions and chloroplasts. It was proposed that the electron produced by excited-state chlorophyll is captured by a pteridine at the photosynthetic reaction center.

The name folic acid was suggested by Mitchell, Snell, and Williams[23] for a material isolated from spinach leaves which was shown to be essential for the growth of certain organisms, and which has since been recognized as a part of the vitamin B complex. The specific substance to which the name folic acid is applied is pteroylglutamic acid (7), and (8) is pteroic acid. Actually, there are a number of "folic acids" consisting of pteroic acid conjugated in peptide linkages with varying numbers of glutamic acid residues. The synthesis and structure of pteroylglutamic acid was first announced in 1945 in a note,[24] and the details of the degradation and synthesis were disclosed about a year later.[25-28] In biological systems, enzymes with the appropriate cofactors are capable of converting pteroylglutamic acid

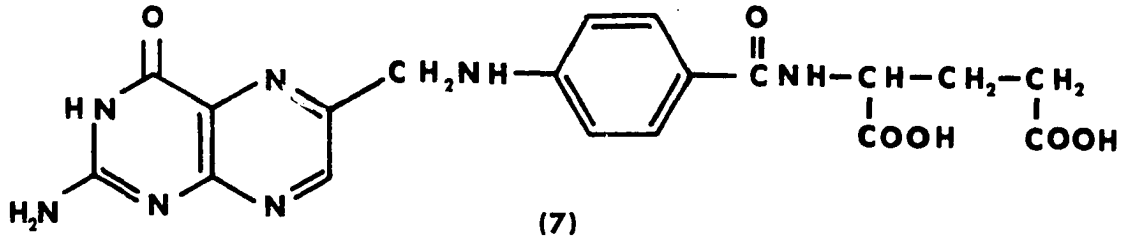

(7)

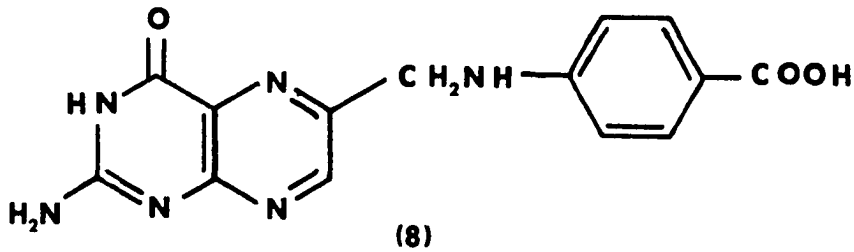

(8)

to the 5,6,7,8-tetrahydro derivative. Under the influence of other enzymes, tetrahydrofolic acid undergoes formylation with the formation of formyltetrahydrofolic acid (9). Formyltetrahydrofolic acid is

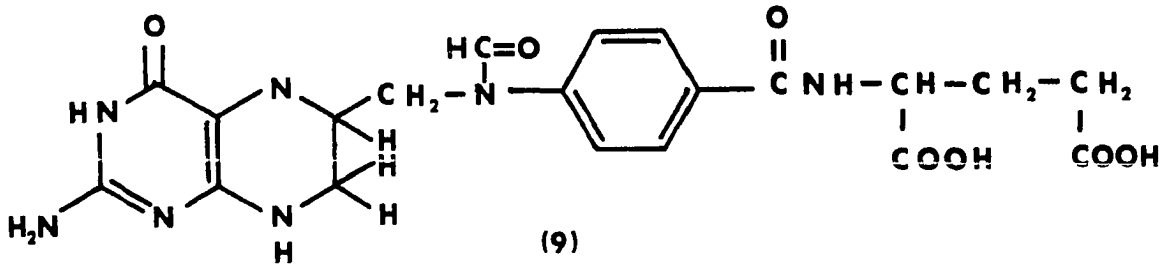

(9)

very important biologically in that it serves as a source of one-carbon-atom fragments in the biosynthesis of many compounds (e.g., purines and pyrimidines).

Although no information is available concerning the oxidation of

pteridines *in vivo*, a considerable amount of work has been done on the *in vitro* oxidation of amino and hydroxy pteridines with mammalian xanthine oxidase. Bergmann and Kwietny[8,9] have reported that xanthine oxidase catalyzes the oxidation of xanthopterin to leucopterin, and 2-amino-4-hydroxypteridine is oxidized to isoxanthopterin. Oxidation of various other mono- and polyhydroxy pteridines can be summarized as follows[9]: a) Pteridines with a free 6-position are all converted finally to 2,4,7-trihydroxypteridine. b) Pteridines with a preformed 6-hydroxyl group are oxidized finally to 2,4,6,7-tetrahydroxypteridine.

Chemical Reduction and Oxidation of Pteridines

Reduction of the pteridine nucleus follows no uniform pathway, although it appears that normally the pyrazine ring is preferentially attacked. Pteridine itself can be reduced to 5,6,7,8-tetrahydropteridine with lithium aluminum hydride.[29] A study of the chemical reduction of all mono- and dihydroxypteridines[30,31] revealed that all are reduced to 5,6- or 7,8-dihydroderivatives, with the exception of 2-hydroxypteridine and 2,7-dihydroxypteridine which are reduced to 3,4-dihydroderivatives.

Oxidation of unsubstituted pteridine with potassium permanganate in 0.1 N NaOH gives 4-hydroxypteridine in 17% yield.[32] Similar treatment of 6-hydroxypteridine produces 6,7-dihydroxypteridine in 65% yield.[32] The oxidation of 7-hydroxypteridine to 6,7-dihydroxypteridine in 15% yield requires hot (60°-70°C) potassium permanganate.[32]

Electrochemical Studies of Pteridines

Many pteridines have been studied electrochemically, principally by Asahi[33,34] and Komenda and co-workers,[35-39] but in general these studies have been quite superficial, involving in most cases only the use of d.c. polarography. These studies for the most part have been confined to derivatives of 2-amino-4-hydroxypteridine, although Komenda and Laskafeld have reported on the polarography of 4-hydroxypteridine, 2-aminopteridine, and pteridine itself.[38] In most cases it was concluded that the polarographic waves observed corresponded to $2\underline{e}/2H^+$ reductions to dihydro compounds. In some instances, two polarographic waves were observed, the second wave presumably representing reduction of dihydropteridines to the tetrahydro derivatives. Reports of studies of the electrochemical oxidation of pteridines have not appeared.

A rather complete study of the electrochemical reduction of folic acid was recently published by Kretzschmar and Jaenicke.[40] Their work indicated that depending on pH, folic acid is reduced to 5,6,7,8-tetrahydrofolic acid, 2-amino-4-hydroxy-5,6,7,8-tetrahydropteridine, or a dimer of tetrahydrofolic acid.

Kwee and Lund[41] have published results of a study of the electrochemical reduction of substituted 4-hydroxypteridines. Generally, the compounds studied were reduced in an initial $2\underline{e}/2H^+$ step to 5,8-dihydro compounds which rearrange to 7,8-dihydro derivatives. The 7,8-dihydro compounds undergo further reduction to 5,6,7,8-tetrahydro derivatives.

REFERENCES

1. F. G. Hopkins, Nature, 45, 197, 581 (1891), Phil. Tran. Roy Soc., B186, 661 (1893).

2. O. Kübling, Chem. Ber., 28, 1968 (1895).

3. C. Schöpf and H. Wieland, Chem. Ber., 59, 2067 (1926).

4. H. Wieland and C. Schöpf, Chem. Ber., 58, 2178 (1925).

5. H. Wieland and P. Decker, Ann. Chem., 547, 180 (1941).

6. S. Kaufman, J. Biol. Chem., 242, 3934 (1967).

7. R. C. Fuller and N. A. Nugent, Proc. Nat. Acad. Sci. U. S., 63, 1311 (1969).

8. F. Bergmann and H. Kwietny, Biochem. Biophys. Acta, 28, 613 (1958).

9. F. Bergmann and H. Kwietny, Biochem. Biophys. Acta, 33, 29 (1959).

10. W. A. Struck and P. J. Elving, Biochemistry, 4, 1343 (1965).

11. G. Dryhurst and P. J. Elving, J. Electrochem. Soc., 115, 1014 (1968).

12. G. Dryhurst and G. F. Pace, J. Electrochem. Soc., 117, 1260 (1970).

13. W. Pfleiderer, Angew. Chem., 75, 993 (1963). Intern. Eng. Ed., 3, 114 (1964).

14. R. Purrmann, Ann. Chem., 544, 182 (1940).

15. R. Purrmann, Ann. Chem., 546, 98 (1940).

16. W. Koschara, Z. Physiol. Chem., 277, 159 (1940).

17. W. Koschara, Z. Physiol. Chem., 263, 78 (1940).

18. R. Tschesche, F. Korte, and G. Heuschkel, Chem. Ber., 88, 1251 (1955).

19. W. Koschara, Z. Physiol. Chem., 279, 44 (1943).

20. E. L. Patterson, M. H. von Saltza, and E. L. R. Stokstad, J. Am. Chem. Soc., 77, 3167 (1955). 78, 5871 (1956).

21. E. L. Patterson, R. Milstrey, and E. L. R. Stokstad, J. Am. Chem. Soc., 78, 5868 (1956).

22. S. Kaufman, Trans. N. Y. Acad. Sci., [II], 26, 977 (1964).

23. H. K. Mitchell, E. E. Snell, and R. J. Williams, J. Am. Chem. Soc., 63, 2284 (1941).

24. R. B. Angeir, J. H. Boothe, B. L. Hutchings, J. H. Mowat, J. Semb, E. L. R. Stokstad, Y. SubbaRow, C. W. Waller, D. B. Cosulich, M. J. Fahrenbach, M. E. Hultquist, E. Kuh, E. H. Northey, D. R. Seeger, J. P. Sickels, J. H. Smith, Jr., Science, 102, 227 (1945).

25. R. B. Angeir, J. H. Boothe, B. L. Hutchings, J. H. Mowat, J. Semb, E. L. R. Stokstad, Y. SubbaRow, C. W. Waller, D. B. Cosulich, M. J. Fahrenbach, M. E. Hultquist, E. Kuh, E. H. Northey, D. R. Seeger, J. P. Sickels, and J. H. Smith, Jr., Science, 103, 667 (1946).

26. E. L. R. Stokstad, J. Am. Chem. Soc., 70, 5 (1948).

27. J. H. Mowat, J. H. Boothe, B. L. Hutchings, E. L. R. Stokstad, C. W. Waller, R. B. Angeir, J. Semb, D. B. Cosulich, and Y. SubbaRow, J. Am. Chem. Soc., 70, 14 (1948).

28. B. L. Hutchings, E. L. R. Stokstad, J. H. Mowat, J. H. Boothe, C. W. Waller, R. B. Angeir, J. Semb, and Y. SubbaRow, J. Am. Chem. Soc., 70, 10 (1948).

29. E. C. Taylor and W. R. Sherman, J. Am. Chem. Soc., 81, 2464 (1959).

30. A. Albert and D. J. Brown, J. Chem. Soc., 1953, 74.

31. A. Albert and S. Matsuura, J. Chem. Soc., 1962, 2162.

32. D. J. Brown and S. F. Mason, J. Chem. Soc., 1956, 3443.

33. Y. Asahi, Yakugaku Zasshi, 79; 1548, 1554, 1559, 1565, 1570, (1959).

34. Y. Asahi, Abhandl. Deut. Akad. Wiss. Berlin, Kl. Chem., Geol., Biol., 1964, 74.

35. J. Komenda, Chem. Listy., 52, 1065 (1958).

36. J. Komenda, L. Kisova, J. Kovdelka, Coll. Czech. Chem. Commun., 25, 1020 (1960).

37. J. Komenda, Pteridine Chemistry, Proc. Intern. Symp., 3rd Stutgart, 1962, 511.

38. J. Komenda and D. Laskafeld, Coll. Czech. Chem. Commun., 27, 199 (1962).

39. L. Kosova, J. Komenda, and J. Hlavaty, Coll. Czech. Chem. Commun., 30, 2460 (1965).

40. K. Kretzschmar and W. Jaenicke, Z. Naturforsch, 26B, 999 (1971).

41. S. Kwee and H. Lund, Biochem. et Biophys. Acta, 297, 285 (1973).

CHAPTER 2

ELECTROCHEMICAL REDUCTION OF PTERIDINE

Introduction

In order to obtain information relating to the electrochemistry of the pteridine nucleus which might be applied later to the understanding of the electrochemistry of more complex, biologically important pteridines, a detailed study of the electrochemistry of pteridine itself was initiated.

Previous work has shown that pteridine is electrochemically reducible at the DME,[1] presumably in a 2e process. However, the latter work was limited to a study of the d.c. polarography of pteridine, and consequently no information is available concerning final product, rate constants or mechanism. Apparently, the electrochemical oxidation of pteridine has not been investigated.

The present study was directed toward a detailed examination of the electrochemical reduction of pteridine, including a determination of heterogeneous and, on occasion, homogeneous rate constants, isolation and identification of reaction products, and elucidation of reaction mechanisms. Experiments revealed that pteridine is not electrochemically oxidizable at the pyrolytic graphite electrode over the pH range 1-13.

Results and Discussion

Chemical Equilibria of Pteridine. To understand the electrochemistry of pteridine, it is first necessary to review the rather complex equilibria of this compound in aqueous solution. This equilibria has been studied extensively by Perrin[2] and Albert et al,[3] using UV and NMR spectrometry. When pteridine is initially dissolved in neutral aqueous solution, it exists entirely as the anhydrous neutral molecule (1, Fig. 2-1), but over several minutes attains equilibrium with the neutral 3,4-hydrate (2, Fig. 2-1). At equilibrium in neutral solution, the mixture consists of 79% (1) and 21% (2).[3] The formation of 3,4-hydrate (2) is acid or base catalyzed, with the rate of hydration being slowest at pH 7 and increasing at higher and lower pH.[2] The rate of dehydration is slower than hydration, but like hydration, is slowest at pH 7 and increases at higher and lower pH. In acidic solutions (pH <3), pteridine exists initially as the cation of the 3,4-hydrate (3, Fig. 2-1) which slowly equilibrates with the cation of the 5,6,7,8-dihydrate (4, Fig. 2-1). In very basic solution (pH >11) the anion of the 3,4-hydrate (5, Fig. 2-1) is formed.

D.C. Polarography. Over the pH range 1-13, pteridine shows three polarographic reduction waves, the $E_{1/2}$ of which shift linearly more negative with increasing pH (Fig. 2-2). The variation of $E_{1/2}$ with pH for the three waves can be represented as follows:

wave I (pH 3-13) $E_{1/2} = 0.04 - 0.064\ pH$ (2-1)

wave II (pH 1-13) $E_{1/2} = -0.36 - 0.070\ pH$ (2-2)

wave III (pH 11-13) $E_{1/2} = -0.54 - 0.080\ pH$ (2-3)

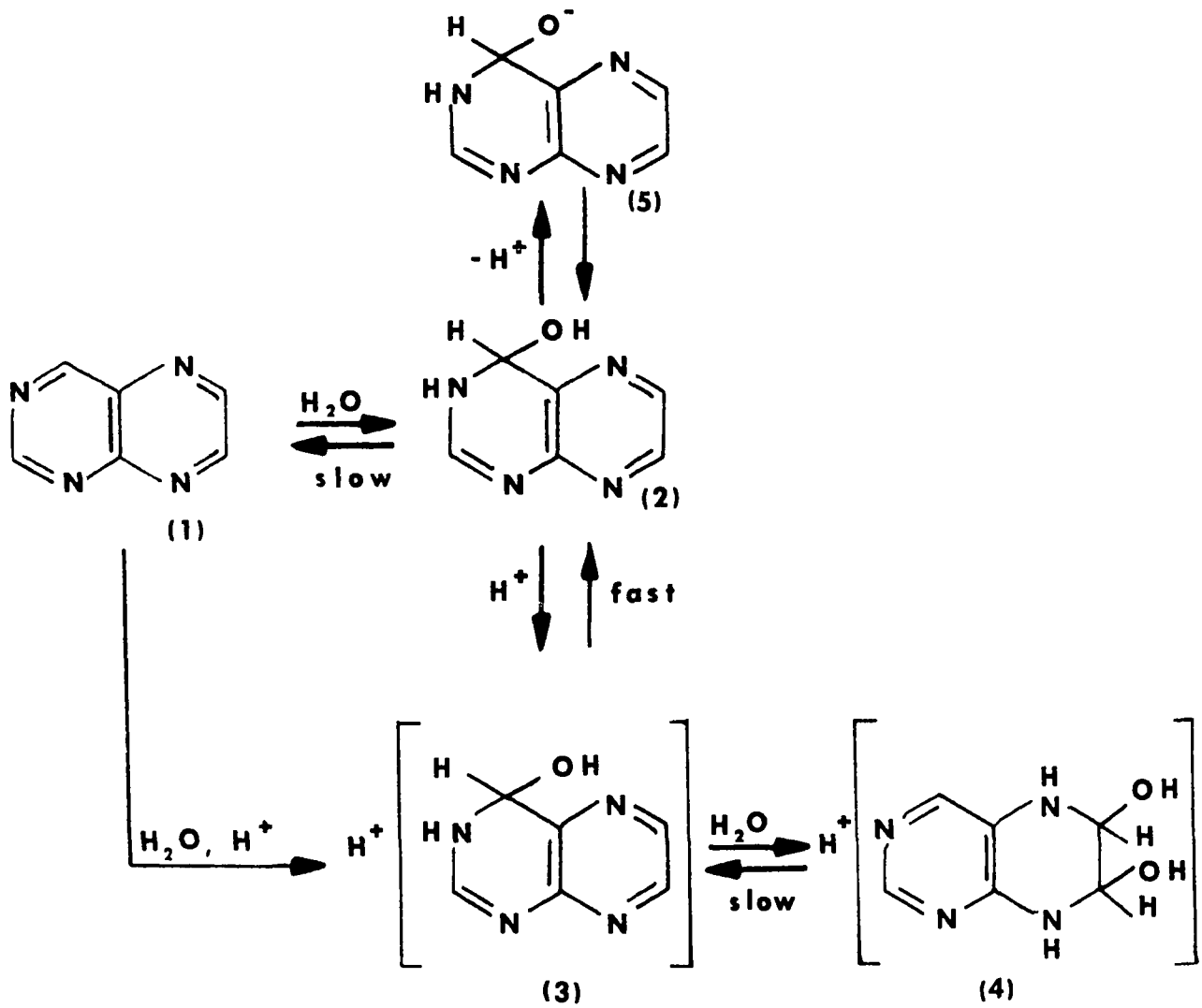

FIGURE 2-1. Equilibrium between the neutral non-hydrated form of pteridine (1), the neutral 3,4-hydrate (2), the cation of the 3,4-hydrate (3), the cation of the 5,6,7,8-dihydrate (4) and the anion of the 3,4-hydrate (5).

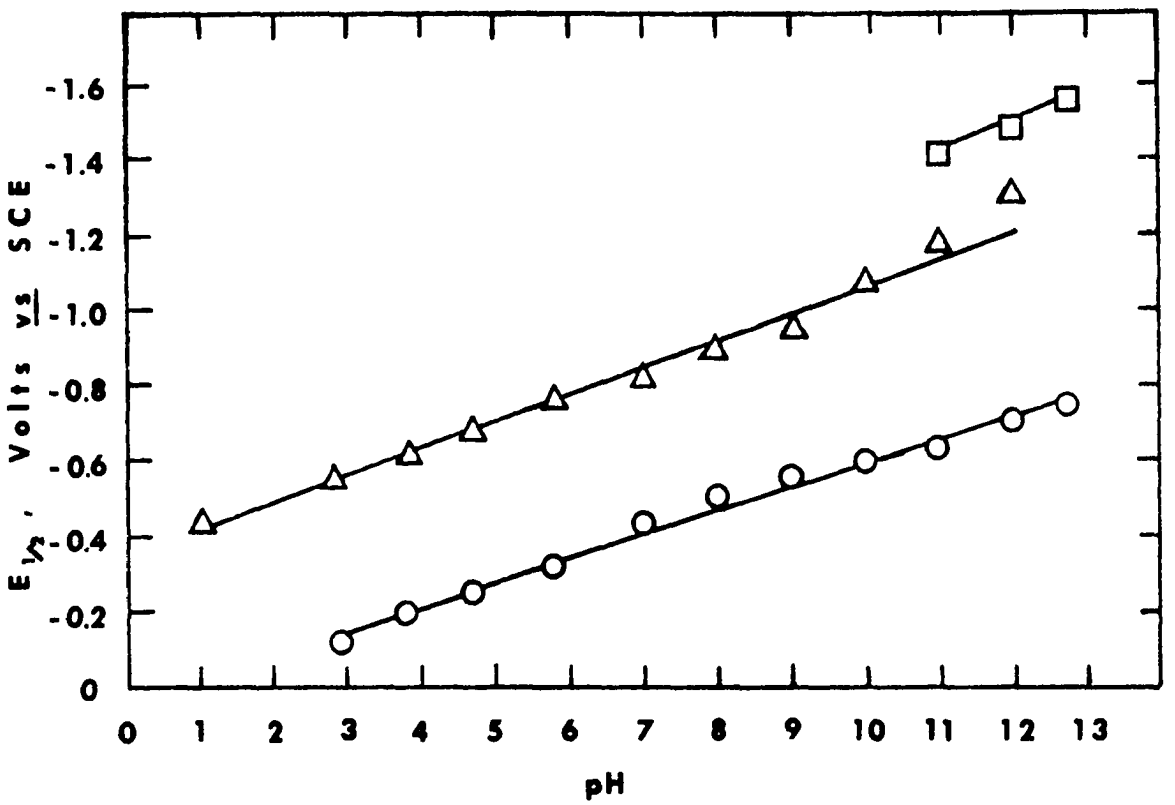

FIGURE 2-2. Variation of $E_{1/2}$ with pH for pteridine wave I (○——○), wave II (△——△), and wave III (□——□).

The variation of the diffusion current constant ($I = i_l/Cm^{2/3}t^{1/6}$) with pH is presented in Fig. 2-3. It should be noted that due to the slow chemical equilibria involved, I values at a given pH will change as a function of time. Therefore, values of I were measured at a specific time (5 min.) after preparation of pteridine test solutions.

The species responsible for each polarographic wave was readily established by comparison of the changes in polarography of pteridine at various pH as a function of time to the well known slow equilibria processes. For example, at pH 7.0 a freshly prepared solution of pteridine shows a well-defined wave at $E_{1/2}$ = -0.44 V (wave I) and a very small wave at $E_{1/2}$ = -0.82 V (wave II) (Fig. 2-4A). After about 15 minutes, however, wave I has decreased in height while wave II is somewhat larger (Fig. 2-4B). This behavior implies that wave I is due to the reduction of anhydrous pteridine, and wave II to the reduction of the 3,4-monohydrate. Similarly, in 1 M acetic acid (pH 2.3), pteridine shows a very small wave I and a much larger wave II (Fig. 2-5A). After a few minutes, wave II has decreased in height due to formation of the non-electroactive 5,6,7,8-dihydrate (Fig. 2-5B). Wave III was ascribed to reduction of the anion of the 3,4-hydrate. That these decreases in wave heights are due to equilibria and not decompositions can be shown, for example, by neutralization of a solution of pteridine in 1 M acetic acid (Fig. 2-5B) to pH 7. After several minutes, a polarogram of the equilibrium mixture of pteridine and the 3,4-hydrate is observed (i.e., a polarogram similar to Fig. 2-4B). Wave assignments are also supported by controlled potential coulometry.

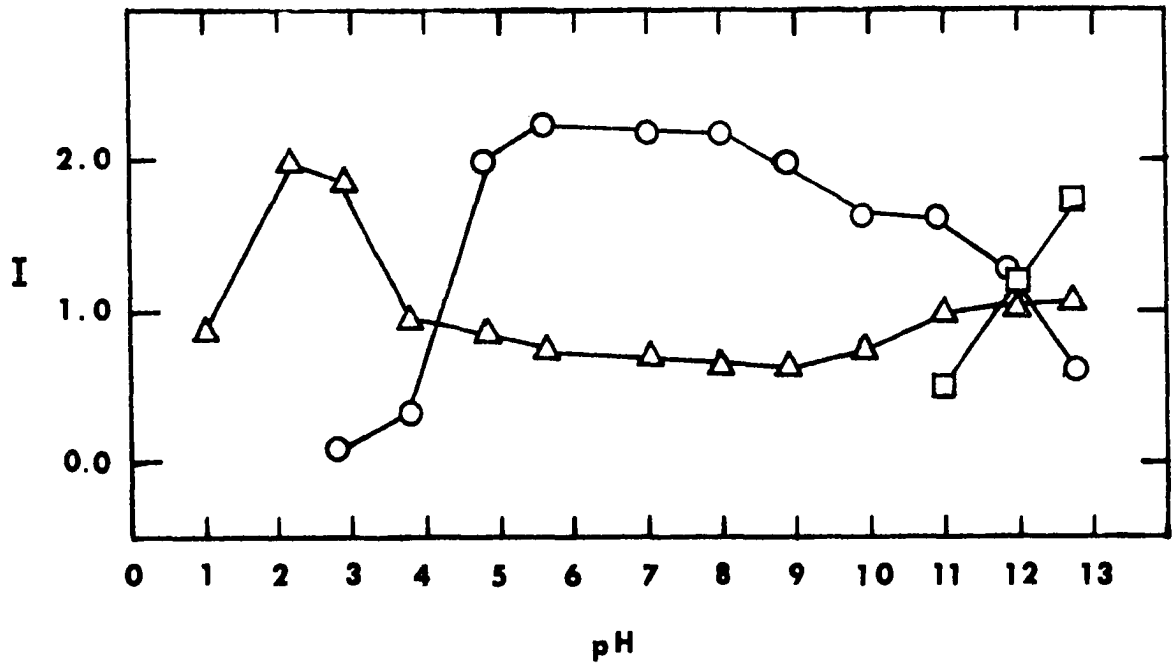

FIGURE 2-3. Variation of the diffusion current constant, I, with pH for pteridine wave I (○——○), wave II (△——△), and wave III (□——□).

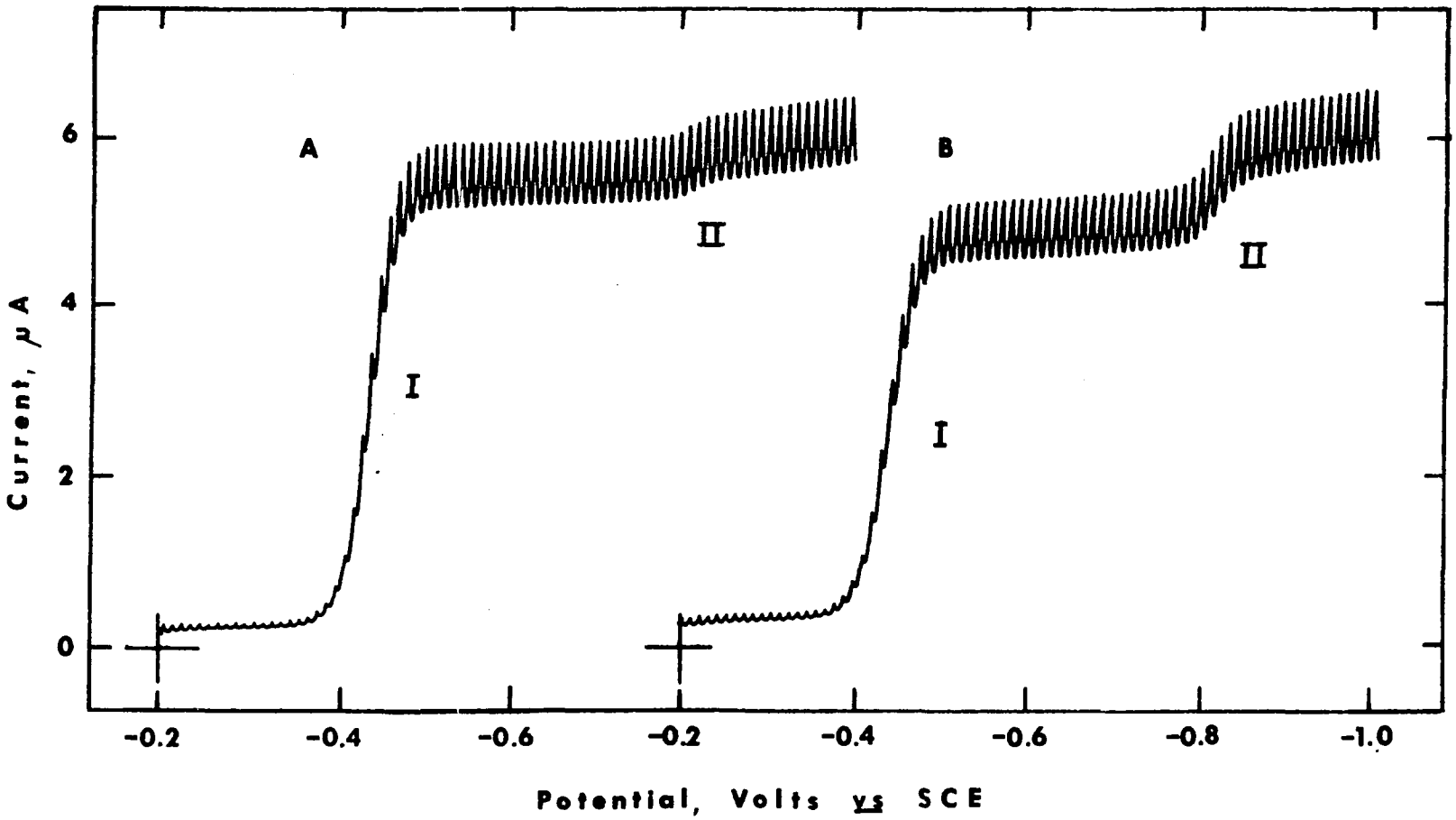

FIGURE 2-4. D.c. polarograms of pteridine (1 mM) in pH 7.0 McIlvaine buffer. (A) Immediately after dissolution, (B) After 15 minutes.

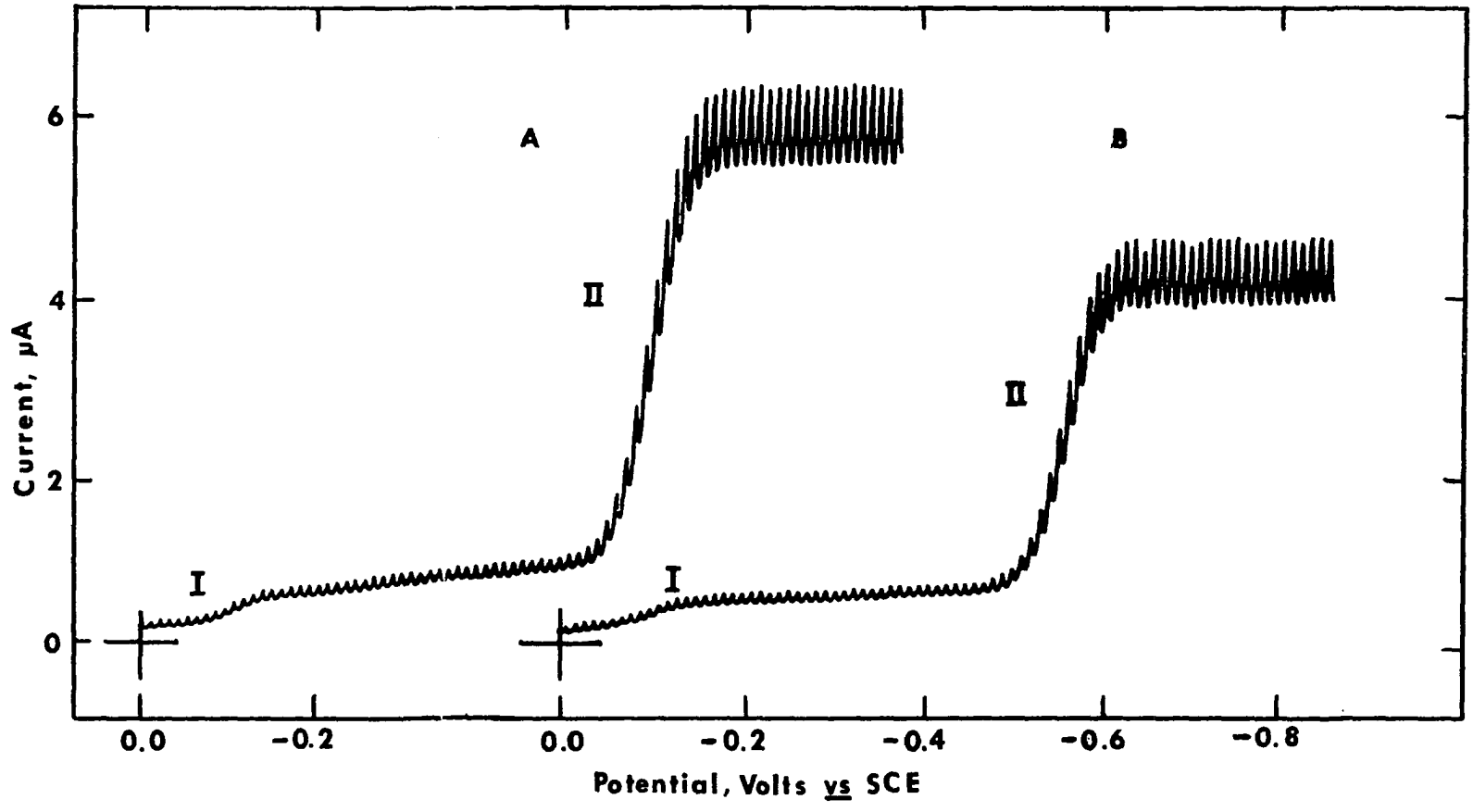

FIGURE 2-5. D.c. polarograms of pteridine (1 mM) in 1 M acetic acid. (A) Immediately after dissolution, (B) After 15 minutes.

Owing to the fact that at least two pteridine species are in equilibrium at any pH, values of I for waves I, II, or III did not allow definite conclusions regarding the number of electrons involved. However, over the pH range 2-13, the sum of I for waves I, II, and III at any pH ranges from 2 to 3, suggesting a 2 electron polarographic process. For reasons described below, the n-value for wave I was of particular interest, and was determined from polarographic data by the log plot method.[4] This method involves plotting potential, $(E + E_{1/2})$, as a function of log $(\frac{i}{i_1-i})$, over the rising portion of the polarographic wave, where

E = potential at any point on the wave

$E_{1/2}$ = half-wave potential, or potential at which $i = i_1/2$

i = current at potential E

i_1 = limiting current of polarographic wave

The evaluation is independent of concentration of electroactive species, and, in addition, allows conclusions to be drawn concerning the reversibility of the electrode process. For a reversible process the plot should be linear for values of the log term from -1.5 to 1.5. The n-values are determined from the slope of the plot. Theoretically, the slope should be $\frac{59}{n}$ mV at 25°C. Log plots at representative pH values for pteridine wave I are shown in Fig. 2-6. The linear nature of these plots suggests that the wave I process is electrochemically reversible (reversibility is supported by cyclic voltammetric experiments). The values of the slope for pH 7.1 (31.9 mV) and 8.1 (36.6 mV) are clearly indicative of n = 2, while the value for pH 10.8 (46.7 mV) is intermediate between that expected for n = 1 and n = 2.

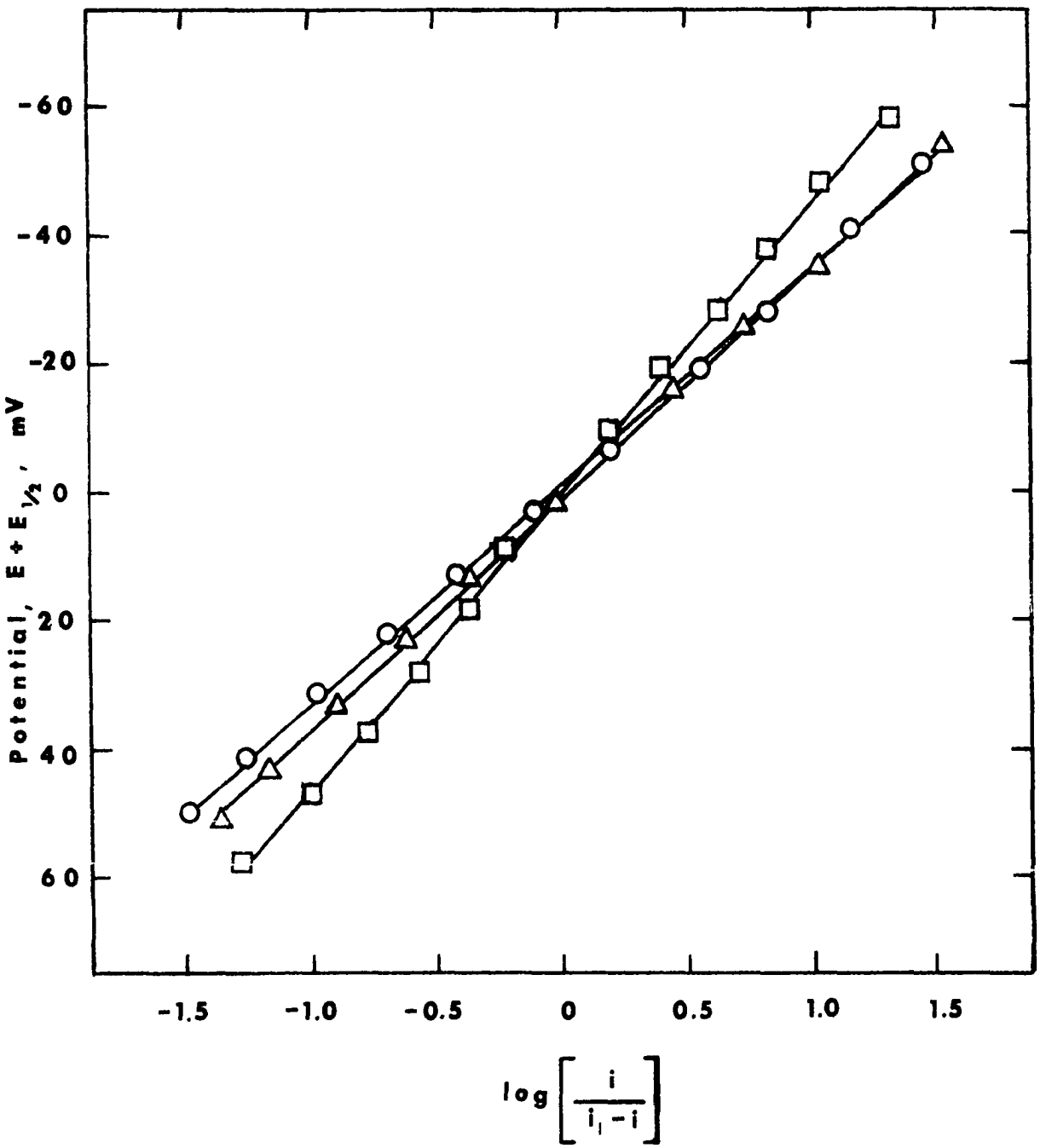

FIGURE 2-6. Log plots of pteridine wave I at pH 7.1 (○——○), pH 8.1 (△——△) and pH 10.8 (□——□).

The mercury column height dependence of the limiting current is indicative of diffusion control for waves I, II, and III at all pH values. That is, the term $i_l/h_{corr}^{1/2}$ is independent of mercury column height[5] (Table 2-1). Values of the temperature coefficient generally confirm diffusion control of polarographic wave height, falling within the range of 1-2%/°C, which is expected for a diffusion-controlled process[5] (Table 2-1). The somewhat higher value of the temperature coefficient at pH 2.8 for wave I probably reflects the small contribution of a kinetic process to wave I at this pH. At this pH, the kinetic process could clearly involve the equilibrium of the anhydrous molecule and the 3,4-hydrate (Fig. 2-1).

Cyclic and Linear Scan Voltammetry. In cyclic voltammetry, a triangular waveform of the type shown in Fig. 2-7A is applied to the electrode, and the current is monitored during the entire voltage sweep. Voltage sweep rates of from 10 mV sec^{-1} to 100 V sec^{-1} are usually employed, and the amplitude of the triangular wave is in the range of 0.5 - 3.0 V. The data are recorded on an x-y recorder or an oscilloscope. Since cyclic voltammograms are observed at stationary electrodes in quiet solution and the time internal between reverse sweeps is relatively short, products of a reduction, for example, are available at and near the electrode surface for oxidation on the positive-going segment of the voltage sweep. It is apparent, then, that a reversible charge-transfer process will show a cyclic voltammogram such as that in Fig. 2-7B. For a reversible system, the anodic and cathodic peaks are not at exactly the same potential, but a separation is theoretically predicted. It should be mentioned that $(i_p)_a$ as

TABLE 2-1

Effect of Mercury Column Height and Temperature on the Limiting Current of Pteridine

pH	Wave	$i_1/h_{corr}^{1/2}$, μA $cm^{-1/2}$ at indicated h_{corr} [a]				Temperature coefficient [b]
		31.4 cm	46.4 cm	61.4 cm	76.4 cm	
2.8	I	0.038	0.037	0.038	0.036	3.27
2.8	II	0.280	0.274	0.268	0.265	1.43
5.6	I	0.584	0.580	0.580	0.575	1.39
5.6	II	0.191	0.183	0.178	0.194	1.00
8.9	I	0.320	0.334	0.315	0.310	1.29
8.9	II	0.105	0.115	0.105	0.107	1.30
11.9	I	0.305	0.303	0.295	0.308	1.69
11.9	II	0.330	0.318	0.330	0.325	2.36
11.9	III	0.454	0.445	0.436	0.429	0.92

[a] $h_{corr} = h_{meas} - \frac{3.1}{(mt)^{1/3}}$

[b] $TC = [\frac{2.303}{T_2 - T_1} \log \frac{i_2}{i_1}] (100)$

where i_2 is the limiting current at T_2 (40°C) and i_1, the current at T_1 (25°C).

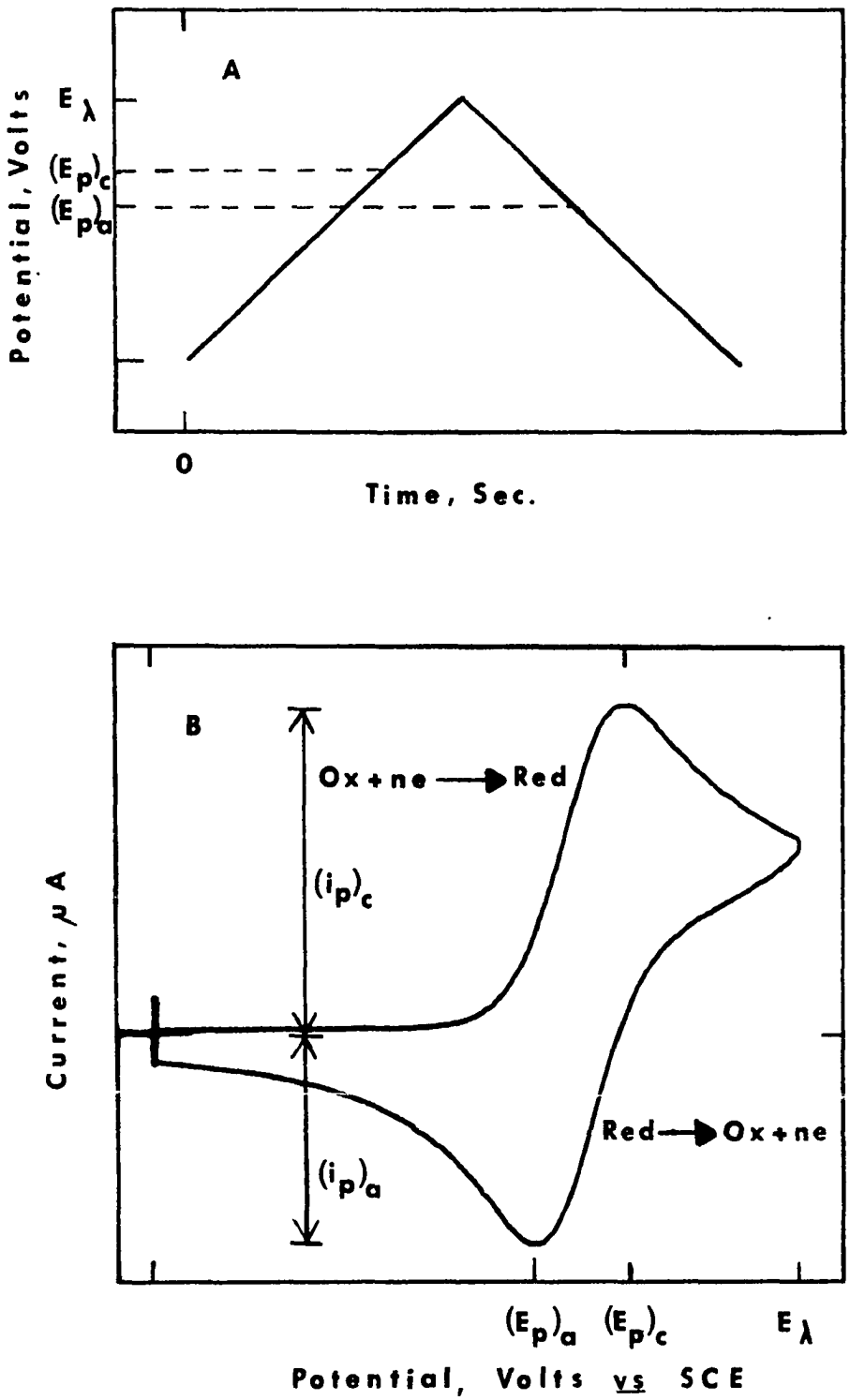

FIGURE 2-7. A. Triangular waveform for cyclic voltammetry, E_λ=switching potential; $(E_p)_c$=cathodic peak potential; $(E_p)_a$=anodic peak potential. B. Cyclic voltammogram for a reversible electrochemical reaction. $(i_p)_c$=cathodic peak current; $(i_p)_a$= anodic peak current.

depicted in Fig. 2-7B does not represent the total anodic current, but is a value which is sometimes used in calculations of homogeneous rate constants (see Appendix 2), and which is useful for purposes of illustration. To obtain the actual anodic current it is necessary to take into account the cathodic current which is flowing at $(E_p)_a$.

At both the pyrolytic graphite electrode (PGE) and the hanging mercury drop electrode (HMDE), pteridine exhibits three reduction peaks (I_c, II_c, III_c) corresponding to polarographic waves I, II, and III. No oxidation peaks are observed on the initial positive-going scan at a clean PGE. However, once having scanned peak I_c, and then sweeping toward more positive potentials, two anodic peaks are observed. One, peak I_a, occurs at potentials slightly positive of cathodic peak I_c, and the other, peak II_a, is observed at more positive potentials at the PGE (Fig. 2-8). The dependence of peak potentials upon pH for peaks I_c, II_c, III_c, I_a, and II_a are shown in Fig. 2-9. The variation of E_p with pH for the five peaks can be represented as follows:

peak I_c (pH 2-13)	$E_p = 0.005 - 0.068$ pH	(2-4)
peak II_c (pH 1-13)	$E_p = -0.33 - 0.079$ pH	(2-5)
peak III_c (pH 10-11)	$E_p = -0.38 - 0.108$ pH	(2-6)
peak I_a (pH 1-13)	$E_p = 0.12 - 0.071$ pH	(2-7)
peak II_a (pH 2-13)	$E_p = 1.08 - 0.080$ pH	(2-8)

At low pH (e.g., pH 2.8 McIlvaine buffer), if the initial scan at the PGE or HMDE is in the negative direction, a very small peak I_c is observed. If, after scanning past peak I_c, the sweep direction is reversed, a small peak I_a appears (Fig. 2-10A). If the negative-going sweep is continued after scanning past peak I_a, a large peak II_c,

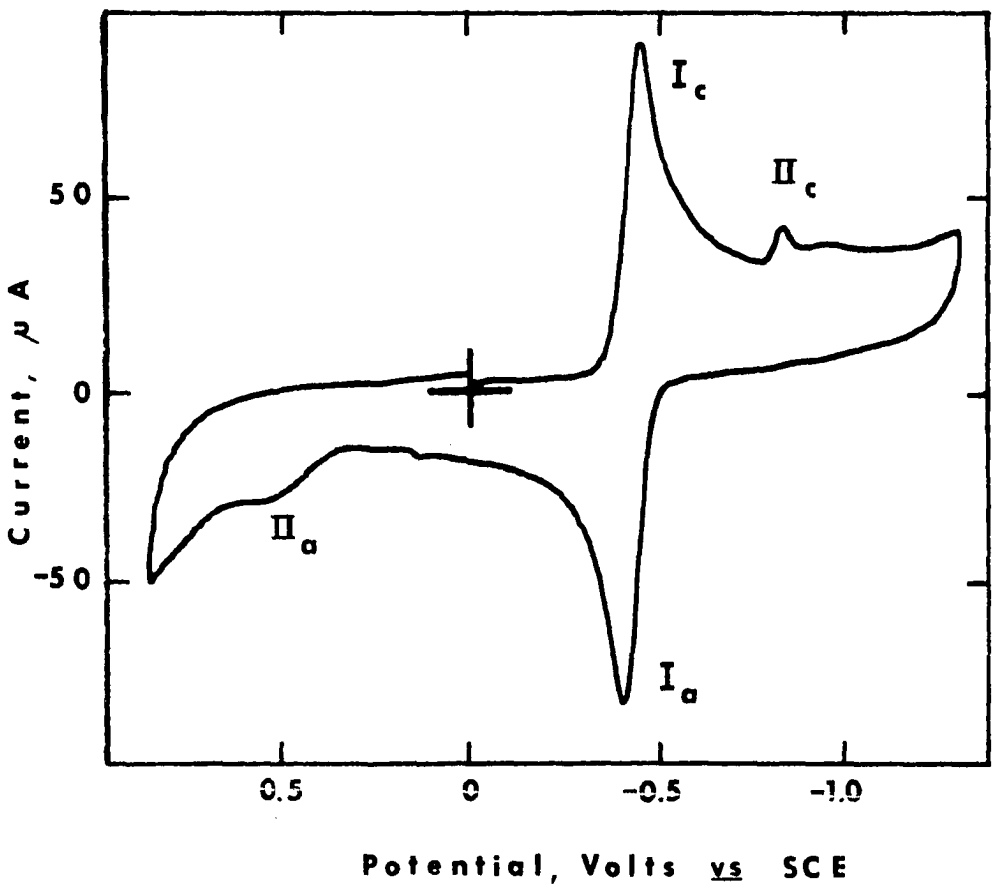

FIGURE 2-8. Cyclic voltammogram of 1 mM pteridine at pH 7.0 at the PGE. Potential scan pattern: 0.00 V → -1.30 V → +0.90 V → 0.00 V. Sweep rate 200 mV sec^{-1}.

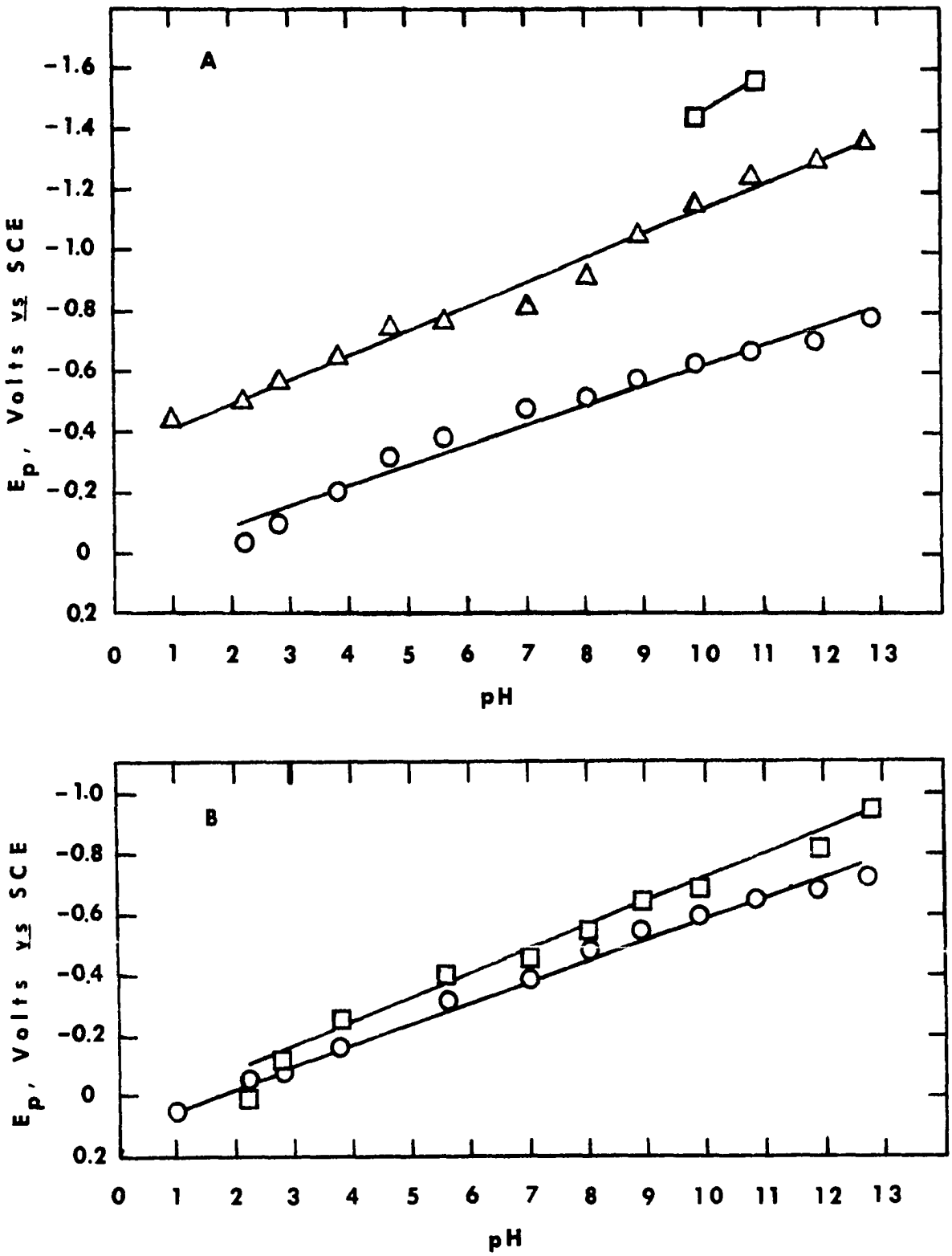

FIGURE 2-9. Variation of E_p with pH for pteridine at the PGE. A. Cathodic peak I_c (○—○), peak II_c (△—△), and peak III_c (□—□). B. Anodic peak I_a (○—○) and peak II_a (□—□); Left axis corresponds to peak I_a, right axis to peak II_a.

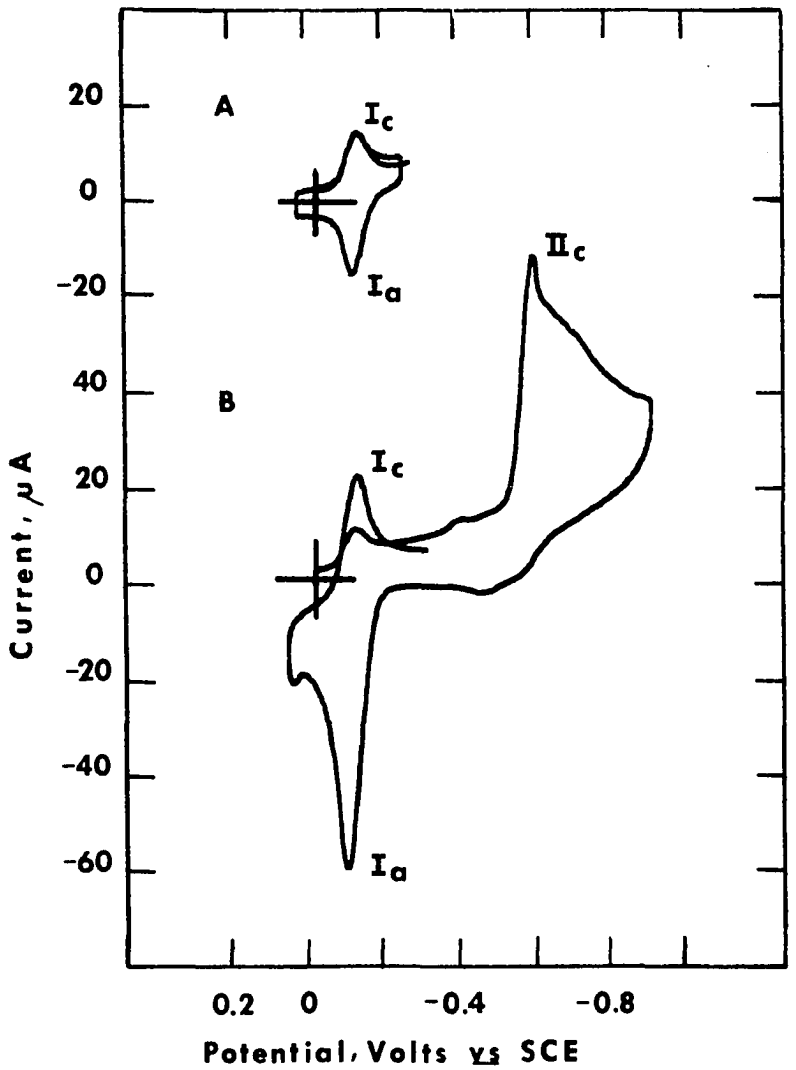

FIGURE 2-10. Cyclic voltammogram of 1 mM pteridine at the PGE in pH 2.8 McIlvaine buffer. Voltage sweep pattern (A) 0.00 → -0.23 V → 0.05 V → -0.23 V. (B) 0.00 V → -0.90 V → 0.05 V → -0.23 V. Voltage sweep rate, 100 mV sec^{-1}.

corresponding to the reduction of the 3,4-hydrate, is observed. If the sweep direction is reversed after scanning past peak II_c, a large peak I_a is observed. If after scanning past this peak, the scan is again reversed, peak I_c is much larger (Fig. 2-10B). This behavior implies that the initial electrode product of peaks I_c and II_c is the same and this product can be oxidized at peak I_a, producing pteridine or its cation.

D.c. polarography had indicated that the reaction responsible for polarographic wave I was an electrochemically reversible 2-electron process, and cyclic voltammetric experiments confirmed this. Theoretical calculations have shown that for a reversible system the potential increment between the cathodic and anodic peaks, at sweep rates slow with respect to the rate of electron transfer, will be[6,7]

$$(E_p)_a - (E_p)_c = \frac{59}{n} \text{ mV} \qquad (2\text{-}9)$$

where $(E_p)_a$ = anodic peak potential

$(E_p)_c$ = cathodic peak potential

n = number of electrons involved in electrode reaction.

Experimental peak separations for pteridine peaks I_a and I_c at the PGE and HMDE are shown in Table 2-2 for various sweep rates and pH values. In all cases the values are close to the theoretical 29 mV predicted by eq. (2-9) at slow sweep rates. As the sweep rate becomes fast relative to the rate of electron transfer, peak separations increase.

Nicholson[8] has shown that the separation of anodic and cathodic peak potentials can be used to measure the rate constant for electron

TABLE 2-2

Separation of Anodic and Cathodic Peak Potentials for Pteridine at Various Sweep Rates and pH Values at the PGE and HMDE. $\Delta E_p = (E_p)_a - (E_p)_c$

		ΔE_p (mV) at sweep rate (V sec^{-1})						
pH	Electrode	0.01	0.05	0.1	0.5	1.0	5.0	10.0
3.8	PGE	33	36	41	48	55	73	81
	HMDE	31	32	35	42	45	56	70
5.6	PGE	35	37	43	55	63	81	106
	HMDE	31	33	35	42	45	62	69
7.0	PGE	34	41	44	58	70	98	120
	HMDE	35	35	37	45	48	60	68
9.0	PGE	33	39	42	53	60	90	105
	HMDE	30	32	33	35	42	50	55
11.0	PGE	a	a	a	55	65	88	a
	HMDE	a	a	a	45	52	73	a

a = peak I_a not sufficiently well-defined.

transfer. Application of absolute rate theory to the electrode process and numerical solution of an integral equation provides a correlation of the separation in peak potentials ΔE_p with a function ψ given by

$$\psi = \gamma^{\alpha} \frac{k_s}{\pi^{1/2} D_o (nF/RT)^{1/2} v^{1/2}} \qquad (2\text{-}10)$$

where $\gamma = (\frac{D_o}{D_R})^{1/2}$

D_o = diffusion coefficient of oxidized species, $cm^2\ sec^{-1}$

D_R = diffusion coefficient of reduced species, $cm^2\ sec^{-1}$

α = electron transfer coefficient

k_s = heterogeneous rate constant for electron transfer at $E=E^\circ$

n = number of electrons involved in reaction

F = 96,500 coulombs

R = gas constant = 8.31 joules $deg^{-1}\ mol^{-1}$

T = absolute temperature

v = voltage sweep rate, Volts sec^{-1}

Since D_o is usually approximately equal to D_R, γ^{α} can be taken as unity. The variation of ψ with ΔE_p is presented in tables and working curves in ref. 8. To determine k_s, ΔE_p is measured at sweep rates at which the system shows peak separation in excess of reversible behavior, and ψ is determined from the tables or working curve. Since all other parameters are known, k_s can then be calculated from eq. (2-10). Rate constants are given in Table 2-3, and a sample calculation is included in Appendix 2.

The involvement of 2 electrons in the peak I_c process is also supported by comparison of experimental and theoretical peak currents. For an uncomplicated perfectly reversible electrode reaction, the peak

TABLE 2-3

Heterogeneous Rate Constants (k_s) for Pteridine Wave I at the PGE and HMDE.[a]

pH	k_s HMDE[b]	k_s PGE[c]
3.8	3.3×10^{-2}	1.7×10^{-2}
5.6	2.7×10^{-2}	1.2×10^{-2}
7.0	2.5×10^{-2}	1.0×10^{-2}
9.0	3.6×10^{-2}	1.3×10^{-2}
11.0	2.0×10^{-2}	1.1×10^{-2}

[a] Voltage sweep rate 1 V sec^{-1}. Pteridine concentration, 1 mM.
[b] Hanging mercury drop electrode, area = 0.022 cm^2.
[c] Pyrolytic graphite electrode, area = 0.12 cm^2.

current is given by[9]

$$i_p = 2.69 \times 10^5 \, AD^{1/2}v^{1/2}n^{3/2}C \qquad (2\text{-}11)$$

where i_p = peak current, μA

A = electrode area, cm^2

D = diffusion coefficient of electroactive substance, cm^2 sec^{-1}

v = sweep rate, V sec^{-1}

n = number of electrons involved in electrode reaction

C = bulk concentration of electroactive species, mM.

Peak currents calculated using eq. (2-11) are tabulated with experimental peak currents in Table 2-4. It is obvious from Table 2-4 that the agreement between theoretical and experimental values is quite good, indicating that the voltammetric peak currents observed are consistent with a 2e process.

Studies of the cyclic voltammetry of pteridine as a function of

TABLE 2-4

Comparison of Experimental and Theoretical Peak Currents for Pteridine Peak I_c.[a]

	Peak current, μA			
	pH 7		pH 8	
v, Volts sec^{-1}	Experimental	Theoretical	Experimental	Theoretical
0.01	3.60	3.67	3.84	3.67
0.02	5.10	5.15	5.46	5.15
0.05	8.18	8.20	8.90	8.20
0.10	11.55	11.60	12.70	11.60
0.20	16.70	16.40	18.25	16.40
0.50	26.00	25.50	28.00	25.50
1.00	35.00	36.70	40.00	36.70

[a] At the HMDE, area = 0.022 cm^2, pteridine concentration, 1.00 mM, n = 2, $D^{1/2} = 2.05 \times 10^{-3}$.

voltage sweep rate and also as a function of pH disclosed variation in the relative magnitude of currents for peak I_c and peak I_a with changing pH and sweep rate. That is, at low sweep rate the value of the ratio $(i_p)_c/(i_p)_a$, where $(i_p)_c = I_c$ peak current and $(i_p)_a = I_a$ peak current, was much larger than at faster sweep rates (Fig. 2-11). Also, the ratio $(i_p)_c/(i_p)_a$ was larger at high pH than at lower pH, at constant sweep rate (Fig. 2-12). This behavior indicates that during the time of the cyclic voltammetric experiment, a portion of the initial electrode reduction product has reacted to form an electroinactive species, which cannot be electrochemically oxidized on the reverse sweep. This reaction could be one of several types: (1) a chemical reaction followed by a secondary electrochemical reaction, (2) a decomposition of the initial electrode product, (3) reaction of the electrode product with solvent or supporting electrolyte, (4) dimerization of the electrode product,

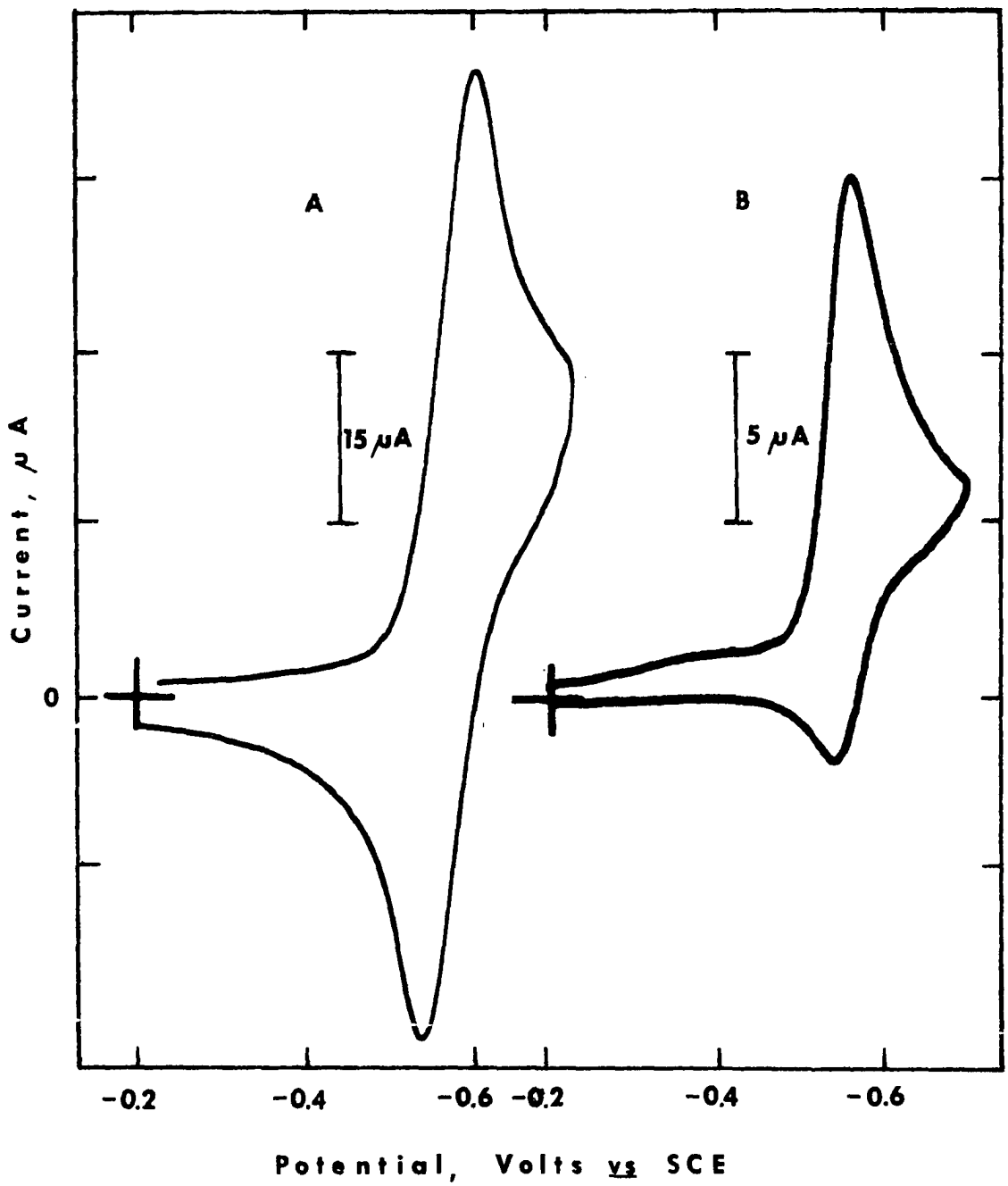

FIGURE 2-11. Cyclic voltammograms of 1 mM pteridine in pH 9.0 borax buffer at the PGE. Sweep rate (A) 200 mV sec^{-1}, (B) 10 mV sec^{-1}.

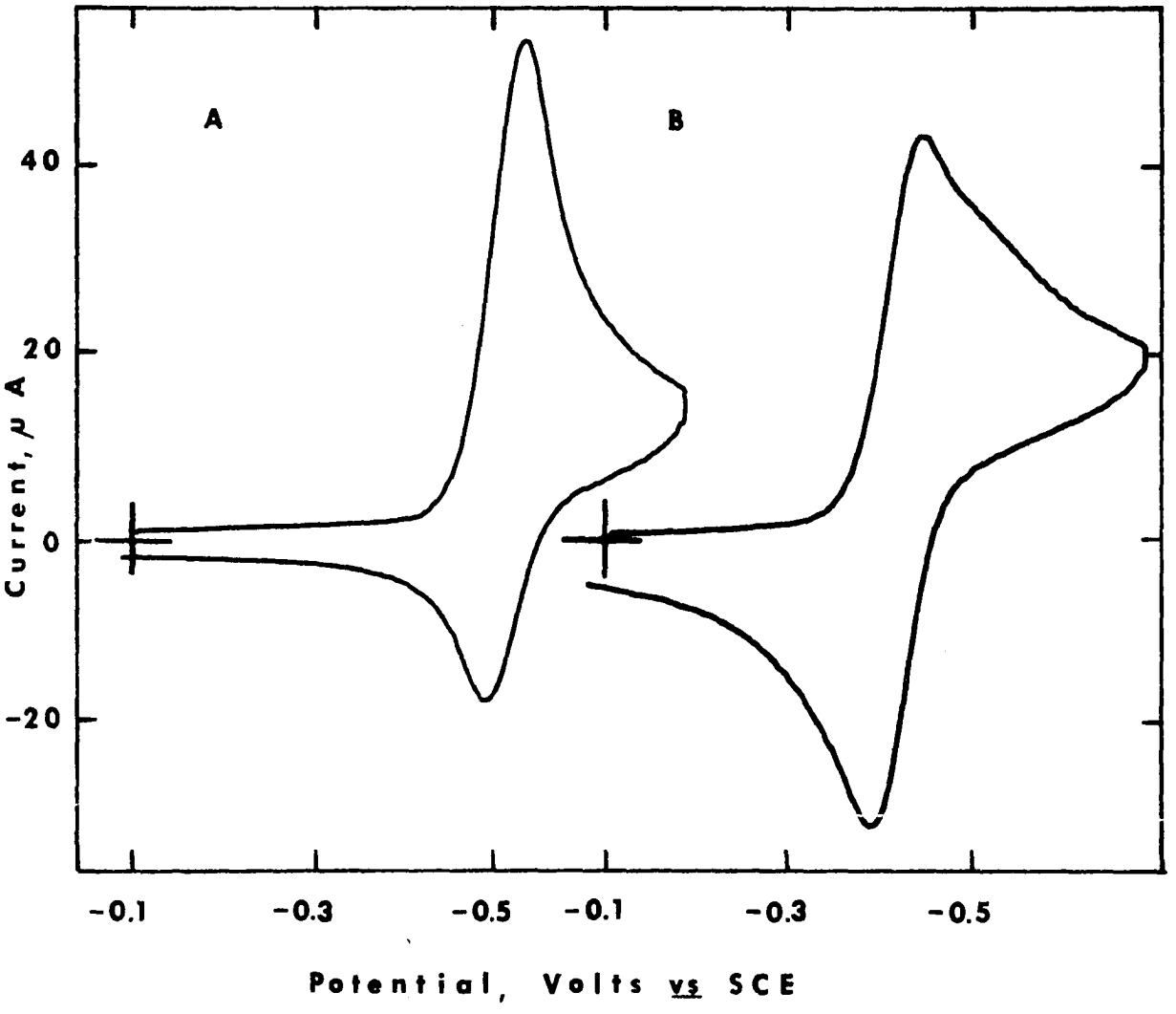

FIGURE 2-12. Cyclic voltammograms of 1 mM pteridine in (A) pH 10.0 borax buffer and (B) pH 7.0 McIlvaine buffer, at the PGE. Sweep rate 100 mV sec^{-1}.

or (5) reaction of the electrode product with starting material.

The possibility of a secondary electrochemical reaction was eliminated by a study of the variation of the peak current for peak I_c with voltage sweep rate. According to eq. (2-11) $i_p/v^{1/2}$ should remain constant with changes in v. However, if the initial electrode reaction is followed by a chemical reaction which is then followed by another electrochemical reaction (i.e., an ECE mechanism), it has been shown that $i_p/v^{1/2}$ should decrease with increasing voltage sweep rate.[10] In the present case (Table 2-5) $i_p/v^{1/2}$ for peak I_c was constant at pH 7 and pH 8, indicating that no secondary electrochemical reaction is involved. At pH 9 and pH 10 the value of $i_p/v^{1/2}$ is somewhat lower at slow sweep rates. An explanation of this observation is presented later.

A study of the effect of pteridine concentration upon the cyclic voltammograms revealed that the reaction following the initial electron transfer occurred much more rapidly at high pteridine concentrations. At the same voltage sweep rate, the height of peak I_a relative to peak I_c was much less at a pteridine concentration of, for example, 2 mM than at 0.2 mM. This information implies that the reaction is second order in pteridine, and eliminates possibilities (2) and (3) which would be first order and pseudo first order, respectively. On the basis of coulometric evidence (vide infra) it was concluded that the reaction is best represented by (5) above. The mechanism for such a reaction can be written as (reaction scheme A):

$$Ox + ne \rightleftharpoons Red \qquad (2\text{-}12)$$

TABLE 2-5

Variation of $i_p/v^{1/2}$ as a Function of $v^{1/2}$ for Voltammetric Peak I_a of Pteridine[a]

v, V sec^{-1}	$v^{1/2}$, $V^{1/2}$ $sec^{-1/2}$	$i_p/v^{1/2}$, $\mu AV^{-1/2}$ $sec^{1/2}$			
		pH 7	pH 8	pH 9	pH 10
0.01	0.1	36.0	38.4	31.7	23.4
0.02	0.141	36.2	38.7	32.1	24.1
0.05	0.224	36.5	39.5	34.2	27.6
0.10	0.316	36.5	40.2	35.7	29.8
0.20	0.447	37.4	40.8	36.0	32.6
0.50	0.707	36.8	39.6	36.8	33.9
1.0	1.0	35.0	40.0	37.0	35.0
2.0	1.41	34.0	36.9	36.8	35.4
5.0	2.24	33.9	35.7	37.5	38.0
10.0	3.16	34.8	38.0	38.0	39.6

[a] At the HMDE, area 0.022 cm^2, pteridine concentration 1 mM.

$$\text{Red} + \text{Ox} \xrightarrow{k_2} \text{Z} \qquad (2\text{-}13)$$

where the electron transfer is reversible (eq. 2-12) and Ox, Red and Z are soluble in the solution phase. The homogeneous reaction (eq. 2-13) is irreversible and is characterized by a rate constant k_2, and the product, Z, is electroinactive. The isolation of a dimeric product (vide infra) provides additional support for the above mechanism.

As was stated earlier, the reaction (eq. 2-13) occurs more rapidly at higher pH. Thus at pH 9 and 10, the reaction of electrode product with starting material is quite fast, and at slow sweep rates, decreases the amount of pteridine available for reduction at and near the electrode surface, causing the quality $i_p/v^{1/2}$ (Table 2-5) to be lower than at pH 7 or 8. At fast sweep rates, however, the voltammetric experiment is complete before a significant amount of starting material can react, leading to higher values of $i_p/v^{1/2}$.

Nicholson and Shain have developed methods for calculating rate constants of chemical reactions following reversible electron transfer processes based upon the variation in $(i_p)_a/(i_p)_c$ as a function of sweep rate.[9,11,12] Specifically, the reaction scheme (B):

$$\text{Ox} + ne \rightleftharpoons \text{Red} \qquad (2\text{-}14)$$

$$2\ \text{Red} \xrightarrow{k_2} \text{Z} \qquad (2\text{-}15)$$

was assumed to be operative. Although the reaction scheme (A) represented by eq. (2-12) and (2-13) was not discussed by the latter workers, the application of the treatment of Nicholson and Shain to the present case (eq. 2-12, 2-13, scheme A) seemed justifiable because of the similarity of the mechanism to that studied by Nicholson and Shain (eq. 2-14, 2-15). The major difference in the cyclic voltammetry of

the reaction scheme (A) and (B) should be a decrease in the values of cathodic peak current, $(i_p)_c$, at slow sweep rates and relatively large values of k_2 in scheme (A) because of reaction of Red with Ox diffusing to the electrode, causing a decrease in the amount of Ox available for reduction. As a consequence of this, however, the amount of Red produced would decrease causing a decrease in $(i_p)_a$, and the ratio $(i_p)_a/(i_p)_c$ (from which k_2 is calculated) should remain essentially constant. Because of the lack of rigor in the application of the Nicholson and Shain treatment to the present case, the absolute values of k_2 remain questionable. However, for comparative purposes (e.g., variation in reaction rate with pH) the calculated values of k_2 are certainly useful.

Nicholson and co-workers[11] developed an equation relating the kinetic terms k_2 and v through ψ, the kinetic parameter:

$$\psi = \frac{k_2 CRT}{nFv} \qquad (2\text{-}16)$$

where k_2 = homogeneous rate constant for dimerization

v = voltage sweep rate, V sec^{-1}

and the remaining terms have their usual significance.

It was shown that the anodic portion of the cyclic voltammogram was most sensitive to the rate of dimerization, and this is easy to see intuitively. The amount of Red in the vicinity of the electrode, available for oxidation on the anodic portion of the cyclic voltammogram, and thus the anodic peak current, depends upon k_2 and upon the time which has elapsed since the initial generation of Red. This time depends upon the voltage sweep rate and the potential at which the

voltage sweep is reversed and is specified as:

$$\tau = \frac{(E_\lambda - E^\circ)}{v} \qquad (2\text{-}17)$$

where τ = time from E° to E_λ, sec.

E_λ = switching potential (Fig. 2-7A)

E° = standard potential of the couple (i.e., potential at which $i = 0.85\ (i_p)_c$)[9]

v = voltage sweep rate, V sec^{-1}

A number of cyclic voltammograms were calculated by Nicholson et al[11] for several values of ψ and at constant switching potential, $(E_\lambda - E^\circ)n$. For each voltammogram the ratio $(i_p)_a/(i_p)_c$ was evaluated and plotted against the quantity $\log (\psi a\tau) = \log (k_2 C\tau)$

where $$a = \frac{nFv}{RT} \qquad (2\text{-}18)$$

and $$a\tau = \frac{nF}{RT}(E_\lambda - E^\circ) \qquad (2\text{-}19)$$

This plot is reproduced in Fig. 2-13, and the values used in constructing the plot are presented in Table 2-6.[11] By comparison of an experimentally determined $(i_p)_a/(i_p)_c$ with Fig. 2-13, it is possible to obtain a value for $\log (k_2 C\tau)$, and, since C and τ are known, to calculate k_2. Experimental values of $(i_p)_a/(i_p)_c$ and k_2 are given in Table 2-7. The relationship between k_2 and pH can be expressed mathematically as

$$k_2 = \frac{k'}{[H^+]^{1/2}} \qquad (2\text{-}20)$$

where $k' = 1.5 \times 10^{-2}$. The significance of this equation is questionable, especially in view of the uncertainty in the values of k_2. The most significant fact would seem to be simply that k_2 increases with pH.

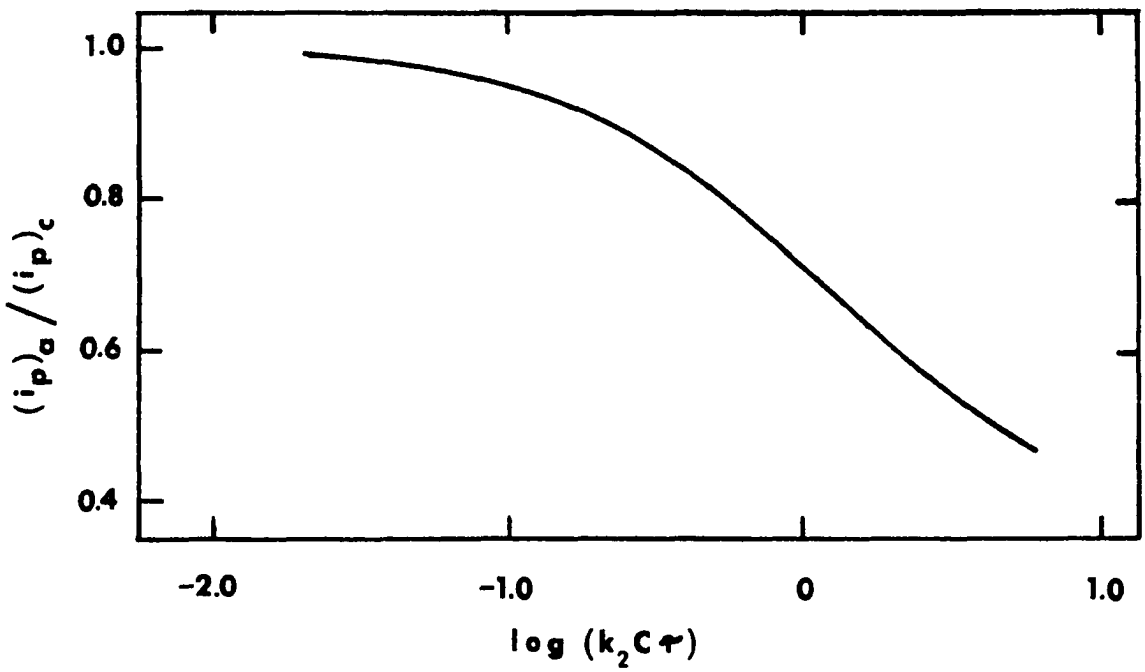

FIGURE 2-13. Variation of $(i_p)_a/(i_p)_c$ with log $(k_2 C\tau)$ for $a\tau = 4$.

TABLE 2-6

Variation of $(i_p)_a/(i_p)_c$ with $k_2 C\tau$, for $a\tau = 4$

$k_2 C\tau$	$(i_p)_a/(i_p)_c$	$k_2 C\tau$	$(i_p)_a/(i_p)_c$
0.02	0.99	0.60	0.78
0.04	0.98	0.90	0.73
0.06	0.97	1.30	0.67
0.10	0.95	1.90	0.61
0.16	0.92	2.70	0.56
0.25	0.89	4.00	0.51
0.40	0.84	6.00	0.47

TABLE 2-7

Values of $(i_p)_a/(i_p)_c$ and k_2 for Pteridine at the HMDE[a]

pH	v, V sec^{-1}	$(i_p)_a/(i_p)_c$	k_2, M^{-1} sec^{-1}
7.0	0.01	0.844	7.4 x 10
	0.02	0.932	5.1 x 10
8.0	0.01	0.814	1.1×10^2
	0.02	0.895	1.0×10^2
	0.05	0.980	1.1×10^2
9.0	0.01	0.658	3.2×10^2
	0.02	0.767	2.8×10^2
	0.05	0.921	1.6×10^2
9.9	0.05	0.646	1.7×10^3
	0.10	0.775	1.4×10^3
	0.20	0.895	1.0×10^3
11.0	0.20	0.630	7.7×10^3
	0.50	0.812	5.3×10^3
11.8	2.00	0.814	2.0×10^4

[a] Electrode area 2.22 mm^2, pteridine concentration 1 mM, $(E_\lambda - E^\circ)$ = 50 mV.

A sample calculation of k_2 is presented in Appendix 2.

Controlled Potential Electrolysis and Coulometry. Because of the many possible forms of pteridine in aqueous solution (Fig. 2-1), it is necessary to choose carefully the conditions for controlled potential electrolysis to ensure that a single species is available to react at the electrode surface at the desired potential. For example, electrolysis on the plateau of wave II at pH 7 (Fig. 2-4) would result in reduction of both non-hydrated pteridine and the 3,4-hydrate. For this reason, electrolysis on wave II must be carried out at low pH (2-3) where essentially all of the pteridine is in the form of the 3,4-hydrate. On the other hand, electrolysis of wave I can be performed at almost any pH, except low pH. Since the concentration of non-hydrated pteridine at pH 2-3 is very low, and the equilibrium between the non-hydrated form and the 3,4-hydrate is slow, electrolysis of wave I at this pH proceeds very slowly.

Electrolysis of pteridine on the plateau of wave I at the mercury pool electrode results in the transfer of one electron (Table 2-8). This is rather surprising in view of the n-value of 2 which was obtained from polarographic and voltammetric data. The only apparent explanation is that the initial reaction product resulting from the transfer of 2 electrons reacts with starting material (pteridine) on a 1:1 basis forming an electroinactive (at this potential) compound. Upon completion of the electrolysis the solution showed two polarographic waves, one (wave IV) at a potential slightly negative of pteridine wave II, and another smaller very poorly defined wave (wave V) at more negative potential (Fig. 2-14). The $E_{1/2}$ of both wave IV and V

TABLE 2-8

Coulometric Determination of the Number of Electrons Involved in the Reduction of Pteridine on the Plateau of Polarographic Wave I[a]

Background	pH	Controlled Potential[b]	n-value
McIlvaine	3.6	-0.30	1.06
McIlvaine	3.6	-0.30	0.97
McIlvaine	4.7	-0.40	1.01
McIlvaine	4.7	-0.40	0.97
Acetate	6.0	-0.60	1.14
Acetate	6.0	-0.60	1.15
McIlvaine	7.0	-0.60	1.01
McIlvaine	7.0	-0.60	1.06
McIlvaine	8.0	-0.60	1.00
McIlvaine	8.0	-0.60	1.07
Ammonia	8.9	-0.60	0.94
Ammonia	8.9	-0.60	0.93
Hydroxide/Chloride	11.9	-1.00	0.95
Hydroxide/Chloride	11.9	-0.80	0.90

[a] At a mercury pool electrode area ≈ 16 cm^2. Pteridine concentration approximately 1 mM in all cases.

[b] Volts vs SCE.

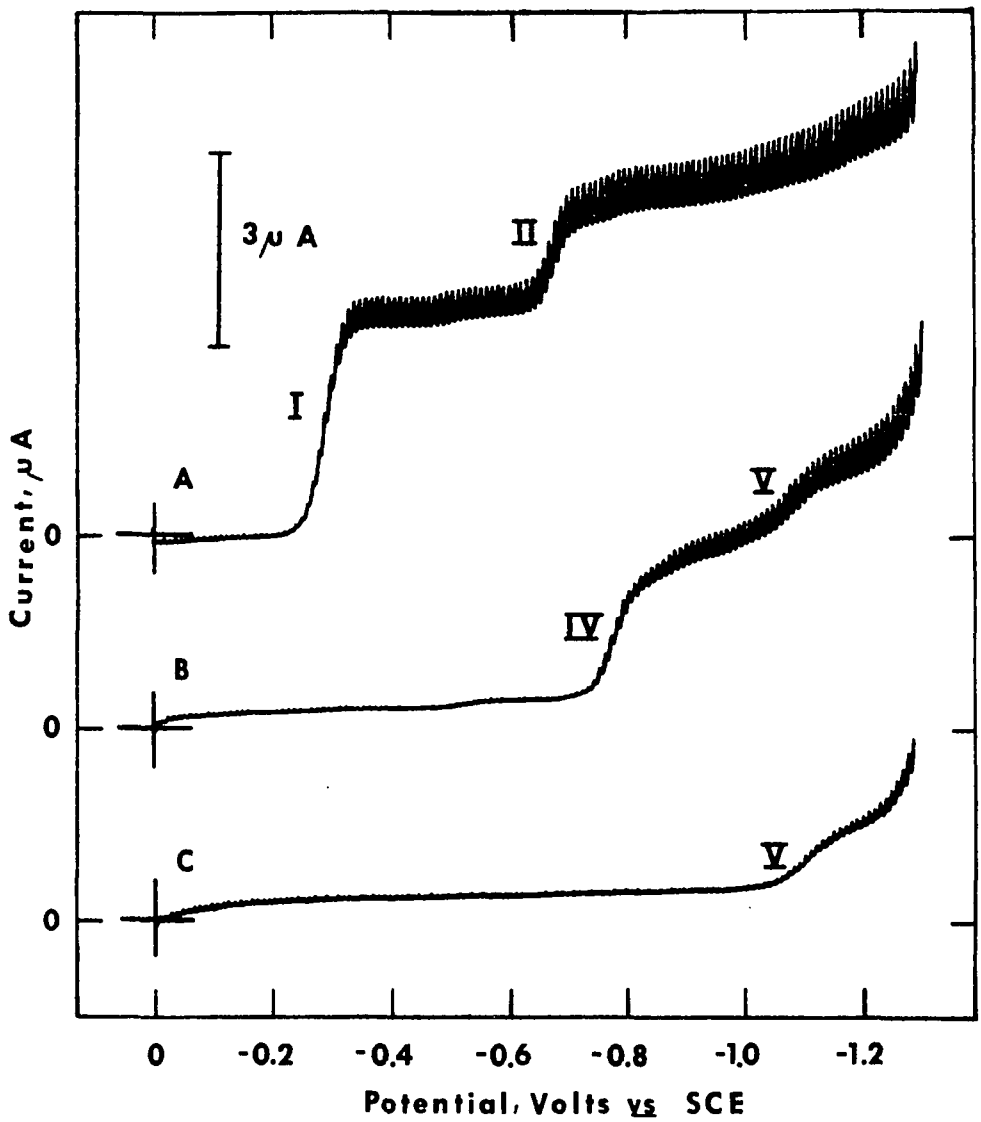

FIGURE 2-14. Polarograms of a 1 mM solution of pteridine at pH 4.7 (A) Before electrochemical reduction (B) After reduction at -0.45 V, and (C) After reduction at -1.00 V.

shift linearly to more negative potential with increasing pH (Fig. 2-15A); wave IV (pH 2.3-12), $E_{1/2}$ = -0.48 - 0.068 pH; wave V (pH 2.3 - 8), $E_{1/2}$ = -0.80 - 0.055 pH. Wave V is not observed if the electrolysis is carried out above pH 8. Also after electrolysis, an oxidation peak is observed at the PGE; E_p = 0.76 - 0.034 pH (Fig. 2-15B). The UV spectrum of the electrolysis product (λ_{max} = 307 nm at pH 4.7, 308 nm and 263 nm at pH 7) was quite different to that of pteridine (λ_{max} = 309 nm and 298 nm at pH 7) (Fig. 2-16A,B). At every pH, electrolysis at potentials corresponding to wave I resulted in the disappearance of wave II.

Electrolysis of pteridine at wave II always resulted in identical electron numbers and products as electrolysis at wave I. However, due to the proximity of wave II to the wave remaining after electrolysis (wave IV, Fig. 2-14, 2-15), it is necessary to select the electrolysis potential very carefully at about the $E_{1/2}$ for wave II rather than on the plateau. These results support the findings from cyclic voltammetry which indicated that the wave I and wave II products are identical.

After electrolysis on wave I or II, electrolysis on the plateau of wave IV results in the transfer of one electron, based on the amount of pteridine initially present. The diffusion current for wave IV, when compared to the diffusion current for wave I (previously shown to be a 2e process under polarographic conditions) is about half as large, indicating a 1e process for wave IV. Analysis of wave IV by the log plot method indicates that the electrode process is irreversible (i.e., the plot is not linear over the range of the log term from

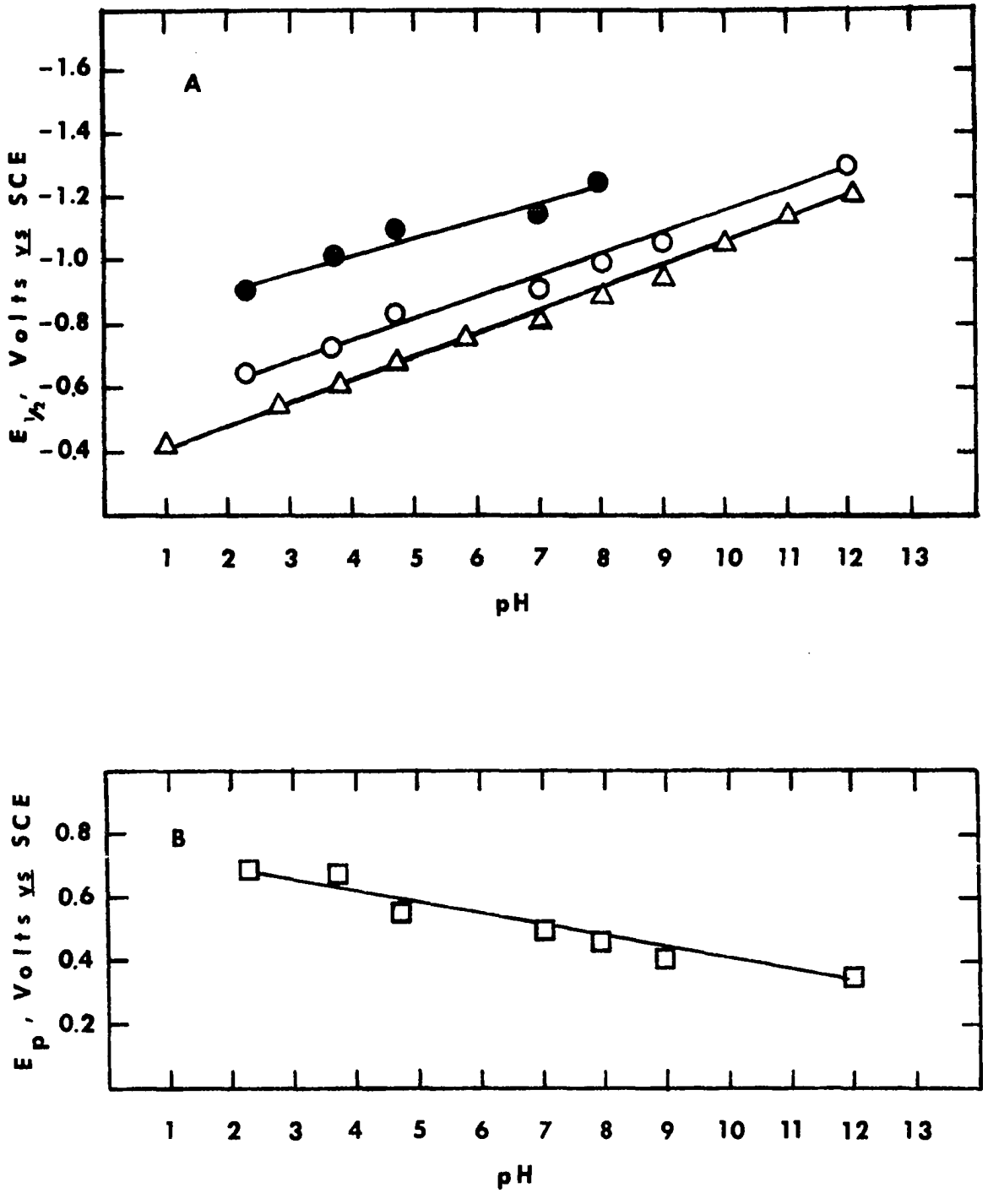

FIGURE 2-15. Dependence of $E_{1/2}$ and E_p upon pH for (A) pteridine wave II (△——△), wave IV (○——○), and wave V (●——●) and (B) the oxidation peak observed at the PGE after reduction of pteridine (□——□).

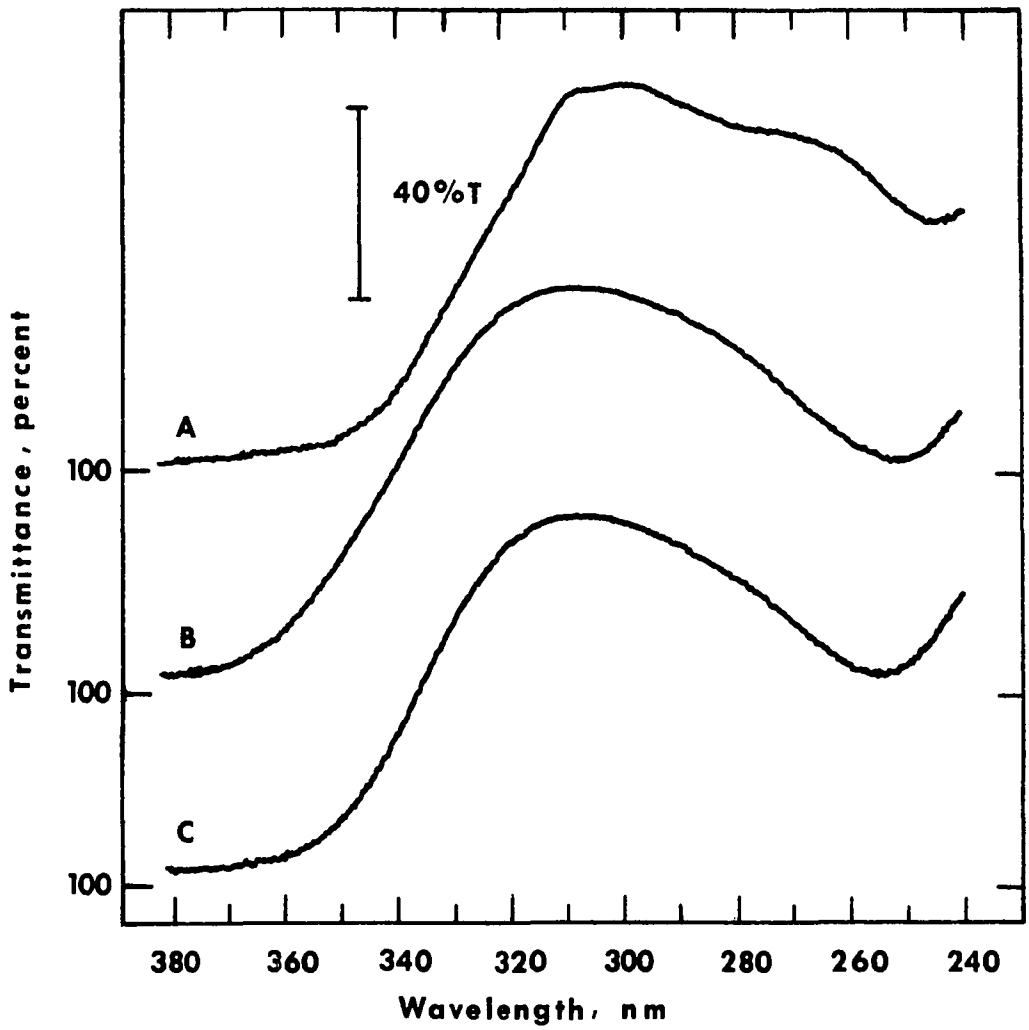

FIGURE 2-16. Ultraviolet spectra recorded during the electrochemical reduction of 1 mM pteridine solution at pH 4.7. (A) Before reduction, (B) After reduction at -0.45 V, and (C) After reduction at -1.00 V. The electrolysis solution was diluted to 0.1 mM with pH 4.7 buffer before the spectra were recorded.

-1.5 to 1.5, vide supra) (Fig. 2-17). In addition, a reversible couple is not observed via cyclic voltammetry at the hanging mercury drop electrode. As for the case of reversible system, the number of electrons involved in an irreversible electrochemical process may be estimated from the slope of the log plot, although a different approach is required for the irreversible case.

For an irreversible electrode reaction:[15]

$$\frac{d(E+E_{1/2})}{d[\log(\frac{i}{i_l-i})]} = -\frac{54.2}{\alpha n_a} \text{ mV} \qquad (2\text{-}21)$$

where α = electron transfer coefficient

n_a = number of electrons involved in the rate-controlling step of the reaction

and the remaining terms have the significance previously stated. At pH 7, αn_a for pteridine wave IV, calculated from the slope of the log plot (Fig. 2-17) and equation (2-21), is 0.98. Since in most cases α is approximately 0.5,[15] n_a must have a value of 2.

The apparent contradiction between the coulometric n-value for wave IV and the n-value obtained from the log plot is easily explained if the compound responsible for wave IV is a form of pteridine dimer. In this case, if the number of electrons transferred per molecule of dimer is 2, as the log plot indicates, the n-value calculated on the basis of pteridine originally present will be 1. Also, since the molar concentration of dimer is one-half the original pteridine concentration, the polarographic diffusion current will be approximately half as large as the diffusion current for the original pteridine.

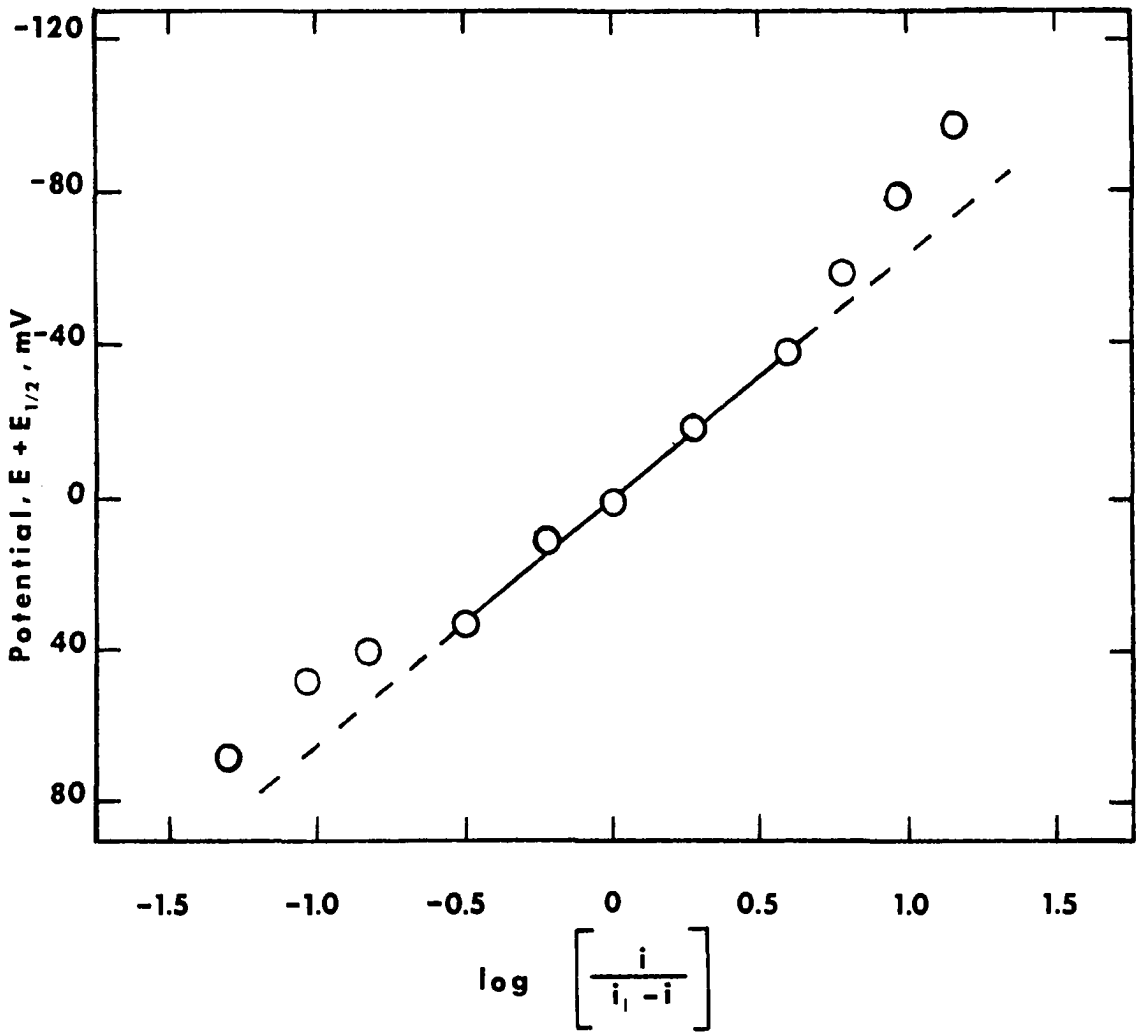

FIGURE 2-17. Log plot for pteridine wave IV at pH 7.0.

Following reduction at a potential corresponding to the plateau of wave IV, only polarographic wave V is observed (Fig. 2-14C), and the oxidation peak at the PGE remains essentially unchanged (Fig. 2-18). The wavelength of the UV absorption maximum is also unchanged, but the absorbance decreased by about 25 percent (Fig. 2-16C).

Reduction on the plateau of wave V, after first having removed waves I, II, and IV, results in fractional n-values (0.2 - 0.3). No change is noted in the UV spectrum after electrolysis.

Electrolysis of pteridine on the plateau of wave III at pH 12 results in the transfer of two electrons and a product which has a UV spectrum identical to that observed following reduction of pteridine on Wave I or wave II followed by reduction of wave IV. Following reduction at a potential corresponding to wave III, a voltammetric oxidation peak, corresponding to that observed following reduction of wave IV, is present, but no polarographic waves are observed.

Macroscale Electrolyses, Product Isolation and Characterization. To obtain a sufficient amount of material for characterization, solutions of 10 to 40 mM pteridine concentration were electrolyzed. Based upon voltammetric and polarographic studies, the electrochemical behavior of pteridine in solutions of pH 2.0 (0.01 M HCl with acid added periodically to adjust pH to 2) and pH 7.0 (McIlvaine or phosphate buffer) was judged to be representative, and macroscale electrolyses were conducted almost exclusively in these media.

Although the definite structures of the products were not established (primarily because of their instability), the evidence obtained from mass and NMR spectrometry, thin layer chromatography,

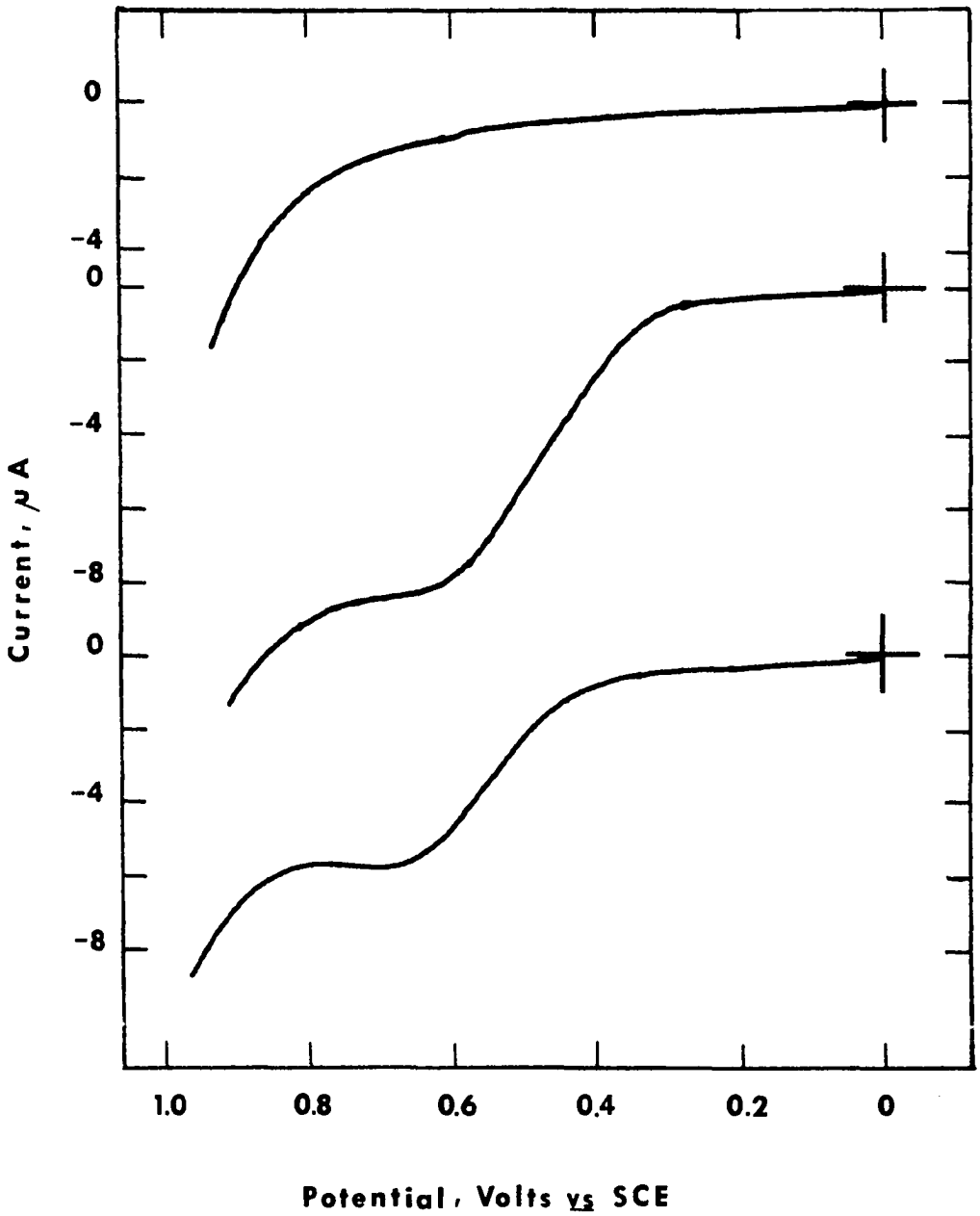

FIGURE 2-18. Voltammogram at the PGE of pteridine solution at pH 7.0 after reduction at a potential corresponding to (A) wave I and (B) wave IV. Sweep rate 10 mV sec^{-1}.

voltammetry, and UV spectroscopy allowed conclusions to be drawn regarding the nature of the electrochemical products.

Lyophilization of the solution after reduction of 500 mg pteridine at pH 7 on the plateau of wave I gave a light brown residue. The reduction product was separated from buffer by extraction with methanol. When the methanol was removed by evaporation, a brown powder remained. Thin layer chromatography of the powder (silica gel developed with methanol) showed three major spots (UV visualization). The most intense had an R_f value of 0.55, and spots of lesser intensity were observed at R_f = 0.40 and R_f = 0.00. The voltammetry and UV spectrum of the brown product were identical to that of the electrolyzed solution. By comparison of UV spectra of the product in water and ethanol, it was determined that above a pH of 6.5 the predominant species in solution is a free base, and below this pH a protonated form exists.

Attempts to purify the crude electrolysis product by recrystallization or chromatography were largely unsuccessful. Recrystallization could not be accomplished in any of a variety of solvents. The electrolysis product was insoluble in all but the most polar solvents (water, methanol, acetonitrile) and heating of the product in the polar solvents caused decomposition (changes in UV spectra and thin-layer chromatography). When the product was dissolved in a polar solvent and reprecipitated by addition of a non-polar solvent, a very fine precipitate was obtained, and TLC showed that purification had not been achieved.

Chromatographic purification was attempted on several supports -- silica gel, alumina, Sephadex, and ion exchange resins. All chromato-

graphic methods resulted in either decomposition of the sample, incomplete separation, or both.

Even though the reduction product could not be purified, NMR and mass spectrometry of the crude material yielded information regarding possible structures. The mass spectrum of the reduction product is shown in Fig. 2-19A. Of particular significance is the group of peaks at m/e 264-266, indicating the presence of a pteridine dimer.

The NMR spectrum of the wave I reduction product in deuterated methanol shows 3 groups of peaks at δ values of 5.5, 7.3 and 7.8 (Fig. 2-19B). The NMR spectrum of pteridine is included for purposes of comparison (Fig. 2-20B). The most significant difference in the two spectra is the presence of the peaks at 5.5 δ in the reduced product. This peak indicates the presence of methylene or methine protons, probably located at C_6 or C_7. Proposed assignments are shown in Fig. 2-19B. The shift of the signals for the C_2, C_4 and C_6 protons is caused by the increased saturation in the pyrazine ring. A similar shift was noted by Albert, et al for 5,6,7,8-tetrahydro-6,7-dihydroxypteridine.[3] Because of the position of the water peak and the poor separation of the signals at δ = 7.5 and 7.8, integration of the spectrum was of little value. However, visual inspection shows that the approximate area ratio is consistent with the proposed assignments.

Infrared spectra of pteridine and the wave I reduction product are shown in Fig. 2-20C and 2-19C, respectively. Mason[16] assigned the bands of pteridine between 1500 - 1600 cm^{-1} to ring stretching vibrations (C=N and C=C). The band of 3000 cm^{-1} is C-H stretch, and the broad band at 3500 cm^{-1} is caused by the presence of a small amount of water

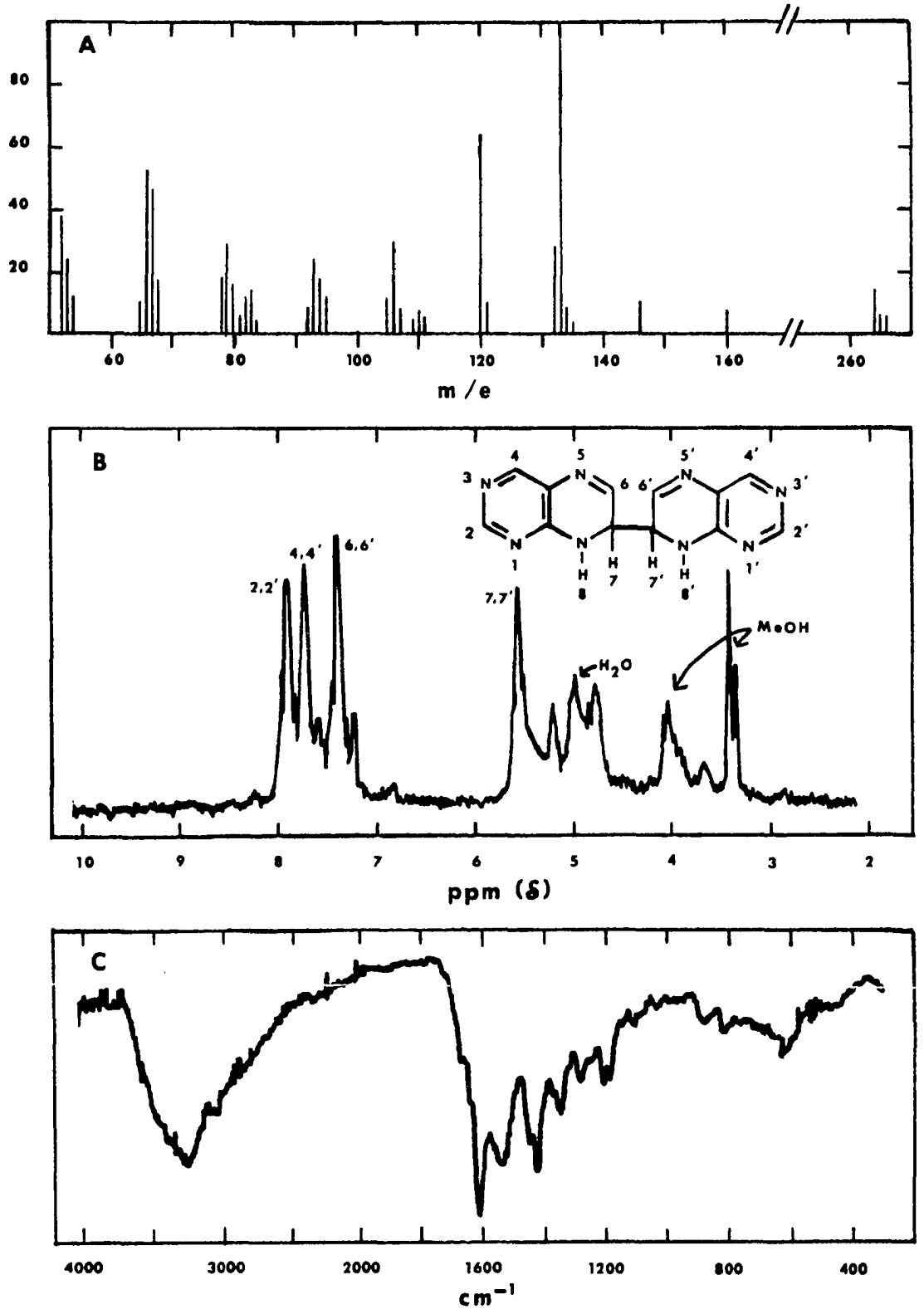

FIGURE 2-19. Mass (A), NMR (B), and IR (C) spectra of pteridine wave I reduction product. NMR solvent, deuterated methanol, IR is KBr disc.

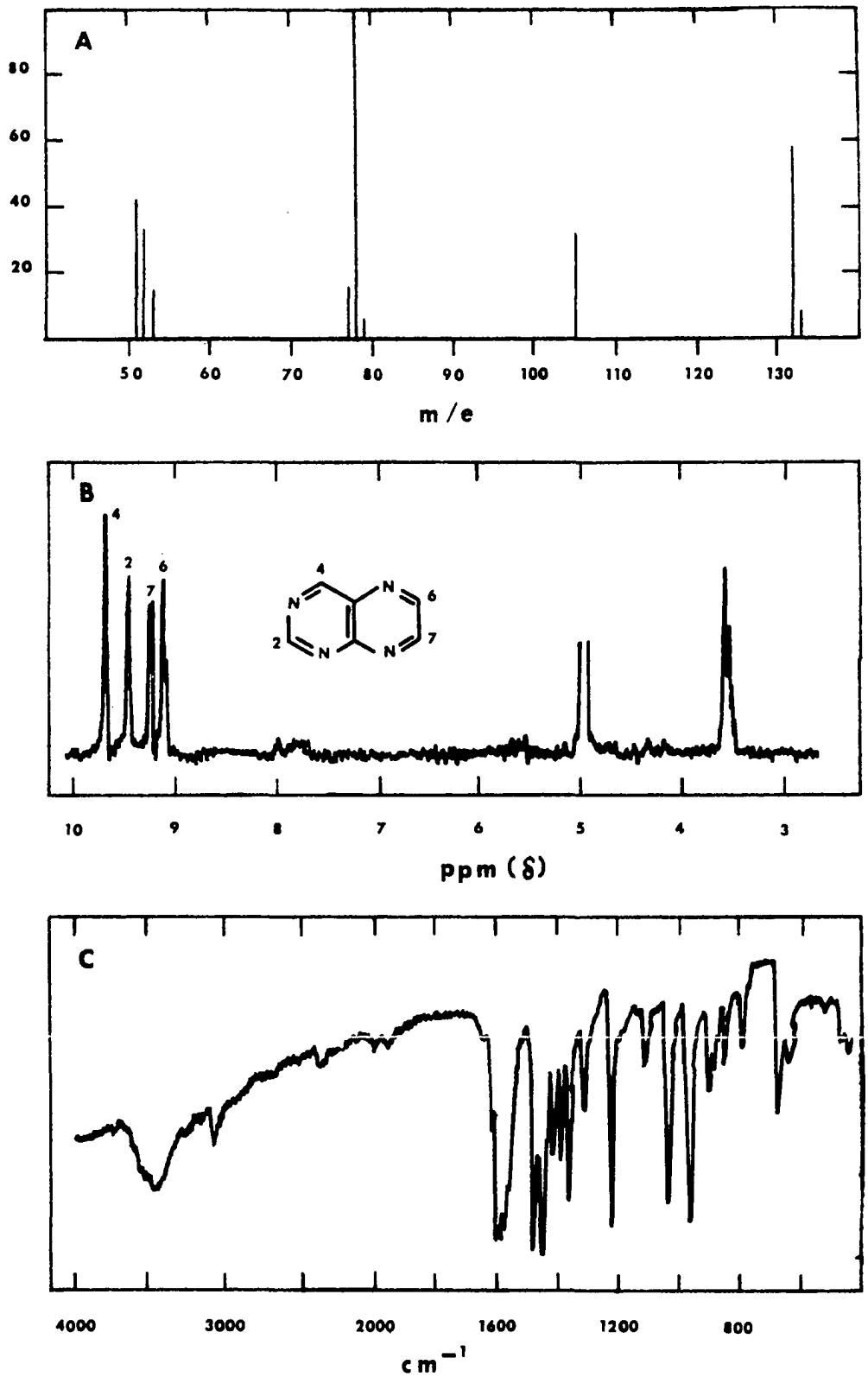

FIGURE 2-20. Mass (A), NMR (B), and IR (C) spectra of pteridine. NMR solvent, deuterated methanol. IR is of KBr disc.

in the KBr disc. Bands from 700 - 1050 cm^{-1} were assigned to out-of-plane C-H bending vibrations. In particular the band at 800 cm^{-1} is associated with the C-H bond in position 4. On reduction a broad band at 3500 - 3000 cm^{-1}, corresponding to various N-H stretches, is observed. The shoulder at 3000 cm^{-1} may be caused by the presence of additional C-H bonds. Ring stretching vibrations remain in the region 1500 - 1600 cm^{-1}, and the band at 800 cm^{-1} (4-C-H) is present.

The similarity of the UV spectra of the wave I product (Fig. 2-16B) and the wave IV product (Fig. 2-16C) indicates that the structures of the two compounds are also very similar. Identical basic pK values (pK = 6.5) for each compound were established by UV spectroscopy.

Although the evidence cited above is consistent with the proposed structure (6) the possibility of isomeric forms is not eliminated. Other possible structures (7,8) are shown below.

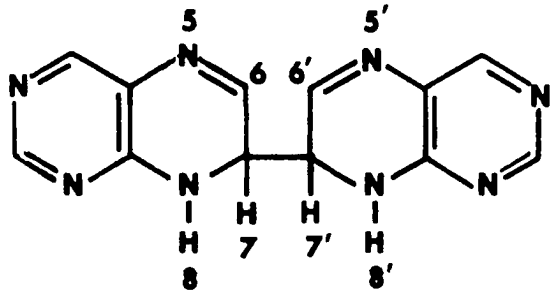

(6)

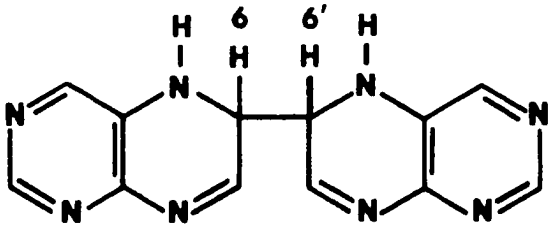

(7)

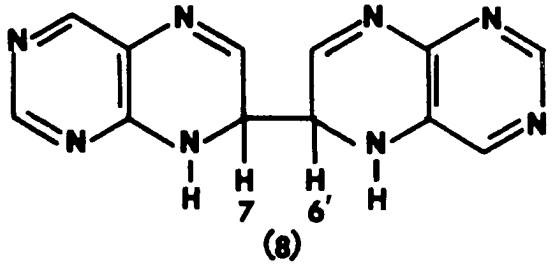

(8)

It would be particularly difficult to distinguish between (6) and (7). Assignment of the proposed structure (6) is based primarily upon published studies of other pteridines[17-19] in which the 7,8-dihydro compound, rather than the 5,6-dihydro, was usually formed. The asymmetric dimer (8) should show two additional signals in NMR, since protons 6 and 6' or 7 and 7' are not equivalent as they are in (6) or (7). Upon reduction, (8) should yield one molecule of 7,8-dihydropteridine and one molecule of 5,6-dihydropteridine. UV and NMR spectrometry seem to indicate that a single compound is produced from the reduction of the dimer.

It would be expected that structures involving dimerization between the pyrazine and pyrimidine rings (9,10) could undergo further electrochemical reduction in the pyrazine ring.

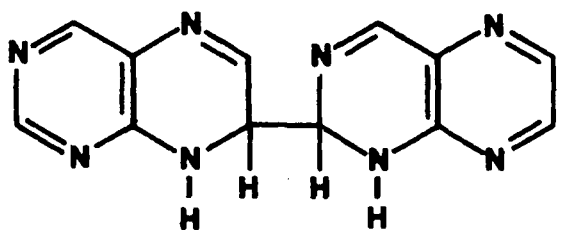

(9)

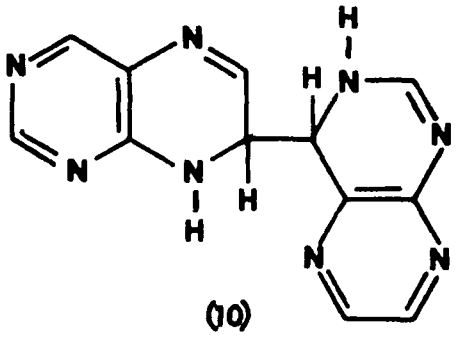

(10)

No such reduction is observed. In addition, infrared spectrometry indicates the presence of the 4-C-H bond, eliminating the possibility of structure (10).

A proposed mass spectral fragmentation pattern for compound (6) is presented in Fig. 2-21. Because of the presence of impurities in the sample it is impossible to assign a detailed fragmentation pattern,

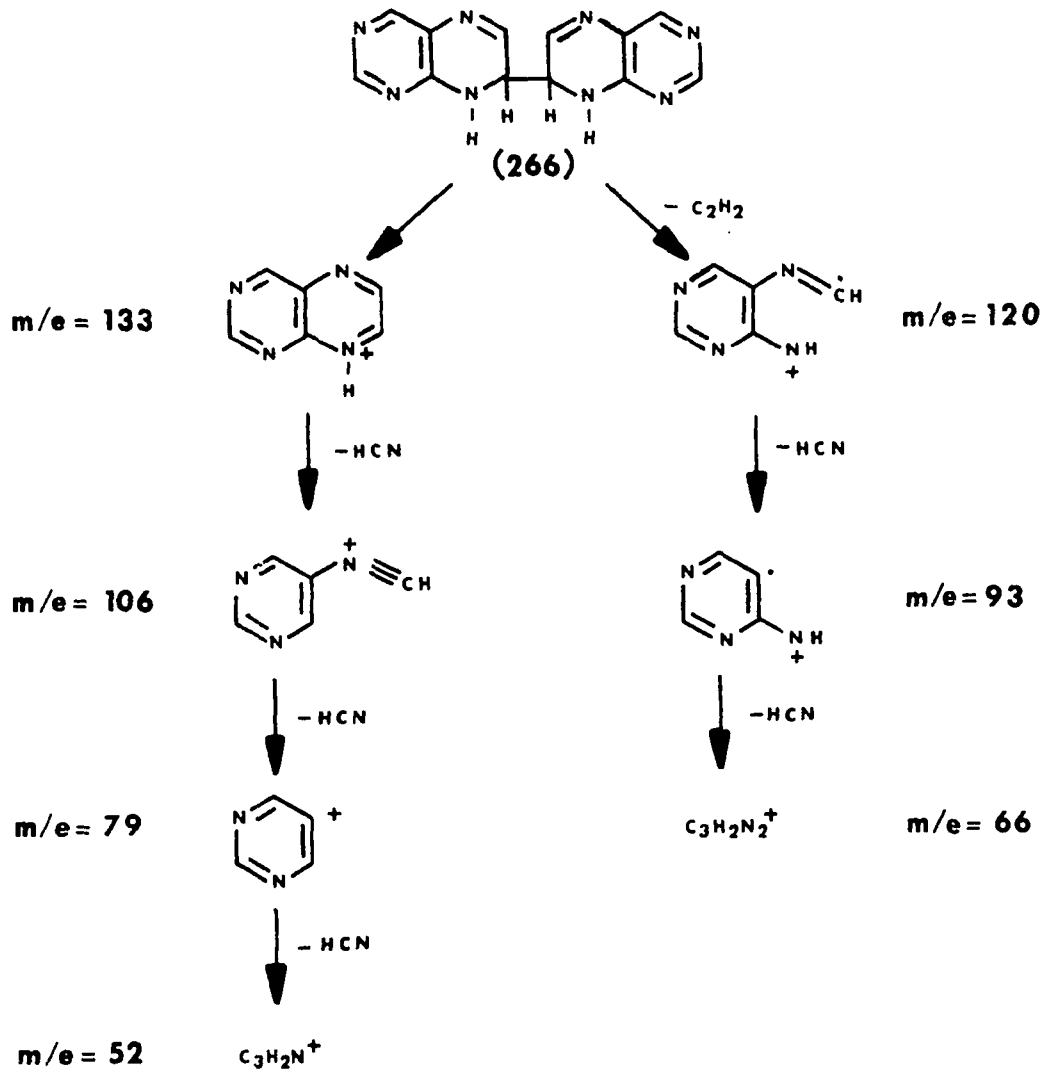

FIGURE 2-21. Proposed fragmentation pattern for pteridine wave I product.

but the proposed pattern accounts for several of the major peaks in Fig. 2-19A.

It seems reasonable to assume that the major spot (R_f = 0.55) observed on thin-layer chromatography of the pteridine wave I reduction product corresponds to the principal reduction product (6), while the less intense spots (R_f = 0.45, 0.00) may correspond to isomeric dimers or side products of the reaction.

Following reduction of 200 - 500 mg pteridine at pH 2 (0.01 M HCl) at a potential more negative than polarographic wave IV, lyophilization of the solution left a brown residue. This material dissolved easily in water, producing a very acidic solution containing a large amount of chloride ion. Although much of the chloride is present as KCl (from salt bridges and reference electrode) the high acidity of the sample indicates the presence of HCl as well. The material was sparingly soluble in methanol. The UV spectrum and voltammetry of the material was identical to that of the electrolyzed solution. Thin-layer chromatography (MeOH on silica gel) showed a major spot at R_f = 0.00, with faint streaking to R_f = 0.50.

To effect separation of the reduction product from potassium chloride and residual hydrochloric acid, the mixture was passed through an ion retardation column (Experimental). The chloride-free effluent was lyophilized, leaving a yellow to buff residue, which was only sparingly soluble in neutral or alkaline aqueous solutions and methanol, but dissolved very readily in acidic solution. The UV spectrum, voltammetry and TLC of this product were again identical to the electrolyzed solution. It was concluded from these observations that the

initial isolated product was a hydrochloride which was converted to the free base by passage through the ion retardation column.

The major impurities in the lyophilized wave IV product are inorganic material (KCl and HCl) with smaller amounts of decomposition products (from starting material and electrode product) and products of chemical or electrochemical side reactions. As in the case of the wave I product, attempts to purify the wave IV product were largely unsuccessful. The purity of the isolated product was determined by measurement of the UV absorbance of a solution containing a known amount of product and comparison to the UV absorbance of the electrolyzed solution. Attempted purification by recrystallization or reprecipitation always resulted in decomposition or a very fine impure precipitate. Decomposition is apparently caused by heating, and is accelerated in acidic or basic solutions. The product was totally retained on silica gel and alumina chromatographic columns, and no improvement in purity was obtained by passage through a Sephadex G-10 column. Best results were achieved simply by passing a solution of the initial lyophilized product through an ion retardation column. In addition to removing the inorganic components, this treatment also removed some of the organic impurities from the sample. Apparently, the ion retardation resin has adsorptive as well as ion-exchange properties. Compared to the electrolyzed solution (UV absorbance, see Experimental), the product was about 85 percent pure.

The mass spectrum of the free base (Fig. 2-22A) shows a molecular ion at m/e = 134, which is that expected for a dihydropteridine.

The NMR spectrum of the reduction product is shown in Fig. 2-22B

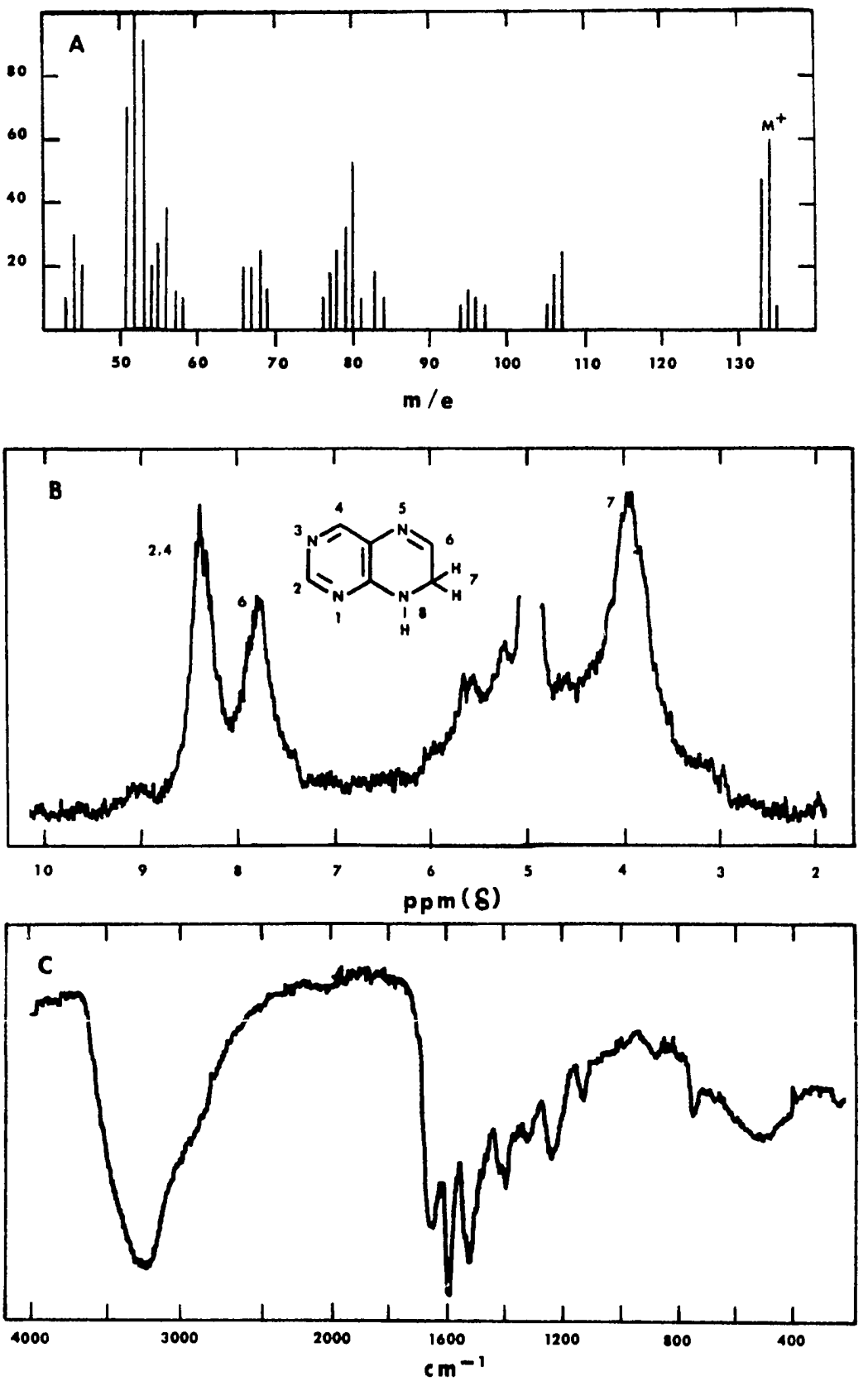

FIGURE 2-22. Mass (A), NMR (B), and IR (C) spectra of the pteridine wave IV reduction product (free base). NMR solvent, 0.5 N DCl in D_2O. IR is KBr disc.

with proposed assignments. Because of the insolubility of the free base in all suitable solvents, NMR spectra were run in D_2O containing deuterated hydrochloric acid. The feature of major significance in the NMR is the chemical shift of the C_7 protons relative to their chemical shift in the wave I product (Fig. 2-19B). In the dimer (6) the C_7 protons are deshielded by the attachment of the pyrazine ring, and thus appear downfield of the C_7 protons in the dihydro compound. As expected, the C_2, C_4 and C_6 protons have almost identical chemical shifts in the dimer and dihydro compound. The broad appearance of the NMR peaks may be caused by the chemical equilibrium between the protonated form of the dihydro compound and the free base.

The infrared spectrum of the wave IV reduction product (Fig. 2-22C) is very similar to that of the wave I product (Fig. 2-19C), and the same comments apply. It should be noted that the band at 800 cm^{-1} (4-C-H) appears in Fig. 2-22C.

Although the wave IV product has been discussed as if it were 7,8-dihydropteridine (11), it should be pointed out that 5,6-dihydropteridine (12) would be expected to have almost identical physical and chemical properties.

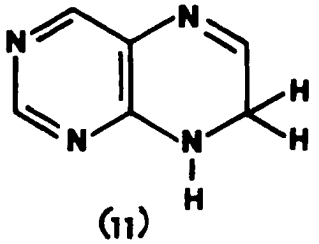

(11)

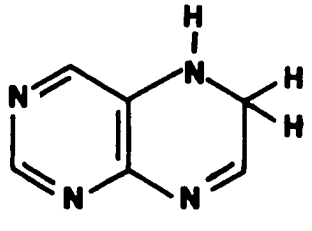

(12)

A decision between these two isomers could probably be made only upon the basis of x-ray crystallographic data, or by comparison with authentic samples. Unfortunately, purification and crystallization could not be effected, and neither 5,6- nor 7,8-dihydropteridine has been previously reported. The available data do, however, allow other dihydro structures to be eliminated as possibilities. The preparation and properties of 3,4-dihydropteridine have been published,[20] and differ considerably from those of the electrochemical reduction product. Also, electrochemical reduction of the pyrimidine ring has never been observed for any pteridine. If the final reduction product were 5,8-dihydropteridine, the C_6 and C_7 vinyl protons would be expected to appear further downfield than the methylene protons of 7,8- or 5,6-dihydropteridine, and no signal for C_6 (or C_7) would appear at $\delta = 7.8$ (Fig. 2-22B). The assignment of the structure as 7,8-dihydropteridine (rather than 5,6-dihydropteridine) is based primarily upon the electrochemical behavior of other pteridines, in which the 7,8-dihydro is always formed, if the structure of the starting compound permits.[17-19] For example, the electrochemical reduction of several substituted 2-amino-4-hydroxypteridines always resulted in initial formation of a 5,8-dihydro compound, followed by rearrangement to the 7,8-dihydro compound.[18] Electrochemical reduction of 7-hydroxypteridine, in which the 7,8-dihydro compound cannot form, gives 5,6-dihydro-7-hydroxypteridine.

The physical properties of the dihydro compound (11) contrast markedly to those of pteridine as shown in Table 2-9.

TABLE 2-9

Comparison of Properties of Pteridine and Dihydropteridine

Property	Pteridine	7,8-Dihydropteridine
Melting point	138-140°C	Does not melt; blackens 200-225°C
Solubility	v. soluble in water, methanol, ethanol; sl. soluble in benzene, chloroform, acetone	sl. soluble in water, methanol, hot ethanol. Insoluble in benzene, chloroform, acetone
Sublimation	Sublimes readily at 100°C, 1 mm vacuum	Does not sublime

Similar contrasts are noted between pteridine and 3,4-dihydropteridine[20] and quinoxaline and 1,4-dihydroquinoxaline.[21]

A proposed mass spectral fragmentation pattern for compound (11) is presented in Fig. 2-23. Again, because of lack of purity a detailed pattern cannot be assigned, but a pattern, similar to that for pteridine,[23] and accounting for several major peaks, is proposed.

Mechanism. The proposed mechanism for the electrochemical reduction of pteridine is shown in Fig. 2-24. Voltammetric and polarographic data clearly indicate that the electrochemical reduction of pteridine at potentials corresponding to polarographic wave I proceeds by an electrochemically reversible process involving 2 electrons and two protons. Studies of the electrochemical reduction of 2-amino-4-hydroxypteridines,[17,18] folic acid,[19] and quinoxalines,[21-23] have shown that these compounds are reduced in an initial $2\underline{e}/2H^+$ reversible process to the 5,8-dihydro derivative (in quinoxaline, the 3,4-dihydro), which then rearranges to the more stable 7,8-dihydro compound (in

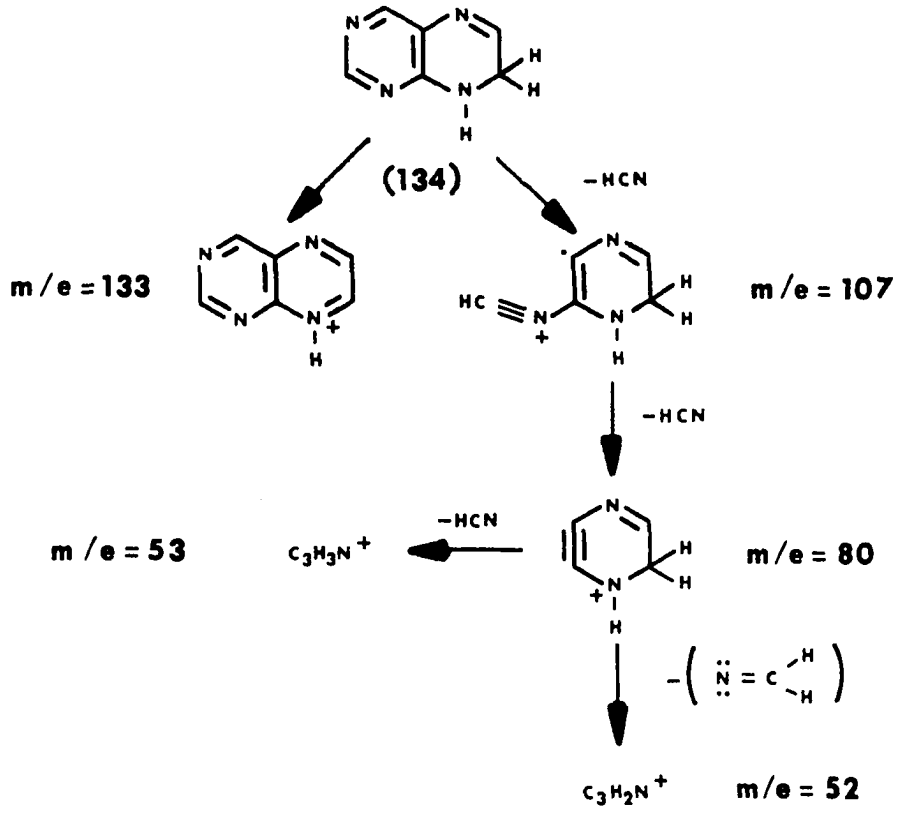

FIGURE 2-23. Proposed mass spectral fragmentation pattern for pteridine wave IV reduction product.

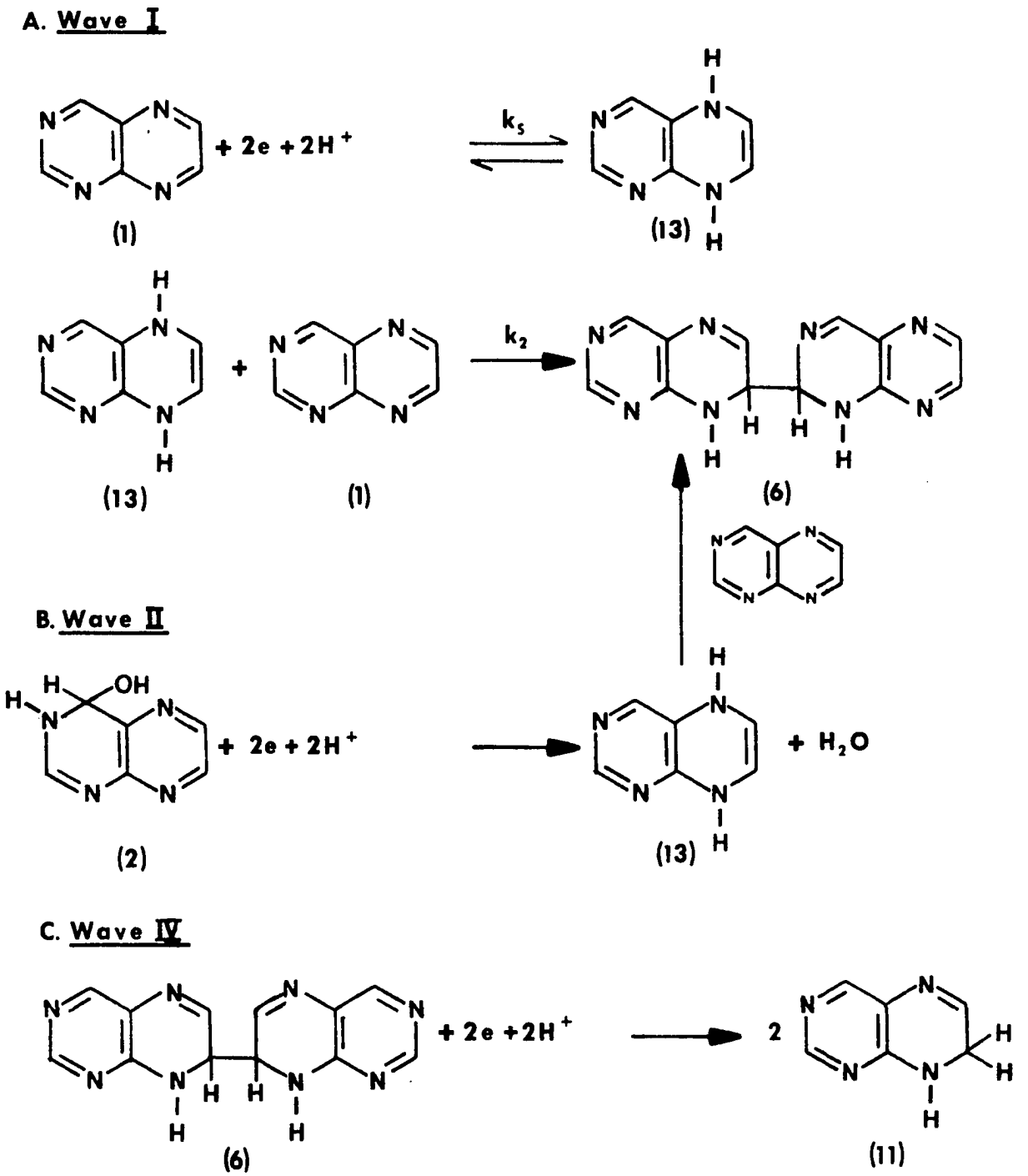

FIGURE 2-24. Proposed electrochemical reduction mechanism for pteridine.

quinoxaline, the 3,4-dihydro) (Fig. 2-25). It seems reasonable to propose that the initial reversible reduction of pteridine proceeds in a similar manner. That the initial reduction of pteridine occurs in the pyrazine ring rather than in the pyrimidine ring is supported by the observation that neither 5,6,7,8-tetrahydropteridine (20) or 5,6,7,8-tetrahydro-6,7-dihydroxypteridine (4) is electrochemically

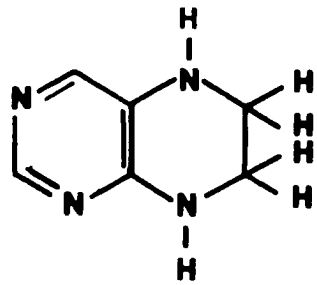

(20)

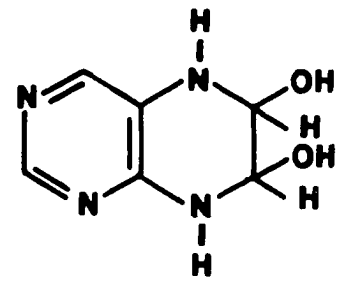

(4)

reducible. In addition, the chemical reduction of pteridine with lithium aluminum hydride results in the formation of 5,6,7,8-tetrahydropteridine.[24] Further evidence favoring the initial formation of 5,8-dihydropteridine was obtained from studies of the electrochemical reduction of 6-hydroxypteridine (21) and 7-hydroxypteridine (22) (Chapter 3).

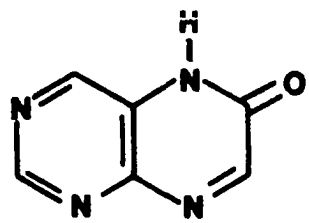

(21)

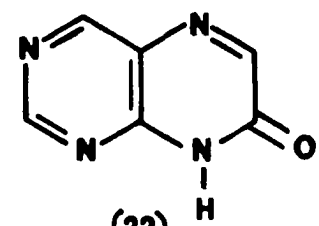

(22)

These compounds are electrochemically reduced in irreversible $2\underline{e}/2H^+$ processes to the 7,8- and 5,6-dihydro compounds, respectively. From

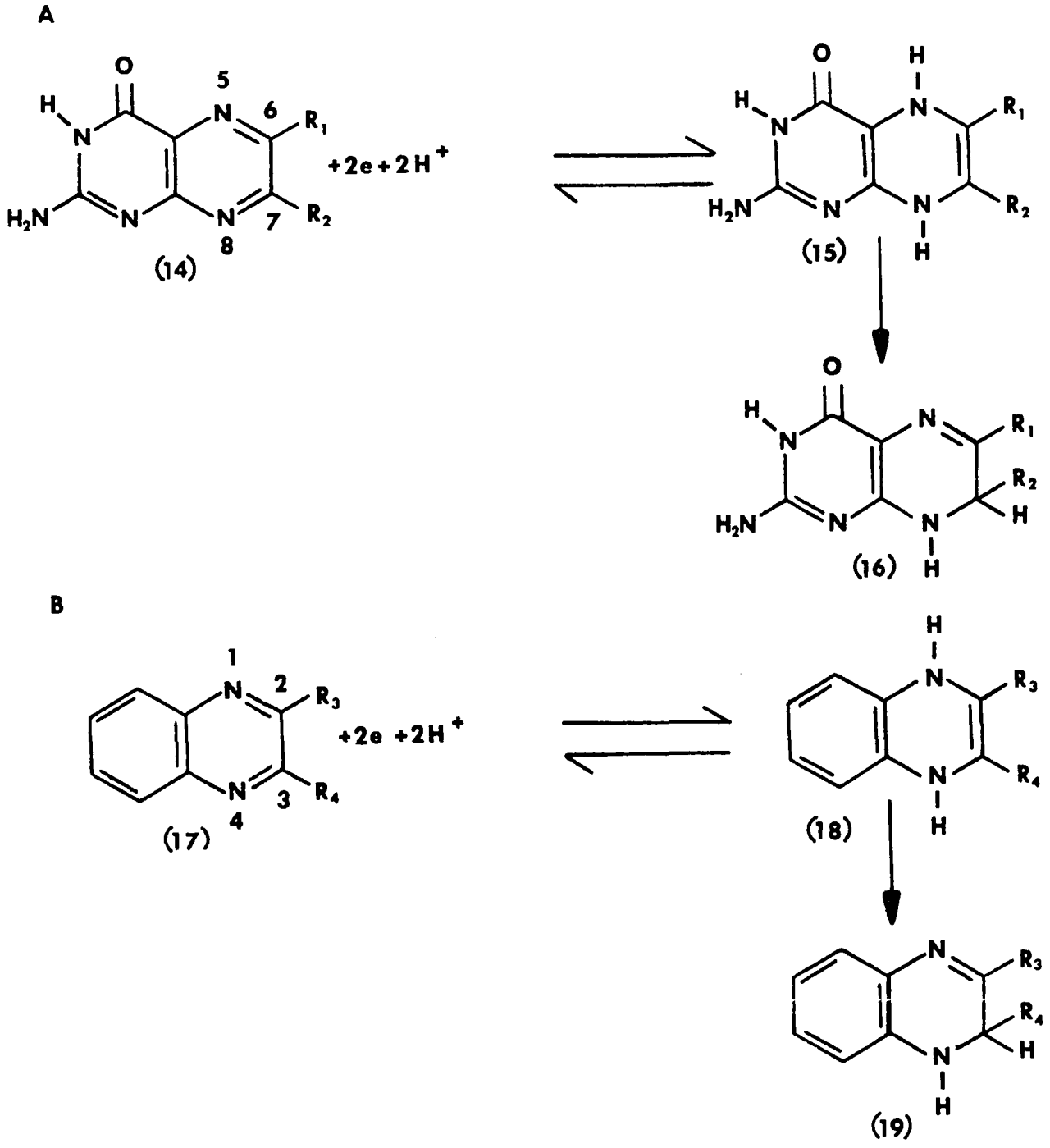

FIGURE 2-25. Electrochemical reduction mechanism for (A) 2-amino-4-hydroxypteridines and (B) Quinoxalines.

the above structures, it is apparent that the 5,8-dihydro compound cannot be formed; thus, a reversible reduction is not observed.

Cyclic voltammetry of pteridine showed that the 5,8-dihydro compound initially formed is not stable, but rather quickly reacts in a reaction which is second order in pteridine. A simple rearrangement to a 5,6- or 7,8-dihydro compound would be expected to be first order in pteridine. Controlled potential coulometry on the plateau of wave I resulted in the transfer of a single electron. The only apparent explanation for these observations is that the dihydro compound produced in the initial electrode reaction reacts with pteridine producing a dihydro dimer. The nature of the dimer has not been unambiguously established, but evidence from NMR, IR, and mass spectrometry and electrochemical studies (vide supra) is consistent with the structure shown in Fig. 2-24 (6), i.e., 7,8,7',8'-tetrahydro-7,7'-dipteridyl. The possibility of isomeric forms of the dimer has been discussed. The chemical reaction resulting in the formation of the dimer (6) is a base-catalyzed Michael addition, similar to the reaction between 7,8-dihydro-6-hydroxypteridine and 6-hydroxypteridine,[25] and to the reaction of 6-hydroxy-7-methyl-7,8-dihydropteridine with 6-methyl-7-hydroxypteridine.[26] A proposed mechanism for the dimerization is shown in Fig. 2-26.

Cyclic voltammetric and coulometric evidence indicates that reduction of pteridine on the plateau of wave II in acidic solution (i.e., reduction of the 3,4-hydrate) is an irreversible process which results in products and n-values identical to those obtained by reduction on the plateau of wave I at higher pH. The reaction clearly

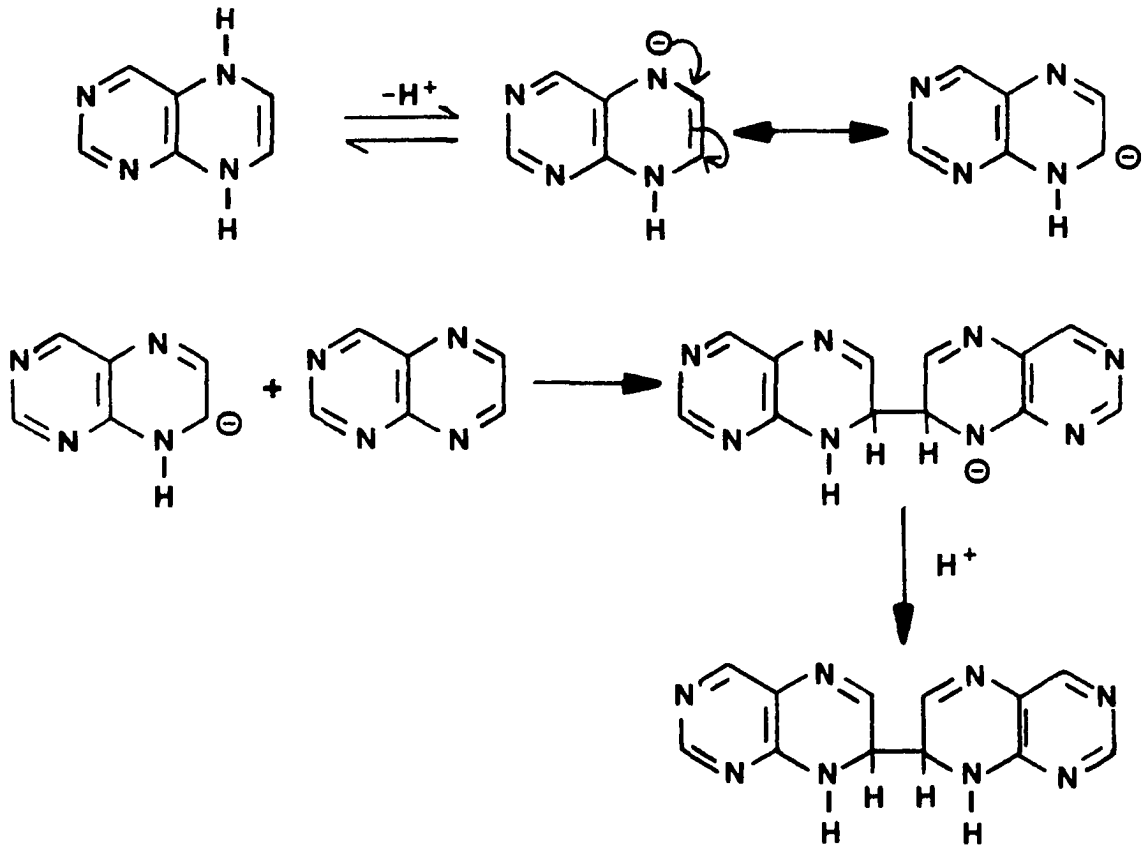

FIGURE 2-26. Proposed mechanism for the reaction of 5,8-dihydropteridine with pteridine to form a dimer.

must involve reduction and loss of water to 5,8-dihydropteridine, which then reacts with pteridine as before (Fig. 2-24B).

Following reduction on wave I or II, coulometric reduction on the plateau of wave IV involves the transfer of a single electron, based upon the amount of pteridine originally present. Polarographic data indicate, however, that two electrons are transferred in an irreversible electrode process. These results are consistent with the mechanism shown in Fig. 2-24C; i.e., a two-electron reduction of the dihydro dimer to two molecules of dihydropteridine.

Reduction of pteridine at a potential more negative than polarographic wave IV apparently proceeds by the mechanism shown in Fig. 2-24A,C. That is, there is no evidence to indicate that at more negative potentials the dihydro compound, (11, Fig. 2-24C) is formed directly from pteridine or by rearrangement of 5,8-dihydropteridine. Indeed, there is no reason to believe that the electrode potential influences the reaction of 5,8-dihydropteridine with pteridine.

Because reduction on the plateau of wave V results in the transfer of only 0.25 electron with no change in the UV spectrum, it was concluded that this wave is not associated with the principal reduction mechanism, but instead represents reduction of a minor wave I product.

Experimental

Chemicals. Chemicals were obtained from the following sources: quinoxaline, 4,5-diaminopyrimidine, 4,5-diamino-6-hydroxy-2-mercaptopyrimidine (Aldrich); glyoxal (Mann Research Laboratories); phosphorus pentasulfide (Eastman); Raney nickel (Sargent-Welch).

The synthesis of 4,5-diaminopyrimidine from 4,5-diamino-2,6-dimercaptopyrimidine was according to the method of Beaman, et al,[14] and 4,5-diamino-2,6-dimercaptopyrimidine was synthesized from 4,5-diamino-6-hydroxy-2-mercaptopyrimidine by the method of Beaman and Robins.[27] Raney nickel catalyst was prepared according to the method of Brown.[28] Pteridine was synthesized from 4,5-diaminopyrimidine and glyoxal by the method of Albert and Yamomoto,[13] except crystalline glyoxal hydrate was used instead of polymeric glyoxal monohydrate. The product was purified by sublimation at 100°C, 1 Torr.

Buffer solutions were prepared with an ionic strength of 1.0 M, giving a 0.5 M ionic strength upon 1:1 dilution, and were constituted as follows: pH 0.5 - 3.0, HCl - KCl; pH 2.2 - 8.0, citric acid - NaH_2PO_4 - KCl (McIlvaine); pH 8.0 - 11.0, $Na_2B_4O_7$ - KCl; pH 11 - 13, NaOH - KCl. 1 M acetic acid was also used. Argon and nitrogen used for deoxygenation were equilibrated with water in a bubbling chamber. All mercury was triply distilled by Bethlehem Apparatus.

Thin-layer chromatography was carried out on Eastman Chromagram sheets, silica gel with fluorescent indicator. Although several developing solvents were tried, the best separations were obtained with absolute methanol. Visualization was with ultraviolet light.

Apparatus. Polarograms and voltammograms were obtained with an instrument of conventional operational amplifier design[29] and employing a function generator patterned after that of Myers and Shain.[30,31] Polarograms and voltammograms were recorded on a Hewlett-Packard Model 7001A X-Y Recorder. Fast-sweep voltammograms were recorded on a Tektronix model 5031 Dual Beam Storage Oscilloscope and photographed

with a Tektronix Model C-70 camera. A water-jacketed three-compartment cell maintained at 25 ± 0.1°C with each compartment separated by a medium-porosity sintered glass disc was used. Salt bridges, inserted on the counter and reference sides of the frits, were prepared by dissolving 4 g agar in 90 ml water and adding 35 g KCl. A saturated calomel reference electrode (SCE) and a platinum gauze counter electrode were used. All potentials are referred to the SCE at 25°C.

A mechanical drop dislodger in conjunction with the dual-channel timing circuit described by Brown et al[32] was used with the dropping mercury electrode (DME) for all d.c. polarograms. A drop time of 2.00 sec was normally employed, except for mercury column height dependence experiments where natural drop times were used. The pyrolytic graphite electrodes were machined from small rods of pyrolytic graphite (Super-Temp Company, Santa Fe Springs, California) to a diameter of 4 mm and length ca. 10 mm, and were sealed into lengths of 4 mm bore glass tubing with Hysol Epoxi-Patch (Hysol Corp., Olean, N.Y.). The electrodes were ground flush with the end of the glass tube, and were resurfaced before each voltammogram was run with 600-grade silicon carbide paper (Buehler Ltd., Evanston, Ill.) mounted on a rotating disc. The electrode was then sprayed with a stream of distilled water to remove the graphite powder from the surface, and dried by touching the surface with absorbent tissue paper. The hanging mercury drop electrode was a Metrohm Model E410 (Brinkmann Instruments, Westbury, N.Y.).

The temperature of the cell and water-jacketed bubbling chamber was maintained by circulating water from a bath heated by an incandescent

bulb in circuit with 25°C or 40°C temperature regulators and a mercury relay (H-B Instrument Co.).

Controlled potential electrolyses were carried out using a Wenking Model 66 TA1, a Tacussel Model ASA4-HT2 or a Princeton Applied Research Model 173 potentiostat. Current integration during electrolysis utilized a Koslow Scientific Model 541 coulometer or a Hewlett-Packard Model 2212A voltage-to-frequency converter and two Hewlett-Packard Model 5321A electronic counters connected in series. Two different three-compartment cells were used for controlled potential electrolysis. Both contained platinum gauze counter electrodes and SCE reference electrodes, but the working compartment of one had a volume of 120 ml and the other, 25 ml. The areas of the mercury pool working electrodes were ca. 16 cm^2 and ca. 3.8 cm^2, respectively. The usual volume of the electrolysis solution was 90 ml or 15 ml. For preparative-scale electrolyses, a two-compartment cell having a working electrode compartment volume of 150 ml was used. With this cell, a platinum gauze counter electrode and a commercial SCE were employed. The working electrode area was ca. 24 cm^2, and the volume of the electrolysis solution was usually 100 ml. In all cells, argon or nitrogen was bubbled through the electrolysis solution via a gas dispersion tube. During electrolysis, solutions were stirred magnetically with a Teflon-covered bar.

The pH measurements were made with a Beckman Zeromatic pH meter. A Buchler Fractomat fraction collector was utilized in column chromatography. Infrared spectra were recorded on a Beckman IR-10 Spectrophotometer. KBr pellets were made with a Barnes Econo-Press. Ultra-

violet spectra were obtained with a Perkin-Elmer Hitachi Model 124 Spectrophotometer using 1 cm quartz cells. NMR spectra were recorded on a Varian T-60 or a Varian XL-100 Spectrometer. Mass spectra were recorded on a Hitachi RMU-6E Spectrometer. Lyophilization was accomplished using a Virtis 12-port manifold and a Welch Model 1400 vacuum pump. Cooling traps contained isopropanol-dry ice.

Polarographic and Voltammetric Procedure. Test solutions were prepared by diluting appropriate quantities of stock solution (usually prepared fresh each day) with a suitable buffer solution. Solutions for voltammetry normally had an ionic strength of 0.5 M. The solutions were deaerated with argon before the polarogram or voltammogram was run, and a stream of argon was passed over the solution during the run.

Coulometric and Macroscale Electrolysis Procedure. For controlled potential coulometry, an appropriate volume of a solution (concentration varied from 0.1 to 2.0 mM but was generally 1 mM) of pteridine in a suitable buffer was placed in the working electrode compartment of the coulometric cell. The solution was deaerated for approximately 10 minutes prior to the beginning of the electrolysis, and argon or nitrogen flow was continued during the electrolysis. When the current decreased to a low, constant value, the counts per unit time produced by the coulometer was noted, and the electrolysis was stopped. For the electrolysis of pteridine solution of low concentration (0.1 - 0.5 mM) the background solution was reduced at the electrolysis potential until a constant current reading was attained. The potentiostat was then turned off, the proper amount of solid pteridine was added and upon dissolution, the electrolysis was continued as before.

Completion of the reduction was confirmed by the absence of the polarographic wave corresponding to the electrolysis potential. The procedure for preparative scale electrolysis was essentially the same, except 200 - 500 mg of pteridine in 100 ml solution was used.

Isolation and Characterization of Electrolysis Products. After completion of the reduction of 200 - 500 mg pteridine on the plateau of wave I (1e) in pH 7 phosphate buffer, the solution was lyophilized, and then extracted with methanol. Thin-layer chromatography of the electrolysis solution and the methanol extract confirmed that the principal reduction products were contained in the extract. The methanol was evaporated and the residue was dissolved in a small amount of water and lyophilized, leaving a brown powder. As described earlier, repeated attempts at purification were unsuccessful. For NMR spectra the brown powder was dissolved in deuterated methanol (100 mg in 0.4 ml), and for IR, a KBr pellet was prepared (1 mg in 100 mg KBr).

During the reduction of pteridine at pH 2 (0.01 M HCl) the pH of the solution tended to increase because of the consumption of protons by the electrochemical reaction. The pH of the electrolysis solution was checked periodically (every 10-15 minutes at the beginning of the electrolysis, less often as the current decayed) with a pH meter, and 2 N HCl was added to adjust the pH to 2. Lyophilization of the solution following reduction of pteridine at pH 2 at -0.80 Volts vs SCE (2e) yielded a brown residue which gave a very acidic solution when dissolved in water. The residue was dissolved in a small amount (3 - 5 ml) water, applied to the top of a 2 x 50 cm column of ion retardation

resin (Bio-Rad 11A8, 50-100 mesh), and eluted with water at a flow rate of 5 ml min^{-1}. Fractions of 100 drops were collected, and the fractions which contained reduction product (detected by UV) but no chloride (absence of precipitate with $AgNO_3$) were combined and lyophilized. The column was regenerated by washing with 1 M HCl (400 ml), 1 M NH_4OH made 0.5 M in NH_4Cl (800 ml), 1 M NH_4Cl (400 ml), and water (3000 ml or until column effluent is chloride-free), in that order. To prevent formation of bubbles in the column, the water used in the final regeneration step was purged with nitrogen. From the electrolysis of 200 mg pteridine, 75 - 100 mg of chloride-free product was usually obtained. The purity of this product was determined by thin-layer chromatography, and by comparison of the UV absorbance of a solution containing a known amount with the absorbance of an electrolyzed solution of known concentration. For NMR spectra, 100 mg of product was dissolved in 0.4 ml 0.5 N DCl in D_2O (solubility of the product in neutral solutions was not sufficient for NMR), and for IR spectra, a KBr pellet was prepared (1 mg in 100 mg of KBr).

Summary

Over the pH range 1 - 12, pteridine is reduced at mercury and pyrolytic graphite in a reversible, $2e/2H^+$ reaction to 5,8-dihydropteridine. The monohydrated form of pteridine which exists at lower pH (3,4-dihydro-4-hydroxypteridine) is also reduced to 5,8-dihydropteridine, but in an irreversible process. The initial electrode product (5,8-dihydropteridine) is not stable, but reacts with starting material (pteridine) in a base-catalyzed Michael reaction producing

a dihydro dimer, probably 7,8,7',8'-tetrahydro-7,7'-dipteridyl. The dimer is also reduced electrochemically in a $2\underline{e}/2H^+$ irreversible reaction to 7,8-dihydropteridine. Rate constants were obtained for the reversible electron transfer and for the dimerization reaction. These reactions were studied by polarography, cyclic voltammetry, controlled potential coulometry, and preparative electrolysis. Products were isolated and examined by mass, NMR, and IR spectrometry.

APPENDIX 2

I. Calculation of heterogeneous rate constant (k_s) from cyclic voltammetric peak separation.

$$\psi = \gamma^{\alpha} \frac{k_s}{\pi^{1/2} D_o (nF/RT)^{1/2} v^{1/2}} \qquad (2\text{-}10)$$

$$\gamma^{\alpha} = [(\frac{D_o}{D_R})^{1/2}]^{\alpha} \cong 1$$

D_o = diffusion coefficient for oxidized species, $cm^2\ sec^{-1}$

D_R = diffusion coefficient for reduced species, $cm^2\ sec^{-1}$

α = electron transfer coefficient

k_s = heterogeneous rate constant for electron transfer at $E = E^{\circ}$

n = number of electrons involved in the reaction

F = 96,500 coulombs

R = gas constant, 8.31 joules $deg^{-1}\ mol^{-1}$

T = absolute temperature

v = voltage sweep rate, Volts sec^{-1}

At 25° for n = 2, assuming $\gamma^{\alpha} = 1$,

$$k_s = 15.64\ \psi\ D_o^{1/2} v^{1/2}$$

For pteridine peak I_a, at pH 7.0 at the HMDE, at a voltage sweep rate of 1 V sec^{-1},

$D_o^{1/2} = 2.4 \times 10^{-3}$

v = 1 V sec^{-1}

ΔE_p = 48 mV

ψ = 0.67 (see Fig. A-2-1 and Table A-2-1)

$k_s = 15.64\ (0.67)\ (2.4 \times 10^{-3})\ (1)$

$= 2.51 \times 10^{-2}$ cm sec^{-1}

D_o was calculated from polarographic data using the Ilković equation

$$i_d = 607\ nD_o^{1/2}Cm^{2/3}t^{1/6} \qquad \text{(A-2-1)}$$

where i_d = average polarographic diffusion current, μA

n = number of electrons involved in the polarographic process

C = bulk concentration of electroactive substance, mM

m = mercury flow rate, mg sec^{-1}

t = drop time, sec.

Since all other terms in eq. (A-2-1) are known, $D_o^{1/2}$ is easily calculated. Values of D_o were also obtained from the slope of current-time curves recorded at the HMDE, as described in Appendix 5. The agreement of the values D_o so obtained were in good agreement with the polarographic values.

II. Calculation of homogeneous rate constant for a dimerization reaction from cyclic voltammetric data.

1. Calculation of $\frac{i_a}{i_c}$, i_a = anodic peak current, i_c = cathodic peak current.

$$\frac{i_a}{i_c} = \frac{(i_{ap})_o}{(i_{cp})_o} + \left[\frac{(i_{sp})_o}{(i_{cp})_o}\right]^2\beta + \frac{(i_{sp})_o}{(i_{cp})_o}\gamma + \xi \qquad \text{(A-2-2)}$$

$(i_{ap})_o$, $(i_{cp})_o$, and $(i_{sp})_o$ are measured as shown in Fig. A-2-2. β, γ and ξ are constants given in Table IV of reference 11. Values of β, γ and ξ are tabulated for values of $a\tau$ = 3.5,

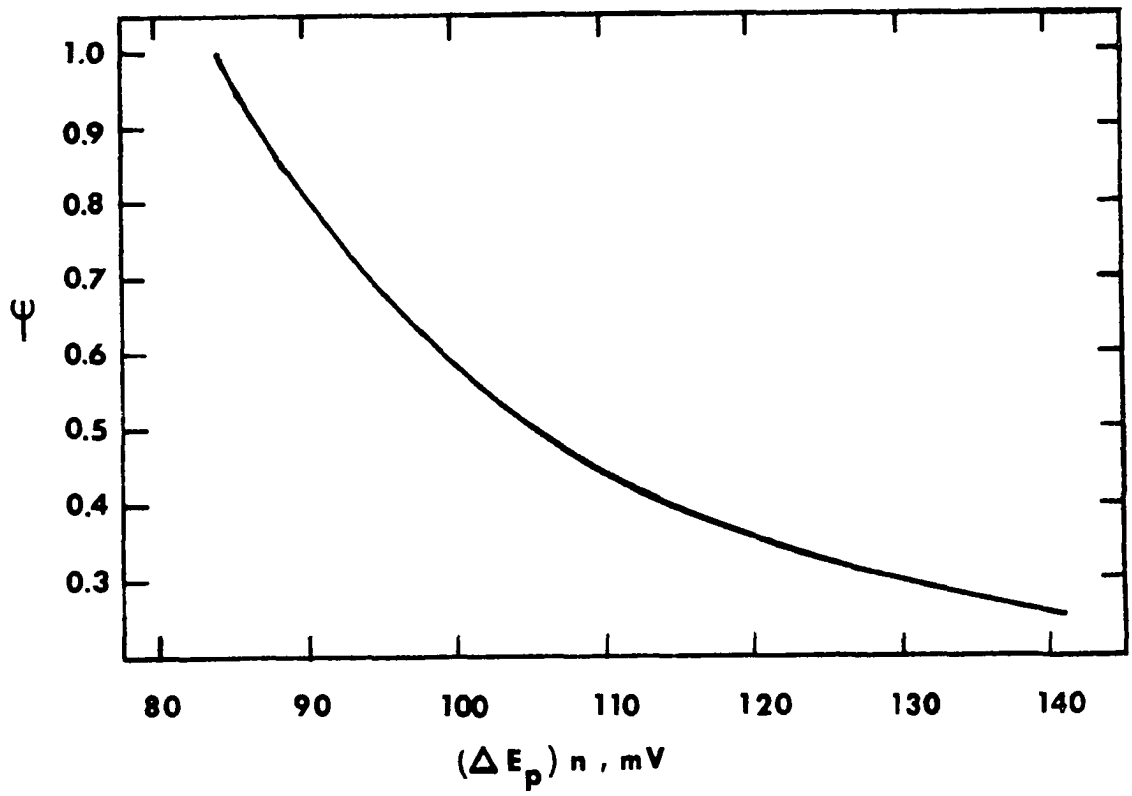

FIGURE A-2-1. Variation of ψ with peak separation. (from ref. 8)

TABLE A-2-1

Variation of ψ with Peak Separation

$(\Delta E_p)n$, mV	ψ	$(\Delta E_p)n$, mV	ψ
61	20	84	1
63	7	92	0.7
64	6	105	0.5
65	5	121	0.35
66	4	141	0.25
68	3	212	0.10
72	2		

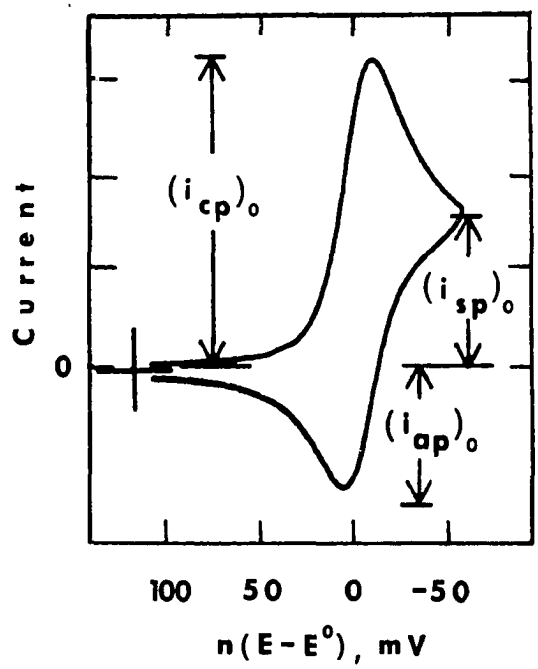

FIGURE A-2-2. Hypothetical cyclic voltammogram for the couple Ox ± ne ⇌ Red.

4.0 and 4.5, so it is best to adjust the switching potential so that a τ falls close to one of these values. Later calculations are somewhat simplified if $a\tau = 4$.

2. Calculation of $a\tau$.

$$a = \frac{nFv}{RT} \qquad \text{(A-2-3)}$$

where n = number of electrons involved in electrode reaction

F = 96,500 coulombs/Faraday

v = voltage sweep rate, V sec^{-1}

R = gas constant, 8.31 joules deg^{-1} mol^{-1}

T = absolute temperature

$$\tau = (E_\lambda - E^\circ)/v \qquad \text{(A-2-4)}$$

where E_λ = switching potential, Volts

E° = potential (Volts) at which $i = 0.85\, i_{cp}$, for a reversible system, or polarographic $E_{1/2}$, if cyclic voltammetry is done at the HMDE

τ = time from E_o to E_λ, sec

combining (A-2-3) and (A-2-4)

$$a\tau = \frac{nF}{RT}(E_\lambda - E^\circ) \qquad \text{(A-2-5)}$$

For n = 2 at 25°C,

$$a\tau = \frac{(2)(96500)}{(8.31)(298)}(E_\lambda - E^\circ) = 77.8\ (E_\lambda - E^\circ) \qquad \text{(A-2-6)}$$

For $a\tau = 4$,

$$(E_\lambda - E^\circ) = \frac{4}{77.8} = 0.0515 \text{ Volts} \cong 50 \text{ mV} \qquad \text{(A-2-7)}$$

Therefore the switching potential should be about 50 mV more negative than E°.

3. Calculation of spherical correction parameter, ρ (not necessary if a planar electrode is used).

$$\rho = \frac{D}{r_o^2 k_2 C_o^*} \qquad \text{(A-2-8)}$$

D = diffusion coefficient of starting material, $cm^2\ sec^{-1}$

r_o = radius of electrode, cm

k_2 = rate constant of dimerization reaction

C_o^* = bulk concentration of starting material

Since ρ depends upon k_2, it is necessary to make a preliminary calculation of k_2 (see (4) below) using $\rho = 0$ in order to solve

eq. (A-2-8).

Example:

For $\rho = 0$, k_2 was calculated to be 2.63×10^2.

$r_o = 0.042$ cm

$D = 5.4 \times 10^{-6}$ cm^2 sec^{-1}

$C_o = 10^{-3}$ moles l^{-1}

$$\rho = \frac{5.4 \times 10^{-6}}{(0.042)^2(2.63 \times 10^2)(10^{-3})} = 0.0116 = 116 \times 10^{-4} \qquad \text{(A-2-9)}$$

It should be noted that changes in k_2 cause changes in ρ. Therefore, whenever k_2 varies (e.g., as with changes in pH), ρ must be recalculated.

4. Calculation of k_2.

$$\log \omega = \log (k_2 C_o^* \tau) + 0.034 (a\tau - 4) \qquad \text{(A-2-10)}$$

Values of ω as a function of i_{ap}/i_{cp} are tabulated in reference 11 for various values of ρ. The value of ρ closest to that calculated in (3) above, should be used. In the example, a ρ value of 100×10^{-4} would be used. When a ρ value is selected, the corresponding i_{ap}/i_{cp} values should be plotted vs ω. Such a plot permits the determination of ω for values of i_{ap}/i_{cp} not tabulated.

In eq. (A-2-10), if $a\tau = 4$, the second term drops out and the expression becomes

$$\log \omega = [\log(k_2 C_o^* \tau)] \qquad \text{(A-2-11)}$$

permitting the calculation of k_2.

For example,

if $\rho = 100 \times 10^{-4}$

and $i_{ap}/i_{cp} = 0.855$,

then $\omega = 0.40$ (from ref. 11).

Let $\tau = 5$ sec

$C_o^* = 10^{-3}$ M

$\log (0.40) = \log k_2 + \log (10^{-3}) + \log (5)$

$- \log k_2 = -3 + 0.7 + 0.4 = - 1.9$

$k_2 = 7.9 \times 10\ M^{-1}\ sec^{-1}$

REFERENCES

1. J. Komenda and D. Laskafeld, Coll. Czech. Chem. Commun., 27, 199 (1962).

2. D. D. Perrin, J. Chem. Soc., 1962, 645.

3. A. Albert, T. J. Batterham, and J. J. MacCormack, J. Chem. Soc. (B), 1966, 1105.

4. L. Meites, Polarographic Techniques, 2nd ed., Wiley, New York, 1965, p. 219.

5. L. Meites, Polarographic Techniques, 2nd ed., Wiley, New York, 1965, pp. 132, 133, 140.

6. P. Delahay, New Instrumental Methods in Electrochemistry, Wiley, New York, 1954, Chap. 3.

7. H. Matsuda and Y. Ayahe, Z. Electrochem., 59, 494 (1955).

8. R. S. Nicholson, Anal. Chem., 37, 1351 (1965).

9. R. S. Nicholson and I. Shain, Anal. Chem., 36, 706 (1964).

10. R. S. Nicholson and I. Shain, Anal. Chem., 37, 178 (1965).

11. M. L. Olmstead, R. G. Hamilton and R. S. Nicholson, Anal. Chem., 41, 260 (1969).

12. R. S. Nicholson, Anal. Chem., 38, 1406 (1966).

13. A. Albert and H. Yamomoto, J. Chem. Soc., 1968C, 2289.

14. A. J. Beaman, J. F. Gerster, and R. K. Robins, J. Org. Chem., 27, 986 (1962).

15. L. Meites, Polarographic Techniques, 2nd ed., Wiley, New York, 1965, p. 240.

16. S. F. Mason, J. Chem. Soc., 1955, 2336.

17. H. Braun and W. Pfleiderer, Ann., 1802 (1973).

18. S. Kwee and H. Lund, Biochem. et Biophys. Acta, 297, 285 (1972).

19. K. Kretzschmer and W. Jaenicke, Z. Naturforsch, 26B, 999 (1971).

20. A. Albert and K. Ohta, J. Chem. Soc., 1970, 1540.

21. J. Pinson and J. Armand, Coll. Czech. Chem. Commun., 36, 385 (1971).

22. T. Goto, A. Tatematsu, and S. Matsuura, J. Org. Chem., 30, 1844 (1965).

23. M. Strier and J. Cavagnol, J. Am. Chem. Soc., 79, 4331 (1957).

24. E. C. Taylor and W. R. Sherman, J. Am. Chem. Soc., 81, 2464 (1959).

25. A. Albert, J. Chem. Soc., 1955, 2690.

26. A. Albert and E. D. Sergeant, J. Chem. Soc., 1964, 3357.

27. A. G. Beaman and R. K. Robins, J. Am. Chem. Soc., 83, 4038 (1961).

28. D. J. Brown, J. Soc. Chem. Ind., 69, 353 (1950).

29. G. Dryhurst, M. Rosen, and P. J. Elving, Anal. Chim. Acta, 42, 143 (1968).

30. R. L. Myers and I. Shain, Chem. Instr., 2, 203 (1969).

31. D. L. McAllister and G. Dryhurst, Anal. Chim. Acta, 64, 121 (1973).

32. E. R. Brown, T. E. McCord, D. E. Smith, and D. D. DeFord, Anal. Chem., 38, 1119 (1966).

CHAPTER 3

ELECTROCHEMICAL REDUCTION OF 6- AND 7-HYDROXYPTERIDINE

Introduction

As outlined in Chapter 2, it is known that under proper chemical conditions 6-hydroxypteridine reacts with 7,8-dihydro-6-hydroxypteridine to form a dihydrodimer.[1,2] The primary reason for initiating a study of the electrochemistry of 6-hydroxypteridine was, then, to discover if this dimerization reaction would proceed with electrochemically generated 7,8-dihydro-6-hydroxypteridine, and, if so, to compare the reaction to that of pteridine. Experiments soon indicated, however, that no dimer was formed during the electrochemical reduction of 6-hydroxypteridine. Nevertheless, the electrochemical reduction of 6-hydroxypteridine did seem to be worthy of investigation, especially in view of the pronounced adsorption effects which were noted. Also, it appeared that the study of the reduction of 6-hydroxypteridine could yield information applicable to the electrochemical reduction of pteridines in general. At all pH values the pyramidine ring of 6-hydroxypteridine is unsaturated, but depending upon pH, the pyrazine ring may be saturated or unsaturated, due to covalent hydration.[1] Study of the electrochemical reduction of 6-hydroxypteridine as a function of pH could show, therefore, whether the pyrazine or pyrimidine

ring is reduced, and also allow conclusions about the effect of covalent hydration upon electrochemical reduction.

Primarily because of its isomeric relationship to 6-hydroxypteridine, the electrochemical reduction of 7-hydroxypteridine was also investigated. Although these compounds are structurally very similar, 7-hydroxypteridine does not undergo covalent hydration. An investigation of 7-hydroxypteridine was accordingly considered of interest since such an investigation could yield information regarding the influence of covalent hydration phenomena on the electrochemistry of such pteridines.

Chemical Properties of 6- and 7-hydroxypteridine. Below a pH of about 7, 6-hydroxypteridine exists primarily as a hydrated species (I, Fig. 3-1A) with water added covalently across the 7,8-bond (i.e., 7-8-dihydro-6,7-hydroxypteridine). At higher pH the principal form of 6-hydroxypteridine is the non-hydrated anion (III, Fig. 3-1A).[3] It appears that the non-hydrated, neutral molecule (II, Fig. 3-1A) does not exist to any appreciable extent in aqueous solution.

Between pH 1.2 and 6.4, 7-hydroxypteridine exists predominantly as the non-hydrated neutral species (II, Fig. 3-1B). At lower pH a non-hydrated cation is formed (I, Fig. 3-1B), while at higher pH a non-hydrated anion is formed (III, Fig. 3-1B).[1,3]

The chemical reduction of 6-hydroxypteridine with potassium borohydride in alkaline solution yields 7,8-dihydro-6-hydroxypteridine (90% yield), and a similar treatment of 7-hydroxypteridine gives 5,6-dihydro-7-hydroxypteridine in 80% yield.[4]

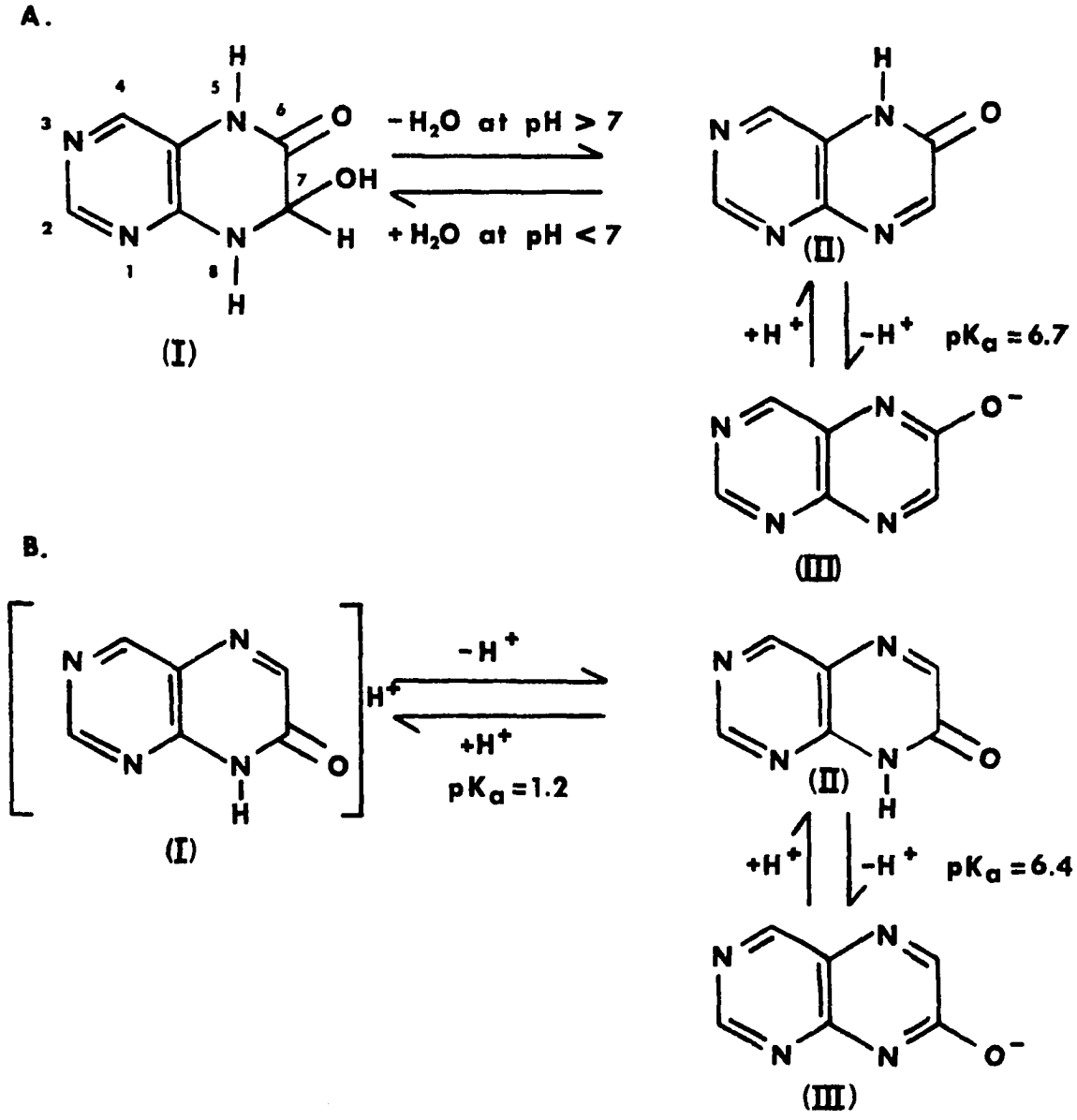

FIGURE 3-1. A. Equilibrium between the neutral hydrated form of 6-hydroxypteridine (I), non-hydrated 6-hydroxypteridine (II), and the non-hydrated anion of 6-hydroxypteridine (III). B. Cationic (I), non-hydrated neutral (II), and anionic (III) forms of 7-hydroxypteridine.

Results and Discussion

6-hydroxypteridine

D.C. Polarography. At pH 7.1 and above, 6-hydroxypteridine exhibits a single polarographic wave, the $E_{1/2}$ of which shifts linearly more negative with increasing pH: $E_{1/2} = -0.162 - 0.064$ pH (Fig. 3-2A). Below pH 7.1 no reduction waves are observed. The height of the wave increases with pH up to pH 10 after which the height remains essentially constant (Fig. 3-3). Kinetic control of the wave might be expected at pH values between about 7-10 where the wave is smaller than its maximum value. In fact, the mercury column height and temperature dependence of the limiting current was indicative of partial kinetic control at pH 7.5 and diffusion control at pH 9.0 and 11.0 (Table 3-1). Kinetic control is indicated by an increase of $i_l/h_{corr}^{1/2}$ with increasing h_{corr} and by a temperature coefficient larger than about 2% per °C.[5] For waves under diffusion control, $i_l/h_{corr}^{1/2}$ is constant with changing h_{corr} and the temperature coefficient is less than 2% per °C.

Over rather well-defined and narrow pH and concentration ranges adsorption effects become apparent in the d.c. polarography of 6-hydroxypteridine. For example, at pH 9.8 at 6-hydroxypteridine concentrations between 0.75 mM and 2.0 mM and at pH 12 at above 4 mM concentrations, a well-defined prewave is observed (Fig. 3-4A). The height of this prewave varied directly with the corrected mercury column height as expected for an adsorption controlled wave[5] (Table 3-2). However, unlike a normal adsorption prewave, its height was greatest at the concentration when it first appeared (e.g., 0.75 mM at pH 9.8) and decreased with increasing 6-hydroxypteridine concentration (Fig.

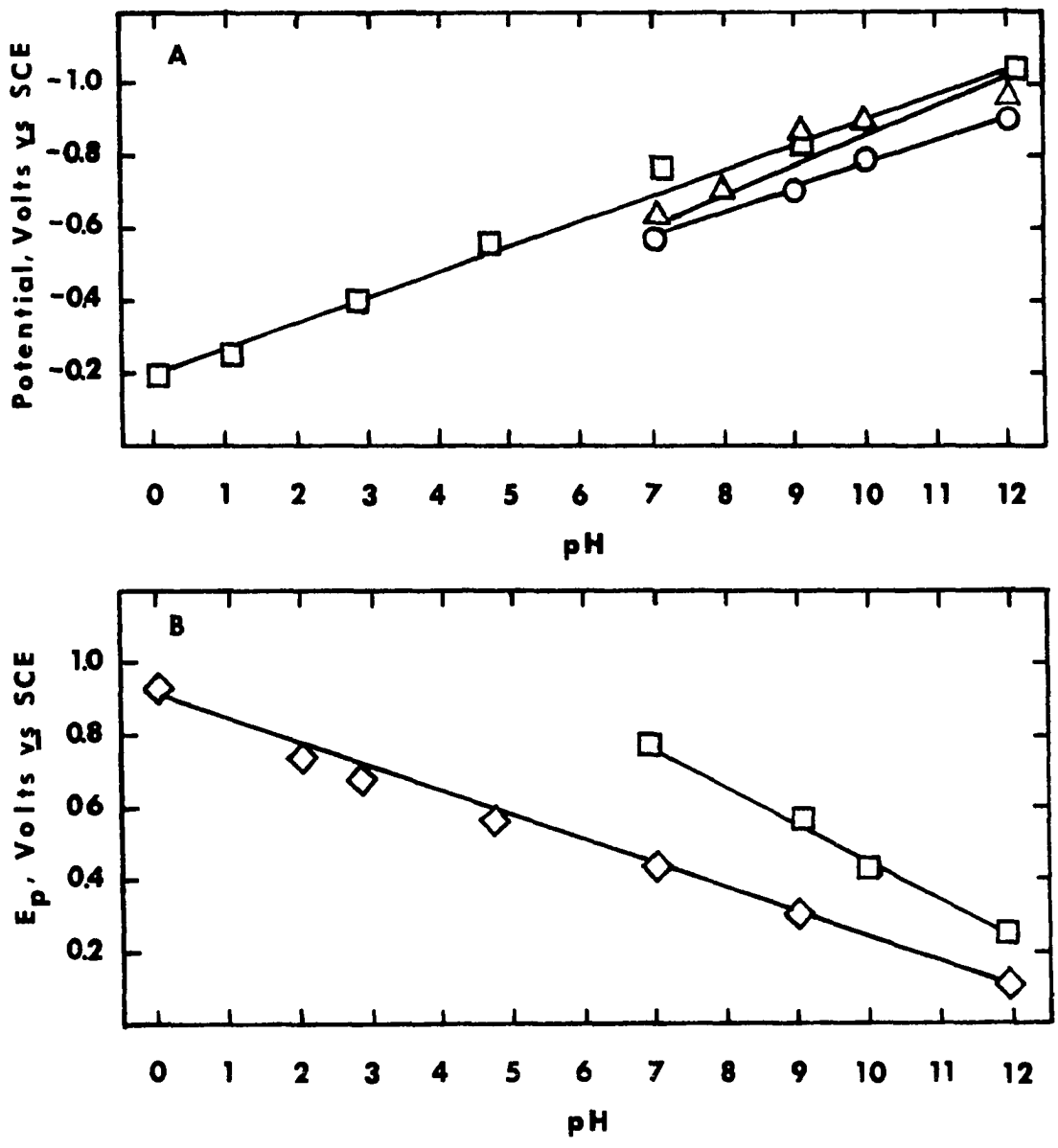

FIGURE 3-2. Variation of $E_{1/2}$ and E_p with pH for 6- and 7-hydroxypteridine. A. O—O = $E_{1/2}$ for 6-hydroxypteridine; Δ—Δ = E_p for cathodic peak of 6-hydroxypteridine at the PGE; □—□ = $E_{1/2}$ for 7-hydroxypteridine. B. ◇—◇ = E_p for anodic peak of 7-hydroxypteridine at the PGE; □—□ = E_p for the anodic peak of 6-hydroxypteridine at the PGE.

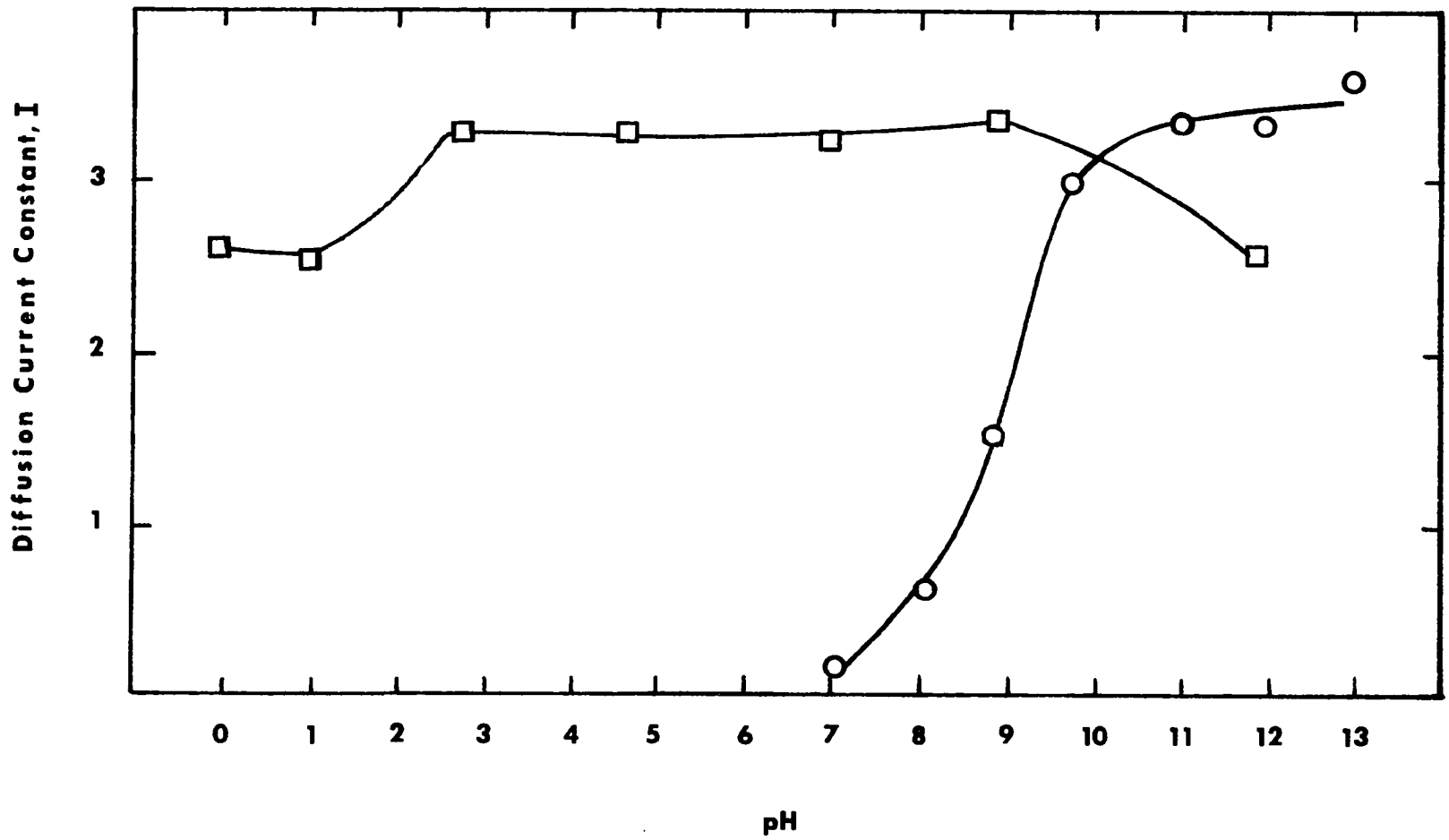

FIGURE 3-3. Variation of the diffusion current constant, I, with pH for 6-hydroxypteridine (○——○) and 7-hydroxypteridine (□——□).

TABLE 3-1

Effect of Corrected Mercury Column Height and Temperature on the Limiting Current for 6-hydroxypteridine

	$i_1/h_{corr}^{1/2}$, $\mu A\ cm^{-1/2}$			Temperature coefficient of i_1[b] percent per °C		
h_{corr}[a], cm	pH 7.5	pH 9.0	pH 11.0	pH 7.5	pH 9.0	pH 11.0
29.8	0.0513	0.697	0.853			
49.8	0.0608	0.703	0.858	3.98	2.06	1.09
69.8	0.0694	0.708	0.861			
89.8	0.0730	0.707	0.865			

[a] $h_{corr} = h_{meas} - \frac{3.1}{(mt)^{1/3}}$

[b] $TC = [\frac{2.303}{T_2-T_1} \log \frac{i_2}{i_1}]\ (100)$

where i_2 is the limiting current at T_2 (40°C) and i_1 the limiting current at T_1 (25°C).

TABLE 3-2

Effect of Mercury Column Height on the Limiting Current of the Prewave for 6-hydroxypteridine in pH 9.8 Borax Buffer at 25°C

h_{corr}, cm	i_1, µA	i_1/h_{corr}, $\mu A\ cm^{-1}$
43.0	1.07	0.025
53.0	1.20	0.023
63.0	1.48	0.024
73.0	1.66	0.023
83.0	1.94	0.023

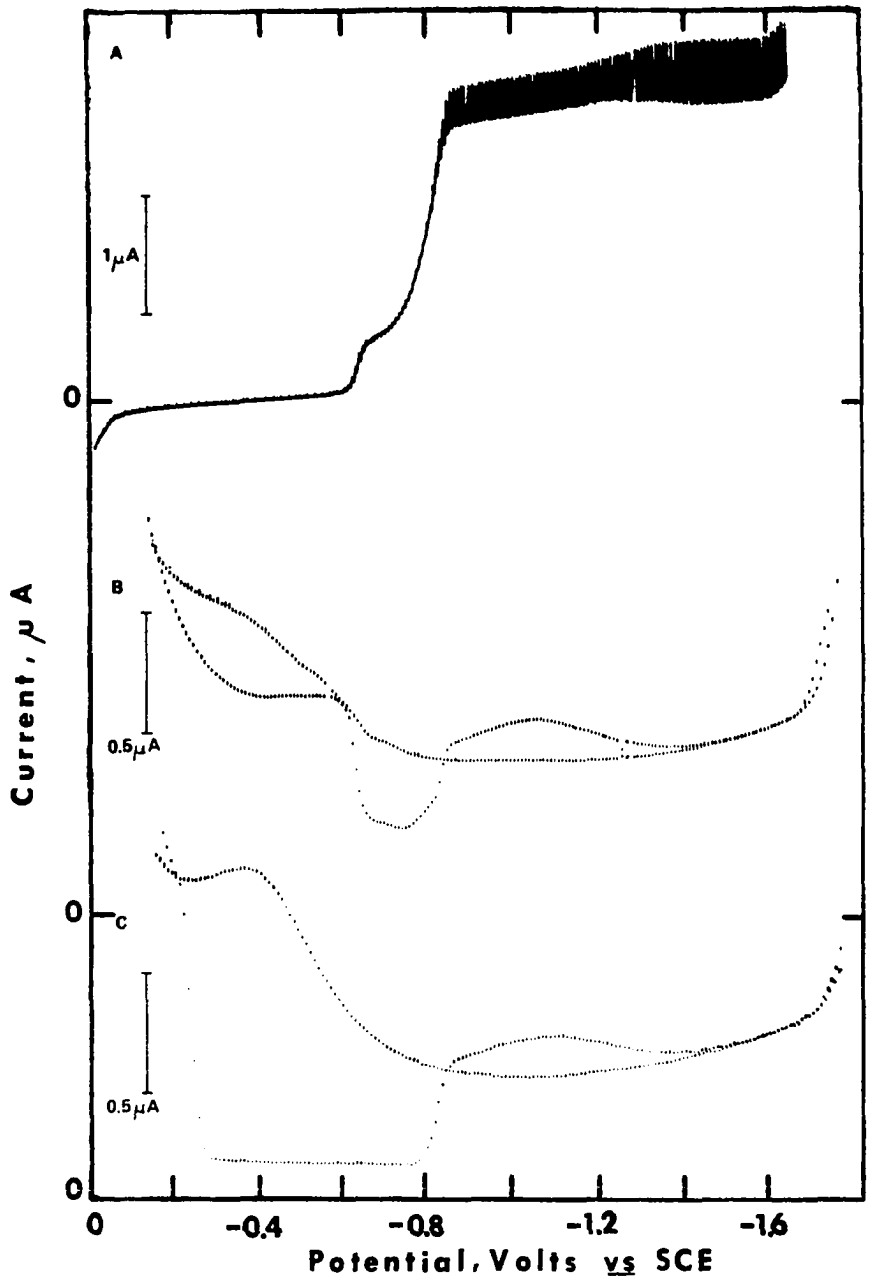

FIGURE 3-4. A. D.c. polarogram of 1 mM 6-hydroxypteridine in pH 9.8 borax buffer.
B. Fundamental a.c. polarogram of 6-hydroxypteridine in pH 9.8 borax buffer.
C. Fundamental a.c. polarogram of 1 mM 7,8-dihydro-6-hydroxypteridine in pH 9.8 borax buffer.
Applied a.c. signal, 100 Hz, 10 mV peak-to-peak.

3-5A). The same behavior was observed at higher pH. Thus at pH 12 the prewave appears at 4 mM 6-hydroxypteridine concentration and decreases in height at higher concentrations. At 6-hydroxypteridine concentrations where the prewave first appears, the $E_{1/2}$ for the principal wave shifts to more negative potentials and continues to do so with increasing concentration (Fig. 3-5B). The $E_{1/2}$ for the prewave, however, shifts to more positive potentials with increasing concentration (Fig. 3-5B). This information, in conjunction with a.c. polarographic data (vide infra), implies that the appearance of the prewave is due to a shift of $E_{1/2}$ for the reduction of 6-hydroxypteridine upon coverage of the electrode surface with an adsorbed layer of reduction product, 7,8-dihydro-6-hydroxypteridine. According to Heyrovský and Kuta,[6] the inhibitory action of surface-active substances that form compact films on the electrode is caused by repulsive forces between molecules reaching the electrode and particles of the adsorbed layer. The penetration of molecules through the film requires a certain energy of activation, which is necessary to overcome the additional energy barrier caused by the presence of the film.

At high 6-hydroxypteridine concentrations (e.g., 5 mM) at pH 9.8 a maximum of the second kind is observed in d.c. polarography (Fig. 3-6A). The a.c. peak appearing in Fig. 3-6B and corresponding to the d.c. wave in Fig. 3-6A is a faradaic wave observed only at high (2-5 mM) concentrations of 6-hydroxypteridine.

At pH 8.1 over the concentration range 0.8-2 mM a small wave is observed at potentials more negative than the main reduction wave (Fig. 3-7A). For reasons discussed below, it is concluded that this

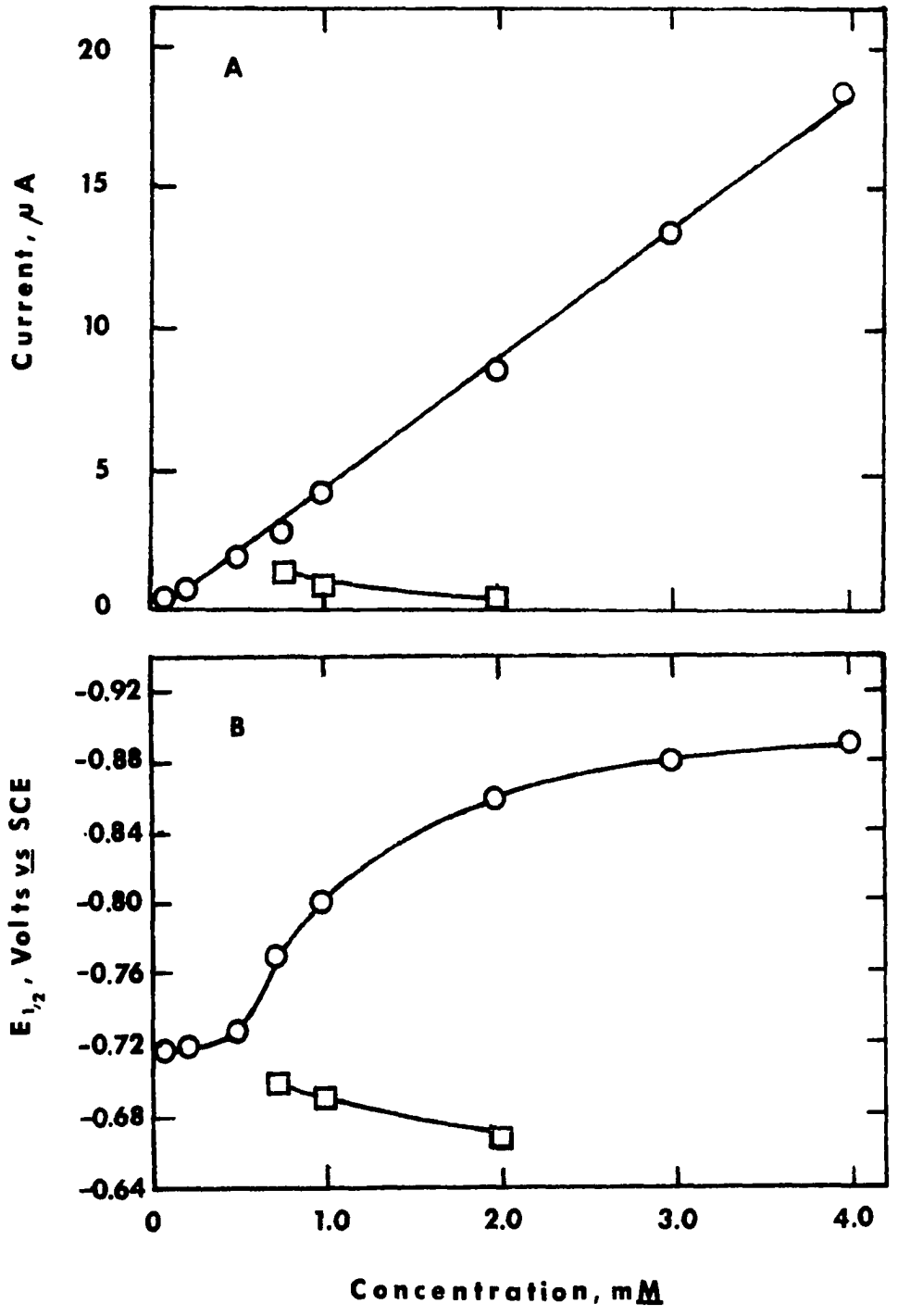

FIGURE 3-5. Variation of wave height (A) and $E_{1/2}$ (B) with concentration for 6-hydroxypteridine in pH 9.8 borax buffer. ○——○, main wave; □——□ prewave.

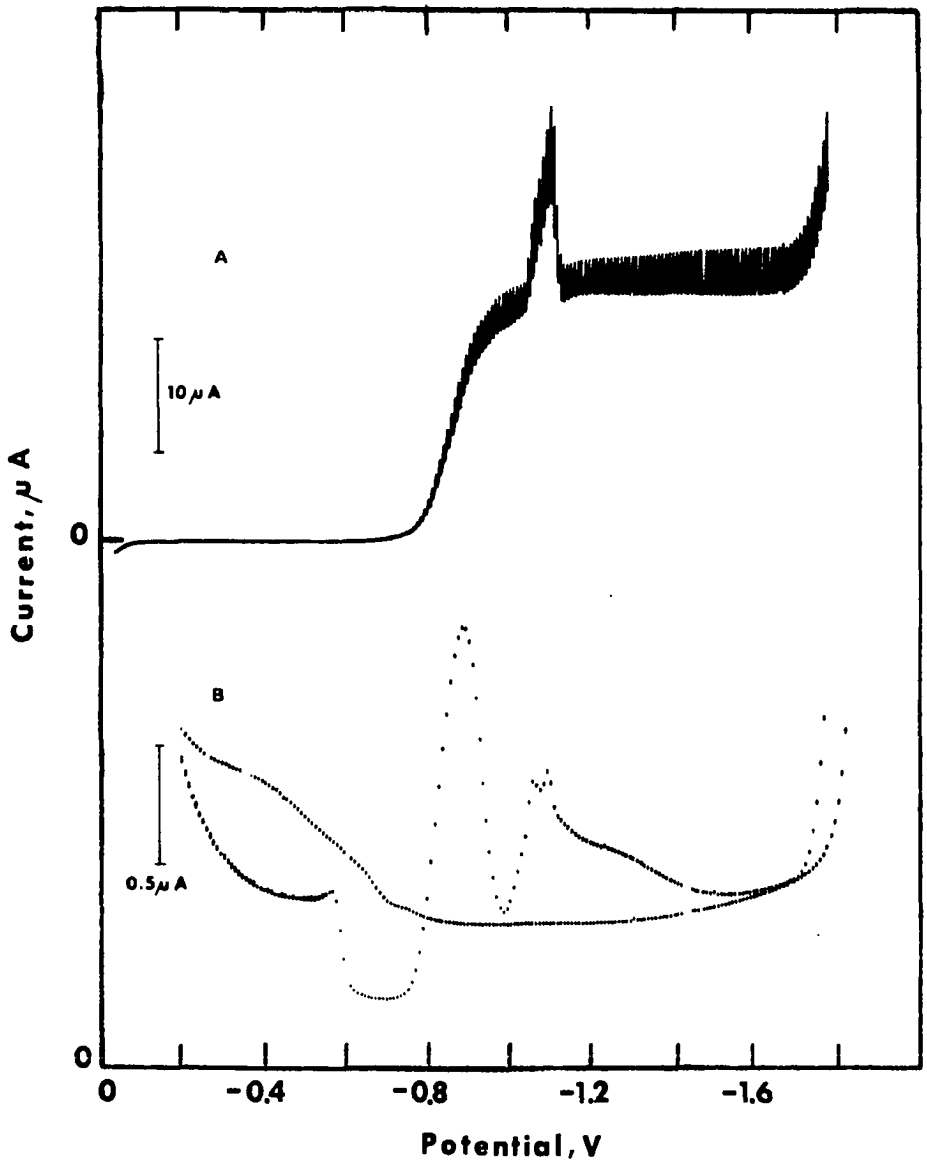

FIGURE 3-6. A. D.c. polarogram of 5 mM 6-hydroxypteridine in pH 9.8 borax buffer.
B. Fundamental d.c. polarogram of 5 mM 6-hydroxypteridine in pH 9.8 borax buffer.
Applied a.c. signal, 100 Hz, 10 mV peak-to-peak.

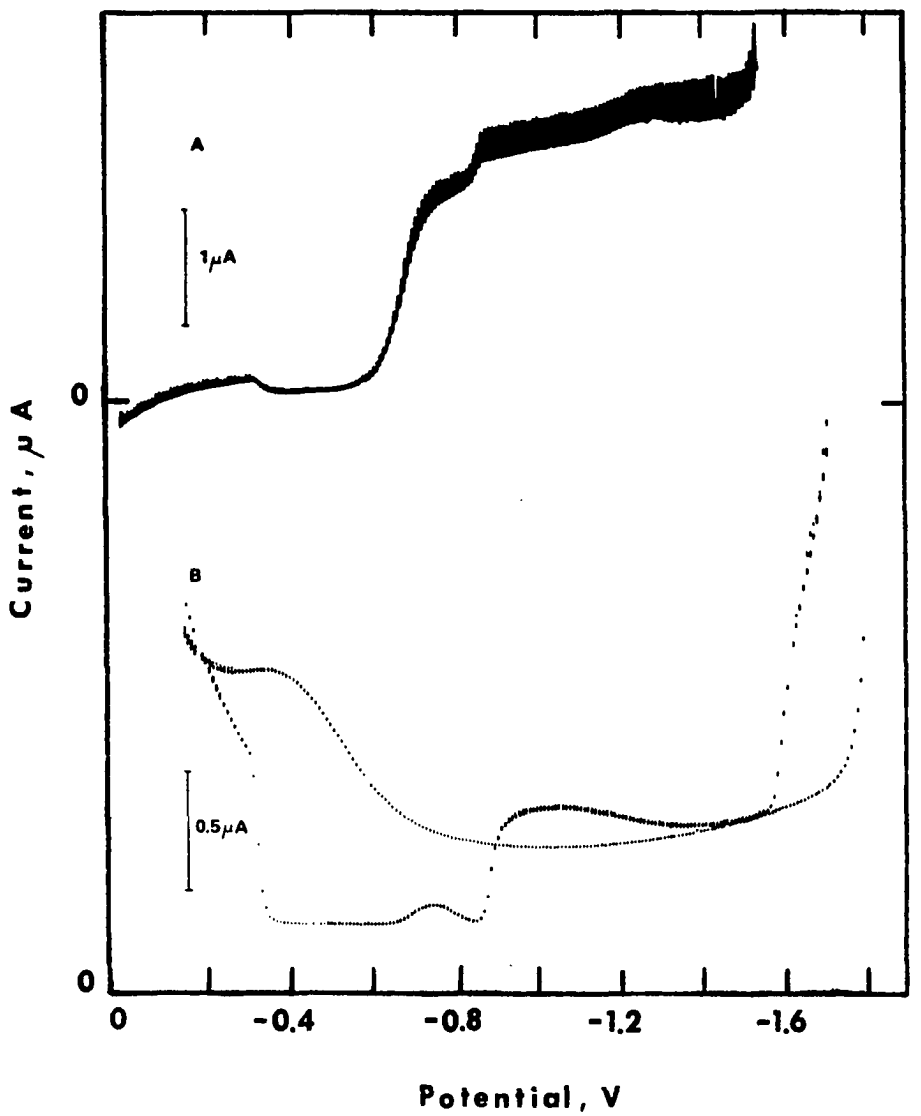

FIGURE 3-7. A. D.c. polarogram of 1 mM 6-hydroxypteridine in pH 8.1 borax buffer.
B. Fundamental a.c. polarogram of 1 mM 6-hydroxypteridine in pH 8.1 borax buffer.
Applied a.c. signal 100 Hz, 10 mV peak-to-peak.

wave is a so-called "capacity" wave.[7]

A.C. Polarography. Before discussing the application of a.c. polarography to the present investigation, a brief description of the method and its application to studies of adsorption at electrodes will be presented.

The term "electrical double layer" or simply "double layer" refers to the interfacial region formed by an electrode dipping into an electrolyte solution. The double layer may be divided into three main parts: (a) the electrode phase, (b) an inner layer of ions adsorbed on or attracted to the electrode, and (c) an outer or diffuse layer which extends into the bulk of the solution. For example, if an electrode at a potential of -1.0 Volts vs SCE is immersed in a solution of potassium chloride, chloride ions will be repelled from the electrode surface while potassium ions will be attracted to it. The separation of electrical charge caused by the negative charge at the surface of the electrode and the layer of positively charged solution adjacent to it is equivalent to the charging of an electrical capacitor. Any material which is preferentially adsorbed at the electrode will change the nature of the double layer and will consequently change the capacity associated with it. Measurement of the capacity of the double layer can therefore yield information related to adsorption at the electrode surface.

One of the simplest and most direct methods used in the measurement of double layer capacity is a.c. polarography. If an alternating signal of low amplitude (10 mV peak-to-peak) and relatively low frequency (100 Hz) is superimposed upon the d.c. potential applied to

the electrode, the alternating current which flows can be directly related to differential double layer capacity (i.e., capacity per unit area), if no depolarizers are present, and if the solution is sufficiently conductive (i.e., supporting electrolyte concentration > 0.1 M in aqueous solution), by the equation:[8]

$$I = CSU\omega \qquad (3\text{-}1)$$

where I = alternating base current, μA

C = differential capacity, μFcm^{-2}

S = surface area of electrode, cm^2

U = amplitude of superimposed a.c. signal, Volts

ω = angular frequency of applied a.c. signal = $2\pi f$, where f is the frequency, Hz.

"Alternating base current" refers to the alternating current observed in the presence of background electrolyte alone.

Over the pH range 3.7 - 9.8, 6-hydroxypteridine causes base current depressions in a.c. polarography indicative of adsorption phenomena at the electrode surface (Figs. 3-4B, 3-6B, and 3-7B). Below pH 7.1, where 6-hydroxypteridine is not electrochemically reducible, the depression must correspond to the adsorption of the hydrated neutral molecule (see Fig. 3-1). In this region it is observed that at concentrations below 0.4 mM, 6-hydroxypteridine gives a broad depression that becomes deeper with increasing concentration (Fig. 3-8ABCD). At about the 0.3 - 0.4 mM concentration level, a very well-defined pit or well is observed (Fig. 3-8E). Further increase of the 6-hydroxypteridine concentration causes no further increase in the depth of the pit, but the potential range over which it occurs increases. Typical

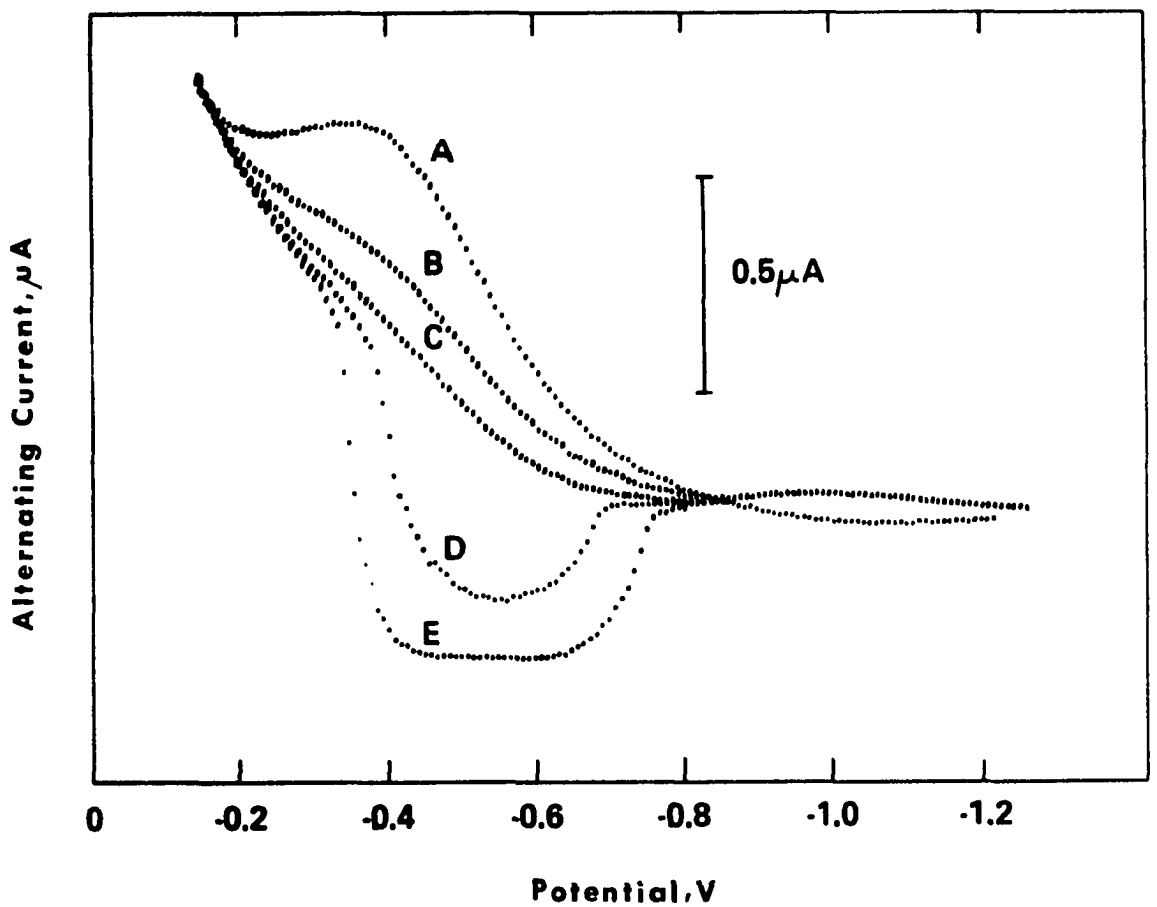

FIGURE 3-8. Fundamental a.c. polarograms of 6-hydroxypteridine at various concentrations in pH 5.6 McIlvaine buffer. (A) Background; (B) 0.1 mM; (C) 0.2 mM, (D) 0.3 mM; (E) 0.4 mM. Applied a.c. signal, 100 Hz, 10 mV peak-to-peak.

data obtained at pH 7.1 is shown in Fig. 3-9 where, for example, it is seen that at the 1 mM concentration level the pit extends from -0.2 V to -0.92 V. Similar curves with only minor variation are observed at other pH values below 7. Depression of the base current at low concentration followed by formation of a sharply defined pit or well in a.c. polarography has been reported, for certain biologically important purine and pyrimidine derivatives, as being indicative of simple adsorption at low concentrations followed by intermolecular association of the adsorbed molecules at higher concentrations.[9,10,11] The adsorbed molecules upon association no doubt form a continuous film on the electrode surface which is reflected in the pronounced decrease in the double layer capacity. The sharply defined walls of the pit reflect the potentials where tears or rips appear in the surface film. As pH is increased above 7.1 the potential range over which the pit extends decreases with increasing pH for a given concentration of 6-hydroxypteridine.

At pH 9.8 a sharp current depression or pit does not appear until a potential is reached sufficient to cause reduction of 6-hydroxypteridine. At pH 9.8 the base current is also depressed in the form of a pit by 7,8-dihydro-6-hydroxypteridine. This pit begins at a potential considerably less negative than that produced by 6-hydroxypteridine at the same pH, but ends at the same potential (Fig. 3-4C). Variations of the potential range of the depression with concentration for 7,8-dihydro-6-hydroxypteridine are very similar to those noted for 6-hydroxypteridine at lower pH, e.g., pH 5.6-7. In these pH regions it will be recalled that the latter compound exists as the

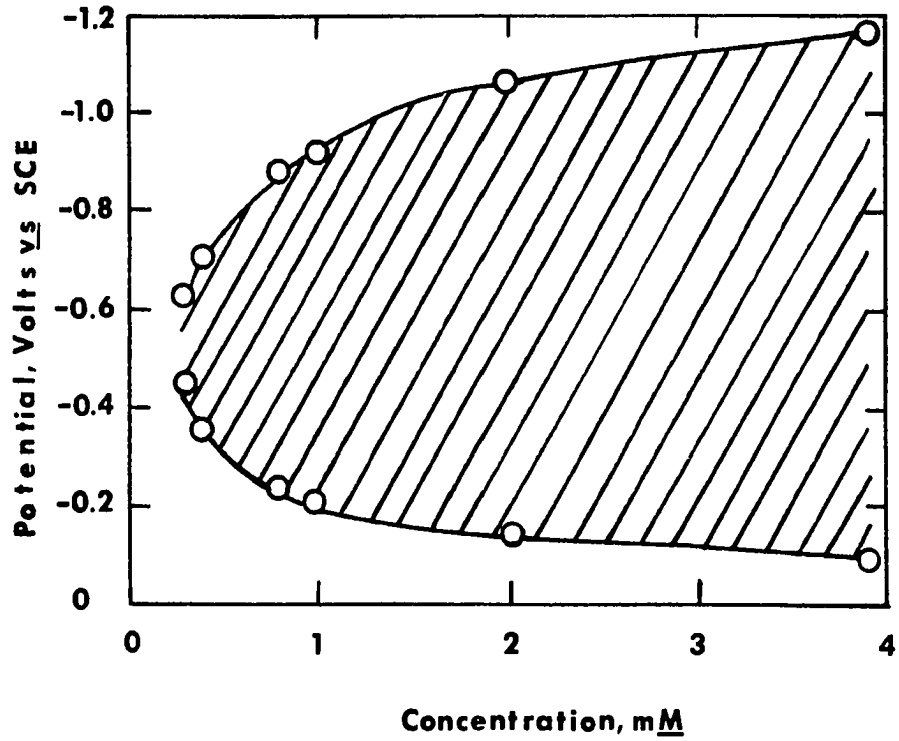

FIGURE 3-9. Potential range of the sharp depression (pit or well) observed in a.c. polarography of 6-hydroxypteridine at pH 7.1 as a function of concentration.

uncharged 7,8-dihydro-6,7-dihydroxypteridine.

At pH 9.8 to 12.5 a smaller depression of the a.c. base current is produced by 6-hydroxypteridine at potentials less negative than the pits and the faradaic d.c. peak (Fig. 3-4B). Such a depression indicates adsorption of the reactant, which at these pH values is the non-hydrated anion of 6-hydroxypteridine.

Using equation (3-1), a.c. polarographic data of the type shown in Fig. 3-8 can easily be converted to differential capacity data which is more readily compared to previous reports of adsorption. Plots of C_o-C (C_o = differential capacity in supporting electrolyte alone) vs concentration are shown in Fig. 3-10 for 6- and 7-hydroxypteridine and their dihydro derivatives. The initial increase in C_o-C (0-0.2 mM) is caused by specific adsorption of the hydroxypteridine. In the case of 6-hydroxypteridine and 7,8-dihydro-6-hydroxypteridine, the sharp rise in C_o-C at 0.2 - 0.3 mM is, by analogy with the reports of Vetterl,[10] most likely caused by association of the adsorbed molecules.

The kinetics of these adsorption-association processes were studied by recording alternating current vs time curves at the hanging mercury drop electrode (HMDE). Plots of differential capacity as a function of time for various concentrations of 6-hydroxypteridine are shown in Fig. 3-11. For higher concentrations (0.3 - 0.5 mM) adsorption-association occurs so rapidly that only the fully associated state is observed experimentally. At lower concentrations (i.e., below about 0.2 mM), the curve can be divided into three distinct portions: a gently sloping initial portion, probably representing simple adsorption; a steeper central part in which association occurs; and a final linear

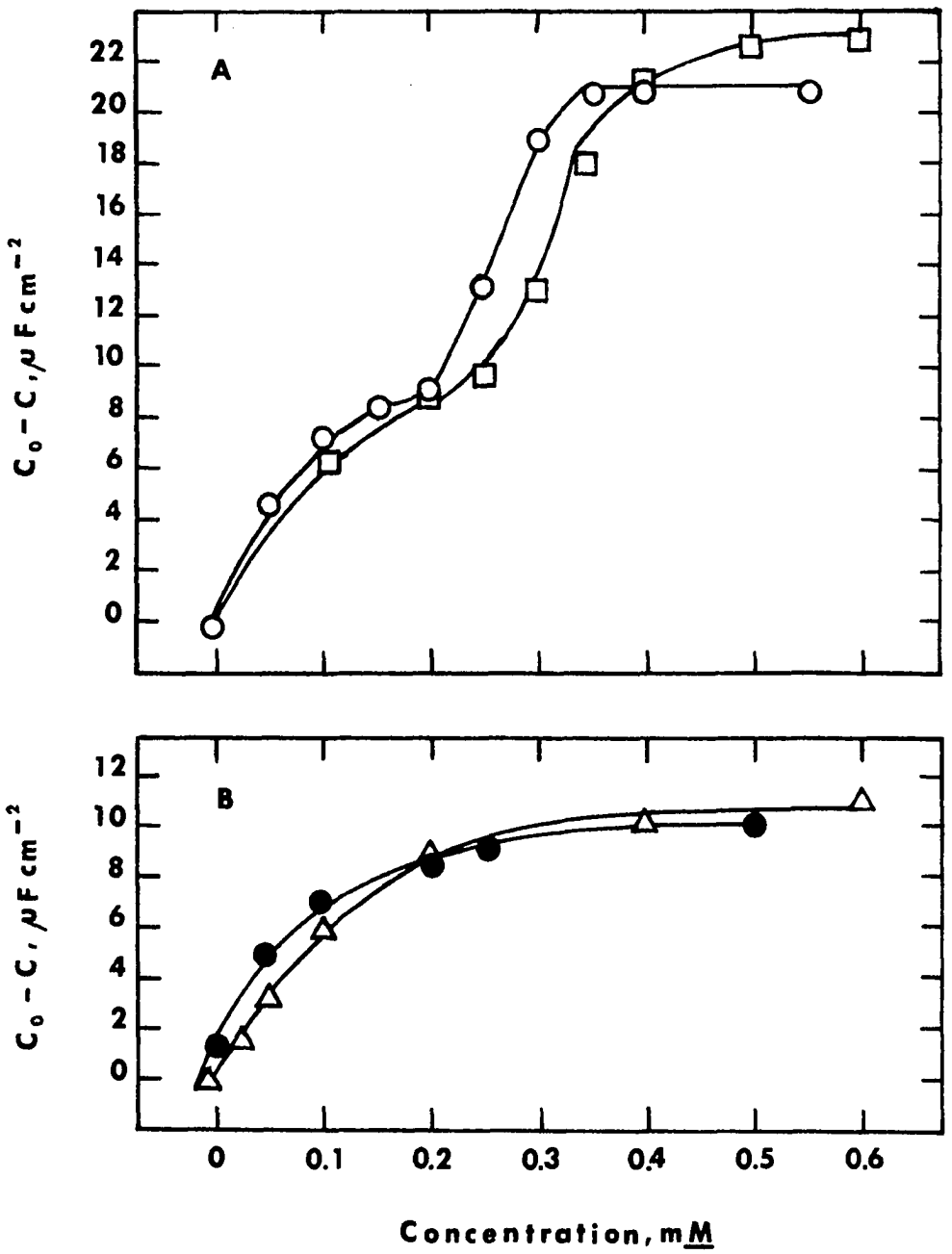

FIGURE 3-10. Change in differential capacity at -0.55 V as a function of concentration for (A) ○——○, 6-hydroxypteridine, pH 6.0; □——□, 7,8-dihydro-6-hydroxypteridine, pH 9.8. (B) △——△, 7-hydroxypteridine, pH 6.0; ●——●, 5,6-dihydro-7-hydroxypteridine, pH 6.0.
At the DME, t = 2.00 sec. Applied a.c. signal, 100 Hz, 10 mV peak-to-peak.

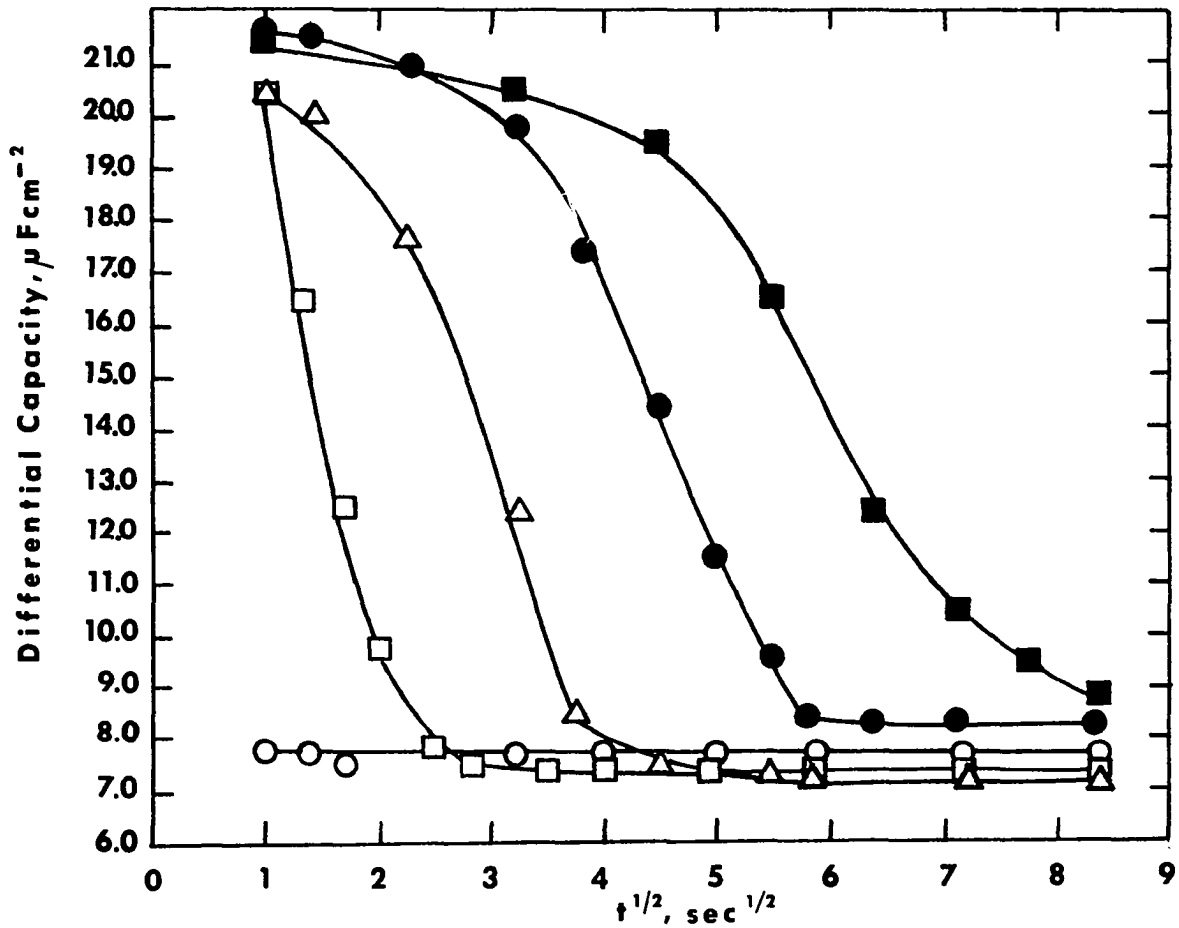

FIGURE 3-11. Differential capacity vs $t^{1/2}$ curves for 6-hydroxypteridine at pH 6.0 at the HMDE. ○—○, 0.5 mM; □—□, 0.2 mM; △—△, 0.17 mM; ●—●, 0.15 mM; ■—■, 0.13 mM. Electrode area, 0.022 cm^2. Potential, -0.55 V vs SCE. Applied a.c. signal, 100 Hz, 10 mV peak-to-peak.

portion representing complete surface coverage and association. Although it has been postulated that the change in differential capacity of an electrode (C_o-C) is directly proportional to the fraction of the surface covered with adsorbed molecules,[12] there appears to be some disagreement on this point.[13] In the present case, if the adsorption of 6-hydroxypteridine is diffusion controlled, the slope of the differential caapcity vs $t^{1/2}$ plot should not change when association begins unless upon intermolecular association the differential capacity is not proportional to surface coverage, or the differential capacity changes in a more pronounced fashion when association occurs. The fact that the first two portions of the curve are approximately proportional to $t^{1/2}$ supports the view that the processes occurring in both regions are diffusion controlled.[14] This suggests, therefore, that upon initiation of intermolecular association the differential capacity of the electrode is affected more drastically than when simple adsorption occurs. That is, the rate of diffusion of molecules to the electrode surface cannot increase when association begins, so the differential capacity must change significantly with only a relatively small change in surface coverage during film formation.

It should also be noted that at concentrations of 6-hydroxypteridine of 0.12 mM and below, differential capacity vs $t^{1/2}$ curves did not have the appearance of the curves shown in Fig. 3-11. In fact, at these concentrations only a single gently sloping curve was obtained, similar to the initial portion of the curves observed at higher concentrations. This curve ultimately leveled off and became essentially time invariant. This behavior at concentrations of 0.12 mM and below suggests that the

equilibrium between adsorbed 6-hydroxypteridine and that in solution is such that insufficient compound can be adsorbed to permit association to occur.

In view of the shape of the differential capacity vs $t^{1/2}$ curves of the type shown in Fig. 3-11, it should be pointed out that the form of the adsorption isotherms, especially those for 6-hydroxypteridine and 7,8-dihydro-6-hydroxypteridine of the type shown in Fig. 3-10A, depends to a large extent upon the drop time employed. That is, at longer drop times, the sharp inflection in the curves occurs at lower concentrations.

The overall a.c. polarographic and differential capacity behavior indicates therefore that the non-electroactive 7,8-dihydro-6,7-dihyroxypteridine is adsorbed at mercury and above a concentration of ca. 0.2 - 0.3 mM associates on the electrode surface. The electroactive form of 6-hydroxypteridine is the non-hydrated anion. This is not adsorbed nearly so strongly as the hydrated neutral species. The product of the electrochemical reduction of the anionic form of 6-hydroxypteridine is also strongly adsorbed and associates on the electrode surface in much the same way as 7,8-dihydro-6,7-dihydroxypteridine. Further discussion of adsorption-association phenomena will be presented later.

A.c. polarography of 6-hydroxypteridine at pH 8.1 where a small wave is observed on the plateau of the d.c. wave reveals that at potentials corresponding to the small d.c. wave a very sharp rise in the alternating current occurs (Fig. 3-7AB). By comparison of the a.c. and d.c. polarograms, it is apparent that the d.c. wave is due

to an abrupt change in the double layer capacity rather than to an electrochemical reaction, i.e., it is a capacity wave. In addition, it can be noted that at a potential of about -0.3 V, where a sudden decrease in a.c. base current occurs, (Fig. 3-7B), a corresponding decrease occurs in the d.c. charging current (Fig. 3-7A). The increase or decrease in d.c. current always occurs at potentials corresponding to sharp increases or decreases of a.c. current even though these potentials change as the concentration of 6-hydroxypteridine is changed. The magnitude of the capacity wave does not change appreciably with concentration of 6-hydroxypteridine over the range 0.5 - 4.0 mM. This behavior indicates that the wave is not faradaic in nature.

Linear Sweep and Cyclic Voltammetry at the PGE. Generally, a single well-defined cathodic peak is observed for 6-hydroxypteridine at the PGE. The peak potential shifts linearly more negative with increasing pH: E_p = -0.232 - 0.064 pH (Fig. 3-2). At certain sweep rates, concentrations, and pH values, an adsorption pre-peak may often be observed (Fig. 3-12). The adsorption nature of the pre-peak is readily established by sweep rate and concentration studies. The theoretical equation of a linear diffusion controlled irreversible peak voltammogram is:[15]

$$(i_p)_{irrev} = 2.98 \times 10^5 n(\alpha n_a)^{1/2} A D^{1/2} v^{1/2} C \qquad (3\text{-}2)$$

where $(i_p)_{irrev}$ = total peak current, μA

n = total number of electrons transferred in the electrochemical process

n_a = number of electrons involved in the initial electron transfer process

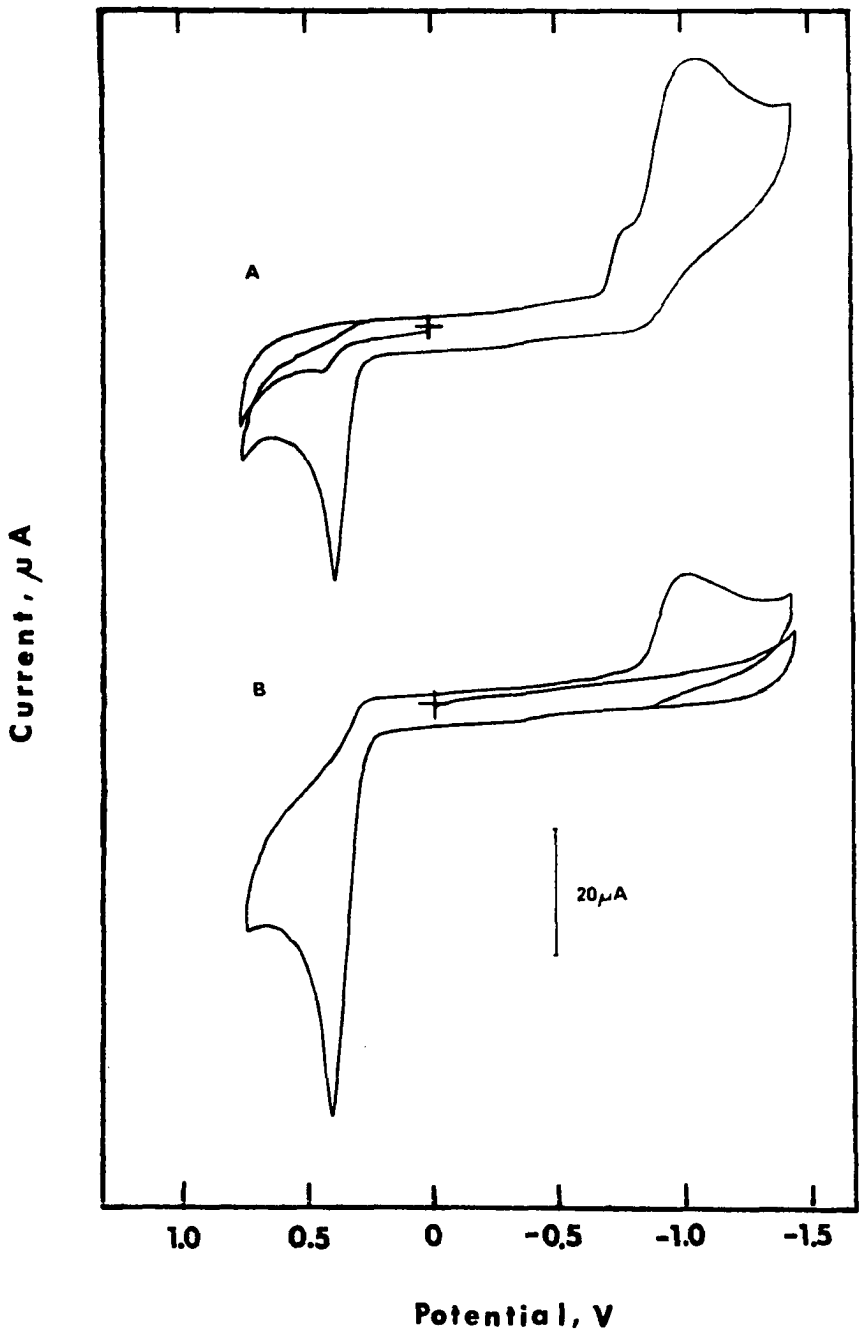

FIGURE 3-12. Cyclic voltammograms of (A) 6-hydroxypteridine and (B) 7,8-dihydro-6-hydroxypteridine at the PGE in pH 11.1 borax buffer. Scan rate 50 mV sec^{-1}. Scan pattern (A) 0.00 V → 0.75 V → -1.50 V → 0.75 V → 0.00 V. (B) 0.00 V → -1.50 V → 0.75 V → -1.50 V → 0.00 V. Current above axis marker is cathodic, below axis marker is anodic.

α = electron transfer coefficient

A = electrode area, cm^2

D = diffusion coefficient of electroactive species, $cm^2\ sec^{-1}$

v = voltage sweep rate, Volts sec^{-1}

C = concentration of electroactive species, mM

According to equation (3-2), the peak current function, $i_p/ACv^{1/2}$, should remain constant with variation in scan rate, and a plot of i_p/C vs C should be linear and parallel to the concentration axis. Thus, for 6-hydroxypteridine, the peak current function ($i_p/ACv^{1/2}$) for the main reduction peak (total peak current above background) is essentially invariant with $v^{1/2}$. However, the peak current function for the pre-peak increases dramatically with increasing voltage sweep rate (Fig. 3-13A), typical of an adsorption controlled process.[16] In addition, a plot if i_p/C vs C for the total peak current is linear and parallel to the concentration axis. However, for the pre-peak a decrease of i_p/C with increasing concentration is noted up to concentrations of 0.4 - 0.6 mM after which i_p/C becomes more or less constant (Fig. 3-13B). This behavior of the pre-peak is typical of a process where the product of an electrode reaction is adsorbed.[15]

Cyclic voltammetry of 6-hydroxypteridine at the PGE exhibits a single cathodic peak on the initial sweep towards negative potentials. On the reverse sweep, a single oxidation peak is observed (Fig. 3-12A). The peak potential for the anodic peak shifts linearly to more negative potentials with increasing pH: $E_p = 1.45 - 0.10$ pH (Fig. 3-2B). Cyclic voltammetry of the reduction product at the PGE is identical with that for 7,8-dihydro-6-hydroxypteridine. Cyclic voltammetry also reveals that 7,8-dihydro-6-hydroxypteridine regenerates 6-hydroxypteridine

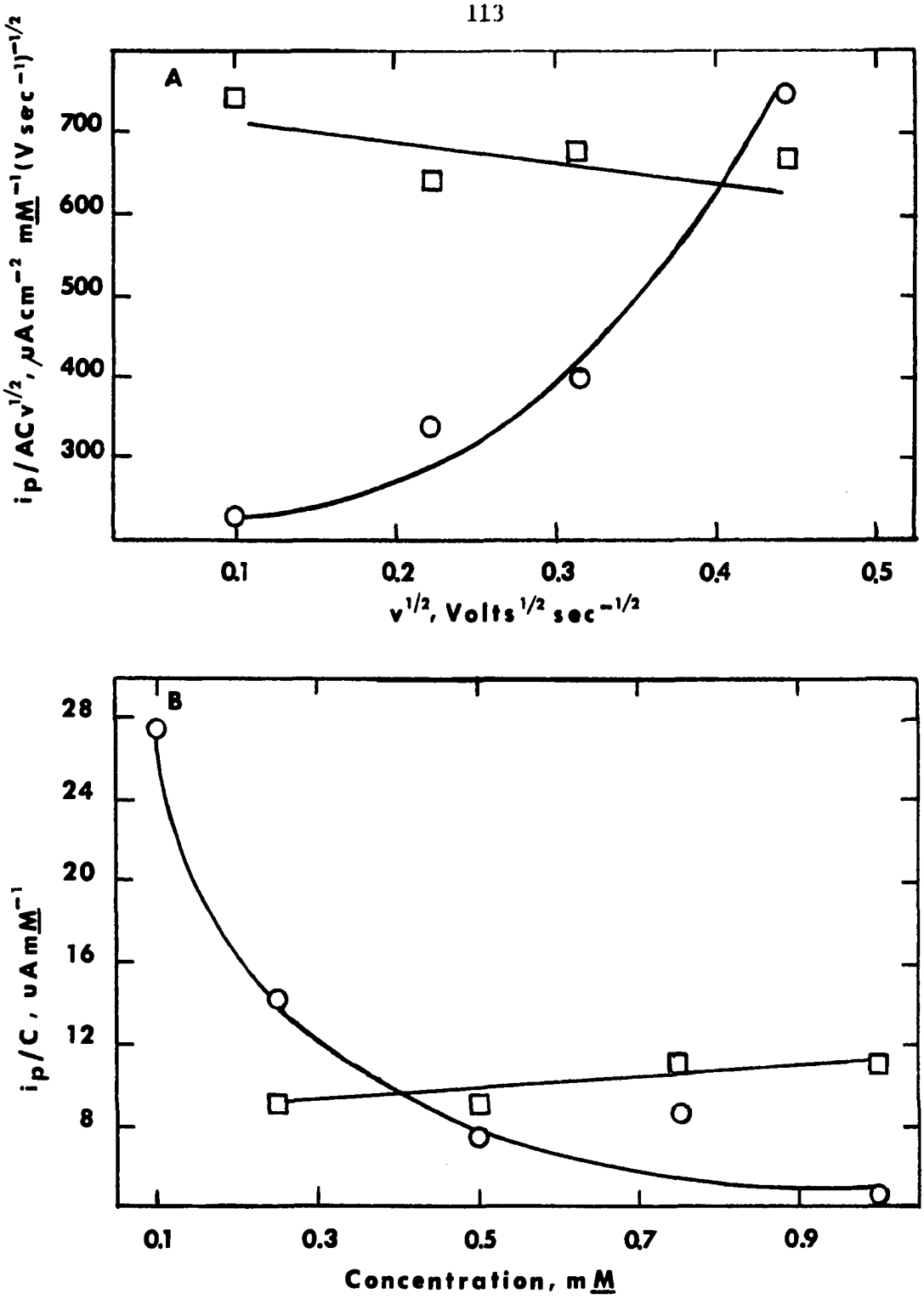

FIGURE 3-13. Variation of (A) peak current function ($i_p/ACv^{1/2}$) with square root of scan rate, and (B) i_p/C with concentration for 6-hydroxypteridine main reduction peak (□——□) and prepeak (○——○), at the PGE.

upon electrochemical oxidation (Fig. 3-12B).

Controlled Potential Electrolysis and Coulometry. Electrochemical reduction of 6-hydroxypteridine at both mercury pool and pyrolytic graphite electrodes over the pH range 8.1 - 12.0 gives faradaic n-values ranging from 1.83 - 2.09 (Table 3-3). In each case, the UV spectrum of the product was identical with authentic 7,8-dihydro-6-hydroxypteridine (Table 3-4). In addition, voltammetry of the product and authentic 7,8-dihydro-6-hydroxypteridine at the PGE gave identical peak potentials (Table 3-4). Thus the product of the electrochemical reduction of the anion of 6-hydroxypteridine is 7,8-dihydro-6-hydroxypteridine.

Quantitative analysis of the product by UV spectrophotometry revealed that 95-100 percent of 6-hydroxypteridine originally present in an electrolysis solution could be accounted for as 7,8-dihydro-6-hydroxypteridine.

Interpretation of Adsorption-Association Phenomena. The a.c. polarographic and differential capacity data clearly support the view that 7,8-dihydro-6,7-dihydroxypteridine and 7,8-dihydro-6-hydroxypteridine are strongly adsorbed at mercury. In addition, at bulk concentrations in excess of ca. 0.13 mM association of the adsorbed molecules occurs, although at 0.13 mM association is observed to occur only after a long time (20-60 sec.). The higher the bulk concentration, the more rapidly the association effects become apparent.

It is noticeable that both of the compounds mentioned above are structurally very similar, differing only in the presence of a hydroxyl group at position 7. Further examination reveals the possibility of hydrogen bonded polymers in the case of both the hydrated neutral form

TABLE 3-3

Coulometric n-values for the Electrochemical Reduction of 6-hydroxypteridine

Buffer system	pH	Electrode	Electrolysis potential Volts vs SCE	n-value
Borax	8.1	Mercury[a]	-0.90	1.83
Borax	8.1	Pyrolytic Graphite[b]	-0.90	1.88
Borax	9.8	Mercury	-1.00	1.97
Borax	9.8	Pyrolytic Graphite	-1.00	2.09
Hydroxide	11.9	Pyrolytic Graphite	-1.20	1.96
1 N NaOH		Mercury	-1.10	1.89
2 N Na_2CO_3		Mercury	-1.00	1.94

[a] Stirred mercury pool, area = 3.8 cm^2

[b] Area = 10.4 cm^2

TABLE 3-4

Comparison of UV Spectra and Voltammetric Oxidation Peak Potentials for 7,8-dihydro-6-hydroxypteridine and Product of Electrochemical Reduction of 6-hydroxypteridine

		Electrochemical product		7,8-dihydro-6-hydroxypteridine	
Buffer system	pH	Peak potential Volts vs SCE	λ_{max} nm	Peak potential Volts vs SCE	λ_{max} nm
Borax	8.1	0.60	289	0.60	290
Borax	9.8	0.50	293	0.50	293
Hydroxide	11.9	0.28	306	0.29	305

of 6-hydroxypteridine (7,8-dihydro-6,7-dihydroxypteridine) and 7,8-dihydro-6-hydroxypteridine. In view of this, it is tentatively proposed that the behavior of 7,8-dihydro-6,7-dihydroxypteridine at pH <7.1 and 7,8-dihydro-6-hydroxypteridine at pH values above and below 7 is as follows. At low concentrations (i.e., below 0.13 mM) simple adsorption occurs with a corresponding decrease of alternating base current and hence differential capacity. At bulk concentrations in excess of ca. 0.13 mM, association of the adsorbed molecules occurs with formation of a continuous polymeric film. At the 0.13 mM concentration level the initiation and completion of the intermolecularly associated film takes a long time (∿1 min.) so that under normal a.c. polarographic conditions association is not observed. Association can be observed under a.c. polarographic conditions (with a drop time of 2 sec.) at bulk concentrations in excess of ca. 0.3 - 0.4 mM. In any event, formation of the intermolecularly associated surface film results in a very pronounced decrease in the double layer capacity and a well-defined pit or well is observed on the a.c. polarogram. A possible form of the polymeric surface layer is shown in Fig. 3-14A. Here it is seen that chains of 7,8-dihydro-6,7-dihydroxypteridine are formed by hydrogen bonding between the pyrimidine and pyrazine ring nitrogens. A two dimensional polymer can be formed by further hydrogen bonding between the $>C_6=O$ and the -OH group at position 7 of the 7,8-dihydro-6,7-dihydroxypteridine molecules. By such hydrogen bonding between two N···H···N hydrogen bonded anti-parallel chains, it is seen that a very large polymeric structure could be formed. Almost identical polymeric hydrogen bonded structures can be drawn for 7,8-dihydro-6-

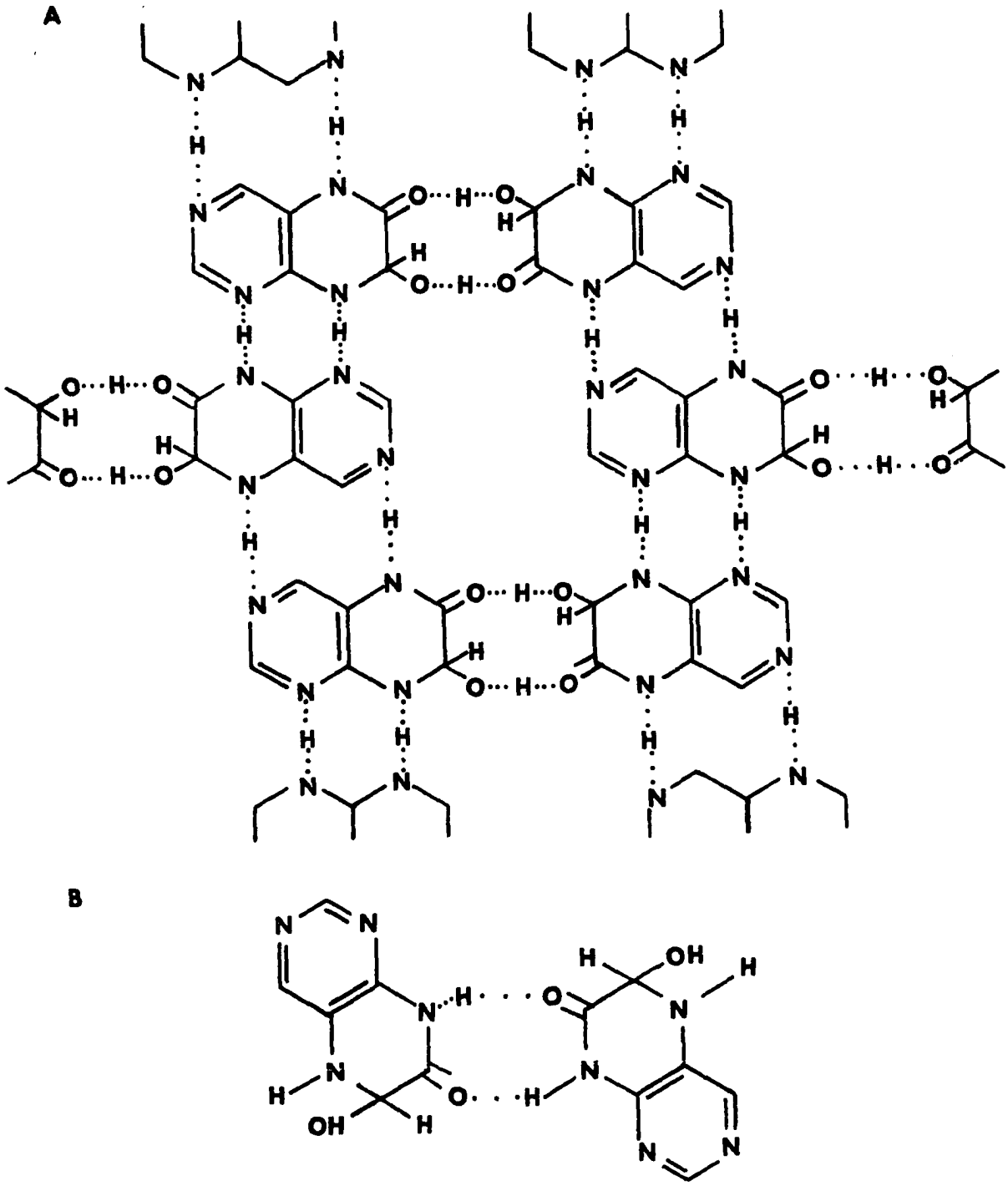

FIGURE 3-14. (A) Possible two-dimensional hydrogen-bonded polymer of 7,8-dihydro-6,7-dihydroxypteridine.
(B) Possible two-dimensional hydrogen-bonded dimeric form of 7,8-dihydro-6,7-dihydroxypteridine.

hydroxypteridine. Other hydrogen bonded structures can be drawn, but in most cases association is limited to dimeric species (Fig. 3-14B).

It is obvious that the non-hydrated anion of 6-hydroxypteridine does not possess the structural features necessary even for the type of association shown in Fig. 3-14B. A.c. polarogrpahy shows no evidence for molecular association of this species.

Reaction Scheme. The electrochemical reduction of 6-hydroxypteridine occurs by a straightforward $2\underline{e}\text{-}2H^+$ reduction of the adsorbed non-hydrated anion (I, Fig. 3-15) to the anion of 7,8-dihydro-6-hydroxypteridine (II, Fig. 3-15). This then presumably rapidly attracts a proton from the solvent to give the neutral dihydro derivative (III, Fig. 3-15). A.c. polarography and d.c. polarography at mercury electrodes and linear sweep voltammetry at the PGE clearly establish that the dihydro derivative is adsorbed at the DME and that above a critical time-dependent bulk concentration association of the adsorbed molecules occurs to give a polymeric species (IV, Fig. 3-15).

7-hydroxypteridine

D.C. Polarography. Over the pH range 0-12, 7-hydroxypteridine gives a single, well-defined polarographic wave, $E_{1/2} = -0.23 - 0.07$ pH (Fig. 3-2). Over the latter pH range 7-hydroxypteridine exists in three different ionic forms but no discontinuities in the $E_{1/2}$ *vs* pH curve were observed. However, the diffusion current constants for the cationic and anionic forms are slightly lower than for the neutral form (Fig. 3-3), possibly because of slightly lower diffusion coefficients for the ionic forms.

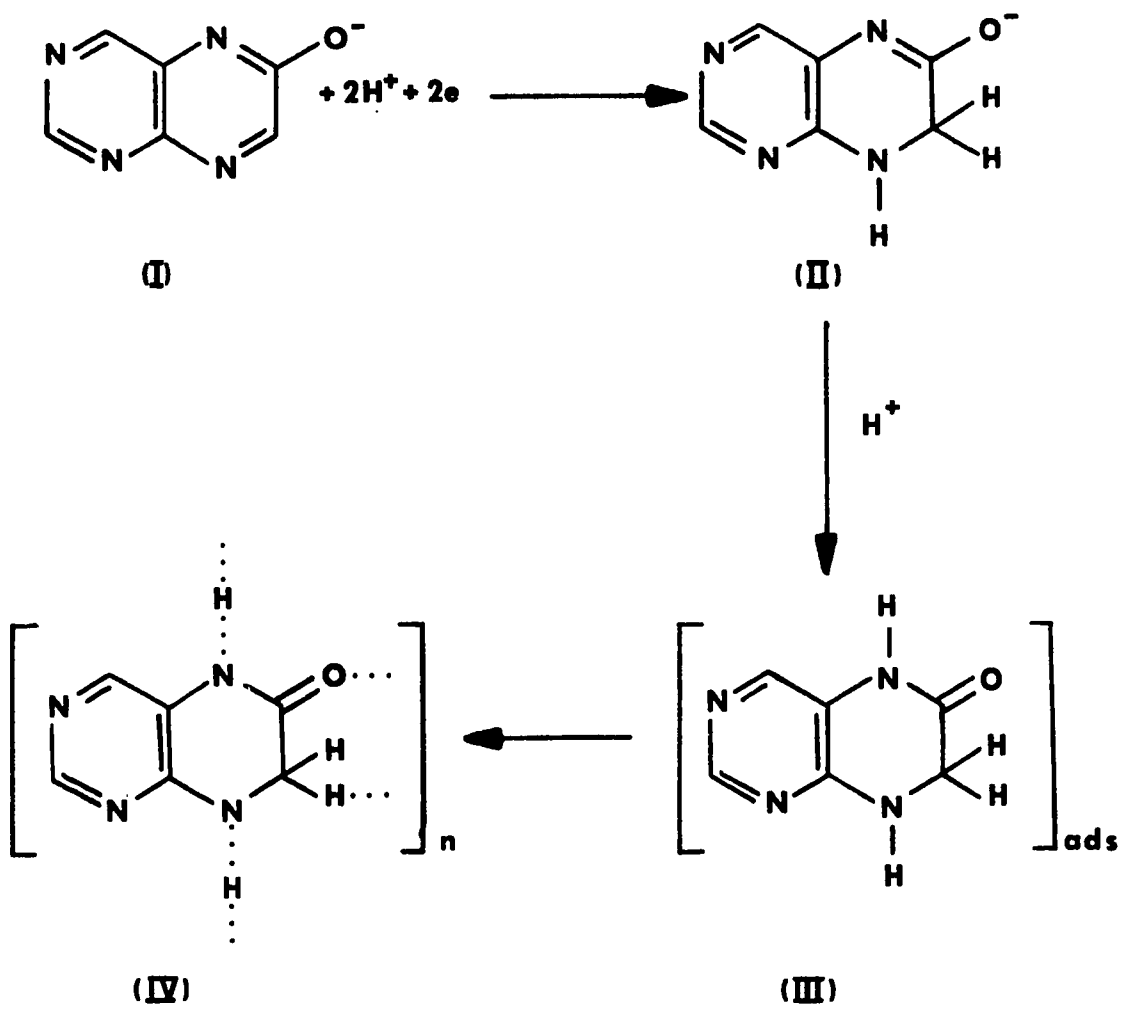

FIGURE 3-15. Proposed reaction scheme for the electrochemical reduction of 6-hydroxypteridine.

D.c. and a.c. polarography of 7-hydroxypteridine gave evidence for simple adsorption (Fig. 3-10), but no association of this compound or its electrochemical reduction product on the electrode surface was indicated.

Controlled Potential Electrolysis and Coulometry. Over the pH range 2.2 - 12.0 faradaic n-values ranging from 1.8 - 2.1 were obtained for the reduction of 7-hydroxypteridine (Table 3-5). At every pH the

TABLE 3-5

Coulometric n-values for the Electrochemical Reduction of 7-hydroxypteridine

Buffer system	pH	Electrode	Electrode potential Volts vs SCE	n-value
McIlvaine	2.2	Mercury	-0.60	1.8
McIlvaine	2.2	Pyrolytic Graphite	-0.60	1.9
McIlvaine	4.7	Mercury	-0.80	1.8
McIlvaine	4.7	Pyrolytic Graphite	-0.80	1.9
Borax	8.1	Mercury	-1.00	1.9
Borax	8.1	Pyrolytic Graphite	-1.00	1.9
Hydroxide/ chloride	12.0	Mercury	-1.40	1.9
Hydroxide/ chloride	12.0	Pyrolytic Graphite	-1.20	2.1

the UV spectrum and voltammetric oxidation peak (vide infra) of the product was identical to that of 5,6-dihydro-7-hydroxypteridine. Quantitative analysis of the product via its UV spectrum showed that

in excess of 95 percent of the electrolyzed 7-hydroxypteridine could be accounted for as the 5,6-dihydro derivative.

Cyclic Voltammetry at the PGE. On the initial negative-going sweep at a clean PGE, a single reduction peak is observed (Fig. 3-16A); E_p = -0.20 - 0.072 pH. The slight inflection which can be noted on this cathodic peak may be indicative of product adsorption, but the poor definition of this pre-peak did not permit a detailed investigation. Upon reversal of the voltage sweep, a well-formed anodic peak is observed, E_p = 0.88 - 0.066 pH (Fig. 3-2). This anodic peak is not observed until the cathodic process has first occurred. The peak potential for the anodic peak is identical to that observed for oxidation of an authentic sample of 5,6-dihydro-7-hydroxypteridine. Once having scanned the anodic peak of the latter compound, the cathodic peak of 7-hydroxypteridine is observed on the next cathodic sweep (Fig. 3-16B).

Reaction Scheme. From the available d.c. polarographic data at mercury, cyclic voltammetry at the PGE, and coulometry at mercury and graphite it is clear that 7-hydroxypteridine (I, Fig. 3-17) is reduced in a straightforward $2\underline{e}$-$2H^+$ process to 5,6-dihydro-7-hydroxypteridine (II, Fig. 3-17). Apparently, both reactant and product lack the structural requirements to cause association at the electrode surface.

Analytical Application

A study of the polarographic behavior of 6- and 7-hydroxypteridine suggests that the compounds can be determined both singly and in mixtures by measurement of their polarographic wave heights. For example, at pH 6.0 only 7-hydroxypteridine gives rise to a polarographic wave, while

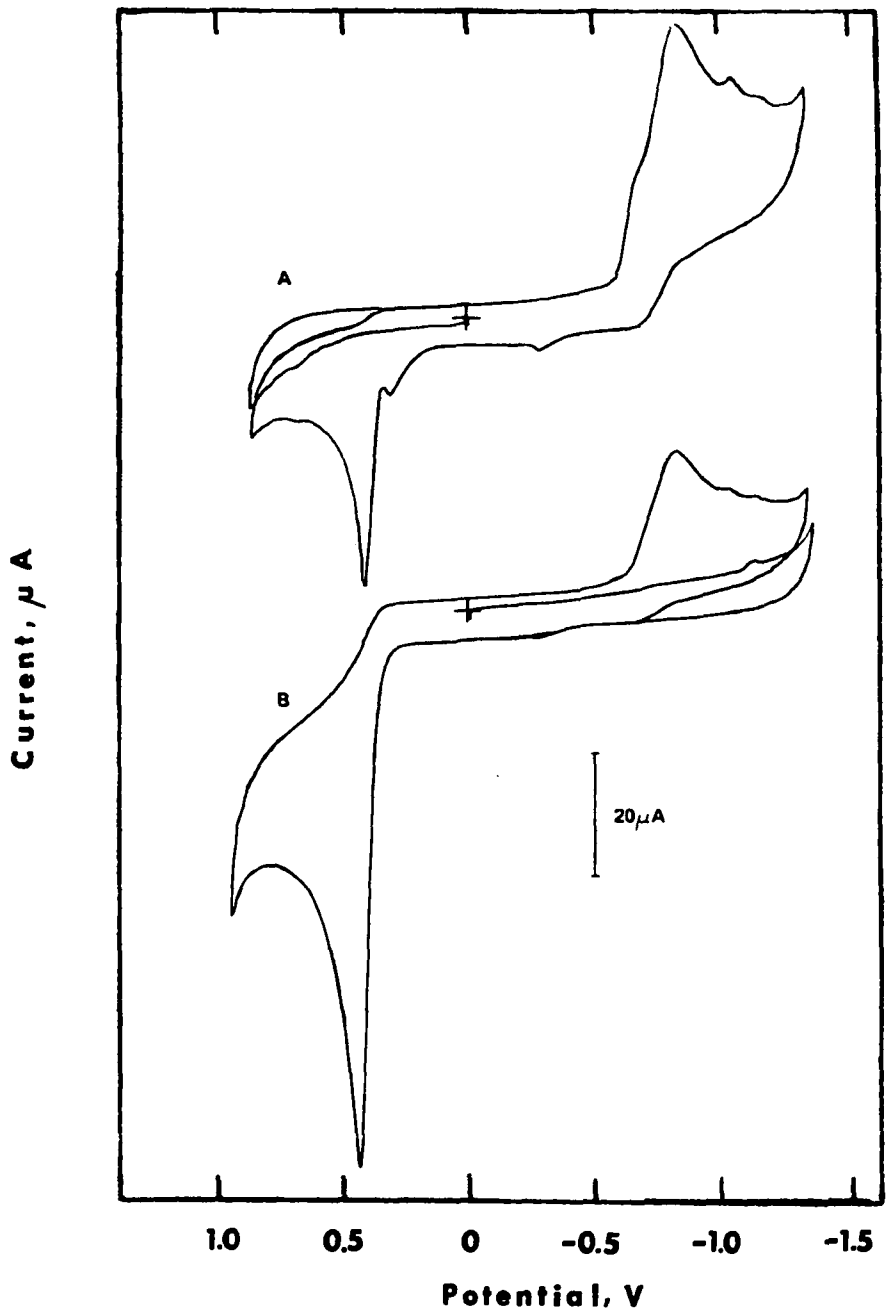

FIGURE 3-16. Cyclic voltammograms of (A) 7-hydroxypteridine and (B) 5,6-dihydro-7-hydroxypteridine at the PGE in pH 7.0 McIlvaine buffer. Scan rate 50 mV sec^{-1}. Scan pattern: (A) 0.00 V → 0.90 V → -1.50 V → 0.90 V → 0.00 V. (B) 0.00 V → -1.50 V → 0.90 V → -1.50 V → 0.00 V. Current above axis marker is cathodic, below axis marker is anodic.

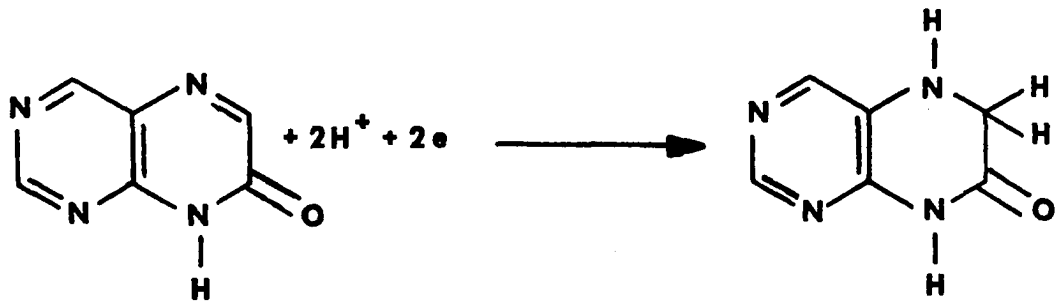

FIGURE 3-17. Proposed reaction scheme for the electrochemical reduction of 7-hydroxypteridine.

at pH 10 both compounds show waves. A typical analysis might involve determination of 7-hydroxypteridine at pH 6.0 by measurement of its wave height and comparison to a standard curve. The concentration of 6-hydroxypteridine could then be determined by measurement of total polarographic wave height at pH 10 (the wave of 6- and 7-hydroxypteridine are too closely spaced at this pH to allow their individual measurement), subtraction of the contribution of 7-hydroxypteridine, and comparison to a standard curve. Experiments have shown polarographic wave heights of both 6- and 7-hydroxypteridine to be linearly proportional to concentration at pH 6 and 10, both separately and as a mixture.

Experimental

Chemicals. Synthesis of 6-hydroxypteridine was according to the method of Albert[1] and 7-hydroxypteridine was prepared by the method of Albert, Brown, and Cheeseman.[17] The preparation of 7,8-dihydro-6-hydroxypteridine and 5,6-dihydro-7-hydroxypteridine was according to Albert and Matsuura.[4] Buffer solutions were prepared from analytical grade reagents. Argon used for deoxygenation was equilibrated with water; no further purification was necessary.

Apparatus. Polarography, linear sweep voltammetry, and cyclic voltammetry were performed with the instrumentation previously described. A.c. polarograms were obtained using a Princeton Applied Research Model 121 Lock-In Amplifier/Phase Detector both as the source of the alternating signal and as an a.c. voltmeter for detection of the alternating component of the current.[18] For a.c. polarography, a sinusoidal signal having a frequency of 100 Hz and 10 mV peak-to-peak

amplitude was employed.

A mechanical drop dislodger in conjunction with the dual-channel timing circuit described by Brown et al[19] was used for all a.c. and d.c. polarograms. A droptime of 2.00 seconds was normally employed. For a.c. polarography, the second channel of the timing circuit was connected to the remote pen input of the x-y recorder and adjusted so that the current was recorded immediately before the drop was dislodged.

Controlled potential electrolysis and coulometry were carried out using the equipment described in Chapter 2. The three-compartment cell used for controlled potential electrolysis employed either a stirred mercury electrode (area ≈3.8 cm^2) or a pyrolytic graphite electrode (area ≈10.4 cm^2), a platinum gauze counter electrode, and a SCE reference electrode.

Summary

Electrochemical reduction of 6-hydroxypteridine over the pH range 7-12 at mercury and pyrolytic graphite electrodes involves a $2e/2H^+$ reaction to 7,8-dihydro-6-hydroxypteridine. A.c. and d.c. polarography showed that 7,8-dihydro-6,7-dihydroxypteridine (the monohydrated form of 6-hydroxypteridine which predominates below pH 7) and 7,8-dihydro-6-hydroxypteridine are strongly adsorbed at the mercury electrode, and under proper conditions of pH and concentration, apparently form hydrogen-bonded polymeric films which cover the electrode surface causing sharp decreases in alternating current. Over the pH range 0-12, 7-hydroxypteridine is reduced at mercury and pyrolytic graphite

in a $2\underline{e}/2H^+$ reaction to 5,6-dihydro-7-hydroxypteridine. Apparently, 7-hydroxypteridine and its reduction product are not strongly adsorbed.

References

1. A. Albert, J. Chem. Soc., 1955, 2690.

2. A. Albert and F. Reich, J. Chem. Soc., 1960, 1370.

3. Y. Inoue and D. D. Perrin, J. Chem. Soc., 1962, 2600.

4. A. Albert and S. Matsuura, J. Chem. Soc., 1962, 2162.

5. L. Meites, Polarographic Techniques, 2nd ed., Wiley, New York, 1965, p. 188.

6. J. Heyrovský and J. Kuta, Principles of Polarography, Academic Press, New York, 1966, p. 301.

7. L. Meites, Polarographic Techniques, 2nd ed., Wiley, New York, 1965, p. 187.

8. V. Vetterl, Coll. Czech. Chem. Commun., 34, 673 (1969).

9. W. Lorenz, Z. Electrochem., 62, 192 (1958).

10. V. Vetterl, Coll. Czech. Chem. Commun., 31, 2105 (1966).

11. V. Vetterl, J. Electroanal. Chem., 19, 169 (1968).

12. A. N. Frumkin, Z. Physik, 35, 792 (1926).

13. P. Delahay, Double Layer and Electrode Kinetics, Wiley, New York, 1965, p. 93.

14. I. R. Miller, J. Mol. Biol., 3, 229 (1961).

15. R. S. Nicholson and I. Shain, Anal. Chem., 36, 706 (1964).

16. R. N. Wopschall and I. Shain, Anal. Chem., 39, 1514 (1967).

17. A. Albert, D. J. Brown, and E. Cheeseman, J. Chem. Soc., 1952, 1620.

18. D. L. McAllister and G. Dryhurst, Anal. Chim. Acta, 58, 273 (1972).

19. E. R. Brown, T. E. McCord, D. E. Smith, and D. D. DeFord, Anal. Chem., 38, 1119 (1966).

CHAPTER 4

THE ELECTROCHEMICAL OXIDATION OF 6- AND 7-HYDROXYPTERIDINE AT THE PYROLYTIC GRAPHITE ELECTRODE

Introduction

Since no previous investigations have been conducted on the electrochemical oxidation of pteridines, the present study was begun with 6- and 7-hydroxypteridine, which are among the simplest pteridines oxidizable electrochemically. Although 6- and 7-hydroxypteridine have not been found in nature, information gained from the oxidation of these compounds should be applicable to pteridines as a class. Also, as more and more groups (especially -OH and $-NH_2$) are added to the pteridine nucleus, solubility in water decreases drastically, rendering electrochemical studies of the more highly substituted compounds more difficult.

Bergman and Kwientny[1] have studied the action of xanthine oxidase upon pteridine and all possible mono-, di-, tri-, and tetrahydroxy isomers. While xanthine oxidase was found not to act upon 6-hydroxypteridine, 7-hydroxypteridine was oxidized to 2,4,7-trihydroxypteridine.

Extensive studies of the chemistry of 6-hydroxypteridine and 7-hydroxypteridine have been conducted by Albert *et al.*[2-6] Upon oxidation with basic potassium permanganate, 6-hydroxypteridine yielded 6,7-dihydroxypteridine at 25°, while 7-hydroxypteridine required a tempera-

ture of 60-70° for oxidation to the same compound.[4]

Results and Discussion

Voltammetry. Over the pH range 2.2 to 10.0, 6-hydroxypteridine shows two well-defined oxidation peaks (peaks I_a and II_a) at the PGE (Fig. 4-1A). The peak potential of these peaks shifts linearly more negative with increasing pH; $(E_p)_I = 1.13 - 0.071$ pH, $(E_p)_{II} = 1.40 - 0.064$ pH (Fig. 4-2). Values of the peak current function are shown in Table 4-1, and a plot of peak current function vs pH for peak I

TABLE 4-1

Peak Current Values for the Oxidation of 6-hydroxypteridine and 7-hydroxypteridine at the PGE

Compound	pH	Background	$i_p/ACv^{1/2}$[a] Peak I	Peak II
7-hydroxypteridine		1 M H_2SO_4	884	
7-hydroxypteridine		2 M H_2SO_4	938	1000
6-hydroxypteridine	3.0	Phosphate-citrate	423	1675
6-hydroxypteridine	3.7	Phosphate-citrate	677	2538
6-hydroxypteridine	4.7	Phosphate-citrate	1261	2769
6-hydroxypteridine	5.6	Phosphate-citrate	1176	2231
6-hydroxypteridine	7.0	Phosphate-citrate	1461	1769
6-hydroxypteridine	8.0	Phosphate-citrate	1423	1615
6-hydroxypteridine	8.9	Borate	730	1307

[a] i_p = voltammetric peak current, μA
A = electrode area, cm^2 = 0.13 cm^2
C = concentration of electroactive species, mM l^{-1} = 1.0 mM l^{-1}
v = voltage sweep rate V sec^{-1} = 0.01 V sec^{-1}

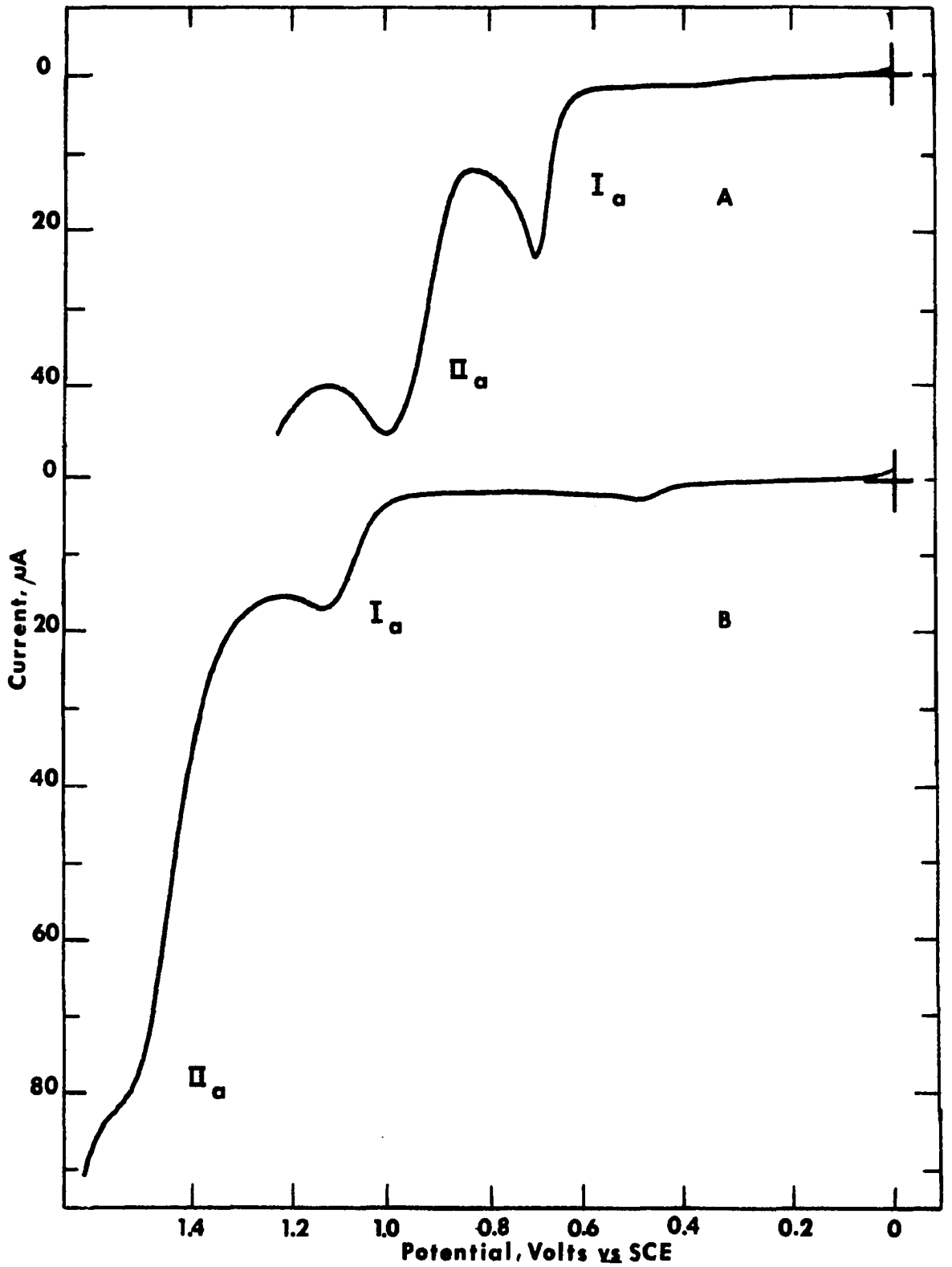

FIGURE 4-1. Voltammograms at the PGE of 1 mM solutions of (A) 6-hydroxypteridine in pH 7.0 McIlvaine buffer, and (B) 7-hydroxypteridine in 2 M H_2SO_4. Sweep rate 10 mV sec^{-1}.

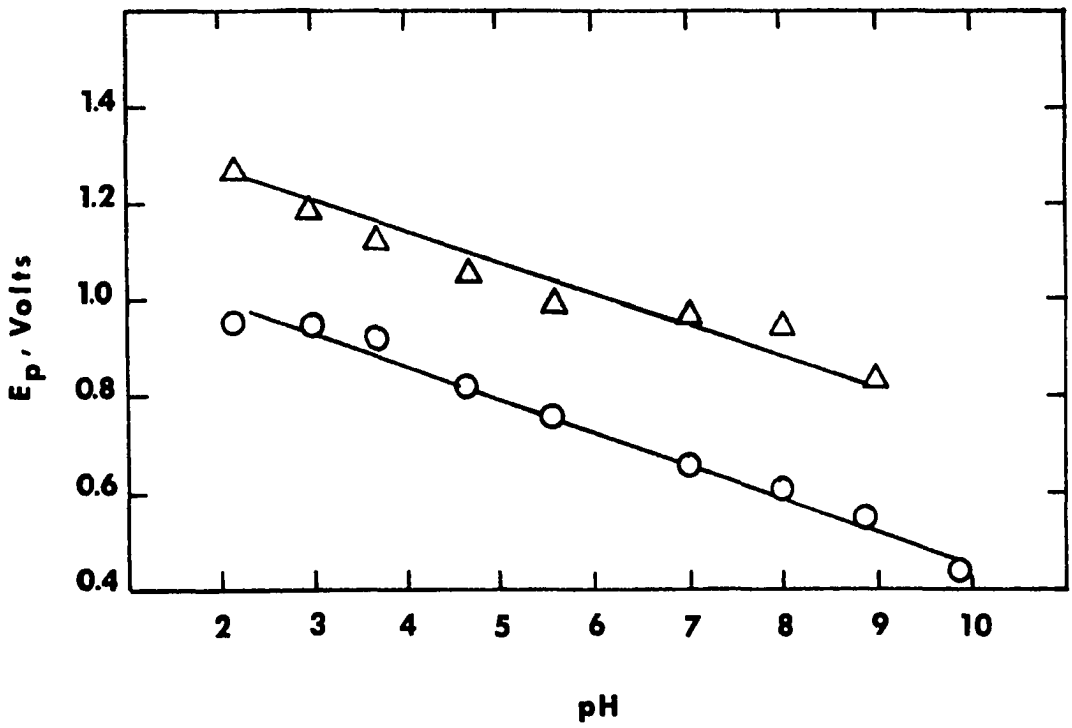

FIGURE 4-2. Variation of E_p with pH for 6-hydroxypteridine at the PGE. Voltage sweep rate 10 mV sec^{-1}. Peak I_a = O—O and Peak II_a = Δ—Δ .

is shown in Fig. 4-3. Adsorption effects undoubtedly influence the dependence of peak current function upon pH somewhat, but the fact that $i_p/ACv^{1/2}$ is greatest between pH 4.7 - 8.0, and falls off sharply above pH 8, implies that only the neutral, hydrated form of 6-hydroxypteridine (see Fig. 3-1A) is oxidized electrochemically.

7-Hydroxypteridine is oxidized only in very acidic solutions (1-2 $\underline{M}$ H_2SO_4) at the PGE. In 1 $\underline{M}$ H_2SO_4 only one oxidation peak is observed (peak I_a), E_p = 1.08 V, while in 2 $\underline{M}$ H_2SO_4 two peaks are present, $(E_p)_I$ = 1.14 V, $(E_p)_{II}$ = 1.52 V (Fig. 4-1B). The small peak at 0.50 V in Fig. 4-1B was observed when a voltammogram of background solution alone was run; i.e., it arises from oxidation of a contaminant in the supporting electrolyte, not from electrochemical oxidation of 7-hydroxypteridine. Values of the peak current function are shown in Table 4-1.

For both 6-hydroxypteridine and 7-hydroxypteridine peak currents were measured by first recording a voltammogram of a solution of the compound of interest, then recording a voltammogram of background solution under identical conditions. Peak currents were then taken as the difference in background current and current in the presence of the electroactive compound at the peak potential.

Studies of the dependence of peak current upon potential scan rate revealed that for both peaks of 6-hydroxypteridine and 7-hydroxypteridine an increase in peak current function, $i_p/ACv^{1/2}$ (where i_p = peak current, μA, A = electrode area, cm^2, C = bulk concentration of electroactive species, $m\underline{M}\ l^{-1}$, and v = voltage sweep rate, V sec^{-1}), with increasing scan rate (Fig. 4-4). Such behavior is usually indicative of reactant

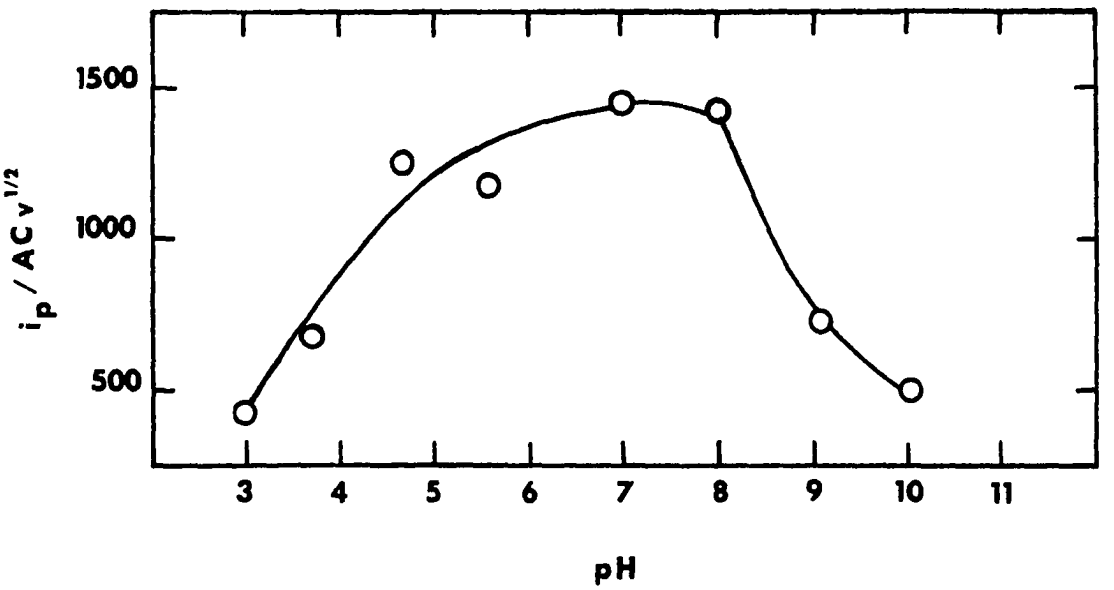

FIGURE 4-3. Variation of $i_p/ACv^{1/2}$ with pH for peak I_a of 6-hydroxypteridine at the PGE, voltage sweep rate 10 mV sec^{-1}, concentration 1 mM.

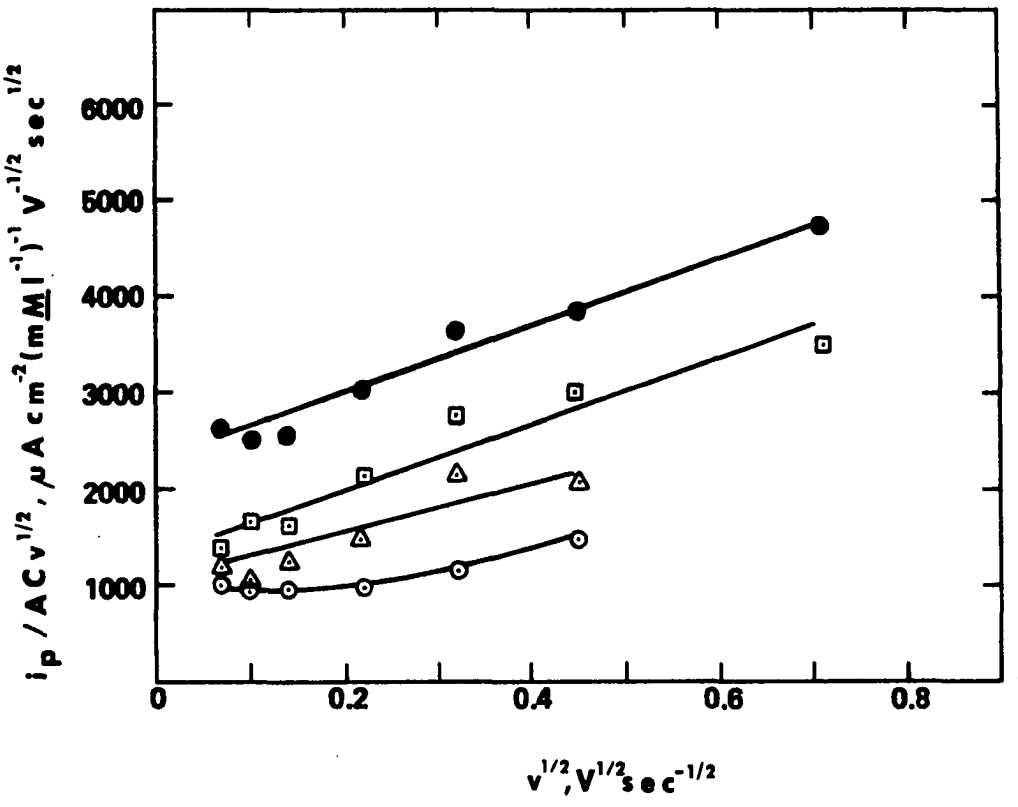

FIGURE 4-4. Variation of peak current function ($i_p/ACv^{1/2}$) with voltage sweep rate for 6- and 7-hydroxypteridine at the PGE. Concentration 1 mM. 6-hydroxypteridine at pH 7.0; peak I_a (□——□), peak II_a (●——●). 7-hydroxypteridine in 2M H_2SO_4; peak I_a (○——○), peak II_a (△——△).

adsorption at the electrode.[7]

The involvement of adsorption, especially for 6-hydroxypteridine, was confirmed by studies of the dependence of peak height upon concentration. For a diffusion-controlled peak, the height of the peak should vary directly as the concentration; therefore, a plot of i_p/C *vs* C should yield a straight line parallel to the concentration axis. However, for a process in which adsorption is a factor, i_p/C decreases with increasing concentration.[8] From Fig. 4-5 it can be seen that both peaks of 6-hydroxypteridine exhibit behavior characteristic of adsorption processes. Adsorption of 7-hydroxypteridine is apparently much less extensive than that of the 6-hydroxy compound; the plot of i_p/C *vs* C is parallel to the C axis and the peak current function changes only slightly with scan rate (Figs. 4-4, 4-5). The second oxidation peak of 7-hydroxypteridine merged with background oxidation at concentrations less than 1 mM, preventing calculation of i_p/C values.

The dependence of peak currents upon concentration for peaks I_a and II_a of 6- and 7-hydroxypteridine is shown in Fig. 4-6. It is apparent from these plots that the peak currents depend upon concentration, but not always in a linear fashion. For analytical purposes, 6-hydroxypteridine peak II_a and 7-hydroxypteridine peak I_a would be most appropriate over the widest concentration range.

Controlled Potential Coulometry. Oxidation of 6-hydroxypteridine at the PGE at a potential corresponding to peak I_a in solutions of pH 3.7 - 8.0 gave n-values of 1.85 - 1.98 (Table 4-2), indicating a 2-electron process. The electrolyzed solution showed an oxidation peak at a potential corresponding to that of peak II_a. The product

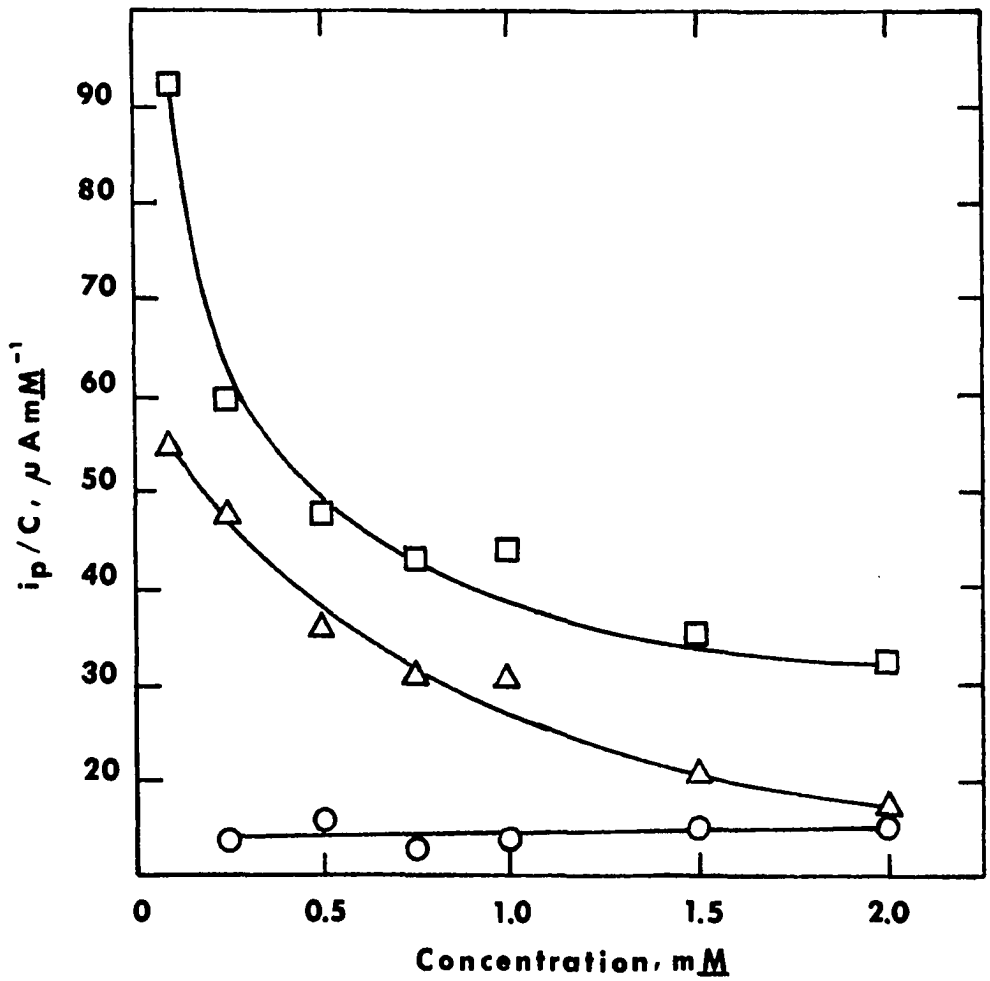

FIGURE 4-5. Variation of i_p/C with concentration at the PGE for peak I_a of 7-hydroxypteridine in 2 $\underline{M}$ H_2SO_4 (○——○), peak I_a (△——△) and peak II_a (□——□) of 6-hydroxypteridine at pH 7.0. Potential scan rate, 20 mV sec^{-1}.

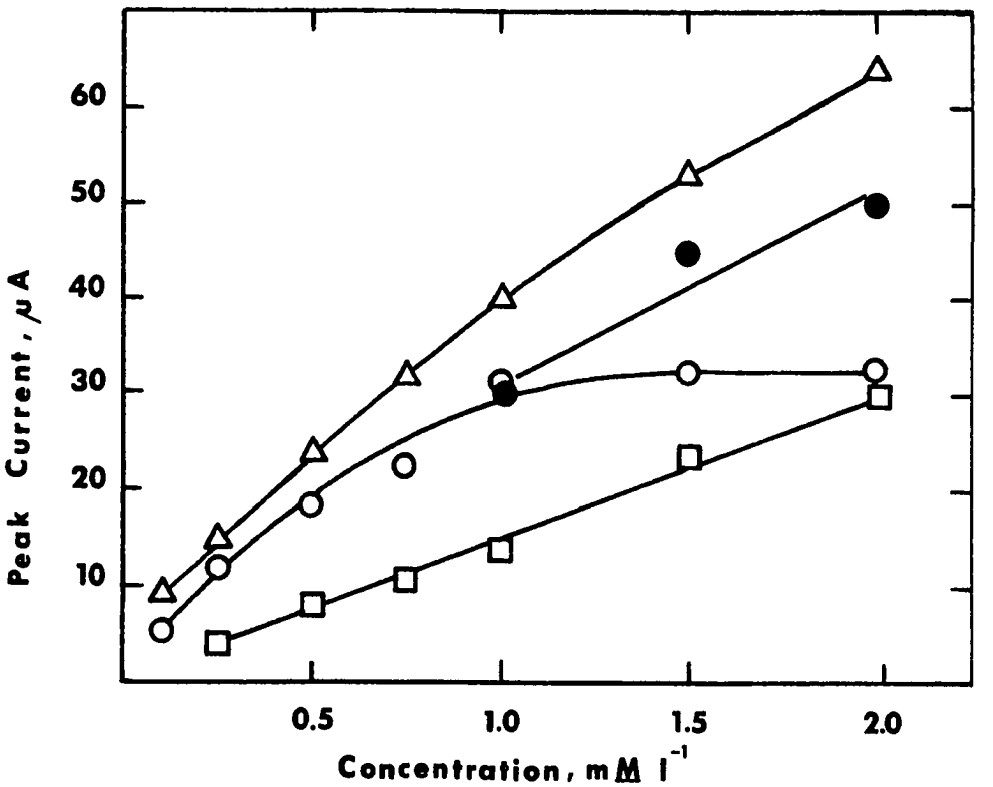

FIGURE 4-6. Plot of peak current vs concentration for 6-hydroxypteridine in pH 7.0 McIlvaine buffer, peak I (○——○), peak II (△——△); 7-hydroxypteridine in 2 M H_2SO_4, peak I (□——□), peak II (●——●). At the PGE, voltage sweep rate 10 mV sec^{-1}.

TABLE 4-2

Coulometric Determination of the Number of Electrons Involved in the Oxidation of Peak I_a of 6-hydroxypteridine

Background	pH	Controlled Potential, Volts *vs* SCE	*n*-Value
McIlvaine	3.7	1.00	1.90
McIlvaine	4.7	0.90	1.85
McIlvaine	7.0	0.75	1.98
Borax	8.0	0.65	1.93

was shown to be 6,7-dihydroxypteridine by comparison of the UV spectrum (λ_{max} = 302 nm at pH 4.7), polarography at the DME ($E_{1/2}$ = -0.96 V at pH 4.7), and voltammetry at the PGE (E_p = 1.08 V at pH 4.7) with the authentic compound. Quantitative analysis by UV showed that 95-100% of the 6-hydroxypteridine oxidized could be accounted for as 6,7-dihydroxypteridine.

Oxidation of 7-hydroxypteridine at the PGE in 2 *M* H_2SO_4 also gave *n*-values indicative of a 2-electron process (1.90 - 1.99). After oxidation, the electrolyzed solution showed no oxidation peak; this was not surprising, however, because the expected product, 6,7-dihydroxypteridine, does not give rise to an oxidation peak in 2 *M* H_2SO_4. The identity of the product was confirmed as 6,7-dihydroxypteridine by comparison with the authentic material (λ_{max} = 307 nm, 223 nm, 207 nm in 2 *M* H_2SO_4, $E_{1/2}$ = -0.60 V in 2 *M* H_2SO_4). Again, quantitative analysis by UV showed the 95-100% of the oxidized 7-hydroxypteridine could be accounted for by 6,7-dihydroxypteridine.

Reaction Scheme. For both 6-hydroxypteridine and 7-hydroxypteridine the data indicate two-electron, two-proton oxidations to 6,7-dihydroxypteridine (Fig. 4-7). In the case of 6-hydroxypteridine, it has been shown[6] that the predominant species in neutral and slightly acid solutions is actually a hydrate with water added covalently across the 7,8 bond (1, Fig. 4-7A). Evidence indicates that this structure facilitates oxidation at the 7,8 bond. For example, 7,8-dihydro-6-hydroxypteridine, which is identical to (1) with the exception of -OH at position 7, is easily oxidized to 6-hydroxypteridine (Chapter 3). Also, the non-hydrated form of 6-hydroxypteridine, which predominates above pH 7, is not electrochemically oxidized. Studies of the dependence of peak height upon scan rate and concentration indicate that the reactant (1, Fig. 4-7A) is adsorbed on the electrode surface.

In the very acidic solutions necessary for the electrochemical oxidation of 7-hydroxypteridine, the reaction must involve oxidation of the cation of 7-hydroxypteridine to the cation of 6,7-dihydroxypteridine[5] (see also Fig. 3-1B).

Voltammetry of 6,7-dihydroxypteridine. Since the product of the electrochemical oxidation of both 6- and 7-hydroxypteridine is 6,7-dihydroxypteridine, the voltammetric behavior of this compound was examined. Over the pH range 2.3 - 9.0, 6,7-dihydroxypteridine shows a single oxidation peak at the PGE. Below pH 2.3 and above pH 9, the peak merges with background oxidation. The peak potential shifts linearly more negative with increasing pH, $E_p = 1.36 - 0.056$ pH (Fig. 4-8).

A study of the dependence of peak current upon potential sweep

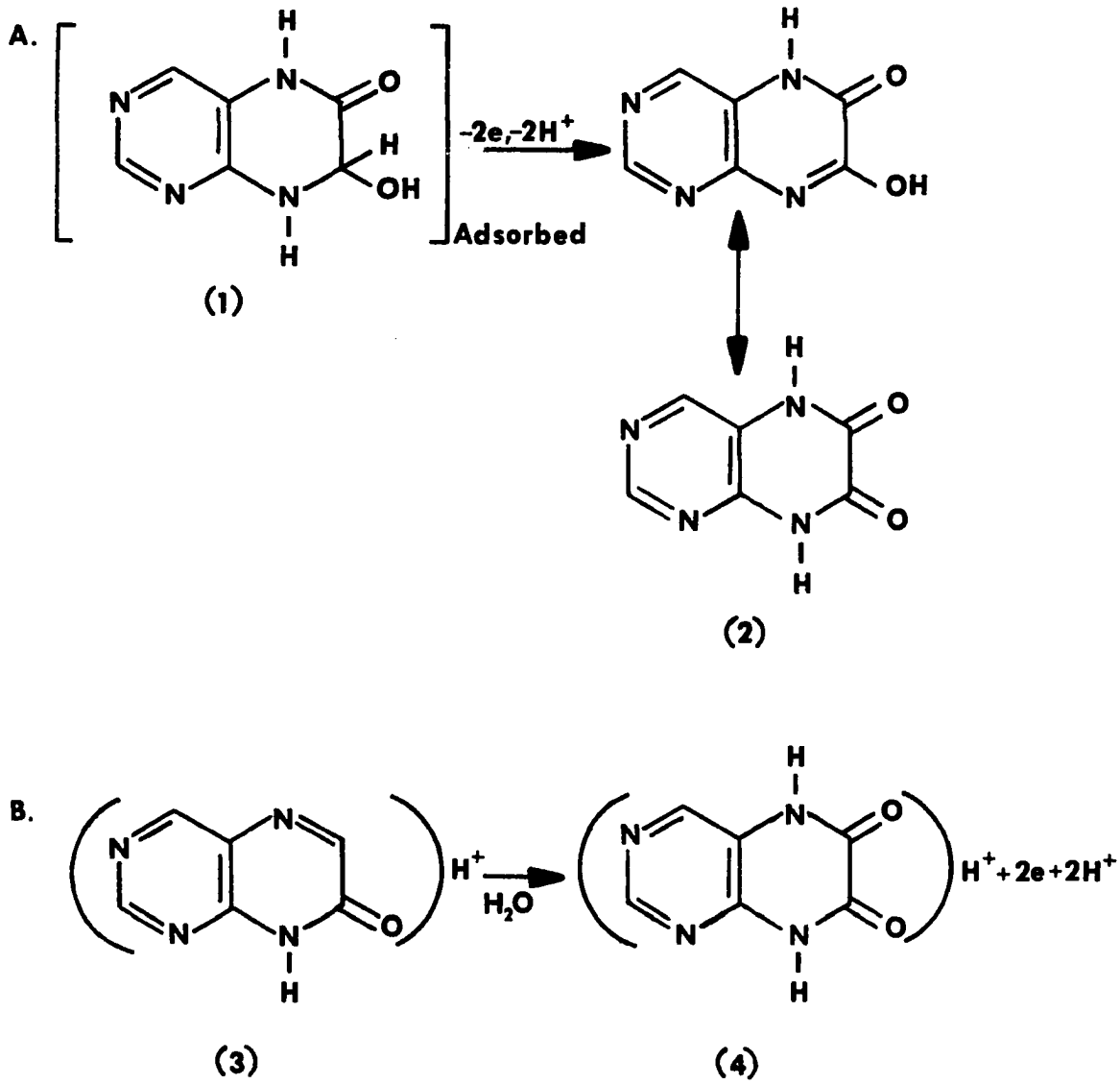

FIGURE 4-7. Proposed reaction scheme for the electrochemical oxidation of (A) 6-hydroxypteridine and (B) 7-hydroxypteridine at the PGE. (1) Hydrated form of 6-hydroxypteridine, (2) 6,7-dihydroxypteridine, (3) cation of 7-hydroxypteridine, and (4) cation of 6,7-dihydroxypteridine.

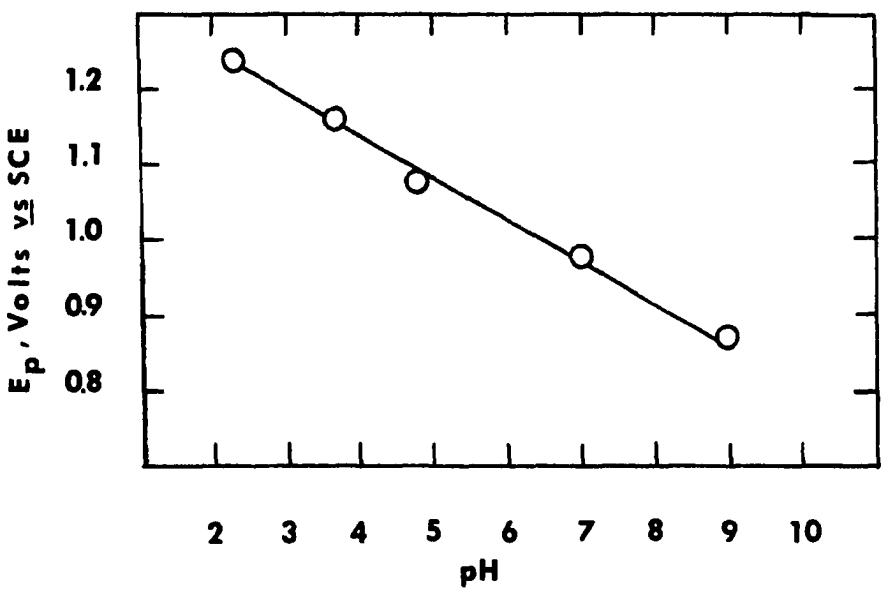

FIGURE 4-8. Variation of E_p with pH for 6,7-dihydroxypteridine at the PGE. Concentration 1 m$\underline{M}$, voltage sweep rate 10 mV/sec.

rate for 6,7-dihydroxypteridine revealed an increase in peak current function at pH 4.7 and 7.0 with increasing scan rate (Fig. 4-9). As previously stated, such beahvior is indicative of reactant adsorption at the electrode.[7]

The magnitude of the peak current function for 6,7-dihydroxypteridine (1543 μA cm^{-2} ($\underline{mM}\ l^{-1}$)$^{-1}v^{-1/2}sec^{1/2}$) at pH 7.0 is indicative of a 2$\underline{e}$ process, by comparison to the oxidation of 6-hydroxypteridine, peak I_a, under similar conditions (1461 μA cm^{-2} ($\underline{mM}\ l^{-1}$)$^{-1}v^{-1/2}sec^{1/2}$, at pH 7.0, sweep rate 10 mV sec^{-1}). However, comparisons of this sort are made less reliable by the involvement of adsorption in these oxidations. The shift of peak potential with pH for 6,7-dihydroxypteridine (56 mV per pH unit) indicates that protons are involved in the rate-determining step of the oxidation.

No short-lived intermediates were detected using cyclic voltammetry at sweep rates up to 50 Volts sec^{-1}.

Coulometry and Macroscale Electrolysis of 6,7-dihydroxypteridine. At pH 2.3, 4.7, and 8.1, coulometry at the appropriate controlled potential showed that between 5.5 and 6.0 electrons per molecule are involved in the oxidation of 6,7-dihydroxypteridine (Table 4-3). Electrolysis of 1 $\underline{mM}$ 6,7-dihydroxypteridine solution usually took 12-18 hours to reach completion. After complete oxidation at the above pH values, the solution no longer showed the characteristic UV spectrum of 6,7-dihydroxypteridine (λ_{max} = 300 nm at pH 2.3), but instead showed only a gradual rise in UV absorbance beginning at about 320 nm and increasing at shorter wavelengths.

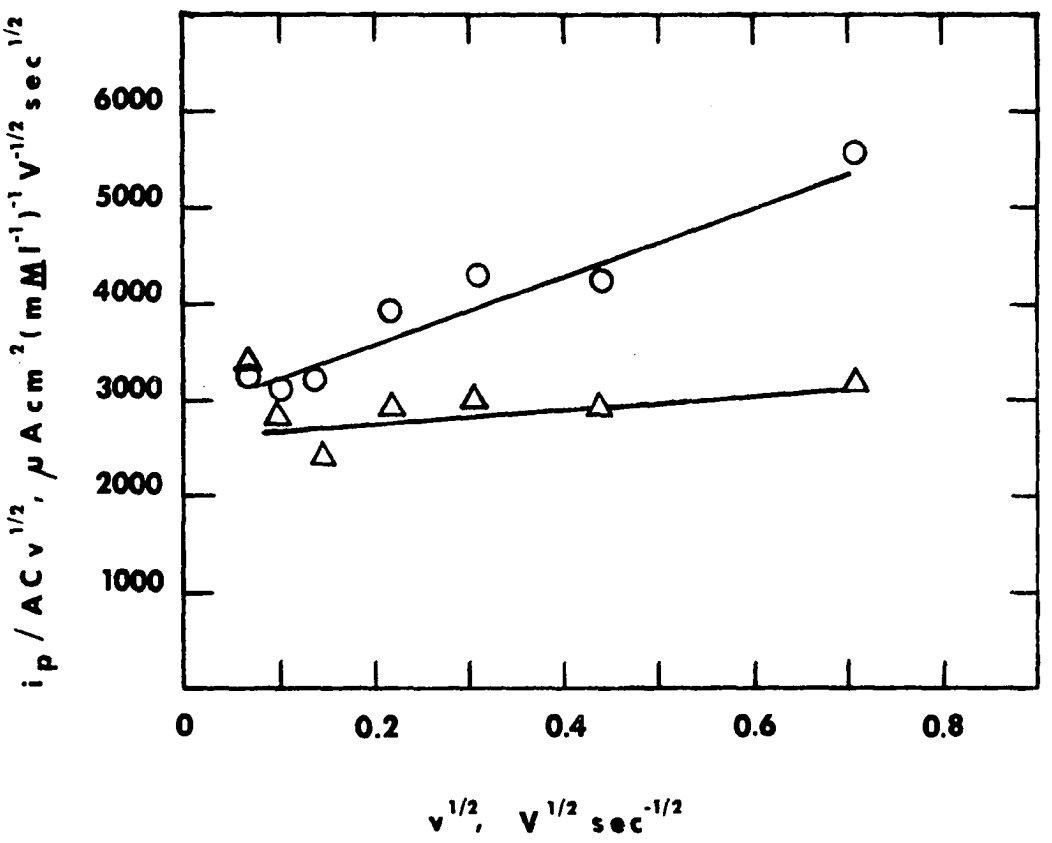

FIGURE 4-9. Variation of peak current function, $i_p/ACv^{1/2}$, with scan rate for 1 mM 6,7-dihydroxypteridine at the PGE.
O——O = pH 4.7, Δ——Δ = pH 7.0.

TABLE 4-3

Coulometric Determination of the Number of Electrons Involved in the Oxidation of 6,7-dihydroxypteridine

Background	pH	Controlled potential volts vs SCE	n-value
1 M Acetic acid	2.3	1.30	5.54
McIlvaine	2.2	1.30	5.51
Acetate	4.3	1.10	5.65
McIlvaine	7.0	1.05	5.90
Borax	8.1	1.00	5.98

Macroscale electrolysis of 6,7-dihydroxypteridine solutions at controlled potential allowed the preparation of sufficiently large quantities of products to permit their isolation, identification, and quantitative determination. A variety of isolation and identification techniques, including lyophilization, column, thin-layer and paper chromatography, polarography, spectrophotometry, and other physical and chemical methods showed that carbon dioxide, ammonia, urea, formaldehyde, formic acid, oxamide (5), oxamic acid (6) and tetraketopiperazine (7) were present in the electrolyzed solution. The procedures

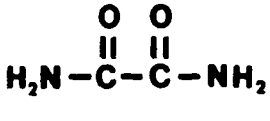

(5)

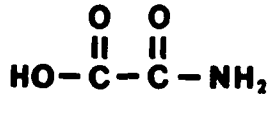

(6)

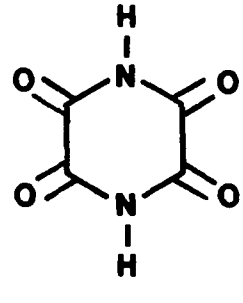

(7)

used and the results obtained in examining the electrolyzed solutions are given in the Experimental section.

After exhaustive electrolysis of 1 mM 6,7-dihydroxypteridine in 1 M acetic acid, polarography at the dropping mercury electrode showed three waves with $E_{1/2}$ of -0.42, -0.85, and -1.05 V (Fig. 4-10A). When the pH was adjusted to 10 by the addition of 2 N NaOH, a single wave was observed, $E_{1/2}$ = -1.62 V (Fig. 4-10B). The waves in 1 M acetic acid were shown to be due to tetraketopiperazine by comparison with the authentic compound and by its tendency to hydrolyze at pH > 4 to oxamide, oxalic acid and oxamic acid. The wave observed at pH 10 is due to the reduction of oxamide, as shown by its $E_{1/2}$ and pH-independence. A detailed study of the oxamide reduction is reported in Chapter 5. After oxidation of 6,7-dihydroxypteridine in pH 4 buffer, no polarographic waves were observed. However, if following electrolysis at pH 4, the pH was adjusted to 10, a polarographic wave appeared at $E_{1/2}$ = -1.62 V. If the electrolysis was conducted in pH 8 buffer, the oxidized solution showed a polarographic wave at $E_{1/2}$ = -1.61 V due to the reduction of oxamide.

Stability Study of Tetraketopiperazine. Because of the reported hydrolysis of tetraketopiperazine in neutral aqueous solution,[9] the stability of this compound was studied in 1 M acetic acid, pH 4.7 McIlvaine buffer, and pH 8 borax buffer. In these studies, polarograms of the solutions were run at intervals of 5 min to 1 hr, and the decrease in the height of the polarographic waves was noted. In 1 M acetic acid, it was found that over a period of 12 hr, the polarographic wave height decreased only 20 percent, indicating very slow

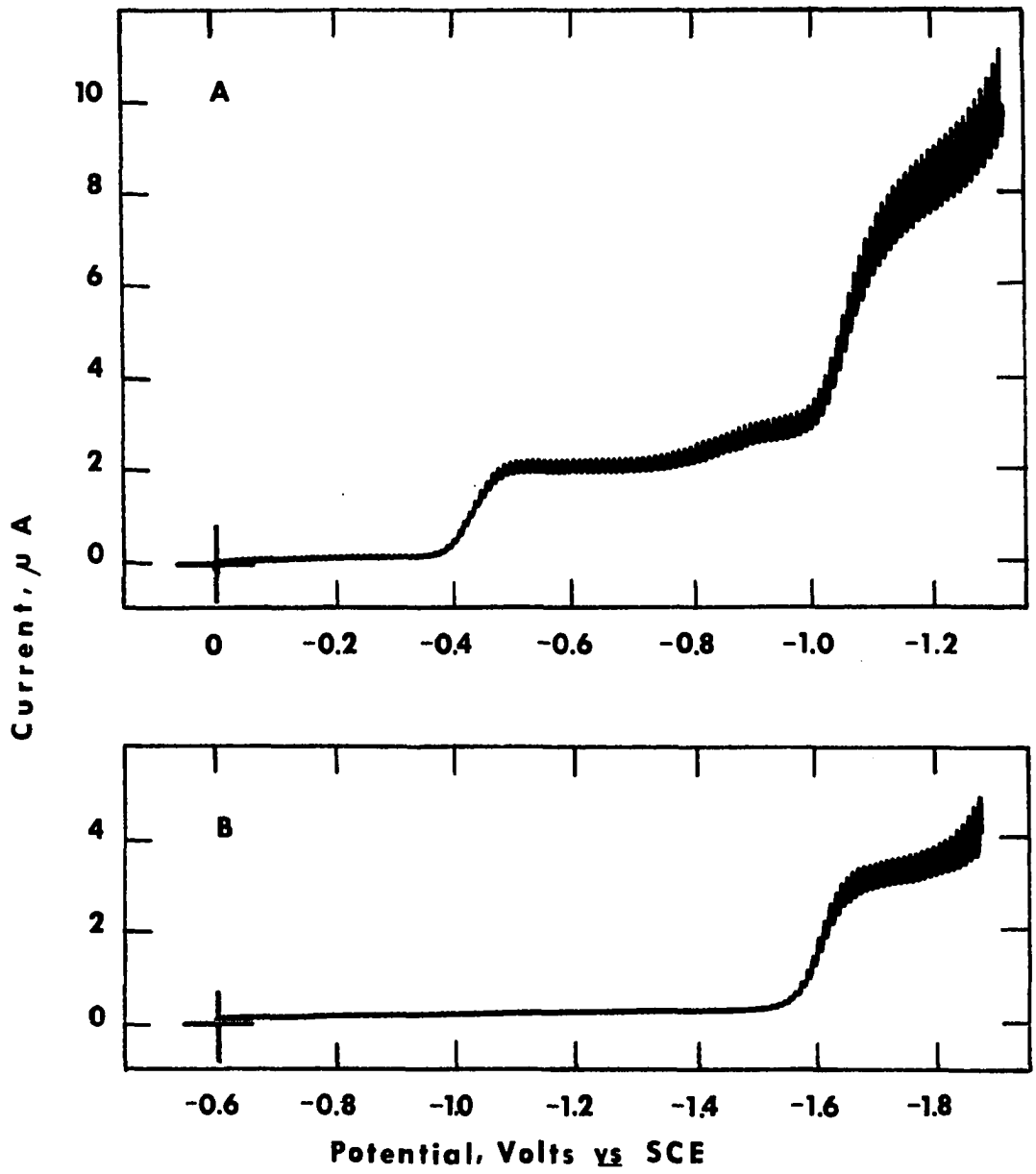

FIGURE 4-10. D.c. polarograms of (A) solution after oxidation of 6,7-dihydroxypteridine in 1 M acetic acid at the PGE, and (B) after adjustment of the pH of the solution to 10.

hydrolysis. However, at pH 4.7, hydrolysis was complete (no polarographic wave could be detected) in about 1 hr; at pH 8, complete hydrolysis required only 10 min. The reported hydrolysis products of tetraketopiperazine are oxamide and oxalic acid;[9] however, quantitative determination of these compounds by polarography at the DME and voltammetry at the PGE (see Experimental) showed that they accounted for only 50 percent of the original tetraketopiperazine. Another expected hydrolysis product, oxamic acid, was shown to be present by paper chromatography, and presumably accounts for the remainder of the original tetraketopiperazine.

Material Balance. By quantitative analysis of most of the identified oxidation products, it was possible to account for 81-97 percent of the oxidized 6,7-dihydroxypteridine. The results in various media are given in Table 4-4. Compounds which are easily hydrolyzed to ammonia under alkaline conditions respond to Nessler's test for ammonia, and the values in Table 4-4 were corrected for such hydrolysis of identified compounds (urea, oxamide, oxamic acid, tetraketopiperazine) by determination of the response of these compounds (at the same concentration levels as in the electrolysis solution) to the test. The values so determined were then subtracted from the total test response. However, ammonia which is derived from the hydrolysis of any unidentified fragments is included in the values of Table 4-4. Because of the severity of the conditions employed in the tests for formic acid and formaldehyde, compounds which are hydrolyzed to formic acid or formaldehyde are detected and are included in the values of Table 4-4. No identified compounds (except formaldehyde and formic

TABLE 4-4

Material Balance for the Oxidation of 6,7-dihydroxypteridine

Compound	Moles per mole of 6,7-dihydroxy-pteridine electrolyzed	Moles nitrogen per mole 6,7-dihydroxy-pteridine electrolyzed	Moles carbon per mole 6,7-dihydroxy-pteridine electrolyzed
pH 2.3			
NH_3[a]	1.70	1.70	
CO_2	1.93		1.93
Formaldehyde	0.36		0.36
Formic Acid[b]	0.44		0.44
Urea	0.24	0.48	0.24
Oxamide	0.40	0.80	0.80
Tetraketopiperazine	0.29	0.58	1.16
Total moles per mole of 6,7-dihydroxypteridine		3.56	4.93
Percent of oxidized 6,7-dihydroxypteridine accounted for		89	82

TABLE 4-4, continued

Compound	Moles per mole of 6,7-dihydroxy-pteridine electrolyzed	Moles nitrogen per mole 6,7-dihydroxy-pteridine electrolyzed	Moles carbon per mole 6,7-dihydroxy-pteridine electrolyzed
pH 4.7			
NH_3[a]	1.62	1.62	
CO_2	2.18		2.18
Formaldehyde	0.46		0.46
Formic Acid[b]	0.36		0.36
Urea	0.26	0.52	0.26
Oxamide	0.51	1.02	1.02
Oxamic Acid[c]	0.30	0.30	0.60
Total moles per mole of 6,7-dihydroxypteridine		3.46	4.88
Percent of oxidized 6,7-dihydroxypteridine accounted for		87	81

TABLE 4-4, continued

Compound	Moles per mole of 6,7-dihydroxy-pteridine electrolyzed	Moles nitrogen per mole 6,7-dihydroxy-pteridine electrolyzed	Moles carbon per mole 6,7-dihydroxy-pteridine electrolyzed
pH 8.0			
NH_3[a]	1.85	1.85	
CO_2	2.34		2.34
Formaldehyde	0.35		0.35
Formic Acid[b]	0.40		0.40
Urea	0.31	0.62	0.31
Oxamide	0.55	1.10	1.10
Oxamic Acid[c]	0.30	0.30	0.60
Total moles per mole of 6,7-dihydroxypteridine		3.87	5.10
Percent of oxidized 6,7-dihydroxypteridine accounted for		97	85

[a] Includes unidentified compounds which are hydrolyzed to ammonia under the conditions of Nessler's test.

[b] Includes unidentified compounds which are hydrolyzed to formaldehyde or formic acid under the conditions of the chromotropic acid test.

[c] Estimated from the decomposition of tetraketopiperazine.

acid) responded to these tests. Although no tetraketopiperazine was detected after electrolysis at pH 4.7 or 8.0, evidence supports the conclusion that this compound was formed, but was rapidly hydrolyzed in these media. The increased amounts of oxamide and CO_2 noted at pH 4.7 and 8.0 were consistent with the hydrolysis of the expected amount of tetraketopiperazine (0.3 mole), with the additional CO_2 resulting from electrochemical oxidation of oxalic acid derived by hydrolysis from tetraketopiperazine. In addition, the quantities of the remaining oxidation products (NH_3, formic acid, formaldehyde, urea) were essentially unchanged at different pH values implying that no gross changes in the reaction scheme occurred as a function of pH. Oxamic acid, which also results from the hydrolysis of tetraketopiperazine, was detected in the electrolyzed solution at pH 4.7 and 8, and the quantity of this compound was estimated from the amount of tetraketopiperazine which was hydrolyzed. The fact that the material balance does not account for 100 percent of the original 6,7-dihydroxypteridine indicates, of course, the presence of unidentified fragments in the electrolyzed solution. However, the relatively low percentage of unidentified products (especially in terms of nitrogen) seems to minimize their importance in the overall reaction scheme.

Oxidation of ^{14}C Labeled 6,7-dihydroxypteridine. Because of the possibility that some of the observed oxidation products (CO_2, oxamide) may originate from various portions of the starting material, and because 6,7-dihydroxypteridine labelled with ^{14}C in positions 6 and 7 is easily synthesized, tracer experiments were conducted. In these experiments, labelled 6,7-dihydroxypteridine was electrochemically

oxidized in 1 M acetic acid, oxamide was isolated, and the evolved CO_2 was trapped. One molar acetic acid was selected as the solvent for the oxidation primarily because of the ease of isolation of oxamide from this medium. The amount of radioactivity in the isolated oxamide and the trapped CO_2 was then determined, and the amounts of these substances originating from the 6,7 positions of the starting material were calculated. The results of these calculations are summarized in Table 4-5. The results reveal that while essentially all of the isolated oxamide at pH 2.3 was derived from the 6 and 7 positions of the starting material, only about 1 percent of the total CO_2 was from position 6 or 7 at this pH. At higher pH, however, a greater percentage of the labelled CO_2 was found. The additional CO_2 undoubtedly resulted from oxidation of oxalic acid, formed by hydrolysis of tetraketopiperazine.

Electrochemical Oxidation of Related Compounds. In an attempt to gain information related to the possibility of certain intermediates in the electrochemical oxidation of 6,7-dihydroxypteridine, the electro-

TABLE 4-5

Percentage of Oxamide and Carbon Dioxide Originating from Positions 6 and 7 of 6,7-dihydroxypteridine

	Percentage from position 6 and 7	
pH	Oxamide	Carbon Dioxide
2.3	95	1.2
4.7	ND[a]	6.9
8.0	ND[a]	8.9

[a] ND = not determined

chemical oxidations of 4,5-dihydroxypyrimidine (8) and 2,4,6,7-tetrahydroxypteridine (9) were briefly examined. Although 4,5-dihydroxy-

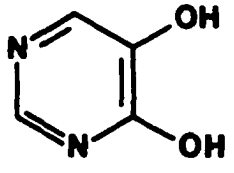

(8)

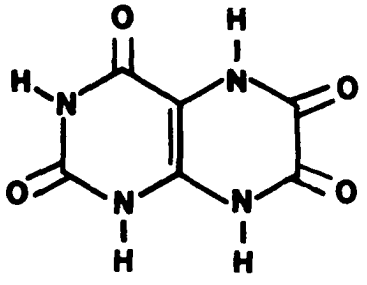

(9)

pyrimidine was not an expected intermediate, its reported electrochemical oxidation product,[10] 4,5-diketopyrimidine, could be formed as an intermediate in the oxidation of 6,7-dihydroxypteridine. In 1 M acetic acid, 4,5-dihydroxypyrimidine is oxidized at the PGE at E_p = 0.72 Volt vs SCE. Controlled potential coulometry in 1 M acetic acid at the PGE at 0.80 Volt resulted in the transfer of 2.7 - 3.0 electrons and the disappearance of the characteristic UV spectrum of 4,5-dihydroxypyrimidine (λ_{max} = 268 nm at pH 2.3). In addition, 1.7 moles of ammonia, 1.5 moles of CO_2, 0.8 moles of formaldehyde, and 0.7 moles of formic acid per mole of original 4,5-dihydroxypyrimidine were liberated. A trace of urea was also detected, but alloxan (10), a possible oxidation product, was not detected in the electrolyzed solution. The same compounds in essentially the same proportions were found when 4,5-dihydroxypyrimidine was oxidized electrochemically at pH 5 (E_p = 0.60 V, λ_{max} = 268 nm). The disappearance of the UV spectrum and the nature of the products of the oxidation of 4,5-dihydroxypyrimidine support the conclusion that upon oxidation, the product (i.e., 4,5-

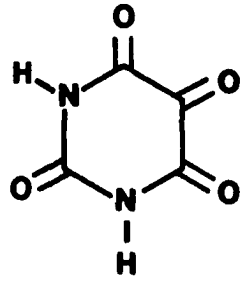

(10)

diketopyrimidine) undergoes extensive fragmentation.

In 1 M acetic acid 2,4,6,7-tetrahydroxypteridine is oxidized (E_p = 0.73 V vs SCE) at the PGE. Controlled potential coulometry at the PGE at 0.80 V in 1 M acetic acid (0.1 m mole 2,4,6,7-tetrahydroxypteridine in 100 ml 1 M acetic acid) resulted in the transfer of 1.7 - 2.1 electrons. Because of its very limited solubility in 1 M acetic acid, only a small part of the 2,4,6,7-tetrahydroxypteridine was initially in solution, but as the electrolysis proceeded the remainder of the material dissolved. Following electrolysis, a small amount of unidentified light yellow precipitate was present, but the characteristic UV spectrum of 2,4,6,7-tetrahydroxypteridine (λ_{max} = 332 nm, 285 nm at pH 2.3) had disappeared, and only a shoulder at 250 nm was observed in the UV. After electrolysis, analysis revealed that 0.5 moles of CO_2, 1.2 moles of NH_3, and 0.33 moles of oxamide per mole of starting material were formed. No tetraketopiperazine, urea, or alloxan was detected. If tetraketopiperazine were formed during the oxidation, a substantial percentage of the compound would hydrolyze during the course of the electrolysis because of the length of time required for complete oxidation (36 - 48 hr). Based upon the rate of hydrolysis

of tetraketopiperazine in 1 M acetic acid, however, if as much as 0.1 mole of tetraketopiperazine per mole of 2,4,6,7-tetrahydroxypteridine were formed in the reaction, a sufficient amount should have remained after electrolysis for polarographic detection.

It was also found that another possible intermediate, oxalic acid, is oxidizable at the PGE. This oxidation occurs at E_p = 0.95 V vs SCE in 1 M acetic acid. This oxidation was not studied in detail, but it is apparent that the most likely product is carbon dioxide.

Reaction Scheme. Summarizing the electrochemical and analytical data presented here, 6,7-dihydroxypteridine is apparently oxidized in an initial 2e, pH-dependent process. Overall, electrochemical oxidation involves approximately 6e and gives a variety of products including NH_3, CO_2, formic acid, formaldehyde, urea, oxamide, oxamic acid, and tetraketopiperazine. Almost all of the oxamide originates at the 6,7 positions of the starting material, while only a small amount of the CO_2 evolved during oxidation is derived from these positions. Electrochemical oxidation of 4,5-dihydroxypyrimidine involves about 2.8 electrons, and the products include CO_2, NH_3, formaldehyde, and formic acid. The electrochemical oxidation of 2,4,6,7-tetrahydroxypteridine results in the transfer of 2e, and CO_2, NH_3, and oxamide are produced. Reactions consistent with these observations are presented in Figs. 4-11 and 4-12.

Primarily on the basis of product analysis, n-values, and the similarity of the pteridine nucleus to the purine ring system, a mechanism is proposed where 6,7-dihydroxypteridine is electrochemically oxidized initially in a $2e\text{-}2H^+$ process to give compound (11) (Fig. 4-11A),

a di-imine. This compound (11) apparently reacts very rapidly with water to give a diol (12, Fig. 4-11A). Similar reactions have been postulated for the initial electrochemical oxidations of uric acid (23) and xanthine (24).[11] However, in the case of these purines (23, 24)

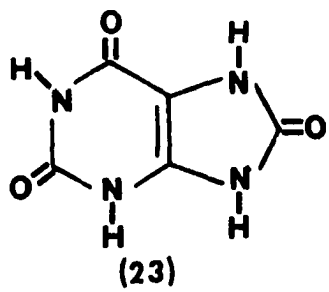

(23)

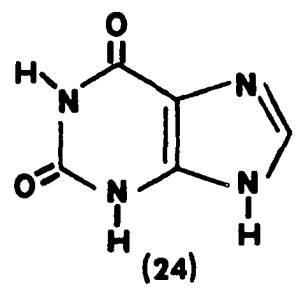

(24)

rapid sweep cyclic voltammetry showed that the di-imine could be reduced back to the starting material. The fact that no such reduction is observed in the case of 6,7-dihydroxypteridine, even at very fast sweep rates (50 V sec^{-1}), implies that the reaction of the di-imine (11, Fig. 4-11A) with water to form the diol (12, Fig. 4-11A) occurs extremely rapidly. A diol such as (12) has been proposed as an intermediate in the chemical oxidation of some pteridines, and in the presence of methanol, a dimethoxy compound was formed.[12] If initial oxidation of 6,7-dihydroxypteridine occurred at C_2 and C_4 to give 2,4,6,7-tetrahydroxypteridine, it would be expected that the products of the oxidation would be very similar to those observed upon oxidation of authentic 2,4,6,7-tetrahydroxypteridine. Such is not the case; in particular, tetraketopiperazine is not formed from the electrochemical oxidation of 2,4,6,7-tetrahydroxypteridine, and following oxidation of 2,4,6,7-tetrahydroxypteridine an unidentified precipitate remains, and a shoulder is observed in the UV at 250 nm.

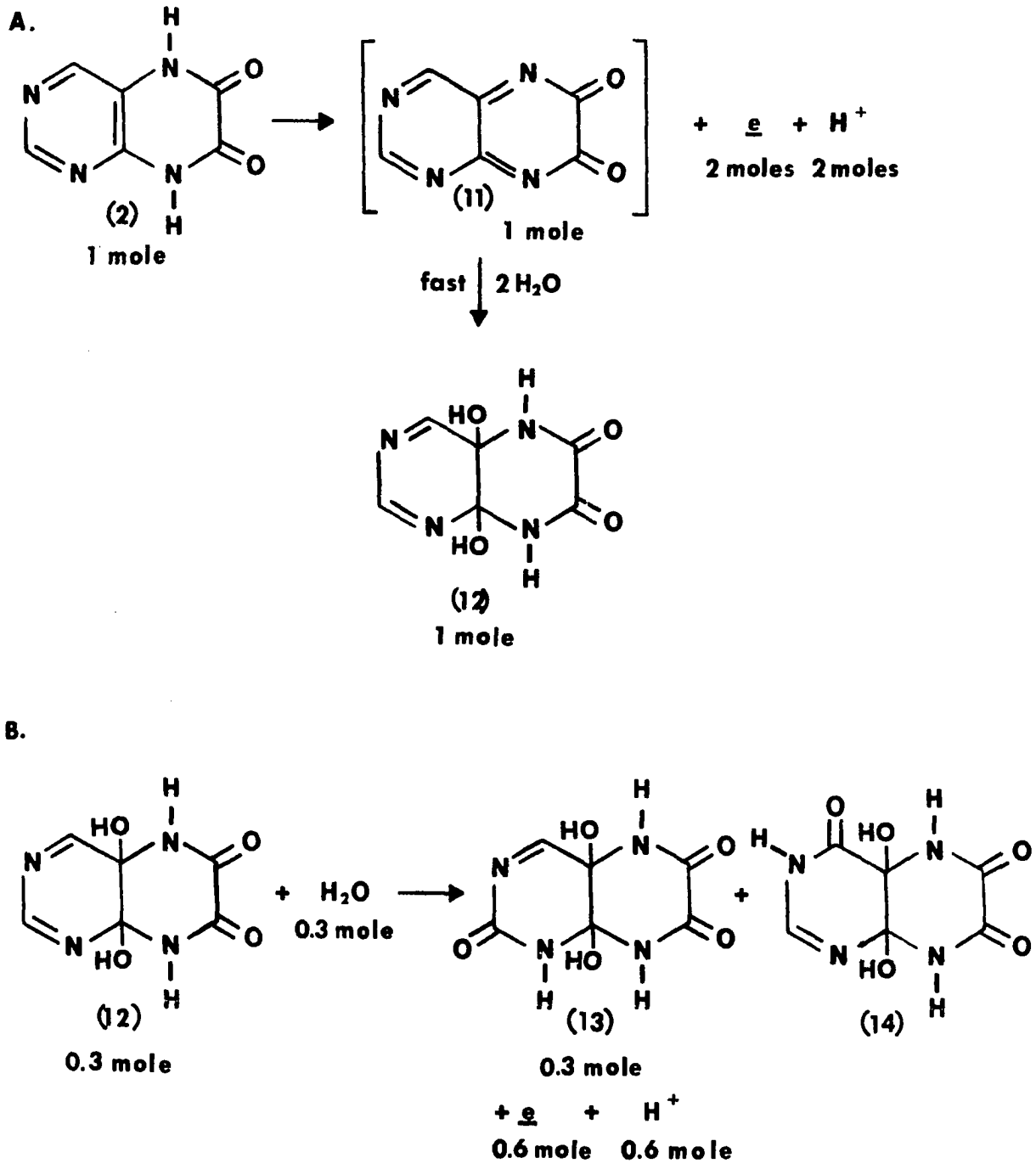

FIGURE 4-11. (A) Proposed initial electrochemical oxidation of 6,7-dihydroxypteridine. (B) Possible secondary electrochemical oxidation of 6,7-dihydroxypteridine.

Following the formation of the diol (12), a variety of chemical and electrochemical reactions are possible. Further electrochemical oxidation of (12) could occur at C_2 or C_4, producing (13) or (14). Although the presence of urea among the electrolysis products supports the formation of (13), it is certainly possible that both (13) and (14) are produced.

Following the electrochemical reactions represented in Fig. 4-11AB, the primary electrochemical products must undergo fragmentation and further electrochemical oxidation to the observed final electrolysis products. Proposed electrochemical and chemical reactions for formation of the ultimate products are presented in Fig. 4-12AB. Except as noted, molar quantities in Figs. 4-11AB and 4-12AB apply to the reactions at all pH values studied. Upon rearrangement, compound (12) gives 4,5-diketopyrimidine (15) and oxamide (5). As demonstrated by the electrochemical oxidation of 4,5-dihydroxypyrimidine, (15) is not stable, but undergoes extensive fragmentation and secondary oxidation, ultimately forming ammonia, carbon dioxide, formaldehyde and formic acid. The quantities of these compounds formed in the oxidation of 4,5-dihydroxypyrimidine are generally compatible with the route shown in Fig. 4-12A for the fragmentation of (15). Under the conditions of the Nessler test or chromotropic acid test, formamidine (16) would be expected to undergo hydrolysis to formamide, which would then be further hydrolyzed to formic acid.[13] Compound (17) is hydrolyzed to formaldehyde and oxalic acid (19), which is then oxidized electrochemically to carbon dioxide.

Because of the approximately equal quantities of urea and tetra-

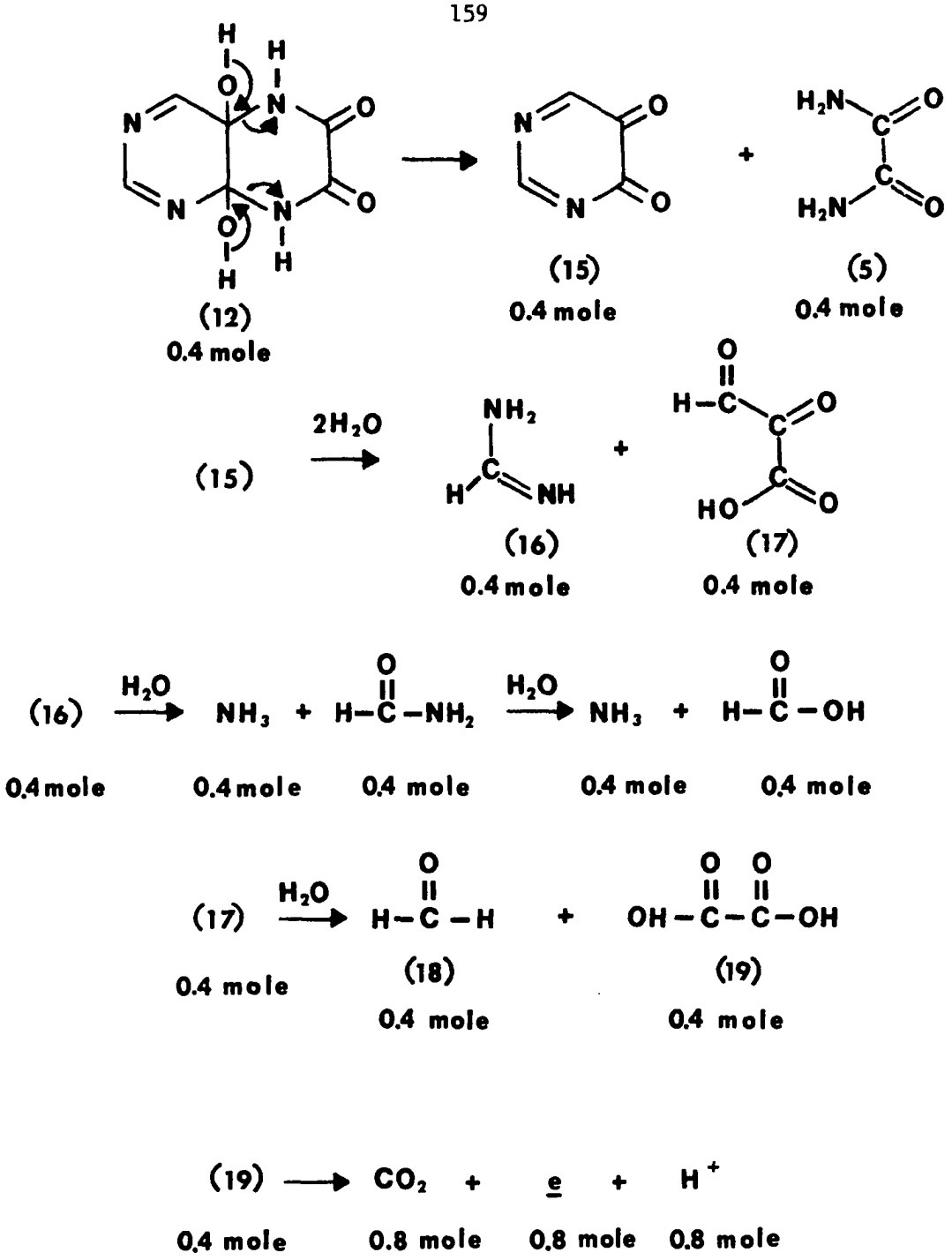

FIGURE 4-12A. Proposed reaction scheme for the rearrangement of the diol (12) to oxamide, followed by fragmentation of 4,5-diketopryimidine.

ketopiperazine obtained from the oxidation of 6,7-dihydroxypteridine at pH 2.3, it seems logical to propose that these compounds arise from a common intermediate. A plausible mechanism for formation of tetraketopiperazine and urea from compound (13) (Fig. 4-12B) involves hydrolysis of the $N_3=C_4$ bond, giving urea and compound (21). Compound (21) undergoes further electrochemical oxidation to the carboxylic acid (22), which by oxidative decarboxylation and dehydration forms tetraketopiperazine (7) and carbon dioxide. At pH > 4, tetraketopiperazine hydrolyzes to oxamic acid (6), oxamide (5), and oxalic acid (19). Oxalic acid is then oxidized electrochemically to carbon dioxide.

Analytical and electrochemical data indicate that no gross changes in the oxidation mechanism of 6,7-dihydroxypteridine occur as a function of pH. Changes which are noted at higher pH (i.e., disappearance of tetraketopiperazine, increased amounts of carbon dioxide and oxamide, and larger n-values) can be satisfactorily accounted for on the basis of tetraketopiperazine hydrolysis and oxidation of the evolved oxalic acid.

It should be pointed out that the primary purpose of a reaction scheme such as that presented in Figs. 4-11AB and 4-12AB is to demonstrate that the observed oxidation products can be derived from the starting material in a logical manner consistent with experimental observations. The intent is not to imply that these reactions represent the only possible route from starting material to product. Indeed, it is highly probable that other chemical and electrochemical reactions are involved, and that the proposed reactions do not occur in the orderly, stepwise fashion depicted.

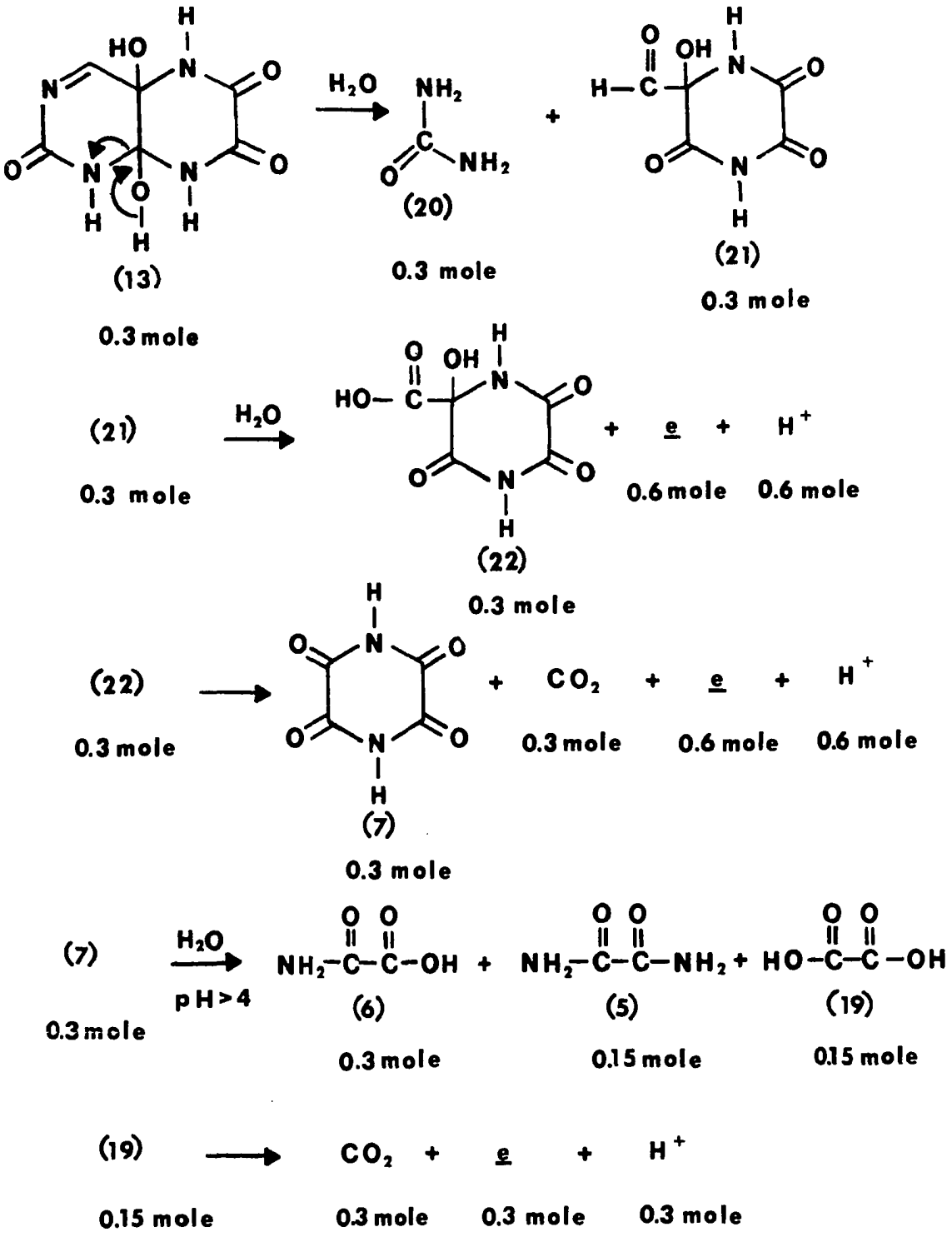

FIGURE 4-12B. Proposed reaction scheme for the rearrangement and oxidation of the diol (13) to tetraketopiperazine and urea.

If the quantities of products predicted by the reactions in Figs. 4-11AB and 4-12AB are compared to the quantities found by analysis (Table 4-4), it is apparent that the reactions presented do not account for all of the products found in the electrolyzed solution, particularly ammonia and carbon dioxide (Table 4-6). In addition, the electron number calculated from the proposed reactions is lower than that found by electrolysis. These observations imply, of course, that a portion of the 6,7-dihydroxypteridine is oxidized via reactions not represented in Figs. 4-11 and 4-12. This is not surprising,

TABLE 4-6

Comparison of Quantities of Oxidation Products of 6,7-dihydroxypteridine Predicted by the Proposed Reaction Schemes with the Quantities Found by Analysis

	Quantities Determined, moles[a]					
	By Analysis			From Reaction Scheme		
Product	pH 2.3	pH 4.7	pH 8.1	pH 2.3	pH 4.7	pH 8.1
NH_3	1.70	1.62	1.85	0.8	0.8	0.8
CO_2	1.93	2.18	2.34	1.1	1.4	1.4
Formaldehyde	0.36	0.46	0.35	0.4	0.4	0.4
Formic Acid	0.44	0.36	0.40	0.4	0.4	0.4
Urea	0.24	0.26	0.31	0.3	0.3	0.3
Oxamide	0.40	0.51	0.55	0.4	0.55	0.55
Tetraketopiperazine	0.29	----	----	0.3	----	----
n-value	5.54	5.80	5.98	4.6	4.9	4.9

[a] Based upon the oxidation of 1 mole of 6,7-dihydroxypteridine

however, since the tetraketopiperazine (0.3 mole) and oxamide (0.4 mole) found following electrolysis in 1 M acetic acid, for example, account for only 70% of the starting material. Assignment of reactions accounting for the production of additional ammonia and carbon dioxide is impossible because of the many positions within the starting molecule from which these compounds could originate. It is obvious, though, that these compounds must be formed via extensive hydrolysis and fragmentation similar to that in Fig. 4-12. The difference in the amount of CO_2 found by analysis and that calculated from the proposed reactions ranges from 0.78 - 0.94 mole, and the difference in n-value is from 0.90 - 1.08. It can be shown that these values are reasonably compatible; i.e., an n-value of 1.0 corresponds to the production of 0.6 mole of CO_2 from compound (12).

In summary, the electrochemical oxidation of 6,7-dihydroxypteridine seems to proceed by two routes, both involving rearrangement of diol intermediates, similar to the intermediates formed in the electrochemical oxidation of certain purines. One route involves rearrangement of the diol in such a way that the pyrimidine ring remains initially intact and oxamide is produced. In the other route, rearrangement of the diol occurs such that the pyrazine ring remains intact in the form of tetraketopiperazine, and urea is formed from the pyrimidine ring.

Experimental

Chemicals. Chemicals were obtained from the following sources: ethyl oxamate, 4,5-diamino-6-hydroxy-2-mercaptopyrimidine, 5,6-diamino-2,4-dihydroxypyrimidine, oxalic acid, oxamic acid, ethyl tartrate

(Aldrich); oxalic-1,2-^{14}C-acid (ICN Isotope and Nuclear Division); sodium bismuthate (Mallinckrodt), Aquasol (New England Nuclear); ethanolamine, 2,5-diphenyloxazole (PPO), p-bis-(O-methylstyryl)-benzene (bis-MSB), (Packard); oxamide (Matheson); phosphorus pentasulfide, p-dimethylaminobenzaldehyde, phenylhydrazine hydrochloride, 2,3-butanedione monoxime, urea (Eastman); Raney nickel (Sargent-Welch); Sephadex G-10 (Pharmacia).

The synthesis of 4,5-diaminopyrimidine was described in Chapter 2. The preparation of 6-hydroxypteridine was according to Albert,[2] and 7-hydroxypteridine and 6,7-dihydroxypteridine were prepared following Albert, Brown, and Cheeseman.[5] The method of Bertho and Bentler[14] was utilized in the synthesis of 2,4,6,7-tetrahydroxypteridine. Ethyl glyoxylate alchoholate was prepared by the method of Rigsby.[15] Tetraketopiperazine was synthesized by the method of de Mouilpied and Rule,[16] and 4,5-dihydroxypyrimidine was prepared following Bredereck, Effenberger, and Österlin.[17]

For thin layer chromatography, silica gel (Eastman 6060) and polyamide (Brinkmann MN-Polygram polyamide-6, UV_{254}) plates were used. Developing solvents were absolute methanol, methanol-glacial acetic acid (95:5), and 1-butanol-glacial acetic acid-water (12:3:5). Paper chromatograms on Whatman No. 1 filter paper were developed with ethylformate-formic acid-water (12:3:5), containing 0.015% bromophenol blue and 0.05% sodium formate, or ethanol-buffer (7:3) containing 0.03% chlorophenol red (buffer, 1.5 N solution of ammonium carbonate in 1.5 N aqueous ammonia).[18]

Buffer solutions for electrochemical studies were prepared as

previously described.

Apparatus. For controlled potential electrolysis and preparative electrolysis, the two-compartment cell described in Chapter 2 was employed. The working electrode consisted of five pyrolytic graphite plates (4.5 cm x 1.5 cm, 0.2 cm thick) suspended in the electrolysis solution. The remainder of the electrochemical apparatus was described in Chapter 2. Radioactive samples were counted in a Packard Tri-Carb Scintillation Spectrometer.

Voltammetric and Coulometric Procedures. Voltammetric and coulometric procedures were the same as described in Chapter 2.

Macroscale Electrolysis. Macroscale electrolyses usually involved the oxidation of 100 - 300 mg 6,7-dihydroxypteridine in 100 ml 1 M acetic acid. At the start of the electrolysis only a small part of the 6,7-dihydroxypteridine was in solution, but as the electrolysis proceeded, the remainder dissolved. Completion of the oxidation was confirmed by the disappearance of the characteristic UV absorption of 6,7-dihydroxypteridine. To reduce contamination of the products of macroscale electrolysis with KCl (from salt bridges and reference electrode), the two compartment cell was employed, one compartment for the working electrode and one for a platinum gauze counter electrode. These two compartments were separated by a fine sintered glass disc and an agar-acetic acid salt bridge. Such salt bridges were made by heating 4 g of agar with 40 ml of water until a homogeneous solution was obtained. Then, 40 ml of 2 M acetic acid was added and the solution cooled to room temperature when a stable gel was formed. The reference electrode was a Coleman fiber-tip SCE inserted into the working

electrode compartment.

Lyophilization of the solution after oxidation of 200 mg 6,7-dihydroxypteridine usually resulted in a buff-colored residue. At times, however, the residue turned to light red while still under vacuum. The red color probably arises from the reaction of ammonia (or ammonium salts) with tetraketopiperazine or small amounts of other unidentified pyrimidines or pyrazines to form murexide-like compounds. It was found that the color change could be prevented if the lyophilization vessel were cooled in an ice bath during the last stages of lyophilization.

Thin-layer and Paper Chromatography. Compounds were spotted on thin-layer and paper chromatograms as aqueous solutions. Identification was based on identical behavior of reference and unknown compounds on the same chromatogram.

Urea was visualized with Erlich's reagent (10% w/v p-dimethylamino-benzaldehyde in concentrated HCl) as a spot with R_f = 0.55 on silica gel plates developed with 1-butanol-acetic acid-water (12:3:5).

A spot having an R_f value of 0.65 on polyamide plates developed with methanol-acetic acid (95:5) was identified as tetraketopiperazine by comparison with the authentic compound.

Isolation and Identification of Oxamide. After lyophilization, about 5 ml of water was added to the residue, and a small amount of white solid failed to dissolve. This solid was isolated by filtration, washed with water and acetone, and identified as oxamide by comparison of its mass and infrared spectrum to that of authentic oxamide (Fig. 4-13). The purity of the isolated oxamide was ascertained by comparison of its polarographic diffusion current at pH 10 with that of

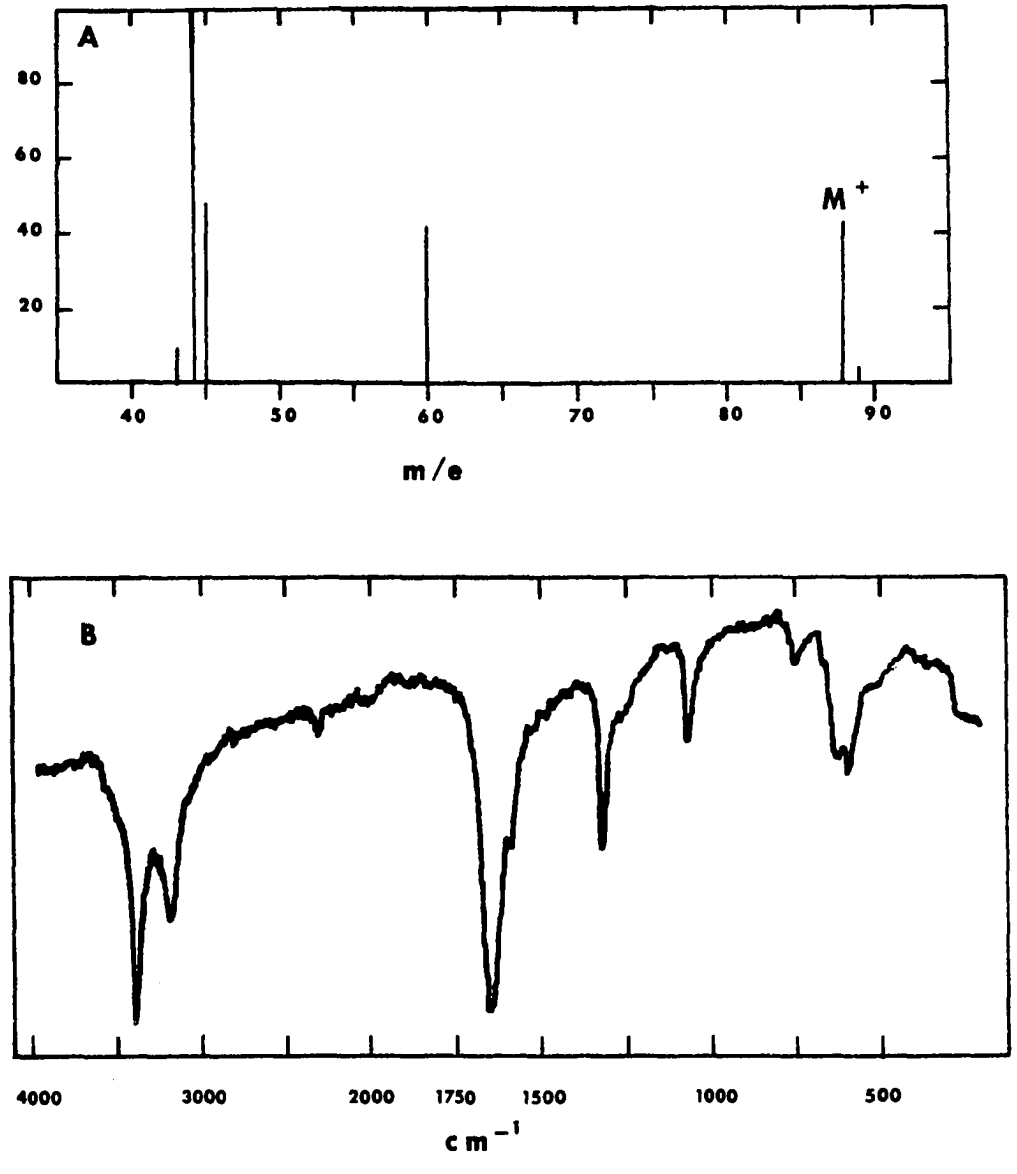

FIGURE 4-13. Mass (A) and IR (B) spectra of oxamide. IR spectrum is of a KBr disc.

authentic oxamide. Oxamide from the radioisotope labelling experiment was isolated in the same manner.

Oxamic acid was identified by comparison of its behavior on paper chromatography, with the authentic compound, using the method of Davies.[18] An appropriate acid-base indicator was incorporated into the developing solvent, and following development and drying, oxamic acid showed up as yellow spots (R_f = 0.65) on blue background (using ethyl formate-formic acid-water, 12:3:5, with 0.015% bromophenol blue) or yellow spots (R_f = 0.60) on a red background (using ethanol-buffer, 7:3, and chlorophenol red indicator).

Column Chromatography. The freeze-dried solid from mass electrolysis was dissolved in a small amount of water, filtered, and applied to a Sephadex G-10 column (1.5 x 100 cm) which had been conditioned by washing with at least one liter of 0.1 M acetic acid.[19,20] The material was eluted with 0.1 M acetic acid, and 100 fifty-drop fractions were collected. One ml was withdrawn from every fifth fraction, and added to 1 ml of pH 2.2 McIlvaine buffer, and a voltammogram at the HMDE was run. When an electroactive component was found, voltammograms were run on each fraction to permit isolation of the fractions containing the electroactive product. In this way, tetraketopiperazine was identified in fractions 40-55. These fractions were freeze-dried, leaving a white solid, which was confirmed as tetraketopiperazine by comparison of its voltammetry and its mass and IR spectra to those of the authentic compound (Fig. 4-14). Because the other major oxidation product, oxamide, shows no voltammetric peaks at low pH, and gives no UV absorbance in 0.1 M acetic acid, fractions 56-100 were freeze-dried

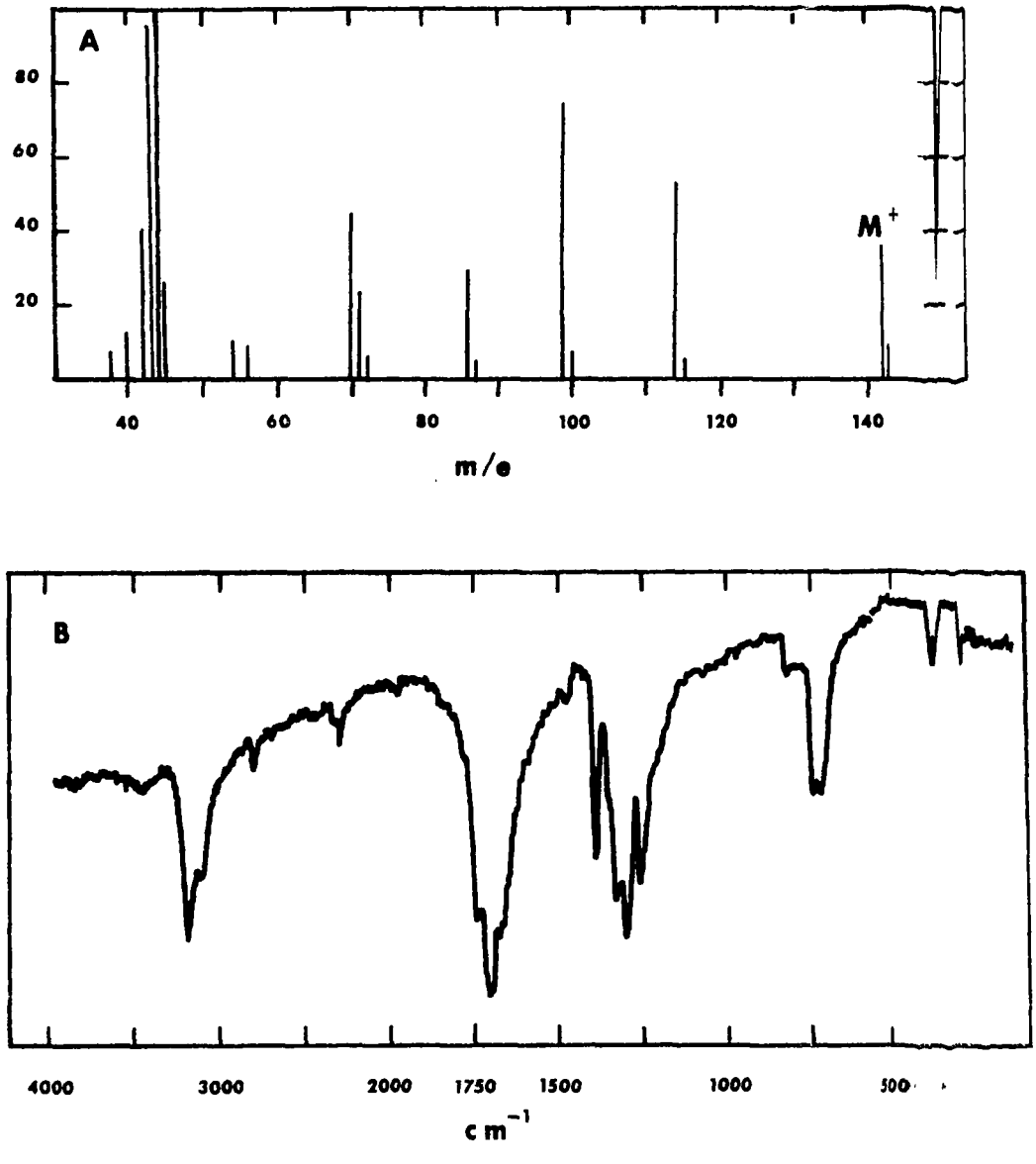

FIGURE 4-14. Mass (A) and IR (B) spectra of tetraketopiperazine . . . IR spectrum is of KBr disc.

individually to determine if oxamide was eluted. After lyophilization, fractions 59-67 and 75-85 appeared to contain the largest quantities of white solid. The material in fractions 59-67 was identified as oxamic acid by comparison of its mass and IR spectra to that of the authentic compound (Fig. 4-15) and the material in fractions 75-85 was similarly found to be oxamide (Fig. 4-13). However, since oxamic acid could not be detected in the original electrolysis solution in 1 M acetic acid, it was concluded that the oxamic acid from the Sephadex column most likely resulted from decomposition of tetraketopiperazine.

Determination of Carbon Dioxide. For the determination of carbon dioxide, the gas train was arranged as follows: argon cylinder, Ascarite tube, bubbling tower, electrolysis cell, dry ice trap, and saturated $Ba(OH)_2$ solution. The purpose of the Ascarite tube was to remove residual CO_2 from the argon, and the dry ice trap prevented water and acetic acid vapor from entering the $Ba(OH)_2$ solution. In a typical determination, the electrolysis solution was deaerated for about 15 minutes before the $Ba(OH)_2$ trap was connected. The $Ba(OH)_2$ trap consisted of a side-arm test tube (2 x 16 cm) into which the gas was passed via a gas dispersion tube or a dropping pipet with a very small opening. The saturated $Ba(OH)_2$ (15-20 ml) was filtered directly into the trap to minimize the possibility of absorption of atmospheric CO_2. After deaeration, the $Ba(OH)_2$ trap was connected to the outlet of the dry ice trap, and the electrolysis was begun. After 10-15 minutes a white precipitate of $BaCO_3$ began to appear. Following completion of the electrolysis, gas flow was continued for an additional 15-20 minutes, after which time the $Ba(OH)_2$ was filtered on a weighed medium

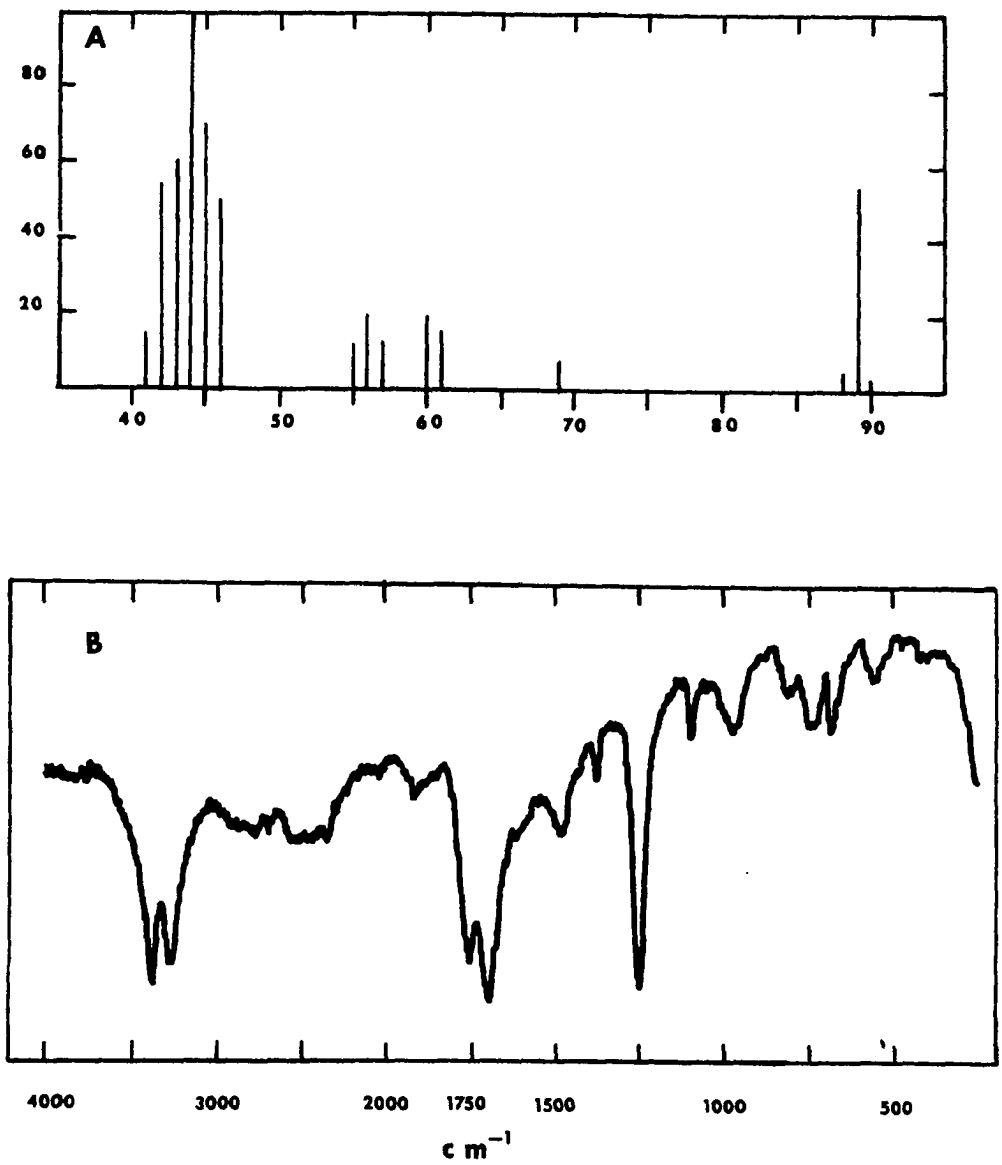

FIGURE 4-15. Mass (A) and IR (B) spectra of oxamic acid. IR spectrum is of a KBr disc.

porosity Büchner funnel. The precipitate was washed with freshly boiled distilled water and acetone, and dried in an oven at 120°C for 1 hour. The funnel plus precipitate was then weighed, and the amount of CO_2 calculated. Standardization experiments using $NaHCO_3$ showed that 95-100 percent of the released CO_2 could be recovered as $BaCO_3$. In ^{14}C labelling experiments, the $Ba(OH)_2$ was replaced with ethanolamine; the remainder of the system was unchanged.

Determination of Oxamide. Oxamide was determined at the completion of the electrolysis by lyophilizing a known volume of the electrolysis solution (usually 25 ml) and dissolving the residue in 10 ml pH 10 carbonate buffer. A polarogram was run of this solution and the concentration of oxamide was determined by comparing the height of the wave at -1.6 V with a calibration curve prepared from authentic oxamide (see Chapter 5).

Determination of Urea. Urea was determined by a modification of Rosenthal's method.[21,22] One milliliter of electrolysis solution was diluted in a test tube (2 x 16 cm) to 6.00 ml with water; 3.00 ml As (V) solution (10 ml concentrated HCl saturated with As_2O_5 and then diluted to 35 ml with HCl) and 1.00 ml 2,3-butanedione monoxime (2.5 w/v percent in 5 percent acetic acid) were added. The tube was placed in a boiling water bath for 30 min and then cooled for 3 min; the absorbance at 480 nm was measured, using a water blank carried through the entire procedure. Concentration was determined by comparison with a calibration curve prepared using samples of 10, 20, 30, 40, and 50 µg urea per 6 ml of water. It was determined that the other known components of the electrolysis solution did not interfere with

the urea determination.

Determination of Ammonia. Ammonia was measured by the Nessler method, following King and Faulconer.[23] Nessler reagent was prepared by slowly adding a saturated mercuric chloride solution to a solution of 50 g KI in 35 ml cold water until a slight precipitate of red mercuric iodide persisted. Then, 400 ml of clarified 9 M NaOH was added and the resultant solution diluted to one liter with water. After standing at room temperature for 24 hr, the clear supernatent liquid was decanted and was ready for use.

Following electrolysis, 1.00 ml of the electrolysis solution was diluted to 10.00 ml with water. Samples of this solution of 1.00 ml, 2.00 ml, or 3.00 ml were diluted to 9.00 ml with water in a 25 ml Erlenmeyer flask, mixed by swirling, and 1.00 ml Nessler reagent was added with swirling. After 5 min the absorbance at 400 nm was measured, using a water blank carried through the procedure. A calibration curve was prepared by diluting aliquots of a stock solution (10 mg NH_4Cl/1000 ml water) so that the weight of NH_3 in the final solution was 5 to 30 μg.

The response of other identified products (urea, oxamide, tetraketopiperazine, oxamic acid) to the Nessler test was determined by running samples of known quantities of these compounds along with the samples of the electrolysis solution. The test results were then corrected to account for the response of these identified products.

Formation of an orange-yellow precipitate on addition of Nessler's reagent to the test solution indicates that the latter is too concentrated in ammonia or that swirling during addition of reagent was

insufficient; such samples were discarded.

Determination of Tetraketopiperazine. Tetraketopiperazine was determined at the completion of the electrolysis by transferring about 10 ml of the electrolysis solution in 1 M acetic acid or pH 2.2 McIlvaine buffer solution to the polarographic cell, deaerating, running a polarogram between 0 and -0.7 V, and comparing the height of the wave at -0.42 V with a calibration curve prepared from authentic tetraketopiperazine.

Determination of Formaldehyde. Aliquots of 0.5 to 1.0 ml of electrolysis solution were transferred to test tubes and diluted to 1.0 ml with water. Then 1 ml chromotropic acid solution (0.6 g of the disodium salt of chromotropic acid in 20 ml of water added to 180 ml of concentrated H_2SO_4) was added and the volume made up to 10 ml with concentrated H_2SO_4. The tubes were heated in a boiling water bath for one hour, cooled to room temperature, and the absorbance was measured at 570 nm against a water blank carried through the same procedure. A calibration curve was prepared with standard formaldehyde solution. No other identified oxidation products respond to this test.

Determination of Formic Acid. Formic acid was determined by a modification of the method of Snell and Snell.[24] A sample of 0.25 - 0.5 ml of electrolysis solution containing not more than 0.015 mg formic acid was added to a test tube containing 40 mg of coiled magnesium ribbon. The test tube was immersed in an ice bath and a drop of concentrated HCl was added after each 1-3 minute interval until 10 drops (0.5 ml) were added. One minute after the last addition, the test tube was removed from the ice bath and 1.5 ml of a reagent, made by mixing 20 ml of water containing 0.6 g of the disodium salt of chromo-

tropic acid with 180 ml concentrated H_2SO_4, was added. The test tube was placed in a boiling water bath for 30 min, the test tube was centrifuged to remove any white precipitate, and the absorbance was measured at 570 nm vs a blank carried through the entire procedure. The absorbance was compared to a standard curve prepared using known quantities of formic acid. Because of the rather severe conditions employed. compounds which are hydrolyzed to formic acid in acid solution (e.g., formamide, formamidine) also respond to the test. These compounds are reported in the results as formic acid. Formaldehyde also responds to the test, but since formaldehyde was determined in a separate procedure, adjustments for its presence could be made.

Determination of Oxalic Acid. In the stability studies of tetraketopiperazine, oxalic acid was determined by linear scan voltammetry at the PGE. Following hydrolysis of a known amount of tetraketopiperazine, the solution was lyophilized and the residue was dissolved in a known volume of 1 M acetic acid. A voltammogram of the solution was run at the PGE, and the quantity of oxalic acid present was determined by comparison of the height of the voltammetric peak at 0.95 V to a standard curve.

^{14}C Labeling Experiments. Labelled 6,7-dihydroxypteridine (6,7-^{14}C) was prepared from 4,5-diaminopyrimidine and oxalic-1,2-^{14}C-acid. The product had a specific activity of 0.45 μc per millimole. Following electrolysis of 200 mg labelled 6,7-dihydroxypteridine, oxamide was isolated as previously described. One milligram of this oxamide was dissolved in 10 ml water, 10 ml of Aquasol was added to 1 ml of this solution in a counting vial, and the radioactivity was

measured in a scintillation counter. For determination of labelled CO_2, 15 mg of labelled 6,7-dihydroxypteridine was oxidized and the CO_2 was trapped in 10.0 ml of ethanolamine. After absorption, 2 ml of ethanolamine was dissolved in 4 ml of methanol, and 2 ml of scintillation solution composed of 16 g PPO and 1 g bis-MSB per liter of toluene was added. Radioactivity was then measured in a scintillation counter. The extent of quenching was determined by addition of an aliquot of oxalic-1,2-^{14}C-acid of known activity to each sample, and noting the increase in the counts per minute.

Summary

Over the pH range 2.3 - 10, 6-hydroxypteridine is oxidized electrochemically at the pyrolytic graphite electrode in a $2\underline{e}/2H^+$ process to 6,7-dihydroxypteridine. In very acidic solution (1 - 2 $\underline{M}$ H_2SO_4), 7-hydroxypteridine is electrochemically oxidized to 6,7-dihydroxypteridine at the PGE. The electrochemical oxidation of 6,7-dihydroxypteridine at the PGE occurs over the pH range 2.3 - 9 and involves approximately 6$\underline{e}$. The initial electrochemical reaction apparently involves formation of a diol on the bridgehead carbon atoms. The diol undergoes rearrangement, further oxidation, and hydrolysis, yielding as final products oxamide, tetraketopiperazine, urea, oxamic acid, ammonia, formaldehyde, formic acid, and carbon dioxide. These electrochemical and chemical reactions were studied by polarography, cyclic and linear scan voltammetry, coulometry, macroscale electrolysis followed by product isolation and identification, and radioisotope tracer techniques.

References

1. F. Bergmann and M. Kwietny, Biochem. Biophys. Acta, 33, 29 (1959).

2. A. Albert, J. Chem. Soc., 1955, 2690.

3. A. Albert and S. Matsuura, J. Chem. Soc., 1962, 2162.

4. D. J. Brown and S. F. Mason, J. Chem. Soc., 1956, 3443.

5. A. Albert, D. J. Brown, and G. Cheeseman, J. Chem. Soc., 1952, 1620.

6. Y. Inoue and D. D. Perrin, J. Chem. Soc., 1962, 2600.

7. R. N. Wopschall and I. Shain, Anal. Chem., 39, 1514 (1967).

8. R. S. Nicholson and I. Shain, Anal. Chem., 36, 706 (1964).

9. Yolanda T. Pratt, in Heterocyclic Compounds, (R. C. Elderfield, ed.), Vol. 6, Wiley, New York, 1957, p. 454.

10. K. Chiang and P. Chang, Hua Hsüeh Hsüeh Pao, 24, 300 (1958).

11. G. Dryhurst, J. Electrochem. Soc., 119, 1659 (1972).

12. R. C. Elderfield and A. C. Mehta, in Heterocyclic Compounds, (R. C. Elderfield, ed.), Vol. 9, Wiley, New York, 1967, p. 18.

13. J. March, Advanced Organic Chemistry: Reactions, Mechanisms, and Structure, McGraw-Hill, New York, 1968, pp. 656, 313.

14. A. Bertho and M. Bentler, Ann. Chem., 570, 127 (1950).

15. W. Rigsby, J. Chem. Soc., 1950, 1912.

16. A. T. de Mouilpied and A. Rule, J. Chem. Soc., 91, 179 (1907); 95, 549 (1909).

17. H. Bredereck, F. Effenberger, and H. Österlin, Chem. Ber., 100, 2280 (1967).

18. C. Davies, R. D. Hartley, and G. J. Lawson, J. Chrom., 18, 47 (1965).

19. J. V. Khym and M. Uziel, J. Chrom., 47, 9 (1970).

20. P. A. Simkin, J. Chrom., 47, 103 (1970).

21. H. L. Rosenthal, Anal. Chem., 35, 1770 (1963).

22. G. Dryhurst and P. J. Elving, J. Electrochem. Soc., 115, 1014 (1968).

23. R. W. King and W. B. N. Faulconer, Anal. Chem., 28, 255 (1956).

24. F. D. Snell and C. T. Snell, Colorimetric Methods of Analysis, Vol. III, Van Nostrand, New York, 1953, p. 304.

CHAPTER 5

THE ELECTROCHEMICAL REDUCTION OF OXAMIDE

Introduction

During the investigation of the electrochemical oxidation of 6,7-dihydroxypteridine, it became necessary to detect and quantitatively determine oxamide, a principal oxidation product. The methods described in the literature generally involve alkaline hydrolysis of oxamide to oxalic acid and ammonia, followed by titration of the acid[1] or titration of the liberated ammonia.[2] These methods were unsatisfactory for analysis of mixtures from the oxidation of 6,7-dihydroxypteridine that contained urea, amides and other species that are hydrolyzed to ammonia, other volatile bases, or organic acids. Investigation revealed that oxamide gives a very well-defined polarographic reduction wave in neutral and alkaline solutions that could be used for its analytical determination.

This chapter describes a detailed examination of the mechanism of electrochemical reduction of oxamide and the use of the d.c. polarographic wave for its analysis.

Results and Discussion

D.C. Polarography. Between pH 5.6 and 11.6 oxamide exhibits a single well-formed polarographic wave. The half-wave potential of this wave is independent of pH, $E_{1/2} = -1.59 \pm 0.01$ V. Between pH 5.6 - 8.0 the polarographic diffusion current constant ($I = \frac{i_l}{Cm^{2/3}t^{1/6}}$) is constant, but at higher pH it systematically decreases with increasing pH (Fig. 5-1). At pH values above 11.6 the hydrolysis of oxamide becomes rapid.[3] Below pH 5.6 the wave is obscured by background discharge. Relatively small but definite changes were noted in the dependence of the limiting current on mercury column height and temperature at different pH values. Thus, at pH 8.1 the ratio of the limiting current to the square root of the corrected mercury column height was constant (Table 5-1), while at pH 11.1 a small but definite decrease in $i_l/h_{corr}^{1/2}$ was noted (Table 5-1). Coupled with the fact that the temperature coefficient of the limiting current at pH 8.1 is 0.4% per °C but 2.0% per °C at pH 11.1, it was concluded that above pH 8.1 the decrease in the limiting current is due to some homogeneous kinetic process. There are only two probable homogeneous kinetic processes the rates of which could explain the decrease in the limiting current with pH. The first is a chemical reaction preceeding the electron transfer reaction, the second a chemical reaction or reactions interposed between two electrochemical reactions, i.e., an ECE mechanism. Before attempting to further elucidate the details of the electrode mechanism it was necessary to decide which of the two homogeneous chemical steps was involved in the overall electrode process. The only reasonable preceeding chemical reactions would

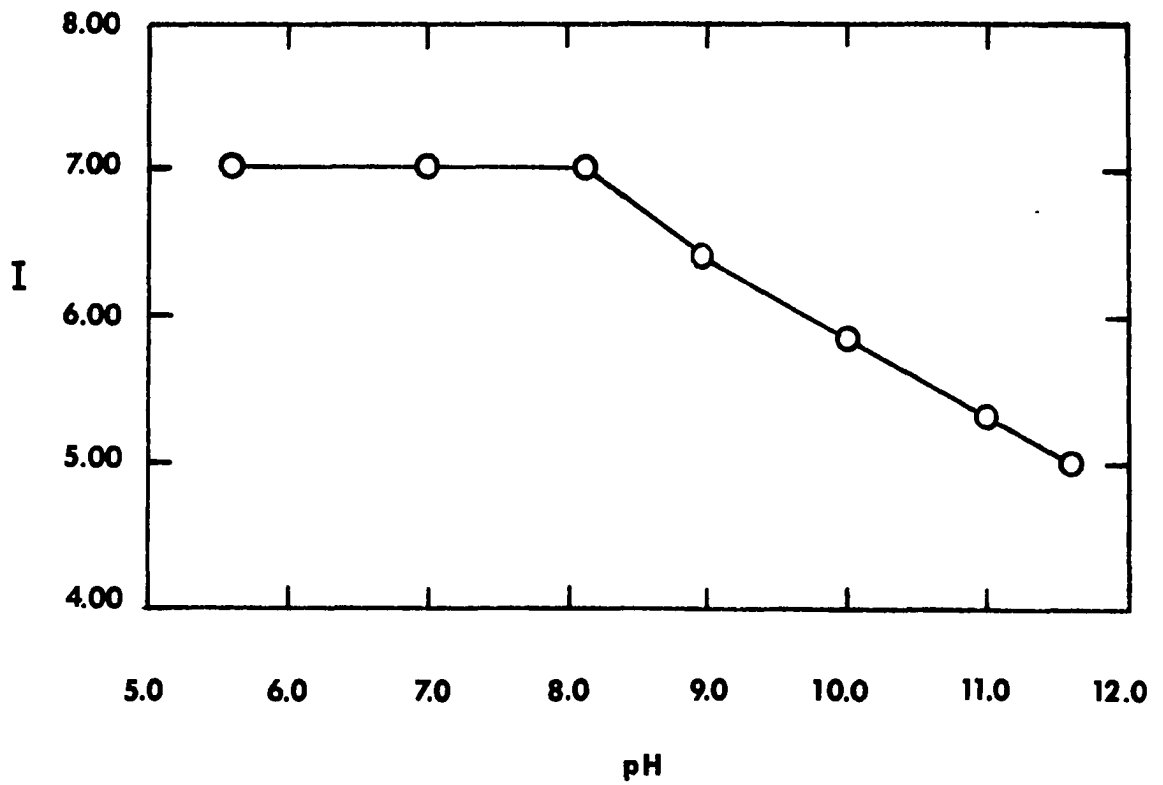

FIGURE 5-1. Variation of the diffusion current constant ($I = i_l/Cm^{2/3}t^{1/6}$) with pH for oxamide.

TABLE 5-1

Effect of Corrected Mercury Column Height and Temperature on the Limiting Current for Oxamide

	$i_1/h_{corr}^{1/2}$, $\mu A\ cm^{-1/2}$		Temperature coefficient of i_1 [b]	
h_{corr} [a], cm	pH 8.1	pH 11.1	pH 8.1	pH 11.1
41.7	0.794	0.665		
51.7	0.797	0.642		
61.7	0.787	0.624	0.4% per °C	2.0% per °C
71.7	0.804	0.622		
81.7	0.803	0.612		

[a] $h_{corr} = h_{meas} - \frac{3.1}{(mt)^{1/3}}$

[b] $TC = \left[\frac{2.303}{(T_2-T_1)} \log \frac{i_2}{i_1}\right] (100)$

where i_2 is the limiting current at T_2 (40°C) and i_1, the limiting current at T_1 (25°C).

involve dissociation or hydration of oxamide. Spectrophotometrically, no evidence for dissociation of oxamide up to pH 11.6 could be obtained. Indeed, compounds similar to oxamide (e.g., acetamide) have acidic pKa values around 30.[4]

In order to investigate the possibility of a hydration-dehydration reaction involving oxamide, the variation of the molar absorptivity as a function of pH was first investigated. Oxamide exhibits two absorption bands in the UV region, one at ca. 280 nm ($\varepsilon \approx 50$) and the

second at ca. 205 nm ($\varepsilon \simeq 10^4$). The former peak is probably due to an $n \rightarrow \pi^*$ transition, the latter to a $\pi \rightarrow \pi^*$ transition, both associated with the carbonyl groups. The peak at 205 nm could only be satisfactorily observed below pH 8 because of solvent absorption. The peak at 280 nm was essentially independent of pH with respect to both λ_{max} and ε_{max}. Addition of dioxane to aqueous buffered solutions of oxamide between pH 7-11 did not result in any significant spectral changes except for minor shifts of λ_{max} (2 nm over dioxane concentration range 0-50%). A temperature change of ca. 40°C also caused no appreciable spectral changes. Bell[5] has indicated that if a carbonyl compound shows an absorption band around 280 nm in aqueous solution which is unaffected by addition of dioxane or change of temperature, then hydration probably does not occur.

In view of these findings it was concluded that oxamide is reduced in a process where one or more chemical reactions are interposed between two electron-transfer reactions. This conclusion was borne out by further electrochemical studies described below.

Controlled Potential Electrolysis and Coulometry. Coulometry of oxamide between pH 7-11 indicated that 4 ± 0.2 electrons per molecule were transferred at all pH values (Table 5-2). Analysis for ammonia liberated during the electrolysis (see Experimental) revealed that 1 ± 0.2 mole of ammonia per mole of oxamide electrolyzed was liberated. Following larger scale electrolyses at controlled potential, glycolamide was found to be the only other product in essentially quantitative yield (see Experimental).

TABLE 5-2

Coulometric n-values for the Electrochemical Reduction of Oxamide at Mercury

Buffer system	pH	Controlled potential, Volts vs SCE	n
Borax	8.1	-1.65	3.82
Borax	8.1	-1.65	3.92
Borax	9.8	-1.65	3.95
Borax	9.8	-1.65	3.77
Carbonate	10.0	-1.65	4.15
Carbonate	10.0	-1.65	3.90

Voltammetry at the HMDE. Linear and cyclic sweep voltammograms of oxamide were run at the HMDE (hanging mercury drop electrode) in aqueous solutions of pH 5.6-11.6. At sweep rates of 5 mV sec^{-1}, oxamide shows a single cathodic peak (peak I_c) the peak potential (E_p) of which is independent of pH, $E_p = -1.63 \pm 0.02$ V. As the potential sweep rate is increased, the peak shifts to more negative potentials, e.g., at 200 Volt sec^{-1} in pH 10.0 carbonate buffer, $E_p = -1.90$ V. Such behavior is expected of an irreversible electrochemical reaction.[6]

At sweep rates below 20 Volt sec^{-1} in aqueous solution, cyclic voltammetry gave no indication of any anodic peaks after having scanned the cathodic peak (Fig. 5-2A). However, at sweep rates above 50 Volt sec^{-1}, a small anodic peak (peak I_a) was observed after having scanned cathodic peak I_c (Fig. 5-2B). Anodic peak I_a was

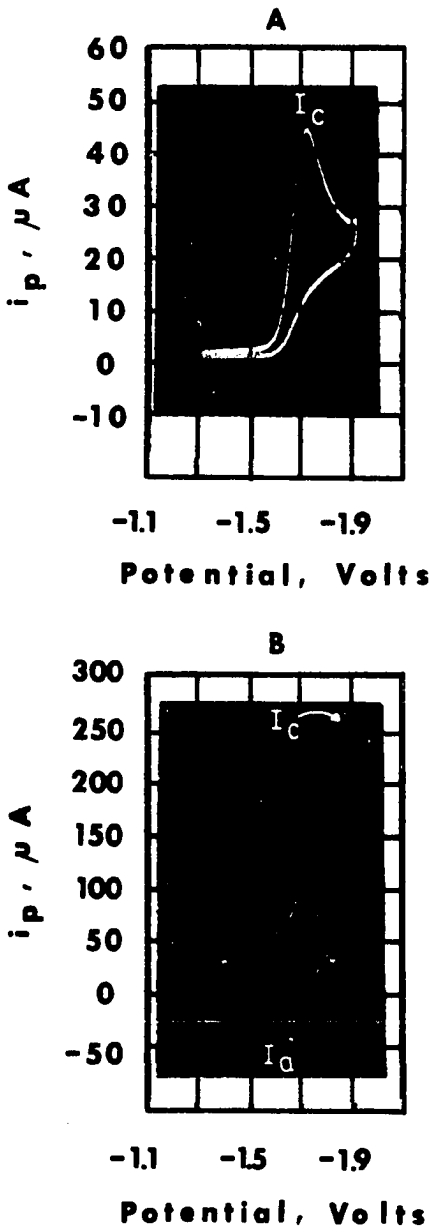

FIGURE 5-2. Cyclic voltammograms of 0.5 mM oxamide at the HMDE in pH 10.0 carbonate buffer. Sweep rate; (A) 2 Volt sec^{-1}; (B) 100 Volt sec^{-1}.

always much smaller than cathodic peak I_c, and its E_p was about 200 mV more positive than peak I_c.

In an attempt to more closely observe the anodic peak I_a observed on cyclic voltammetry of oxamide, some initial studies were carried out in acetonitrile solution. Unfortunately, oxamide is extremely insoluble in pure acetonitrile and other aprotic solvents so that it was not possible to obtain useful data. However, in 50% aqueous buffered solutions - 50% acetonitrile, peak I_a appears at a sweep rate as low as 2 Volt sec^{-1}. At very rapid sweep rates in the latter medium a new cathodic peak (peak II_c) appears at a more positive potential than peak I_c (Fig. 5-3A). As the concentration of oxamide is decreased, peak I_c decreases in height, but the height of peak II_c remains constant (Fig. 5-3B) until very low concentrations are reached. The peak current function for peak II_c increases greatly with increasing scan rate. This evidence supports the view that peak II_c is an adsorption prepeak, corresponding to reduction of oxamide to an adsorbed product.[7]

The fact that peak I_a would be observed by cyclic voltammetry at considerably lower scan rates in partially non-aqueous media suggests that the stability of the species being oxidized in the peak I_a process is considerably less in totally aqueous solution.

The shift of the peak potential for peak I_c with sweep rate, the failure to detect anodic peak I_a except at very fast sweep rate, and the separation of peak potentials for peaks I_c and I_a when both are observed are all consistent with an overall irreversible electrochemical reaction.

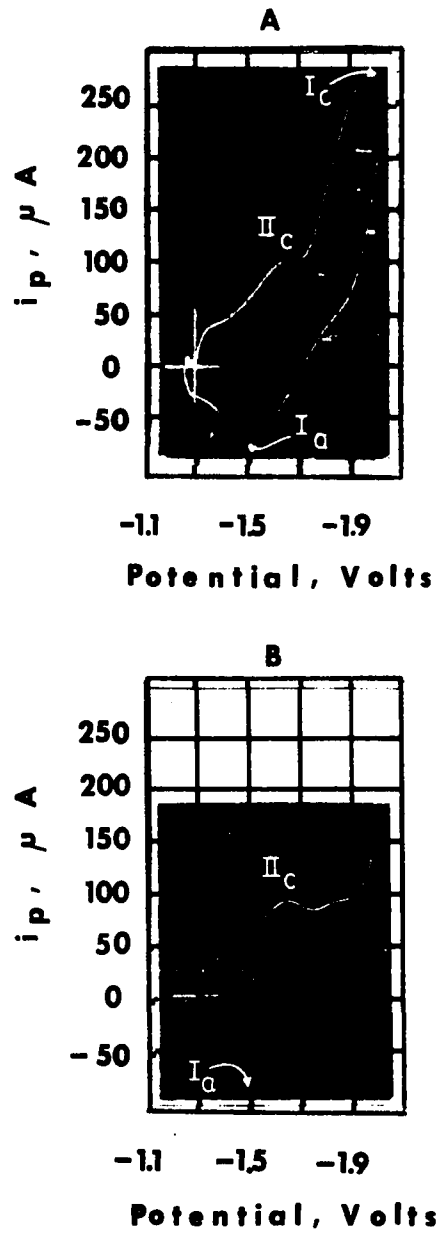

FIGURE 5-3. Cyclic voltammograms of oxamide at the HMDE in 50% acetonitrile - 50% pH 10.0 carbonate buffer. (A) 0.5 mM oxamide; (B) 0.05 mM oxamide. Sweep rate 100 Volt sec^{-1}.

In order to define more completely the reduction process occurring at the electrode, the effect of potential sweep rate on the peak voltammogram of oxamide was examined. The theoretical equation of a linear diffusion controlled irreversible peak voltammogram is:[6]

$$(i_p)_{irrev} = 2.98 \times 10^5 \, n \, (\alpha n_a)^{1/2} A D^{1/2} v^{1/2} C \qquad (5\text{-}1)$$

where $(i_p)_{irrev}$ = irreversible voltammetric peak current, microamperes

n = total number of electrons involved in the electrochemical reaction

α = electron transfer coefficient

n_a = number of electrons involved in the rate-controlling step of the reaction

A = electrode area, cm^2

D = diffusion coefficient of electroactive species, cm^2 sec^{-1}

v = voltage sweep rate, Volts sec^{-1}

C = bulk concentration of electroactive species, millimoles $liter^{-1}$.

According to equation (5-1) the peak current function, $i_p/ACv^{1/2}$, should remain constant with variation in scan rate if chemical complications or adsorption are not involved in the electrode process. In the case of oxamide, the peak current function decreases with increasing scan rate (Fig. 5-4) at all pH values. The onset of this decrease shifts to lower sweep rates with increase in pH.

By computing a value of αn_a from the equation:[8]

$$(E_{p/2})_2 - (E_{p/2})_1 = - \frac{0.0128}{\alpha n_a} \ln \frac{v_2}{v_1} \qquad (5\text{-}2)$$

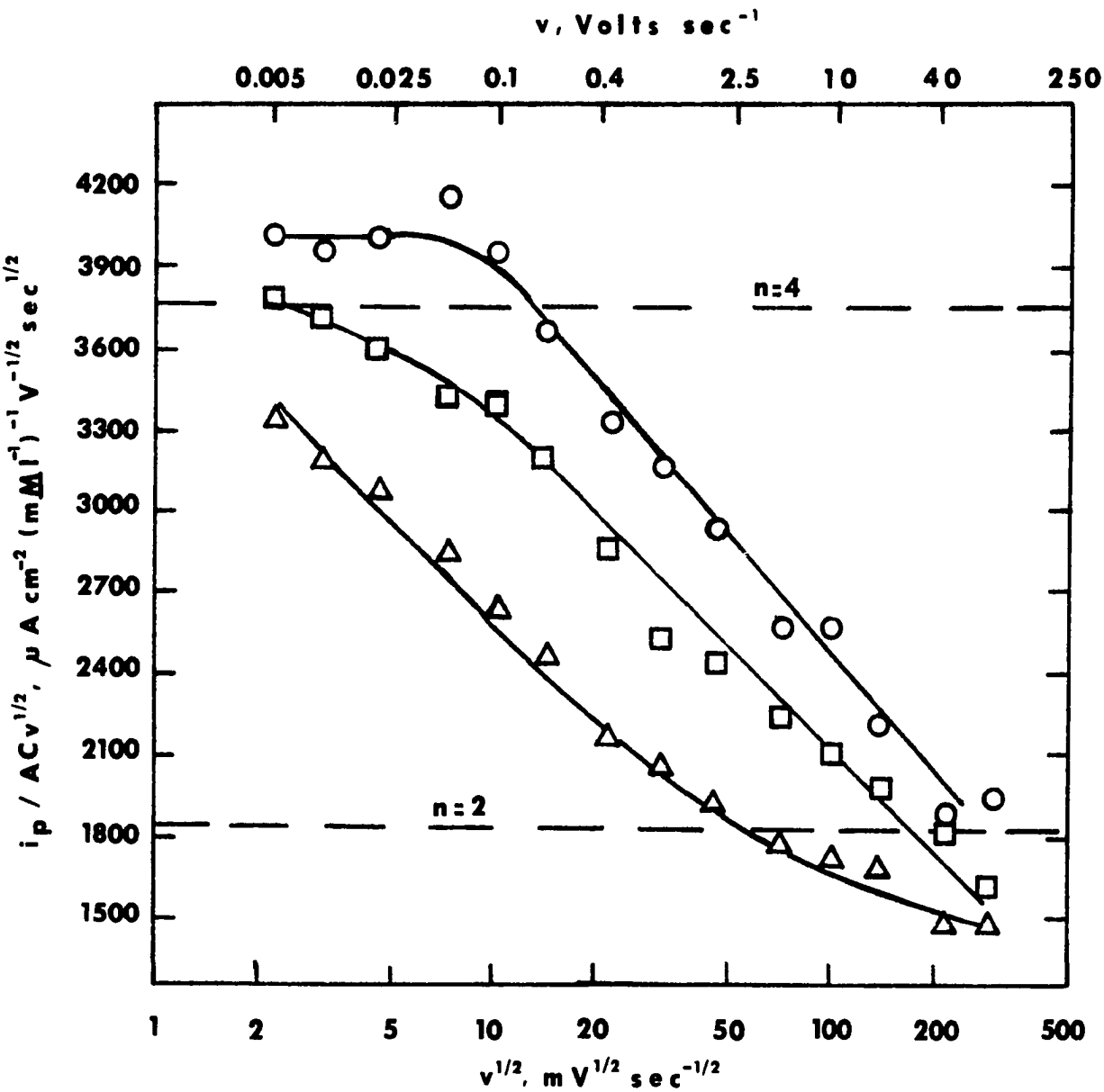

FIGURE 5-4. Variation of the peak current function of oxamide peak I_c at the HMDE with the square root of scan rate in various buffer systems. O—O pH 7.0 McIlvaine, □—□ pH 10.0 carbonate and Δ—Δ pH 11.8 hydroxide-chloride buffer. The dotted lines show theoretical peak current functions for n = 4 and n = 2 when no chemical complications occur.

where $(E_{p/2})_1$ and $(E_{p/2})_2$ are the half-peak potentials (Volts) for oxamide peak I_c at sweep rates v_1 and v_2 (Volts sec^{-1}) it is possible to compute theoretical peak current functions for uncomplicated irreversible electrode reactions. Using an αn_a value of 1.0 (the measured values of αn_a between pH 7-11.6 ranged from 1.04 to 0.80) theoretical peak current functions for n = 4 and n = 2 were calculated (Fig. 5-4). It is clear that at low sweep rates the peak current function of oxamide peak I_c is close to that expected for a 4e reaction while at fast sweep rates it approaches the theoretical value for a 2e reaction. This behavior is indicative of an electrode process in which the initial electron-transfer reaction is followed by one or more chemical reactions which in turn is followed by a further electron-transfer process, i.e., an ECE process,[7] or an electrode process preceeded by a chemical reaction. However, in view of the spectrophotometric studies of oxamide the probability of the latter process was considered remote, and an ECE mechanism was presumed to occur.

The theory of stationary electrode voltammetry for the ECE mechanism has been treated by Nicholson and Shain.[9] According to this treatment, the observed current can be calculated for a process in which both electron-transfer steps are reversible from the expression:

$$i = 6.02 \times 10^5 AD^{1/2}Cv^{1/2}[n_1^{3/2}\sqrt{\pi}\,\chi(at) + n_2^{3/2}\sqrt{\pi}\,\phi(at)] \qquad (5\text{-}3)$$

where $a = \frac{nFv}{RT}$, $\sqrt{\pi}\,\chi(at)$ = current function for the first charge transfer, $\sqrt{\pi}\,\phi(at)$ = current function for the second charge transfer, and n_1 and n_2 = the number of electrons involved in the first and

second charge transfers, respectively. Values for the functions $\sqrt{\pi}\ \chi(at)$ and $\sqrt{\pi}\ \phi(at)$ are tabulated for various values of k_f/a, where k_f is the homogeneous rate constant for the chemical step(s) interposed between the two charge transfer reactions.[9] In order to adapt this theory to the reduction of oxamide in which both electron-transfer reactions are apparently irreversible, equation (5-3) was rewritten in a form that probably approximates this process but still allows the use of theoretical current functions tabulated by Nicholson and Shain,[7,9] as follows:

$$i = 6.02 \times 10^5 AD^{1/2}Cv^{1/2}[n_1(\alpha n_a)_1^{1/2}\sqrt{\pi}\ \chi(bt) + n_2(\alpha n_a)_2^{1/2}\sqrt{\pi}\ \phi(at)] \quad (5\text{-}4)$$

where $\sqrt{\pi}\ \chi(bt)$ is the current function for an irreversible charge transfer and the remaining terms have their usual significance.[7] Theoretical current functions for the second irreversible electron-transfer step have never been derived, and accordingly the function $\sqrt{\pi}\ \phi(at)$ was necessarily employed in the calculations. Using equation (5-4) theoretical peak current functions, $i_p/ACv^{1/2}$, were calculated for ECE processes where the rate constant ranged from 1-200 sec^{-1}. The values of $\sqrt{\pi}\ \chi(bt)$ were obtained from reference 6 and correspond to the maximal values; the values of $\sqrt{\pi}\ \phi(at)$ were obtained from reference 9 and again were maximal values. When these theoretical peak current functions vs square root of sweep rate curves were compared to the experimental curves it was possible to approximate values of k_f (Table 5-3). The value of αn_a used in the theoretical calculations was taken as unity (vide supra). The diffusion coefficient was determined at pH 7 from the slope of current-time curves using

TABLE 5-3

Values of the Homogeneous Rate Constant, k_f, for the Chemical Step in the Electrochemical Reduction of Oxamide at a Mercury Electrode

		k_f, sec^{-1}, From		
Buffer system	pH	Peak voltammetry	Potentiostatic	Polarographic
McIlvaine	7.0	50	30	
Borax	10.0	10	13	6.5
Chloride-Hydroxide	11.6	1	2	1

the method of Shain and Martin[10] (see Appendix 5) and had a value of 9.73×10^{-6} cm^2 sec^{-1}. The values of k_f calculated by this method are of course at best only approximate because of the lack of rigor in the use of equation (5-4). Nevertheless, when compared to values of k_f determined by alternate methods the error involved (vide infra) was clearly not too great and suggests that this method could be applied to other systems if necessary. A sample calculation of k_f is shown in Appendix 5.

Potentiostatic Studies. In an attempt to verify the values of k_f determined by the peak voltammetric methods, the potentiostatic method of Alberts and Shain[11] as applied to the ECE mechanism was employed. In this method the potential of a stationary microelectrode (e.g., the hanging mercury drop electrode) is stepped to a value corresponding to the plateau of a polarographic wave (i.e., a potential such that all molecules of the electroactive substance which reach the electrode are immediately reduced) and the resulting current is monitored as a function of time. At short times the observed current

corresponds to the first charge transfer step, but at longer times there is a transition to a current corresponding to both charge transfer steps. The time at which the transition occurs depends upon the rate of the intervening chemical reaction. The theoretical equation relating current to time for an ECE process is:[11]

$$i_t = \frac{FAD^{1/2}[n_1 + n_2(1 - e^{-k_f t})]}{t^{1/2}\pi^{1/2}} \qquad (5\text{-}5)$$

where i_t is the instantaneous current at time t (sec) in microamperes; n_1, the number of electrons involved in the first electron transfer step; n_2, the number of electrons involved in the second electron transfer step, and t, the time (sec) elapsed since application of the potential step. The remaining terms have their usual significance. Theoretical current-time curves were calculated for n = 4 (i.e., where k_f is infinite) and n = 2 (i.e., where k_f is zero) using the Cottrell equation and the value of D computed previously (see Appendix 5). Experimental current-time curves revealed that at very short times the current was close to that expected for a 2e reaction (Fig. 5-5A,B) and then at longer times the curve deviated and ultimately coincided with the theoretical 4e curve. The transition from the 2e to 4e reaction took considerably longer at high pH (e.g., pH 11.6, Fig. 5-5A) than at lower pH (e.g., pH 7.0, Fig. 5-5B). This of course implies that the value of k_f becomes smaller as the pH increases. The value of k_f at each pH can be obtained from data of the type shown in Fig. 5-5 by use of the working curves prepared by Alberts and Shain.[11] Theoretical curves can then be constructed using equation (5-5). The agreement between theoretical and experi-

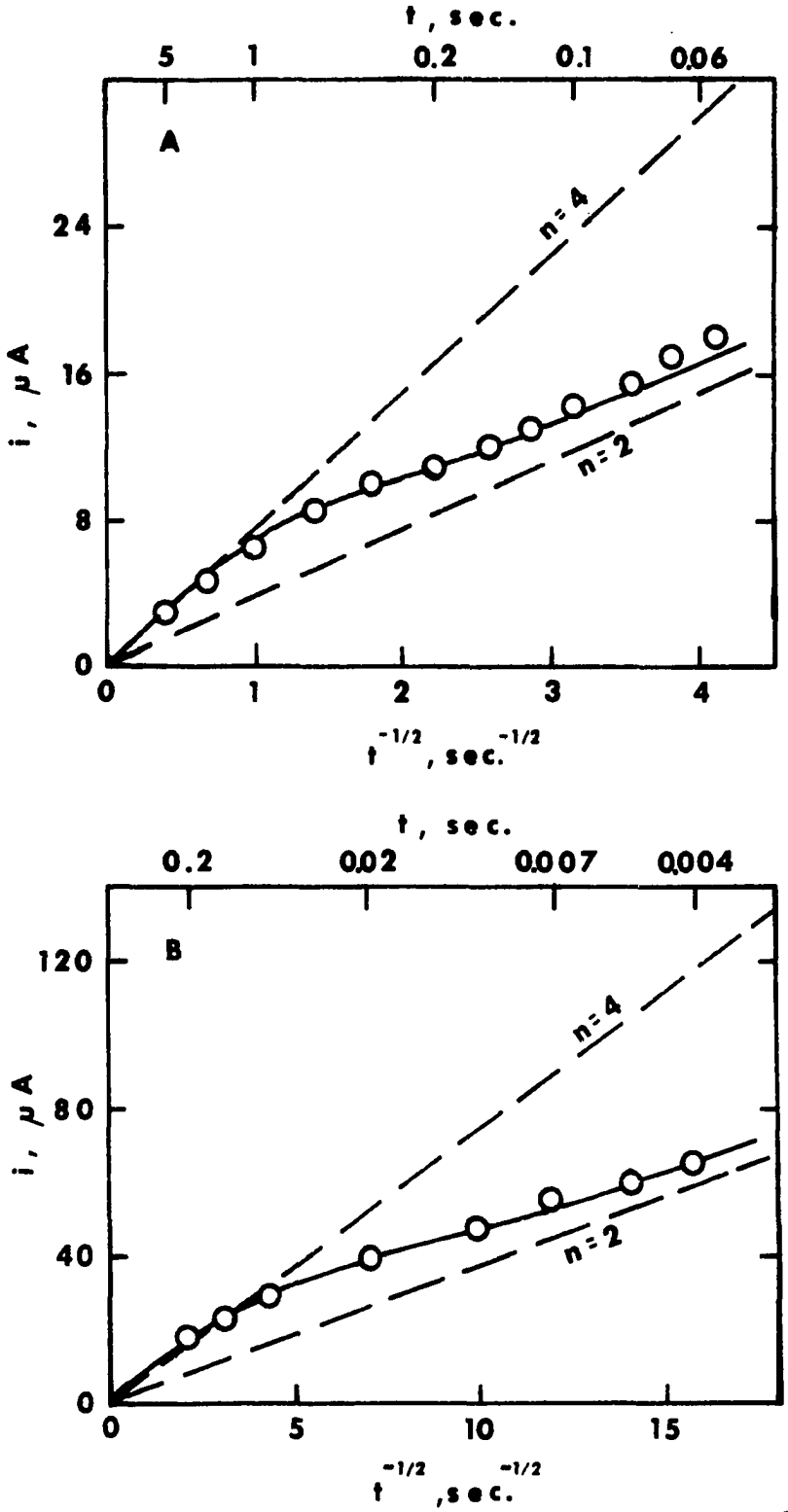

FIGURE 5-5. Comparison of experimental and theoretical current-time curves for the electrochemical reduction of oxamide at the HMDE; (A) pH 11.8, k_f = 2 sec^{-1}, (B) pH 7.0, k_f = 30 sec^{-1}. Circles represent experimental values, solid lines are theoretical curves for the given rate constants calculated from equation (5-5). Dotted lines represent theoretical curves for uncomplicated 2e and 4e processes.

mental current-time curves was excellent. Typical values of k_f computed at representative pH values are shown in Table 5-3 where clearly the agreement between the potentiostatically determined values and those determined by peak voltammetry is quite good. A sample calculation of k_f by the potentiostatic method is shown in Appendix 5.

Further Polarographic Studies. The effect of an ECE mechanism upon a d.c. polarographic wave has been examined by Nicholson and co-workers.[12] Using the approach described by the latter workers the rate constants of rather slow chemical reactions interposed between two charge transfer reactions may be estimated. Applied to the present study, this implies that the value of k_f at pH values above ca 8-9 is sufficiently low to cause a measurable decrease of the polarographic limiting current below the 4e value. Using the working tables of Nicholson and co-workers,[12] values of k_f were calculated and compared to those obtained by the potentiostatic and voltammetric methods. The value of i_d (the diffusion current for the first electrochemical step) used in the latter approach was taken as one-half of the value of the limiting current at the end of the drop life at pH 5.6-7, i.e., where k_f is large and does not affect the polarographic limiting current. The value of i_k was then the measured limiting current at pH values above 9, i.e., where k_f decreases to such a value that the limiting current decreases below the diffusion limited value. Typical values of k_f so calculated are presented in Table 5-3, and a sample calculation is shown in Appendix 5. The polarographic method is probably the least satisfactory method for calculation of k_f. The range of values of k_f which can be determined is rather

limited, and small errors in measurement of i_d and i_k lead to rather large errors in the value of k_f.

Mechanism

Summarizing the previous experimental data it is clear that oxamide is electrochemically reduced between pH 5.6-11.6 in a pH independent, overall 4e process to give glycolamide as the ultimate product. The pH independence of the voltammetric peak potential and polarographic half-wave potential implies that protons are not involved in the rate-determining process. The total electron-transfer process is electrochemically irreversible. The effect of increasing potential sweep rate in peak voltammetric studies and the variation of current with time in potentiostatic studies support the view that the overall electrode process follows an ECE mechanism with both the initial and final charge-transfer steps involving 2e. D.c. polarography also supports the ECE mechanism.

The only reasonable reaction for the initial 2e pH independent charge-transfer reaction of oxamide (I, Fig. 5-6) is formation of a dianion (II, Fig. 5-6). The following chemical processes probably involve protonation of the dianion to an enediol (III, Fig. 5-6) followed by rearrangement to compound IV and loss of ammonia to compound V. Similar reduction mechanisms have been proposed for benzil and other 1,2-diketones.[12,13,14]

The anodic peak I_a observed on cyclic voltammetry of oxamide may correspond either to the oxidation of the dianion or the enediol. The fact that the anodic peak can be observed at lower sweep rates

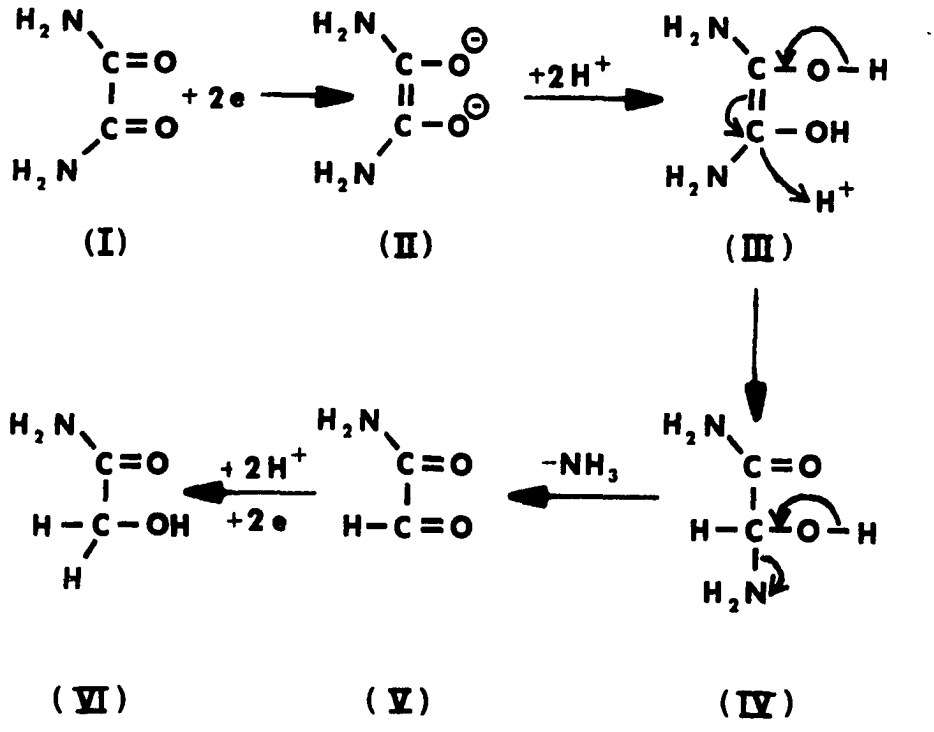

FIGURE 5-6. Proposed mechanism for the electrochemical reduction of oxamide to glycolamide and ammonia.

in a more aprotic solvent (50% acetonitrile) suggests that the dianion is oxidized. In any event, the enediolate (II, Fig. 5-6) or the enediol (III) would both be expected to be readily oxidized species as are many enediols, both chemically[15] and electrochemically.[16]

The chemical reactions describing the transformation of II-V may occur quite separately or proceed via a concerted reaction. Nevertheless, the effect of pH on the overall rate constant of the reaction is obvious, i.e., the rate of the chemical reaction decreases with increasing pH. However, the measured rate constant (k_f) may have a value corresponding to any of the individual reactions or may simply reflect a value for the overall rate. The compound formed by the chemical reactions characterized by k_f is glyoxylamide (V, Fig. 5-6). There is no electrochemical data on this compound; however, gloxylic acid is easily reduced electrochemically to glycolic acid.[17] Also, phenylglyoxylamide is reduced electrochemically to phenylglycolamide.[18] It is not unreasonable that glyoxylamide is also similarly reduced electrochemically.

Analytical Utility of d.c. Polarography. Linear limiting current vs concentration curves were obtained for oxamide in solutions of pH 5.6-11. However, the polarographic reduction wave is best defined in borax buffer pH 8 and carbonate buffer pH 10, i.e., the wave exhibits its best separation from background discharge. Linear concentration curves in these buffers could be obtained between 10^{-5} to $>10^{-3}$ M oxamide (Fig. 5-7). From the viewpoint of quantitative analysis oxamide can be satisfactorily determined by preparation of a calibration curve at the desired pH and over the concentration

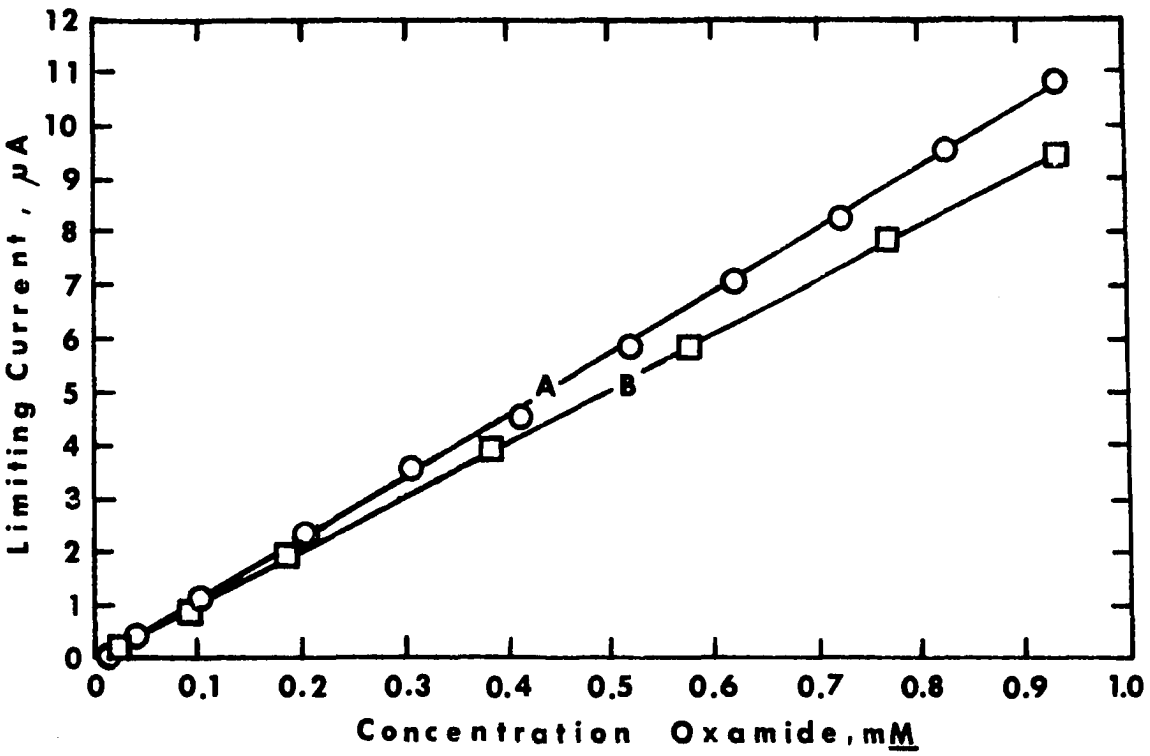

FIGURE 5-7. Linear variation of the limiting current vs concentration of oxamide in (A) borax buffer pH 8.1 and (B) carbonate buffer pH 10.0.

range of interest. The pH employed would probably be selected where the wave of oxamide does not fall in the same potential region as waves of other electroactive components in the sample. It was found that neither oxalic acid nor oxamic acid (the monoamide of oxalic acid) are electrochemically reducible in weakly acidic or basic media, hence these two compounds do not interfere with the determination of oxamide.

Experimental

Chemicals. Oxamide was obtained from Matheson, Coleman, and Bell, glycolamide from Pfalz and Bauer, and acetonitrile from Mallinckrodt.

Buffer solutions were prepared from analytical reagent grade chemicals. Water-saturated nitrogen was used for deoxygenation of aqueous solutions. Dried argon saturated with acetonitrile was used for deoxygenation of acetonitrile solutions.

Apparatus. The apparatus employed has been described in previous chapters.

Polarographic and Voltammetric Procedures. Polarographic and voltammetric procedures were the same as previously described.

Coulometric and Macroscale Electrolysis Procedure. For controlled-potential coulometry, 80 ml of a 1.0 mM solution of oxamide in the appropriate buffer was placed in the working electrode compartment of the coulometric cell, and the electrolysis was carried out as previously described. The procedure for macroscale electrolysis was essentially the same, except that about 200 mg of oxamide in 80 ml

solution was used. At the beginning of the electrolysis only a small portion of the oxamide was in solution, but as the reduction proceeded the remainder dissolved. Macroscale electrolyses of this nature usually required 36-48 hours.

Determination of Ammonia. The working electrode compartment of the cell was sealed with a large rubber stopper through which passed a glass tube. This glass tube was connected via Tygon tubing to a gas bubbling tower containing 80 ml 0.1 N H_2SO_4 in which any ammonia flushed out of the electrolysis solution was trapped. Following electrolysis, ammonia was determined spectrophotometrically in both the H_2SO_4 and in the electrolysis solution using Nessler's reagent,[19] as described in Chapter 4.

Isolation and Identification of Electrolysis Product. To facilitate isolation of electrolysis products other than ammonia, macroscale electrolyses were carried out in carbonate buffer pH 10. After completion of the electrolysis the solution was passed through a column (2 x 50 cm) of Dowex 50w - X8 ion exchange resin (H^+ form) and eluted with 0.1 M acetic acid. The eluent was freeze-dried and a white solid was obtained. This was recrystallized from ethyl acetate, and the product melted at 114.5°C. This material was identified as glycolamide by comparison of its mass, NMR, and infrared spectra (Fig. 5-8ABC) and melting point with that of authentic material. Analysis revealed that the yield of glycolamide was 90 per cent or better based on the amount of oxamide electrolyzed.

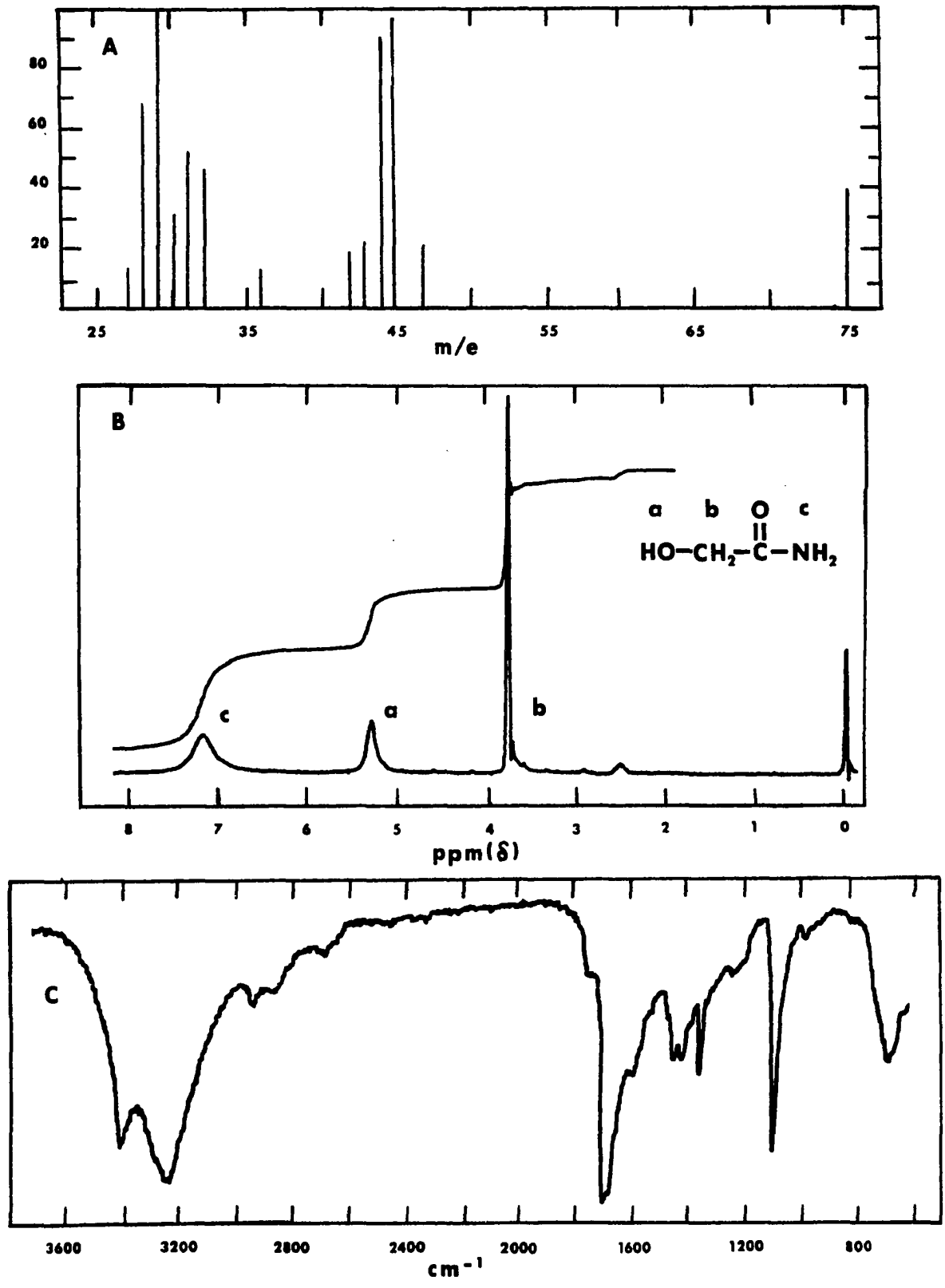

FIGURE 5-8. Mass (A), NMR (B), and infrared (C) spectra of glycolamide, NMR solvent DMSO-d_6, IR is KBr pellet.

Summary

Oxamide is electrochemically reduced at mercury electrodes at pH 5.6-11.6. The overall mechanism proceeds by an initial 2e reduction of the 1,2-carbonyl groups of oxamide to give a dianion. This then protonates, rearranges, and loses ammonia to glyoxylamide, which is reduced in a further $2e/2H^+$ reaction giving glycolamide as the ultimate product. The reaction thus proceeds by an ECE mechanism. The overall homogeneous rate constant for the chemical reaction(s) interposed between the two charge-transfer steps has been measured by peak voltammetric, potentiostatic, and d.c. polarographic methods. The d.c. polarographic wave of oxamide between pH 5.6 and 11 provides the basis for a very simple analytical method for the determination of oxamide.

APPENDIX 5

I. Determination of the diffusion coefficient of oxamide from current-time curves.

If the potential of a stationary microelectrode is stepped to a potential such that all molecules of an electroactive substance diffusing to the electrode are immediately reduced or oxidized (e.g., a potential corresponding to the plateau of a polarographic wave), the manner in which current decays with time is given by the Cottrell equation:

$$i_t = \frac{nFAD^{1/2}C}{(\pi t)^{1/2}} \qquad \text{(A-5-1)}$$

where all terms have their usual significance (see, e.g., eq. 5-5). If i_t is plotted as a function of $t^{-1/2}$, the slope of the curve is given by:

$$\text{slope} = \frac{di_t}{dt^{-1/2}} = \frac{nFAD^{1/2}C}{\pi^{1/2}} \qquad \text{(A-5-2)}$$

$D^{1/2}$ can therefore be calculated from the expression:

$$D^{1/2} = \frac{\text{Slope}}{\frac{nFAC}{\pi^{1/2}}} \qquad \text{(A-5-3)}$$

if all other terms are known. For example, at pH 7, n = 4, F = 96,500 coulombs, A = 0.022 cm^2, C = 0.5 mMl^{-1}, and

$$D^{1/2} = \frac{\text{Slope}}{2400} \qquad \text{(A-5-4)}$$

From the experimental i_t *vs* $t^{-1/2}$ plot (Fig. A-5-1) it was determined that at $t^{-1/2} = 1$, $i_t = 7.80$ and at $t^{-1/2} = 0.5$, $i_t = 4.05$.

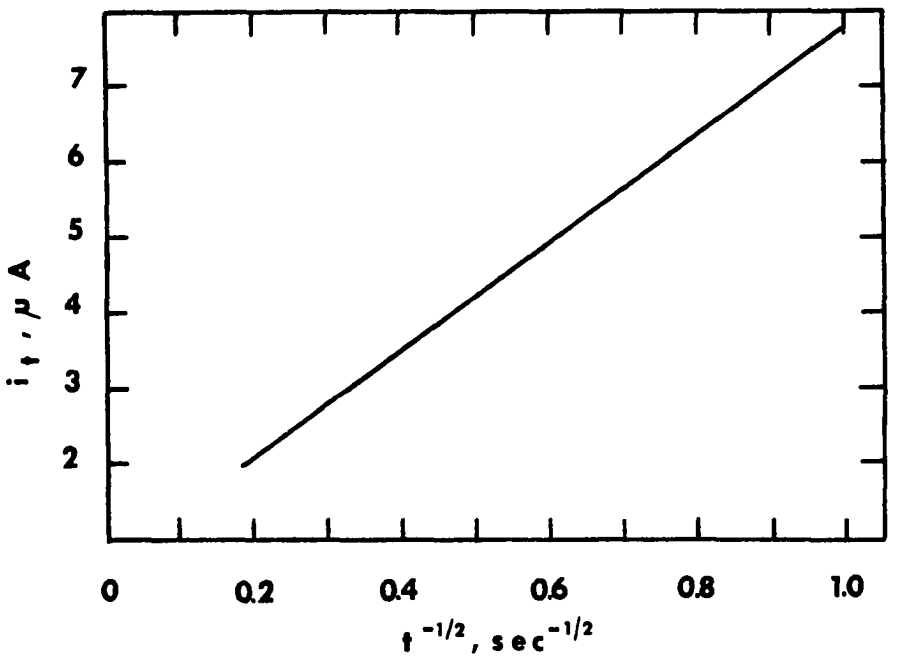

FIGURE A-5-1. i_t *vs* $t^{-1/2}$ for oxamide at pH 7 at the HMDE

Therefore,

$$\text{slope} = \frac{7.8-4.05}{1-0.5} = 7.50$$

and

$$D^{1/2} = \frac{7.5}{2400} = 3.12 \times 10^{-3} \text{ cm sec}^{-1/2}$$

II. Calculation of theoretical peak current versus square root of scan rate curves for oxamide, and determination of k_f.

1. Computation of αn_a at pH 7.

$$(E_{p/2})_2 - (E_{p/2})_1 = -\frac{0.0128}{\alpha n_a} \ln \frac{v_2}{v_1} \qquad (5\text{-}2)$$

$v_1 = 0.01$ V sec^{-1}

$(E_{p/2})_1 = -1.5587$ V *vs* SCE

$v_2 = 0.10$ V sec^{-1}

$(E_{p/2})_2 = -1.5875$ V *vs* SCE

$$\alpha n_a = -\frac{0.0128}{-1.5875-(-1.5587)} \ln \frac{0.10}{0.01}$$

$$= 1.02$$

2. Calculation of peak current function for n = 2.

From eq. (5-1):

$$i_p/ACv^{1/2} = 2.98 \times 10^5 n(\alpha n_a)^{1/2} D^{1/2}$$

$n = 2$

$\alpha n_a = 1.0$

$D^{1/2} = 3.12 \times 10^{-3}$

$i_p/ACv^{1/2} = 1860\ \mu A cm^{-2} (mM l^{-1})^{-1} V^{-1/2} sec^{1/2}$

3. Calculation of theoretical peak current *vs* $v^{1/2}$ curves for ECE mechanism.

From eq. (5-4):

$i = 6.02 \times 10^5 n(\alpha n_a)^{1/2} AD^{1/2} Cv^{1/2} [\sqrt{\pi}\ \chi(bt) + \sqrt{\pi}\ \phi(at)]$,

if $n_1 = n_2$ and $(\alpha n_a)_1 = (\alpha n_a)_2$.

The value of the $\sqrt{\pi}\ \chi(bt)$ was obtained from Table II, ref. 6, and is the maximal (peak) value (0.496) for an irreversible charge transfer. Maximal values of $\sqrt{\pi}\ \phi(at)$ were taken from Table III, ref. 9, and

plotted vs the corresponding values of k_f/a, where k_f = homogeneous rate constant and $a = \frac{nFv}{RT}$, where n = number of electrons involved in second charge transfer, F = 96,500 coulombs, v = voltage sweep rate, Volts sec^{-1}, R = 8.31 Joules $degree^{-1}$ mol^{-1}, and T = absolute temperature, °K (Fig. A-5-2).

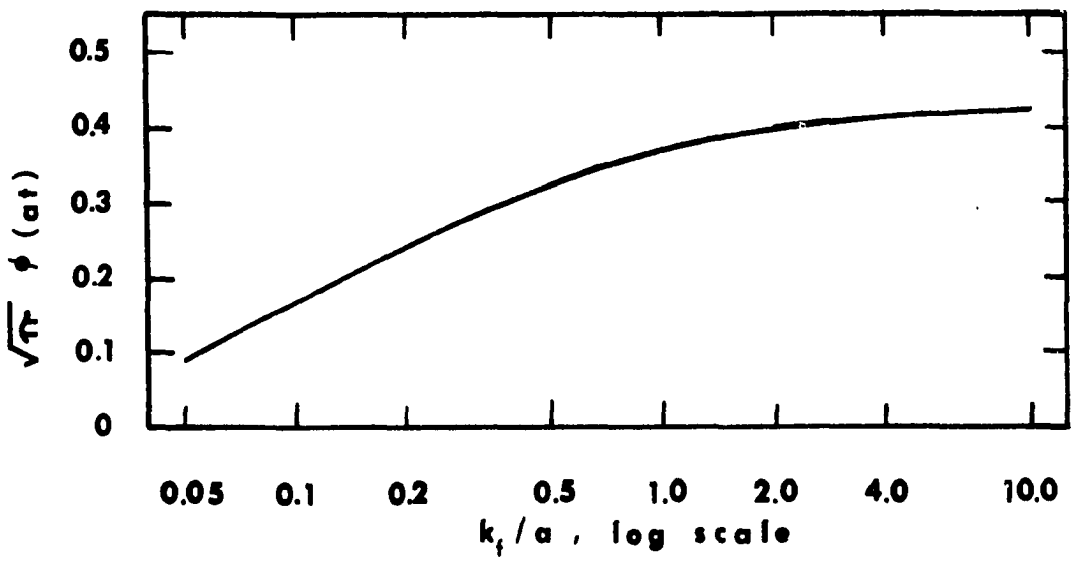

FIGURE A-5-2. Variation of the peak current function, $\sqrt{\pi}\,\phi(at)$, with k_f/a for the second charge-transfer step of an ECE reaction.

Plots of peak current function ($i/ACv^{1/2}$ vs $v^{1/2}$) were then constructed for values of k_f from 1 to 200, and compared to the experimental curves (Fig. 5-4) for determination of experimental k_f values. Details for construction of a sample plot are given below.

$$a = \frac{nFV}{RT} = 77.93v, \text{ if } n = 2$$

From eq. (5-4)

$$i/ACv^{1/2} = 6.02 \times 10^5 n(\alpha n_a)^{1/2} D^{1/2} [\sqrt{\pi}\,\chi(bt) + \sqrt{\pi}\,\phi(at)]$$

$$= 6.02 \times 10^5 (2)(1)(3.12 \times 10^{-3}) = 3770[\sqrt{\pi}\chi(bt) + \sqrt{\pi}\phi(at)]$$

Values of $i/ACv^{1/2}$ calculated at various sweep rates for $k_f = 10$ are shown in Table A-5-1.

TABLE A-5-1

Values of $i/ACv^{1/2}$ at Various Sweep Rates for $k_f = 10$

v	$v^{1/2}$	a	k_f/a	$\pi^{1/2}\chi(bt)$	$\pi^{1/2}\phi(at)$	$i/ACv^{1/2}$
0.02	0.141	1.55	6.45	0.496	0.414	3430
0.05	0.224	3.89	2.57	0.496	0.397	3370
0.10	0.316	7.79	1.28	0.496	0.377	3290
0.20	0.447	15.59	0.64	0.496	0.337	3140
0.50	0.707	38.96	0.26	0.496	0.262	2860
1.00	1.00	77.93	0.13	0.496	0.195	2610
2.00	1.41	155.9	0.064	0.496	0.120	2320

When plots of $i/ACv^{1/2}$ *vs* $v^{1/2}$ were constructed (on the same scale used in Fig. 5-4) for several values of k_f, and compared with the experimental curves (Fig. 5-4), it was found that the theoretical plot for $k_f = 10$ most nearly coincided with the experimental curve for oxamide at pH 10. Therefore, the value of k_f for oxamide at pH 10 is approximately 10.

III. Determination of k_f from potentiostatic data.

1. Calculation of k_f values from experimental data.

Experimental current-time curves were plotted as shown in Fig. 5-5, *i.e.*, as i *vs* $t^{-1/2}$. The curves for n = 4 and n = 2 were calculated from the Cottrell equation (eq. A-5-1). Since the curves for n = 4 and n = 2 are linear, only two or three points must be calculated to

establish the line. The ratio i/i_∞ (where i = experimental current at time t and i_∞ = theoretical current at time t for $k_f = \infty$, i.e., n = 4) was calculated at several times and compared to the working curves given in ref. 11. In these curves, the value i/i_∞ is plotted vs log $(k_f t)$. Therefore, for i/i_∞ at any time t, k_f is easily calculated. For example, in Fig. 5-5A, at t = 0.2 sec, i = 10.5 μA and i_∞ 16 μA, therefore $i/i_\infty = 0.66$. From Fig. 5 in ref. 11, then, log $k_f t$ = -0.4 and $k_f = 2\ sec^{-1}$.

2. Verification of k_f values by comparison of theoretical and experimental curves.

Using equation (5-5), and the values of k_f calculated as shown above, theoretical i vs $t^{-1/2}$ curves were plotted and compared with experimental curves. If necessary, slight adjustments were made in k_f values to obtain the best fit with the experimental points.

IV. Calculation of k_f values from polarographic data.

Using the values of i_d and i_k described in the text, the ratio i_k/i_d was calculated. In the working curve in ref. 12, values of i_k/i_d are plotted vs log $k_f t$, where t is the drop time in seconds. Thus at pH 11.6, with t = 2.00 sec, i_k = 4.9 μA. The value of i_d, obtained at pH 7, was 3.3 μA. Therefore, $i_k/i_d = \frac{4.9}{3.3} = 1.5$, corresponding to a value of 2.0 for $k_f t$, and 1.0 for k_f.

REFERENCES

1. R. D. Tiwari, J. P. Sharma, and I. C. Shulka, Ind. J. Chem., 4, 221 (1966).

2. J. B. Apatoff, J. Cohen, and G. Norwitz, Anal. Chem., 35, 800 (1963).

3. X. V. Voortam, P. Crooy, A. Bruylants, and L. Baczynsky, Bull. Soc. Chim. Belges, 73, 753 (1964).

4. D. J. Cram, Chem. Eng. News, 41, No. 33, 94 (1963).

5. R. P. Bell, in Advances in Physical Organic Chemistry (V. Gold, ed.), Vol. 4, Academic Press, New York, 1966, pp. 1-29.

6. R. S. Nicholson and I. Shain, Anal. Chem., 36, 706 (1964).

7. R. H. Wopshall and I. Shain, Anal. Chem., 39, 1514 (1967).

8. R. N. Adams, Electrochemistry at Solid Electrodes, Marcel Dekker, New York, 1969, p. 137.

9. R. S. Nicholson and I. Shain, Anal. Chem., 37, 178 (1965).

10. I. Shain and K. J. Martin, J. Phys. Chem., 65, 254 (1961).

11. G. S. Alberts and I. Shain, Anal. Chem., 35, 1859 (1963).

12. R. S. Nicholson, J. M. Wilson, and M. L. Olmstead, Anal. Chem., 38, 542 (1966).

13. R. H. Philip, R. L. Flurry, and R. A. Day, J. Electrochem. Soc., 111, 328 (1964).

14. J. Holubek and J. Volke, Coll. Czech. Chem. Commun., 25, 3292 (1960).

15. L. F. Fiesor and M. Fiesor, Reagents for Organic Synthesis, J. Wiley and Sons, New York, 1967, pp. 159-160.

16. G. Dryhurst, J. Electrochem. Soc., 119, 1659 (1972).

17. J. M. Saveant, Bull. Soc. Chim. France, 481 (1967).

18. J. Armand, P. Souchay, and F. Valentini, C. R. Acad. Sc. Paris, Ser. C, 265, 1267 (1967).